



PACIFIC EARTHQUAKE ENGINEERING RESEARCH CENTER

Ground Motions for Earthquake Simulator Qualification of Electrical Substation Equipment

Shakhzod M. Takhirov

University of California, Berkeley

Gregory L. Fennes

University of California, Berkeley

Eric Fujisaki

Pacific Gas & Electric Co.

and

Don Clyde

University of California, Berkeley

Ground Motions for Earthquake Simulator Qualification of Electrical Substation Equipment

Shakhzod M. Takhirov

Earthquake Engineering Research Center
University of California, Berkeley

Gregory L. Fenves

Department of Civil and Environmental Engineering
University of California, Berkeley

Eric Fujisaki

Pacific Gas and Electric Company
Oakland, California

Don Clyde

Earthquake Engineering Research Center
University of California, Berkeley

Sponsor:

California Energy Commission

PEER Report 2004/07
Pacific Earthquake Engineering Research Center
College of Engineering
University of California, Berkeley

January 2005

ABSTRACT

The main objective of the study was to develop a set of strong motion time histories suitable for seismic qualification testing of electrical substation equipment in accordance with the IEEE 693-1997 standard. Although the objective deals with shake table testing of a particular class of equipment, many of the issues investigated are equally relevant to the dynamic testing of other types of equipment and components. This study was motivated by a desire to introduce a standard set of input motions in three orthogonal directions and thus achieve more consistency in earthquake simulator testing. The report focuses on developing with a time domain spectral matching procedure an input strong motion based on a record of an actual earthquake, so that the spectrum-compatible strong motion time history preserves the non-stationary behavior of the actual record.

A selection of 35 three-component historic records from 18 earthquakes was analyzed and the records were compared by using several parameters. From the analysis, the best candidate for the input strong motion was selected and modified by adding non-stationary wavelets to the signal. The resulting strong motion time history preserves the non-stationary behavior of the actual earthquake record, while its response spectra envelop the IEEE target response spectra for a broad range of natural frequencies as required by the standard. The resulting strong motion time history is intended for use by testing facilities and will be considered for a future revision to IEEE 693.

Additional requirements for the input motion specification in the IEEE693-1997 are recommended.

ACKNOWLEDGMENTS

This project was sponsored by the Pacific Earthquake Engineering Research Center's Program of Applied Earthquake Engineering Research of Lifeline Systems supported by the California Energy Commission, the California Department of Transportation, and the Pacific Gas & Electric Company. This financial support is gratefully acknowledged.

This work made use of the Earthquake Engineering Research Centers Shared Facilities supported by the National Science Foundation under award number EEC-9701568 through the Pacific Earthquake Engineering Research Center (PEER). Any opinions, findings, and conclusions or recommendations expressed in this material are those of the author(s) and do not necessarily reflect those of the National Science Foundation.

This report was prepared as a result of work sponsored by the California Energy Commission ("the Commission"). It does not necessarily represent the views of the Commission, its employees, or the State of California. The Commission, the State of California, its employees, contractors, and subcontractors make no warranty, express or implied, and assume no legal liability for the information in this report; nor does any party represent that the use of this information will not infringe upon privately owned rights. This report has not been approved or disapproved by the Commission nor has the Commission passed upon the accuracy or adequacy of the information in this report.

The authors wish to thank the following individuals for their technical contributions to the project: Dr. Anshel Schiff, of Precision Measurement Instruments, for discussion of the project results, and Dr. James Wilcoski, of the U.S. Army Corps of Engineers Construction Engineering Research Laboratory, for providing the IEEE-compatible synthetic time history.

CONTENTS

ABSTRACT	iii
ACKNOWLEDGMENTS	iv
TABLE OF CONTENTS	v
LIST OF FIGURES	vii
LIST OF TABLES	ix
1 INTRODUCTION	1
1.1 Objectives.....	1
1.2 Review of Previous Research	2
1.3 Deliverables	4
1.4 Report Organization.....	4
2 STUDY OF DESIGN AND REQUIRED RESPONSE SPECTRA COMPARED TO IEEE SPECTRA	7
2.1 Required Response Spectra for Seismic Qualification of Electrical Substation Equipment (IEEE 693).....	7
2.2 Design Response Spectra from Building Codes and Related Documents	9
2.2.1 International Building Code 2000.....	9
2.2.2 Uniform Building Code 1997	12
2.2.3 Regulatory Guide 1.60	18
2.3 Required Response Spectra for Nonstructural Component or Equipment Testing.....	20
2.3.1 NEBS Requirements For Telecommunication Equipment (GR-63-CORE).....	20
2.3.2 ICBO ES Criteria for Seismic Qualification Testing of Nonstructural Components (AC156)	22
2.3.3 International Electrotechnical Commission Standard (IEC-1999)	26
2.4 Summary and Conclusions.....	30
3 STUDY OF GROUND MOTIONS AND RECORD SELECTION FOR SPECTRAL MATCHING	33
3.1 Criteria Used to Select Strong Motion Record	33
3.1.1 Earthquake Magnitude and Distance of Site from Source.....	34
3.1.2 Peak Ground Motion Parameters	37

3.1.3	Site Classification and Instrument Location	38
3.2	Summary of Key Computed Parameters and Indices	41
3.2.1	Number of Cycles Histogram	42
3.2.2	Power Spectral Density	42
3.2.3	Elastic Response Spectra.....	44
3.2.4	Number of Cycles in Response of SDOF System.....	44
3.2.5	Parameters Based on Cumulative Energy	47
3.2.6	Duration Based on IEEE-693 Definition	48
3.2.7	Cumulative Specific Kinetic Energy.....	51
3.3	Record Selection for Test Time History and Its Parameters.....	52
3.3.1	Candidate Selection for Test Time History from 35 Records.....	52
3.3.2	SDOF System Response Parameters and PSD for Landers Record (Record 18).....	54
3.3.3	Details of Landers Strong Motion Time History (Record 18).....	59
3.4	Summary and Conclusions.....	59
4	DEVELOPMENT OF RESPONSE SPECTRUM-COMPATIBLE TIME HISTORY	61
4.1	Spectrum Matching Procedure in Time Domain	62
4.1.1	Description of Time Domain Matching Procedure.....	62
4.1.2	Spectral Matching of Landers (Joshua Tree) Record in Time Domain	62
4.2	Spectral Matching of Reference Time History in Frequency Domain	67
4.2.1	Procedure for Response Fit in Frequency Domain	67
4.2.2	Spectral Matching Results for Response Fit in Frequency Domain	68
4.3	Synthetic Accelerogram Matching Target Spectra (SimQke)	68
4.3.1	General Description of Procedure for Generating Synthetic Time Histories ...	68
4.3.2	Results for Synthetic Generation of Strong Motion Time History	73
4.4	Comparison of Frequency Content for Time Histories Modified by Matching Procedures	73
4.4.1	PSD Comparison.....	73
4.4.2	Time-Dependent Frequency Analysis (Spectrogram).....	75
4.5	Conclusions.....	78

5	INPUT TIME HISTORIES FOR EARTHQUAKE SIMULATORS.....	79
5.1	Major Existing and Future U.S. Earthquake Simulators.....	79
5.1.1	Some Examples of Existing Earthquake Simulator Facilities	81
5.1.2	Future Upgrades of Earthquake Simulator Facilities	83
5.2	IEEE-Compatible Landers and Filtering Procedures to Accommodate Simulator Capacity	84
5.2.1	Properties of IEEE-compatible Landers (TestQke4IEEE).....	84
5.2.2	Filtering Procedure Used for EERC Earthquake Simulator.....	92
5.2.3	Filtering Procedure Developed at MTS	93
5.2.4	Two Sample Input Signals Filtered from IEEE-Compatible Landers	94
5.3	Proposed Signal vs. Strong Motion Signals Currently in Use	99
5.3.1	Tabas 1 and Tabas 2 Time Histories (EERC, UC Berkeley)	99
5.3.2	Synthetic Strong Motion History Used at CERL.....	99
5.3.3	Summary of Key Parameters	100
5.3.4	Conclusions	115
6	RECOMMENDED REQUIREMENTS FOR QUALIFICATION TESTING OF ELECTRICAL EQUIPMENT	117
6.1	Analysis for Tolerance Estimation and Filtering Limits.....	117
6.1.1	Frequency Resolution for TRS Verification against RRS	117
6.1.2	Tolerance Zone Estimation	118
6.1.3	Analysis of Limits of Natural Frequency Based on Variation of Stop Frequency of High-Pass Filter	120
6.2	Test Signal Requirements for Electrical Equipment.....	129
6.2.1	Requirements on Generation of Alternative IEEE-Compatible Signal.....	129
6.2.2	Filtering Procedure and Theoretical Response Spectrum of Filtered Signal ..	130
6.2.3	Tolerance and Frequency Resolution for TRS.....	131
6.2.4	Number of Cycles with High Amplitude in SDOF System Response.....	131
6.2.5	Strong Motion Duration	132
7	SUMMARY AND CONCLUSIONS.....	133
7.1	Study of Strong Motion Records and Matching Procedures.....	133
7.1.1	Study of Strong Motion Time Histories.....	133

7.1.2	Study on Spectrum Matching Procedures	135
7.2	Summary and Conclusions for Recommended Input Signal	135
7.2.1	Properties of Recommended Input Signal.....	136
7.2.2	Summary of Recommended Requirements for Qualification Testing.....	137
7.3	Recommendations for IEEE 693 Qualification Procedure	138
7.3.1	Prescribed IEEE-Compatible Landers	138
7.3.2	Requirements on Generation and Filtering Procedure	138
7.3.3	Limitations of RRS Prescribed by IEEE 693 in Central and Eastern U.S.	138
REFERENCES.....		141
APPENDIX A	Parameters of Strong Motion Records and Response Indices.....	147
APPENDIX B	Notes on Fracture Mechanics and Cycle Counting Procedure.....	157
APPENDIX C	Examination of Earthquake Records from Eastern and Central North America.....	169
APPENDIX D	Specification for Input Motion Used for Testing — IEEE 693 (Proposed for New IEEE 693).....	181

LIST OF FIGURES

Fig. 2.1	IBC-2000 design spectra for various S_s and S_I vs. IEEE high PL and high RRS.....	11
Fig. 2.2	UBC-1997 design spectra for source type A vs. IEEE high PL and high RRS.....	14
Fig. 2.3	UBC-1997 design spectra for source type B vs. IEEE high PL and high RRS.....	15
Fig. 2.4	UBC-1997 design spectra for source type C vs. IEEE high PL and high RRS.....	16
Fig. 2.5	USASC (USNGC) Regulatory Guide 1.60 spectrum vs. high IEEE PL spectrum for 5% damping.....	19
Fig. 2.6	GR-63 RRS for various zones vs. high IEEE RRS and high IEEE PL for 2% damping.....	21
Fig. 2.7	TRS (based on VERTEQII) vs. 30% tolerance zone above RRS at 1/6 octave.....	23
Fig. 2.8	TRS (based on VERTEQII) vs. 30% tolerance zone above RRS at 1/12 octave.....	24
Fig. 2.9	AC 156 RRS for various zones vs. high IEEE RRS and high IEEE PL for 5% damping.....	26
Fig. 2.10	IBC-1999 response spectra vs. IEEE high qualification RRS.....	29
Fig. 3.1	Magnitude vs. distance distribution.....	37
Fig. 3.2	Peak ground accelerations for all records.....	39
Fig. 3.3	Distribution of peak ground accelerations.....	39
Fig. 3.4	Peak ground velocities for all selected records.....	40
Fig. 3.5	Distribution of peak ground velocity.....	40
Fig. 3.6	Soil vs. epicentral distance distribution for all selected records.....	41
Fig. 3.7	Maximum, mean, and mean-plus-one deviation of cycle counts for all records.....	43
Fig. 3.8	Total cycle counts with 25% maximum magnitude threshold.....	43
Fig. 3.9	Mean and mean-plus-one deviation PSD for all records.....	45
Fig. 3.10	Mean and mean-plus-one deviation spectra for all records.....	45
Fig. 3.11	Number of cycles in SDOF response for set of 35 records.....	46
Fig. 3.12	Cumulative energy for all records normalized to 1.0g PGA.....	47
Fig. 3.13	RMS acceleration for all records normalized to 1.0g PGA.....	49
Fig. 3.14	Bracketed duration for all records based on cumulative energy (5%–95%).....	49
Fig. 3.15	Strong part to bracketed duration ratio for all records based on cumulative energy..	50
Fig. 3.16	Bracketed duration based on IEEE 693 definition.....	50
Fig. 3.17	Bracketed durations for cumulative energy and IEEE 693 definitions.....	51

Fig. 3.18	Cumulative specific kinetic energy for normalized accelerograms.....	52
Fig. 3.19	Landers record (Record 18) vs. mean and mean-plus-one standard deviation of the set.....	55
Fig. 3.20	Smoothed PSD of Landers000 vs. mean and mean-plus-one deviation for 35 records.....	56
Fig. 3.21	Spectrum of Landers000 vs. mean and mean-plus-one deviation for 35 records.....	56
Fig. 3.22	Smoothed PSD of Landers090 vs. mean and mean-plus-one deviation for 35 records.....	57
Fig. 3.23	Spectrum of Landers090 vs. mean and mean-plus-one deviation for 35 records.....	57
Fig. 3.24	Number of high cycles in SDOF response for Record 18 vs. set of 35 records	58
Fig. 4.1	Original and IEEE spectrum-compatible Landers time histories	63
Fig. 4.2	Response spectra for original and IEEE spectrum-compatible Landers time histories.....	64
Fig. 4.3	Power spectral density for original and IEEE-compatible Landers time histories	65
Fig. 4.4	Smoothed PSD for original and IEEE spectrum-compatible Landers time histories.....	66
Fig. 4.5	Original and IEEE-compatible (frequency domain) Landers time histories	69
Fig. 4.6	Spectra for original and IEEE-compatible (frequency domain) Landers time histories.....	70
Fig. 4.7	PSD for original and IEEE-compatible (frequency domain) Landers signals.....	71
Fig. 4.8	Smoothed PSD for original and IEEE-compatible (frequency domain) Landers signals	72
Fig. 4.9	Synthetic strong motion time history generated by means of SimQke-1	74
Fig. 4.10	Smoothed PSD for IEEE-compatible time histories generated by various matching procedures (X direction).....	76
Fig. 4.11	Time-dependent frequency content of synthetic, reference, and IEEE-compatible signals (X direction)	77
Fig. 5.1a	Tolerance zone for IEEE-compatible Landers at 2% damping (1/24 octave resolution)	86
Fig. 5.1b	Tolerance zone for IEEE-compatible Landers at 5% damping (1/24 octave resolution)	87

Fig. 5.2	Acceleration time histories in three principal directions for IEEE-compatible Landers	89
Fig. 5.3	Velocity time histories in three principal directions for IEEE-compatible Landers	90
Fig. 5.4	Displacement time histories in three principal directions for IEEE-compatible Landers	91
Fig. 5.5	Steps of filtering procedure (from top to bottom)	95
Fig. 5.6	Landers RRS designed for use in high RRS qualification test	97
Fig. 5.7	LandersPL proposed for use at high PL qualification test.....	98
Fig. 5.8	PSD and elastic response spectra for Tabas-1	101
Fig. 5.9	PSD and elastic response spectra for Tabas-2	102
Fig. 5.10	Acceleration time history for CERL synthetic strong motion	103
Fig. 5.11	PSD and spectra CERL synthetic strong motion.....	104
Fig. 5.12	Smoothed PSD for test signals vs. mean of set of 35 strong motions	106
Fig. 5.13	Cycle count results for IEEE-compatible test signals.....	107
Fig. 5.14	Number of high-level cycles in SDOF system response for IEEE-compatible Landers	108
Fig. 5.15	Number of high-level cycles in SDOF system response for Tabas-1	109
Fig. 5.16	Number of high-level cycles in SDOF system response for Tabas-2.....	110
Fig. 5.17	Number of high-level cycles in SDOF system response for IEEE-compatible CERL	111
Fig. 5.18	Cumulative energy for IEEE-compatible test signals.....	113
Fig. 5.19	Duration of IEEE-compatible Landers signals	113
Fig. 5.20	Strong part to duration ratio for test signals	114
Fig. 5.21	Cumulative specific kinetic energy for IEEE-compatible signals.....	114
Fig. 6.1	Tolerance analysis conducted for 35 historic strong motion time histories	119
Fig. 6.2	Normalized peak values for all filtered versions	122
Fig. 6.3	Count of high cycles for various filtered versions.....	123
Fig. 6.4	Difference in cycle counts at 1/12 octave resolution: part 1	124
Fig. 6.5	Difference in cycle counts at 1/12 octave resolution: part 2	125
Fig. 6.6	Elastic response spectra computed for various filtered versions	126
Fig. 6.7	Normalized difference in elastic response spectra: part 1	127

Fig. 6.8	Normalized difference in elastic response spectra: part 2	128
Fig. A.1	Example of CE computation: difference between general trends of CE for actual record (Landers000) and synthetically generated (CERL in X direction) time history	149
Fig. A.2	Misleading difference in spectral shape for linear vs. 1/24 octave frequency resolutions.....	153
Fig. A.3	Strong part of the IEEE high PL response spectrum (solid line).....	154
Fig. B.1	Points where slope changes its sign.....	164
Fig. B.2	Points where slope changes its sign (close view)	164
Fig. B.3	Modified Landers000 that starts from and ends by the same maximum value	165
Fig. B.4	Cycle count for Landers000.....	165
Fig. B.5	First 4 steps for a sample load history (ASTM simplified procedure)	166
Fig. B.6	Last steps and final result for a sample load history (ASTM simplified).....	167
Fig. C.1	Comparison for mean PSD and spectra: set of 35 records and ENA and CNA se...	171
Fig. C.2	High IEEE PL spectra vs. ENA and CAN set anchored at 1.2g.....	173
Fig. C.3	IBC-2000 response spectra for MCE at major seismic regions (New York excluded).....	175
Fig. C.4	IBC-2000 response spectra for MCE at sites of New York seismic region	177
Fig. C.5	IBC-2000 response spectra for Memphis region vs. scaled IEEE spectrum	179

LIST OF TABLES

Table 2.1	Percent ratio of the UBC-1997 plateau value to the IEEE RRS plateau	17
Table 2.2	Summary of design and required response spectra and requirements of test time history from various regulatory documents	31
Table 3.1	Strong motion records selected for consideration	34
Table 3.2	Parameters of strong motion time histories	35
Table 3.3	Geomatrix classification of geotechnical subsurface characteristics.....	41
Table 3.4	List of records with duration longer than 20 sec (IEEE and CE definitions).....	53
Table 5.1	Existing major earthquake simulators of the U.S.	80
Table 5.2	Future NEES earthquake simulators in the U.S.....	81
Table 5.3	Deviation of IEEE-compatible Landers from IEEE spectra (in percents at 1/24 octave frequency resolution)	88
Table 6.1	Peak values for filtered versions of the IEEE-compatible Landers record.....	121
Table C.1	Strong motion records from eastern and central North America.....	170
Table C.2	Mapped MCE spectral accelerations and PGA for site type B (IBC-2000).....	174

1 Introduction

1.1 OBJECTIVES

The main objective of this study was to develop a set of earthquake ground motion time histories suitable for seismic qualification of electrical substation equipment in accordance with the IEEE 693-1997 standard (IEEE, 1998). Although the study's objective deals with shake table testing of a particular class of equipment, many of the issues investigated are equally relevant to the dynamic testing of other types of equipment and components.

As currently written, the IEEE standard requires that the response spectra for an earthquake input motion envelop only (match or exceed) the IEEE target response spectra. IEEE 693 recommends spectral matching at 2% damping, and requires at least 20 sec of strong motion shaking be present in each earthquake record. This study was motivated by a desire to improve the equipment qualification procedures by introducing a standard strong motion, and thus achieve more consistency in earthquake simulator testing. There are two general ways to specify the input strong motion: the first is based on modification of a record from an earthquake, while the second is based on synthetic generation of the input signal. The study focuses on developing an input strong motion based on actual earthquake records with a time domain spectral matching procedure so that the spectrum-compatible strong motion time history preserves the non-stationary behavior of the real record.

The study reviews the design spectra and required response spectra (RRS) used and specified in various standards in the United States and internationally. This part of the study shows the relation between the IEEE RRS spectra and other response spectra. The difference between two spectral matching techniques, namely the time domain and the frequency domain procedures, is presented in detail. Both approaches can produce adequately matched time histories, but the time domain method preserves the non-stationary behavior of the original time history and closely matches the target spectra for more than one damping value. The limitations

of the test equipment and the performance of the largest shake tables currently in use are discussed. In order to accommodate the limits of a particular earthquake simulator, the input strong motion would typically require filtering, which is also addressed.

The main part of the study focuses on the analysis of recorded strong motion time histories and the selection of the best candidates for the input record. Based on relevant criteria for substation electrical equipment, 35 historic strong motion records from 18 earthquakes that occurred in the United States, Canada, Mexico, Iran, Taiwan, and Turkey were examined. Most of the strong motion time histories were recorded in the free field or at the base of lightweight structures on moderately stiff soils and locations within 20 km of the epicenter. The strong motion records were normalized and compared based on the use of several parameters including, but not limited to, duration of strong motion, duration of strongest shaking, several energy parameters, number of cycles, power spectral density, and elastic response spectra. Based on the analysis, the best candidate for the input strong motion was selected and modified by adding non-stationary wavelets to the signal. The resulting time history preserves the non-stationary behavior of an actual strong motion record, while its response spectra envelop the IEEE target response spectra in a broad range of frequencies. The resulting strong motion time history is intended to be offered for use to any interested testing facilities and will be considered for inclusion in a future revision to IEEE 693.

The strong motion time history developed was successfully used for a qualification test of a 500 kV disconnect switch (Takhirov et al. 2004) on the Earthquake Engineering Research Center (EERC) shake table at the Richmond Field Station of the University of California, Berkeley. The site is the headquarters of the Pacific Earthquake Engineering Research (PEER) Center.

1.2 REVIEW OF PREVIOUS RESEARCH

The review focused on the most important trends in developing test strong motion time histories for earthquake simulator testing and on discussion of the available strong motion histories in current use.

There are two major approaches for developing a spectrum-compatible test history. The first approach creates a synthetic time history that consists of a set of tapered harmonics selected to achieve similarity to an actual earthquake record. However, because of its stationary content,

the synthetic signal does not have non-stationary behavior associated with an actual earthquake. The second approach is based on using a recorded strong motion record that is modified to match a specified spectrum. If the modifications are achieved by adding non-stationary wavelets, the resultant strong motion time history preserves the non-stationary content of the original strong motion record.

A good example of the test strong motion developed by means of the first approach is a signal developed and used at the Construction Engineering Research Laboratory (CERL) to conduct seismic qualification testing (see Westcoast Subcommittee's website: <http://www.westcoastsubcommittee.com/ieee693/qualified.php>). It is designed for use in three-dimensional testing and has a spectrum compatible with the IEEE spectrum. (IEEE, 1998).

In recent years the equipment qualification tests conducted by PEER used the IEEE 693 spectrum-compatible strong motion time histories based on a record from the Tabas, Iran, earthquake (Gilani, et al. 2000; Gilani, et al., 1998). The original record was modified using a non-stationary response spectrum matching technique developed by Abrahamson (Abrahamson 1996). In this time domain matching algorithm, short duration wavelets are added to the original earthquake history at optimal times to match the spectral amplitude at each frequency to the target value. The test signals consisted of two test histories selected for the low- and high-frequency ranges, respectively. In order to qualify the equipment, it had to be tested twice. The disadvantage of this approach is that the equipment should perform adequately during two test runs for low and high frequencies, which can cause overtesting of the equipment.

The IEEE-compatible strong motion time histories vary from one test laboratory to another. The commercial laboratories tend to not release the strong motion time histories used at their facilities; therefore limited literature is available on these test records and their properties. This was an important reason to develop a time history that would be suitable for any test facility and thereby have test results that could be compared between laboratories in order to achieve a consistency in experimental qualification studies. In addition, there was an increased necessity of assuring that the input motions satisfy applicable requirements. The study represents an attempt to specify the limitations and tolerance zones (between test response spectra and RRS) for the test strong motion, and to avoid overtesting and undertesting of electrical equipment during qualification testing.

1.3 DELIVERABLES

The main objective of the study was achieved and a three-component set of earthquake ground motion time histories suitable for seismic qualification of electrical substation equipment in accordance with the IEEE 693-1997 standard (IEEE, 1998) was developed. The strong motion time histories in three principal directions of testing are available for download from the Westcoast Subcommittee's website: <http://www.westcoastsubcommittee.com/ieee693/qualified.php>.

Along with the set of strong motion time histories, the study provides specifications for a spectral matching procedure and extended requirements for the IEEE-compatible time history. The recommendations on the requirements for the test response spectrum (TRS) are also provided. The specifications and requirements are summarized in "Specification for Input Motion Used in Earthquake Simulator Testing under IEEE 693" in Appendix D of this report and are available on the PEER website: http://peer.berkeley.edu/lifelines/Task408_411/Task408.html.

Matlab (The MathWorks, 2001) codes developed in the study form another set of the deliverables. The set consists of implementations of the filtering procedure and of the high cycle counting procedure in single-degree-of-freedom system response. The codes are also available at: http://peer.berkeley.edu/lifelines/Task408_411/Task408.html.

1.4 REPORT ORGANIZATION

In Chapter 2 the design and required response spectra specified in various codes and regulations are presented and compared with the required response spectra specified in IEEE 693-1997 (IEEE, 1998). The requirements for qualification testing that include the acceptance criteria, the time history for the earthquake simulator, and the tolerance between TRS and RRS are also discussed.

Chapter 3 presents the study of 35 strong motion time histories recorded during 18 earthquakes in the U.S. and abroad. Based on a number of parameters, the best candidate for further modification in the spectral matching procedure was selected from the records.

Chapter 4 discusses the advantages and disadvantages of the time domain and frequency domain procedures that are generally used for development of a response-spectrum-compatible strong motion time history. Due to a number of advantages outlined in the discussion, the time domain procedure was selected as a spectrum matching procedure to develop the IEEE response-spectrum-compatible time history from the Landers (Joshua Tree) record.

Chapter 5 presents information on existing and future earthquake simulators in the U.S. A filtering procedure needed to modify the IEEE-compatible time history and to accommodate limitations of the simulators is also discussed. Two versions of an input time history for the EERC simulator filtered from the IEEE-compatible Landers (TestQke4IEEE) are presented. The chapter presents characteristics of the IEEE-compatible Landers time history (TestQke4IEEE) compared to other input time histories for earthquake simulators used in qualification testing of electrical substation equipment.

Chapter 6 presents recommended requirements for a strong motion time history intended for use in qualification testing of electrical substation equipment by means of an earthquake simulator. Although the study provides the recommended strong motion time history, a user has the option of creating a user-specific input signal that would comply with the requirements.

All major achievements and recommendations on a generating procedure of the test time history and on the seismic qualification procedure itself are summarized in Chapter 7.

Appendix A presents definitions and discussions of parameters and indices used to characterize the strong motion records. The parameters and the indices are used to describe the severity of the earthquake records and are divided into two groups. The first group consists of parameters obtained directly from the recorded strong motion data, and the second consists of parameters and indices obtained by computing the response of a single-degree-of-freedom (SDOF) system to a strong motion record and by manipulating the system response.

Appendix B presents information on fracture mechanics that addresses the necessity of cycle counting and details of the cycle counting procedure used in the study.

A discussion of earthquakes that have occurred in eastern North America (ENA: the eastern U.S. and the southeastern Canada) and in central North America (CNA: the central U.S.) is presented in Appendix C. The discussion is based on analysis of five strong motion records and the comparison of IBC-2000 design spectra for these regions with the IEEE spectra.

The recommended specifications and requirements for qualification testing of electrical equipment are summarized in “Specification for Input Motion Used in Earthquake Simulator Testing under IEEE 693,” presented in Appendix D.

2 Study of Design and Required Response Spectra Compared to IEEE Spectra

In this chapter the design and required response spectra specified in various codes and regulations are presented and compared with the required response spectra specified in IEEE 693-1997 (IEEE, 1998). The requirements for qualification testing that include the acceptance criteria, the time history for the earthquake simulator, and the tolerance between TRS and RRS are also discussed.

2.1 REQUIRED RESPONSE SPECTRA FOR SEISMIC QUALIFICATION TESTING OF ELECTRICAL SUBSTATION EQUIPMENT (IEEE 693)

The IEEE spectrum originates from research conducted by Newmark in the 1960s and 1970s for the U.S. Nuclear Regulatory Commission (NRC) (Newmark, 1973) and uses a median spectrum (with 50% probability of not being exceeded) for a large number of historic acceleration records. The IEEE 693-1997 spectrum is not site specific and presents a broadband response spectrum that envelops the effects of earthquakes in different areas considering site conditions ranging from rock to soft soil. However, as noted in the standard, the spectrum may not adequately cover sites with very soft soils. Design of buildings and bridges is usually based on using site-specific spectra because the structures are built at a particular location. In contrast with buildings and bridges, electrical equipment of the same design may be used at any location and, as such, it is not practical to use site-specific spectrum for qualification. A new version of the IEEE 693 (IEEE, 2004) standard is currently being developed that uses the same response spectra as its predecessor. This chapter presents a comparison between the IEEE spectra and other response spectra recommended by various codes and regulatory documents.

The IEEE 693-1997 (IEEE, 1998) was developed as a recommended practice for the seismic design and qualification of substation electrical equipment. To streamline the

qualification process, IEEE 693 provides discrete levels of qualification (high, moderate, and low). For a given level of qualification, the standard defines the required response spectrum (RRS), and the performance level (PL) spectrum (the low RRS does not have the corresponding PL), the former of which is 50% of the latter. Equipment qualified to the standard's RRS must remain functional and sustain no structural damage. Based upon the acceptance criteria, qualified equipment is expected to perform acceptably up to the PL spectral loading, although minor structural damage may occur. For highly active seismic regions, the IEEE 693 standard anchors the RRS to 0.5g peak ground acceleration (PGA), and the PL spectrum to 1.0g PGA.

The selection procedure for the appropriate IEEE seismic qualification level (high, moderate, or low) for a site consists of a series of steps. According to the latest draft of the IEEE 693 standard (IEEE, 2004), the procedure can be performed by using the IBC-2000 ground motion maps (ICC, 2000). Using the appropriate IBC-2000 map for a maximum considered earthquake (MCE) ground motion, the 0.2 sec spectral response acceleration is determined for the site. Depending on the soil properties of the site, the value has to be multiplied by a factor presented in Table 1615.1.2(1) (ICC, 2000). Finally the soil-corrected 0.2 sec spectral response acceleration is divided by 2.5 to estimate the peak ground acceleration presented in fractions of g. If the value is less than or equal to 0.1g, the low qualification level should be used. If the peak ground acceleration is greater than 0.1g but less than or equal to 0.5g, the moderate qualification level should be used. If the value is greater than 0.5g, the high qualification level should be used. The study focuses on sites with high seismic activities where the peak ground acceleration is greater than or equal to 0.5g.

The design response spectra described in building codes are intended to specify earthquake loading on a building or a structure for life-safety performance. In such an event, the building would be expected to yield (sometimes significantly) but maintain a substantial margin against collapse. The IEEE approach for seismic qualification testing of electrical equipment is very different. The standard specifies two options: seismic testing at the RRS level and the PL testing. The stresses in critical components of tested electrical equipment under the IEEE RRS strong motion should remain within allowable stresses. Another option is PL testing when the electrical equipment must withstand the impact of the strong motion time history with some possible minor damage but with the equipment able to perform its major functions. Therefore all discussion related to the required response spectra is focused on the two levels of testing and the corresponding spectra for RRS and PL.

Due to the low damping associated with electrical equipment, the IEEE 693 specifies required response spectra at 2% damping. Most codes specify design response spectra for 5% damping, therefore this damping value was used for comparing the spectra of the various codes. The IEEE high PL spectrum at 5% damping, as a relationship between spectral acceleration, S_a , and frequency, f , has the following form (IEEE, 1998):

$$S_a = \begin{cases} 0.92f & 0 < f < 1.1 \text{ Hz}, \\ 2.50 & 1.1 \text{ Hz} \leq f \leq 8.0 \text{ Hz}, \\ 6.34/f + 0.21 & 8.0 \text{ Hz} < f \leq 33.0 \text{ Hz}. \end{cases} \quad (2.1)$$

The IEEE spectrum has a plateau with constant spectral acceleration that covers frequency from 1.1–8.0 Hz. The spectral acceleration linearly (relative to the frequency) increases up to the plateau value at 1.1 Hz, and decreases after 8.0 Hz with an inverse relationship between the spectral acceleration and the frequency.

2.2 DESIGN RESPONSE SPECTRA FROM BUILDING CODES AND RELATED DOCUMENTS

2.2.1 International Building Code 2000

The International Building Code 2000 (ICC, 2000) specifies a design response spectrum that depends on the location of a site relative to the source of a possible earthquake and the soil property of the site. The maximum considered earthquake (MCE) spectral response acceleration at a short period (0.2 sec), S_s , and at a 1 sec period, S_l , are the key parameters in the determination of the response spectra. These parameters can be obtained from provided contour maps. The design spectral accelerations are at two thirds of those for the MCE.

Based on S_s and S_l , and site amplification factors F_a and F_v , tabulated and presented separately for both S_s and S_l , the design spectral accelerations are computed and the response spectra is specified. The spectral acceleration can be expressed in a form similar to Eq. (2.1) (ICC, 2000):

$$S_a = S_{DS} \begin{cases} (5 T_0) f & 0 < f < 1/(5 T_0), \\ 1.0 & 1/(5 T_0) \leq f \leq 1/T_0, \\ (0.6/T_0)/f + 0.4 & 1/T_0 < f. \end{cases} \quad (2.2)$$

Where S_{DS} and T_0 are parameters that depend on S_s , S_l , F_a , and F_v .

The IBC-2000 and the IEEE spectra have similar shapes and consist of a plateau with constant spectral acceleration, a linear ramp-up in low frequency, and a hyperbolic ramp-down in high frequencies. The plateau of the IEEE spectrum has a fixed range from 1.1–8.0 Hz, whereas the IBC-2000's plateau end frequency is five times greater than the plateau's start frequency, and these frequencies strongly depend on the site conditions.

Figure 2.1 presents these response spectra for various soil types, epicentral distances from the strong motion source, and types of the source. As an example, sites in the Bay Area are considered and the IBC-2000 spectral acceleration parameters are obtained from the corresponding map. The top plot in Figure 2.1 presents the IBC-2000 design spectra for various soil types and mapped spectral accelerations: $S_s = 2.0$ and for $S_I = 1.5$ (5 km from possible strong motion source). All the IBC-2000 design spectra are presented for 5% damping and are based on mapped spectral accelerations for an earthquake with a 2% probability of exceedance in 50 years (those correspond to a probabilistic MCE; to simplify the analysis the deterministic limit on the probabilistic MCE was ignored throughout the study). The IEEE spectra represent high qualification level spectra for 5% damping and 0.5g PGA for the RRS and 1.0g PGA for the PL. In this case only the spectrum for hard rock (type A) is enveloped by the IEEE RRS.

The middle plot in Figure 2.1 shows the IBC-2000 spectra for $S_s = 1.75$ and for $S_I = 1.0$ obtained for a site located at about 7 km from the source. The plateau of each spectrum is completely enveloped by the IEEE RRS, although at high frequencies the IBC-2000 spectra (for soil types B — rock, C — very dense soil and soft rock, and D — stiff soil) are slightly higher than the IEEE spectrum. The bottom plot in Figure 2.1 presents the IBC-2000 spectra with no near-fault factors with $S_s = 1.5$ and for $S_I = 0.6$. The IEEE RRS completely envelops the low-frequency range for all soil types and slightly underestimates structural response for soil type B for frequencies greater than 10 Hz.

Although the IBC-2000 spectra are close to the IEEE RRS, with some dependence on the location of the site relative to the fault, the IEEE PL spectrum anchored at 1.0g PGA completely envelops all the IBC-2000 spectra. For instance, if $S_s = 2.56$ (the maximum value of the parameter for the western U.S.), the IBC-2000 spectral plateau is 1.37 times greater than that for the IEEE RRS anchored at 0.5g. Nevertheless, the IBC-2000 spectral acceleration at the plateau is still less than that for the IEEE high performance level (twice higher than the IEEE RRS).

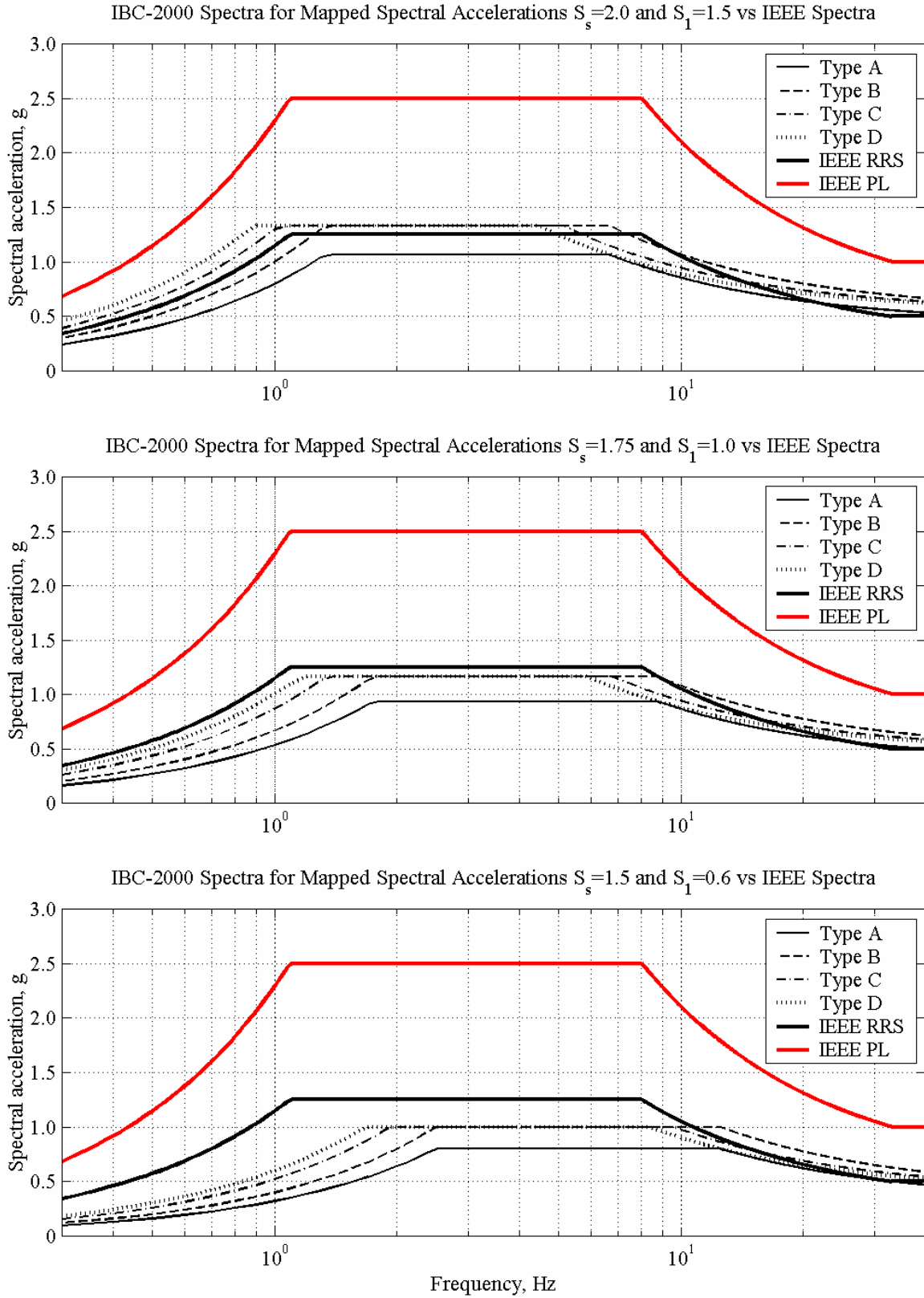


Fig. 2.1 IBC-2000 design spectra for various S_s and S_1 vs. IEEE high PL and high RRS

One of the least conservative acceptance criteria for qualification of electrical equipment is the PL testing: the equipment has to withstand the performance level testing with some acceptable minor damage but with no collapse and the major functionality of the equipment preserved. In contrast with this acceptance criterion, the IBC-2000 approach intends to prevent building collapse with some margin; the building can be damaged and sometimes significantly.

It is worth noting that the general procedure for generating design response spectra proposed in the NEHRP (BSSC, 1997) and ASCE provisions (ASCE, 2000) is similar to that adopted in IBC-2000.

In summary, the IEEE spectrum has a broad range of frequencies with constant spectral acceleration representing a plateau of the spectrum that can be broader than the corresponding range of the IBC-2000 spectra. The IEEE RRS envelops the IBC-2000 spectra for a site 7–10 km from a source of a possible earthquake where the near-fault effects are not significant. For a distance on the order of 10 km, a small difference exists for the soil type B site and for frequencies greater than about 10 Hz, when the plateau of the IBC-2000 spectra is not enveloped by the IEEE RRS. The IEEE PL spectrum envelops the IBC-2000 design response spectra for all types of soils, while the IEEE RRS is close to the latter. In general, the IEEE test spectra are greater than those of the IBC-2000.

2.2.2 Uniform Building Code 1997 (UBC-1997)

UBC-1997 (ICBO, 1997) uses a design response spectrum that depends on the soil properties of a site and the site's location relative to a source of a possible earthquake. The effect of site proximity to active seismic sources are accounted for by near-source factors, which depend on the type of seismic source.

The definition of the UBC design response spectra is the same as that of the IBC-2000 except for parameters, and has the following form (ICBO, 1997):

$$S_a = 2.5 C_a \begin{cases} (5 T_0) f & 0 < f < 1/(5 T_0), \\ 1.0 & 1/(5 T_0) \leq f \leq 1/T_0, \\ (0.6/T_0)f + 0.4 & 1/T_0 < f. \end{cases} \quad (2.3)$$

where C_a and T_0 are the UBC-1997 parameters representing site location and soil conditions.

Figure 2.2 presents the UBC-1997 design response spectra for sites located in seismic Zone 4 for various distances from a seismic source A. The UBC response spectra are plotted for various soil conditions (soil type definition adapted in the UBC-1997 code is identical to that in IBC-2000) at the site and 5% damping. The IEEE spectra are plotted for 5% damping for a high qualification level anchored at 0.5g PGA (RRS) and for high PL anchored at 1.0g. The IEEE RRS does not envelop any of the UBC-1997 spectra for locations within 2 km from a source, as shown in the top plot of Figure 2.2. When the distance from the source is 2–5 km, the UBC-1997 spectra and the IEEE RRS are similar, as shown in the middle plot of Figure 2.2. In this case the IEEE RRS envelops two spectra for soil types A and C. For distances greater than 10 km from the source, the IEEE RRS envelops all the UBC-1997 spectra, as shown in the bottom plot of Figure 2.2.

Figure 2.3 presents the UBC-1997 design spectra for sites located in seismic Zone 4 for various distances from a seismic source B. The top plot shows spectra at less than 2 km from the source, the middle plot presents the spectra at 5 km, and the bottom plot shows the spectra at 10 km or more from the source. Similar to seismic source A, the IEEE RRS does not envelop the UBC-1997 spectra for locations close to the source (less than 2 km) except in cases of soil type A. The middle plot shows that the IEEE RRS envelops all the UBC-1997 spectra in a wide range of frequencies for sites at 5 km from the possible source. The situation slightly changes for distances more than or equal to 10 km, shown in the bottom plot of Figure 2.3. The UBC-1997 design spectrum for soil type B shifts toward high frequencies, and the IEEE RRS does not envelop the spectrum from about 10.5 Hz. The IEEE RRS envelops the UBC-1997 spectra for all other soil types.

The UBC-1997 spectra for seismic source type C are presented in Figure 2.4. The top plot shows that the IEEE RRS envelops the UBC-1997 spectra for all soil types except for soil type B. This comparison is the same for other distances from a source (middle and bottom plots of Fig. 2.4).

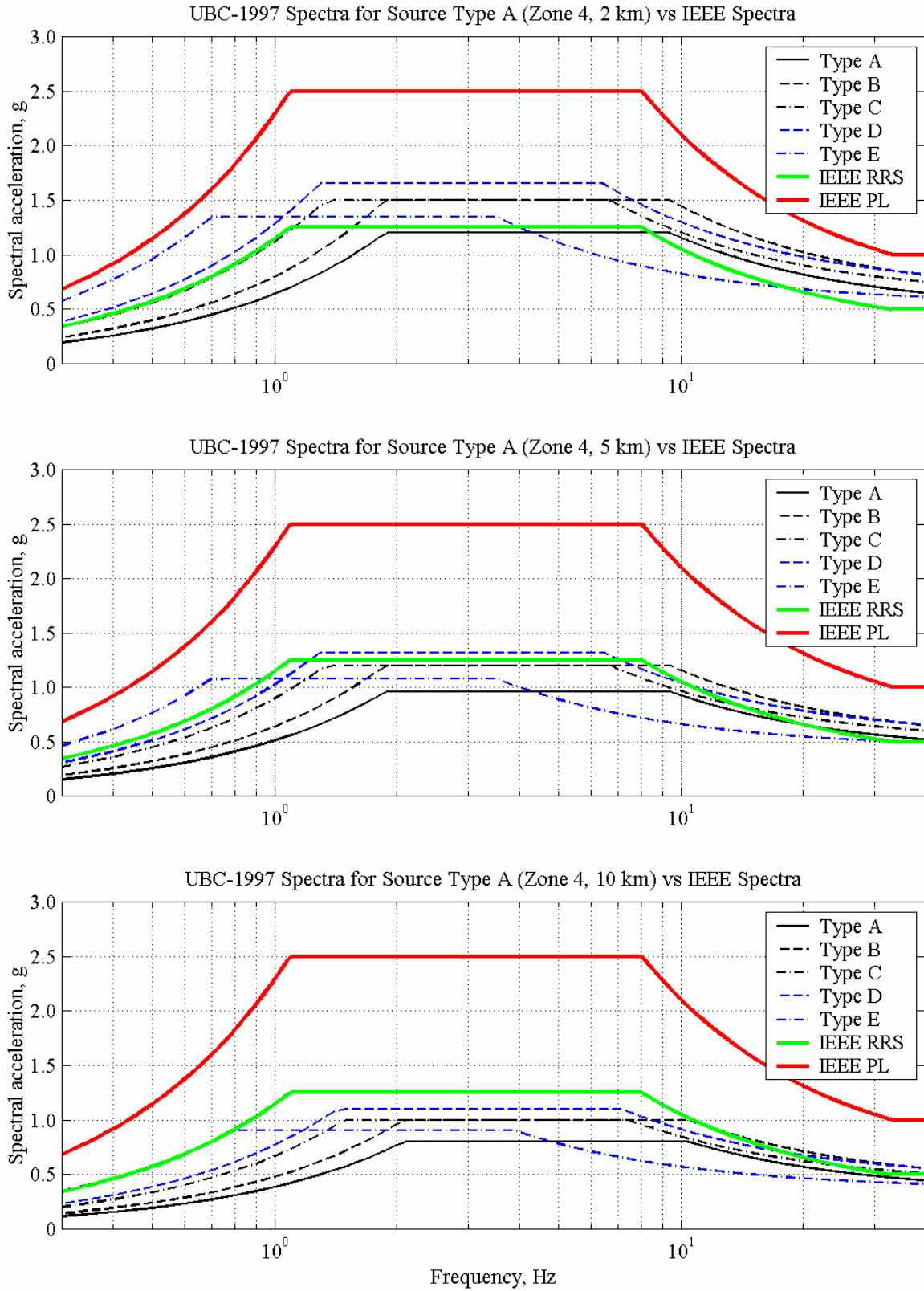


Fig. 2.2 UBC-1997 design spectra for source type A vs. IEEE high PL and high RRS

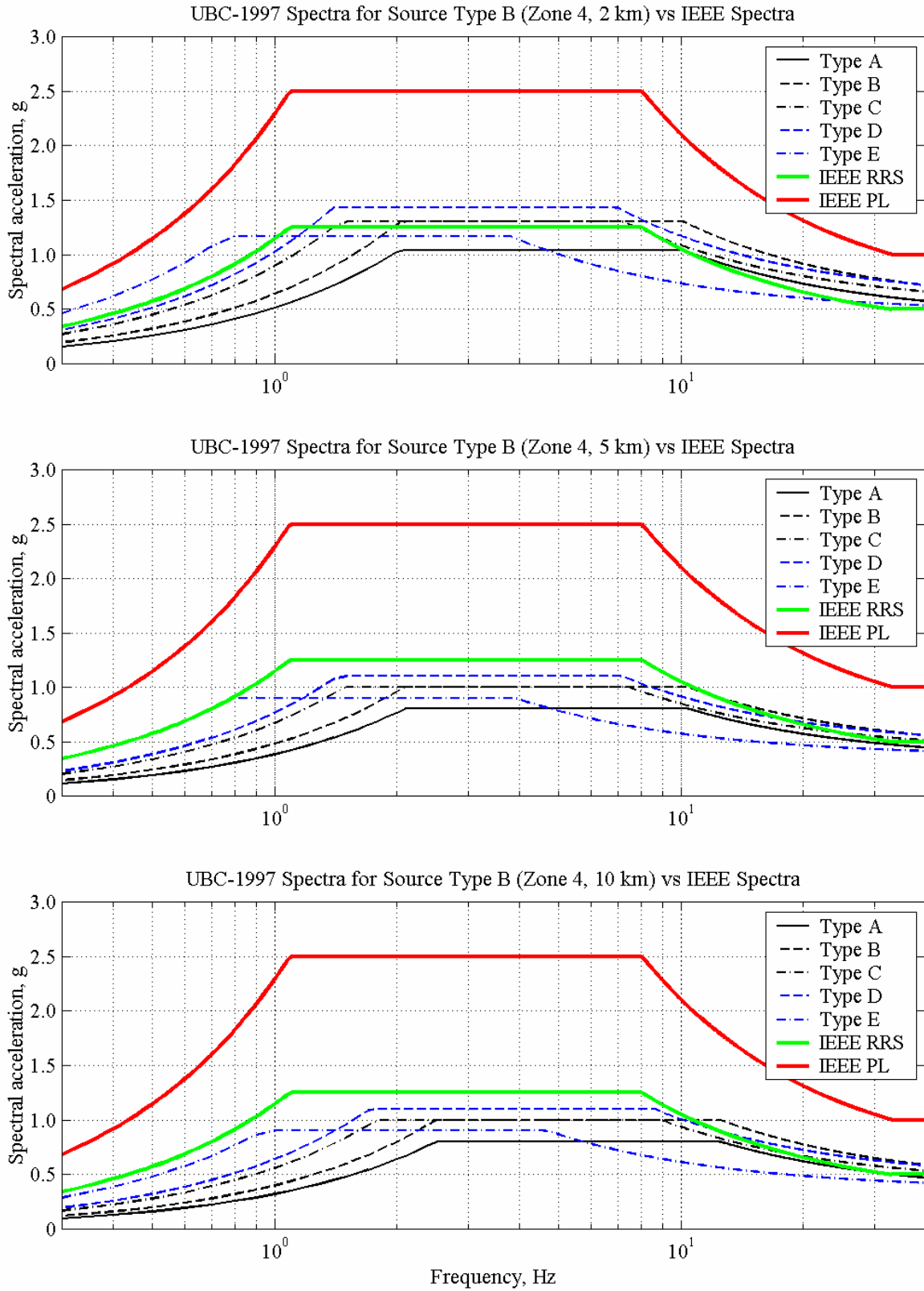


Fig. 2.3 UBC-1997 design spectra for source type B vs. IEEE high PL and high RRS

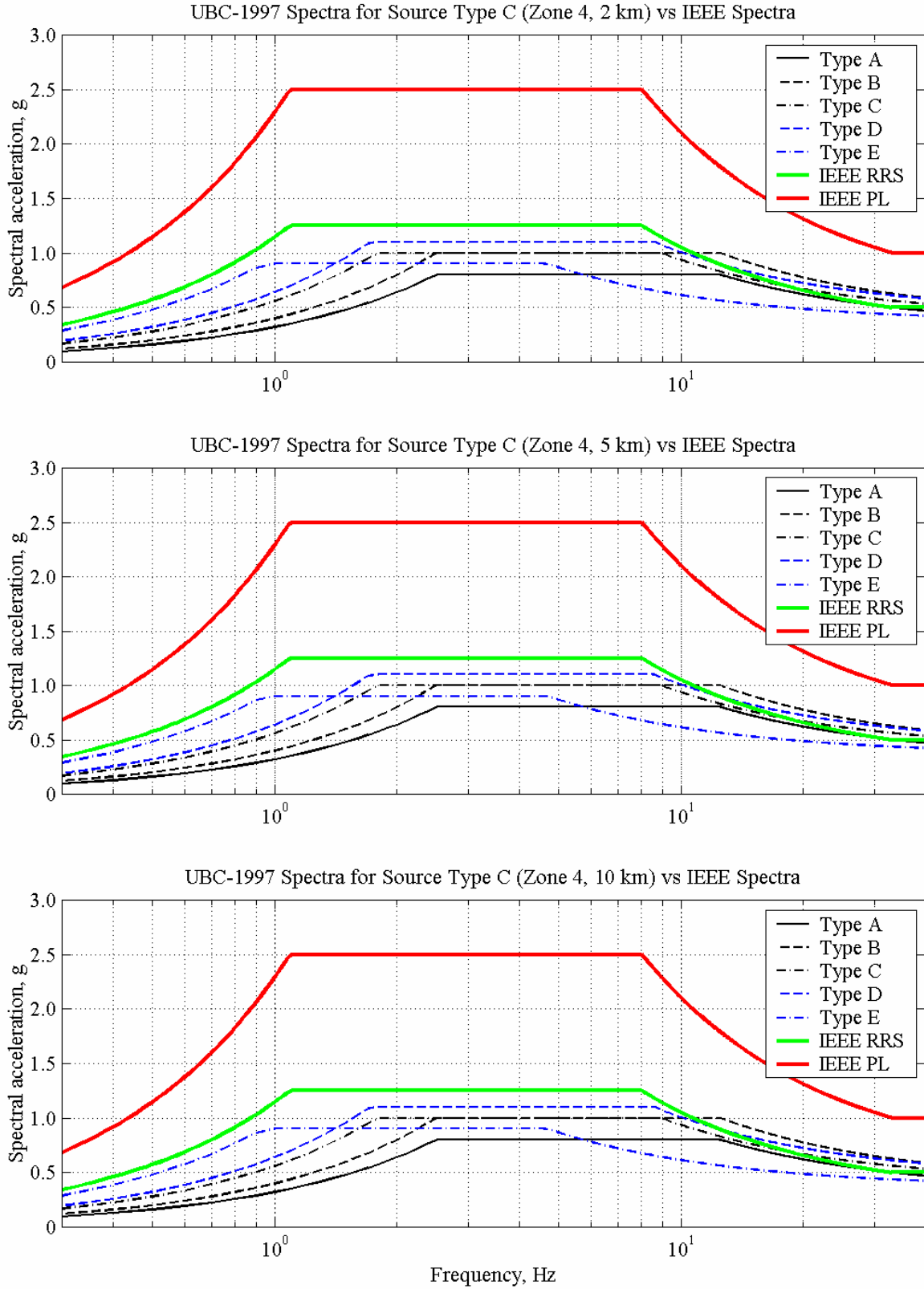


Fig. 2.4 UBC-1997 design spectra for source type C vs. IEEE high PL and high RRS

The plateau spectral acceleration of the UBC spectra can be as large as 1.32 times greater than the plateau value for the IEEE RRS but less than the plateau spectral acceleration for the IEEE PL spectrum. Table 2-1 shows the percentage of the UBC plateau value relative to the corresponding one of the IEEE RRS. The cases of when the UBC plateau value exceeds the IEEE RRS plateau value are presented in bold.

The UBC-1997 design approach is similar to that of the IBC-2000 and intends to prevent building collapse with some margin. In contrast with the IBC-2000, the UBC-1997 is based on a design earthquake that has 10% exceedance in 50 years. The acceptance criterion for electrical equipment during qualification is different: equipment has to withstand the performance level of testing with some acceptable minor damage, but with no collapse and the major functionality of the equipment preserved.

Table 2.1 Percent ratio of the UBC-1997 plateau value to the IEEE RRS plateau

Soil type	Source type	Closest distance to known seismic source		
		<= 2km	5 km	>= 10 km
S_a	A	96%	77%	64%
	B	83%	64%	64%
	C	64%	64%	64%
S_b	A	120%	96%	80%
	B	104%	80%	80%
	C	80%	80%	80%
S_c	A	120%	96%	80%
	B	104%	80%	80%
	C	80%	80%	80%
S_d	A	132%	106%	88%
	B	114%	88%	88%
	C	88%	88%	88%
S_e	A	108%	86%	72%
	B	94%	72%	72%
	C	72%	72%	72%

In summary, the IEEE RRS does not envelop the UBC-1997 response spectra for sites located very close to a source in seismic Zone 4. As the distance from the source increases, the IEEE RRS envelops the UBC-1997 spectra for most cases. The IEEE PL spectrum envelops the UBC-1997 design response spectra for all types of soils, while the IEEE RRS is close to the

UBC-1997 design spectra. Overall, the IEEE test spectra represent more conservative design approach than that of UBC-1997.

2.2.3 Regulatory Guide 1.60

Regulatory Guide 1.60 (referred to below as “RG-1.60”) of the U.S. Atomic Energy Commission (USAEC) was published in 1973 (USASC, 1973) and established a design response spectra for the seismic design of nuclear power plants. At the time, it was based on the results of Newmark’s research (Newmark, 1973). The normalized design response spectra in this guide correspond to a maximum horizontal ground acceleration of 1.0g. The maximum ground displacement is taken as proportional to the maximum ground acceleration, and is set at 36 in. (0.91 m) for a peak ground acceleration (PGA) of 1.0g. The spectral shapes are the same for all sites and earthquake sources and depend only on maximum ground acceleration (assuming that the value of maximum ground acceleration includes the effects of all other parameters) and the damping of the structure. Although the spectra were applicable for use at any sites including soft soils, the guide calls for cautious use of the spectra for sites with very soft soils. The design response spectrum has two levels that represent the safe shutdown earthquake (SSE) and the operating basis earthquake (OBE). The latter is usually taken as one half of the former. From a performance point of view, it is worthy to note that safety systems in nuclear power plants are expected to remain functional after a SSE.

More recent work by the U.S. NRC (USNRC, 1996) to assess the probability of the SSE that would quantify the annual probability of the SSE and would estimate PGA of the SSE have led to the following results. The target annual probability of exceedance for the SSE is estimated as 1E-05, or 0.05% in 50 years versus 2% for the MCE (or more than 2% if deterministic limits are applied), so the SSE is much larger than the MCE. It should be noted that some approved SSEs for a number of existing nuclear plants probably do not meet the 0.05% in 50 years criterion.

Figure 2.5 compares the IEEE high PL spectrum and the RG-1.60 spectrum at 5% damping and is plotted for 1.0g PGA. The IEEE spectrum is greater than the RG-1.60 spectrum in the low-frequency range, but has a lower peak of spectral acceleration. The peak spectral acceleration in the RG-1.60 spectrum anchored at 1.0g is 3.14g, whereas the spectral acceleration in the IEEE PL spectrum is limited by 2.5g at 5% damping. Frequency points marking the end of

ramp-up and the start of the ramp-down in the RG-1.60 spectrum are also different from that in the IEEE PL spectrum. Namely, a zone of high spectral acceleration in the RG-1.60 spectrum is from 2.5–9.0 Hz, whereas the plateau of the IEEE spectrum runs from 1.1–8.0 Hz.

Taking into account the definition of the SSE and its extremely low annual probability of exceedance, the RG-1.60 response spectrum represents a much more conservative design approach than the IEEE PL spectrum.

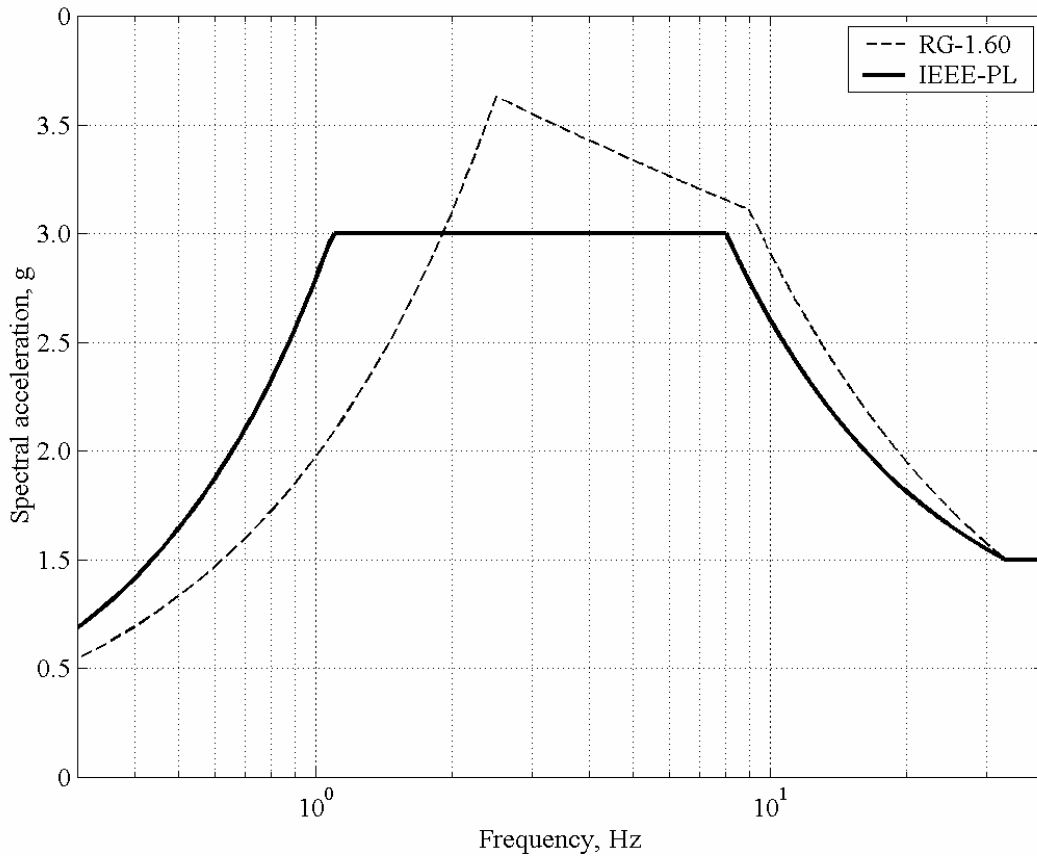


Fig. 2.5 USASC (USNGC) Regulatory Guide 1.60 spectrum vs. high IEEE PL spectrum for 5% damping

2.3 REQUIRED RESPONSE SPECTRA FOR NONSTRUCTURAL COMPONENT OR EQUIPMENT TESTING

2.3.1 NEBS Requirements for Telecommunication Equipment (GR-63-CORE)

GR-63-CORE (Telcordia Technologies, 2002) has requirements for the physical protection of Network Equipment-Building Systems (NEBS) that include protection from earthquakes. It identifies the minimum criteria for all new telecommunication equipment systems used in telecommunication networks. The requirements specified in GR-63-CORE and required response spectra are exactly the same as those for the similar European Standard (ETSI, 2003). The GR-63-CORE document (Telcordia Technologies, 2002) is referred to below as “GR-63.”

The required response spectrum is calculated for 2% damping and is site independent, with three levels of seismic testing severity. A region where the testing equipment is designated for installation shall be associated with an earthquake risk zone that varies from 1–4. For example, equipment designated for installation in Zone 4 is tested at the highest acceleration level. The RRS is the same for Zones 1 and 2 that represent the lowest level of seismic testing. The moderate level of seismic qualification testing is associated with Zone 3. The earthquake risk zone for an installation is determined from a zoning map in the document. In contrast to the IEEE RRS, the plots of the GR-63 RRS have different shapes for various zones.

The amplification factor due to elevated mounting of the equipment is included in the RRS. For other elevations the RRS can be reduced by some factors, but this is rarely done in equipment testing, since most equipment is designed for all locations of the building.

Figure 2.6 presents the GR-63 RRS compared with the high RRS (anchored at 0.5g) and high PL (anchored at 1.0g). The IEEE 693-1997 high PL response spectrum envelops all the GR-63 required response spectra except that for Zone 4 anchored at 1.6g PGA. The Zone 4 anchor is greater than that for the IEEE high PL spectrum, because the GR-63 RRS includes an amplification factor reflecting elevated mounting of the telecommunication equipment.

The GR-63 document (Telcordia Technologies, 2002) requires acceptance criteria for qualification testing. The major requirement is that a network of multiple units of telecommunication equipment should maintain integrity during and after an earthquake. Therefore equipment should be fully operational with no major structural damage and with no

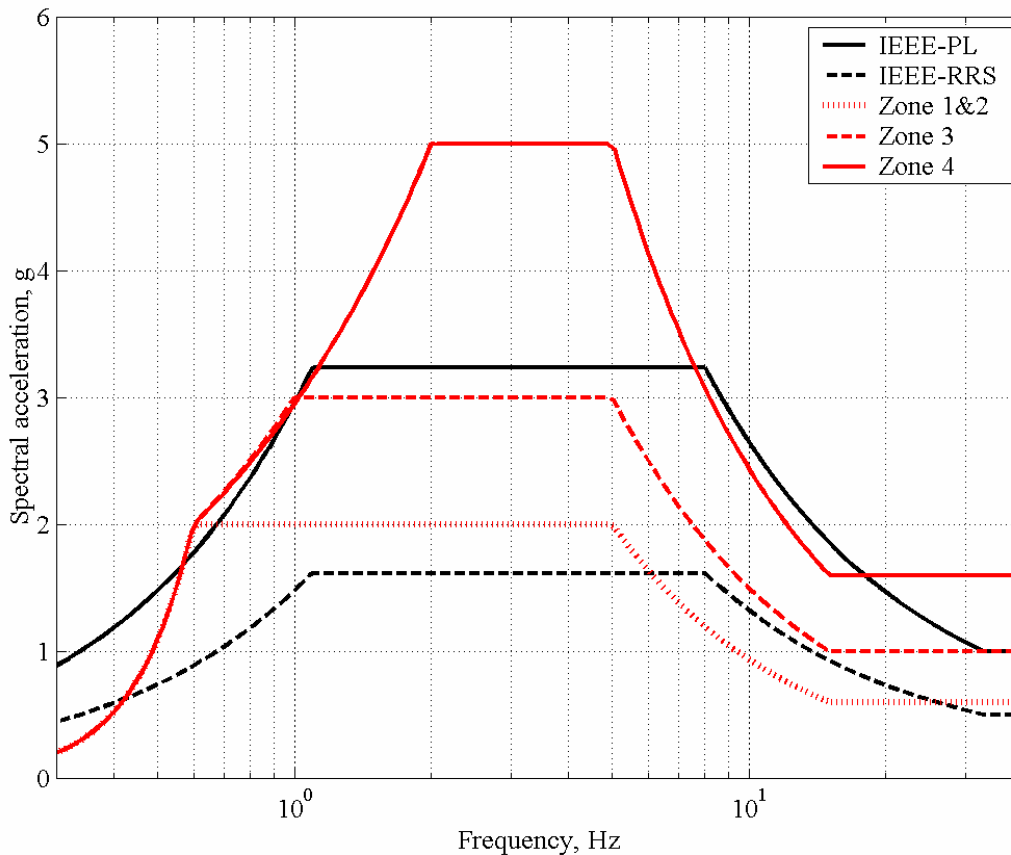


Fig. 2.6 GR-63 RRS for various zones vs. high IEEE RRS and high IEEE PL for 2% damping

impact on other network systems. These acceptance criteria is quite close to those of IEEE 693 (IEEE, 1998).

In summary, the IEEE spectrum at high PL envelops all GR-63 required response spectra except that for Zone 4, but the GR-63 spectra include the amplification factor due to elevated mounting of equipment. Since the GR-63 input motion is intended to account for telecommunications equipment located high in a building, it cannot be easily compared with IEEE 693. However, since amplification factors at the upper levels of buildings may be several times higher than ground spectra, the IEEE 693 PL spectra appear to match or exceed the GR-63 spectra.

The GR-63 standard (Telcordia, 2002) also specifies requirements for input time history and provides a recommended strong motion time history test called “VERTEQII” that complies with all these requirements. The input signal for an earthquake simulator can be selected from the recommended one or can be replaced with another that satisfies the same requirements.

According to GR-63, during the dynamic tests the TRS shall meet or exceed the RRS in the frequency range of 1.0–50 Hz; in other words, the TRS shall envelop the RRS in this frequency range. The TRS is determined using a damping level of 2%. The reproduction of the prescribed strong motion shall be verified against the RRS by analyzing the TRS at one-sixth-octave frequencies from 0.5–50 Hz. The total number of frequency points at this resolution is 41, with only 18 points in the frequency range from 1.0–7.0 Hz.

GR-63 establishes the upper bound for the TRS variation as follows: the TRS should not exceed the RRS by more than 30% in the frequency range from 1.0–7.0 Hz. A test may be invalid if an equipment failure occurs when the TRS exceeds the RRS by more than 30% in this frequency range. The requirements are presented in Figure 2.7. The TRS based on the prescribed VERTEQII input time history approximately fits in the 30% tolerance zone above the RRS at the one-sixth-octave resolution. An increase in the frequency resolution to one-twelfth octave shows significant mismatch with the 30% tolerance zone above the RRS (Fig. 2.8). There is at least one dip below the RRS at any test level, and the highest peak for Zone 4 testing is about 80% higher than the RRS.

Such a significant difference between the TRS and the RRS for higher frequency resolution can be avoided in the requirements for qualification testing of electrical equipment achieved in the study and presented in Chapter 6.

2.3.2 ICBO ES Criteria for Seismic Qualification Testing of Nonstructural Components (AC156)

The International Conference of Building Officials Evaluation Service, Inc. (ICBO ES) publishes acceptance criteria and requirements for seismic qualification testing of nonstructural components that is usually referred to as “AC156” (ICBO ES, 2000). The criteria are intended to provide guidelines on implementing performance features for nonstructural components consistent with the UBC-1997, IBC-2000, and other related documents.

The required response spectrum is presented in a normalized form for 5% damping using the expressions similar to those for IBC-2000 and UBC-1997 with slightly different parameters (ICBO ES, 2000):

$$S_a = A_{FLX} \begin{cases} f/(1.3)^{0.90} & 0.1 < f < 1.3 \text{ Hz,} \\ 1.0 & 1.3 \text{ Hz} \leq f \leq 8.3 \text{ Hz,} \\ (8.3/f)^{0.67} & 8.3 \text{ Hz} \leq f \leq 33.3 \text{ Hz} \end{cases} \quad (2.4)$$

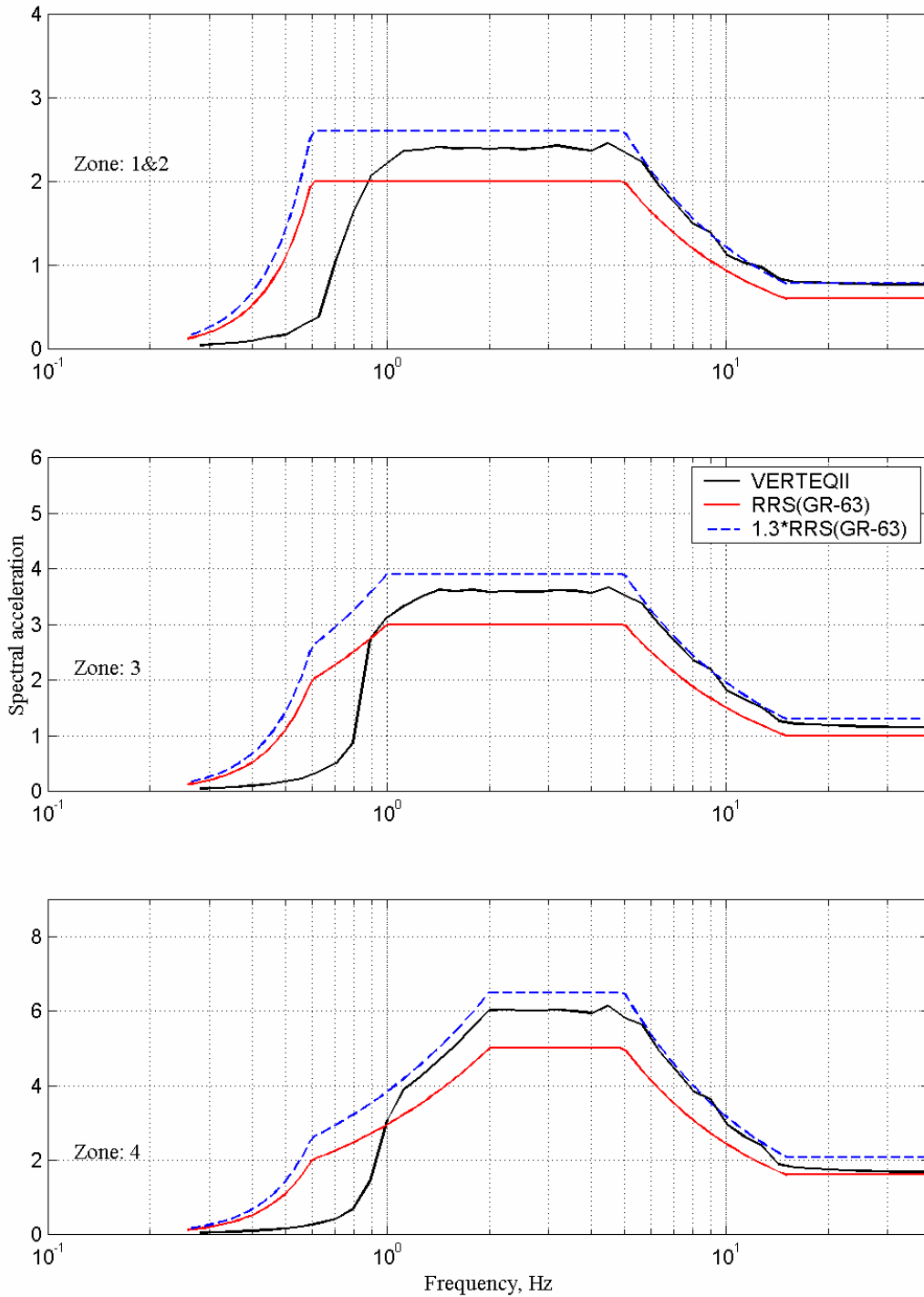


Fig. 2.7 TRS (based on VERTEQII) vs. 30% tolerance zone above RRS at 1/6 octave

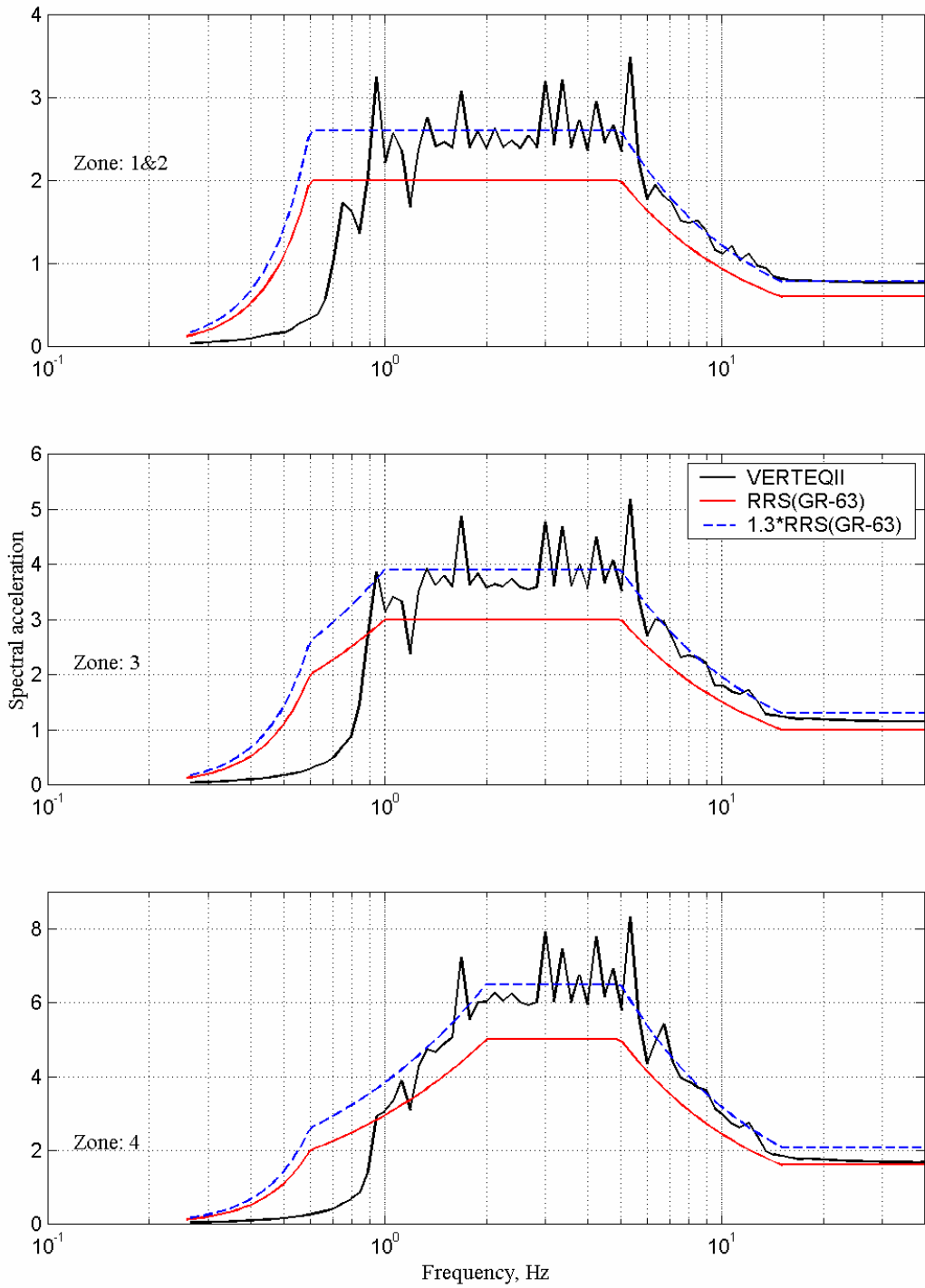


Fig. 2.8 TRS (based on VERTEQII) vs. 30% tolerance zone above RRS at 1/12 octave

in which A_{FLX} is a parameter reflecting the demands of the particular code.

For equipment attached at grade level A_{FLX} is:

$$A_{FLX} = 2.5 C_a \text{ for IBC-2000 code or } A_{FLX} = S_{DS} \text{ for UBC-1997} \quad (2.5)$$

Therefore in this case the plateau start and end frequencies are fixed and equal to 1.3–8.3 Hz, so its width is almost the same as the IEEE spectrum plateau. In log-log scale the ramp-up and the ramp-down are linear. Spectral acceleration at 33.3 Hz is 2.5 times less and spectral acceleration at 0.1 Hz is 10 times less than that at the spectral plateau. An amplification factor due to elevated mounting is limited to a maximum value of 1.6.

Figure 2.9 compares the IEEE 693 and the AC156 spectra for various soil types (the site coefficients, F_a , are the same for soil types B, C, and D; therefore the spectrum plots for these soil types are identical and only the spectrum for soil B is plotted as a representative). The AC156 spectra are obtained for the same values of mapped spectral accelerations, namely, $S_s = 2.14$ and $S_I = 1.59$, respectively (San Francisco, California). The IEEE high seismic performance level response spectrum envelops the AC156 required response spectra for all soil types as shown in the last figure. Also shown is that the IEEE RRS better covers the low-frequency range than does the AC156 spectrum and that the spectra are similar at high frequencies.

As discussed previously, there are sites where the plateau value of the IEEE RRS is less than the corresponding one from IBC-2000 or UBC-1997. The limits of the IEEE RRS in the AC156 criteria formulation are the same, as presented earlier for the IBC-2000 code and in discussion related to the UBC-1997. Although the AC156 spectra can be in the vicinity of the IEEE RRS anchored at 0.5g PGA, the IEEE high PL spectrum envelops the AC156 spectra for all site conditions and locations.

The acceptance criterion for qualification testing as specified in the AC156 document is similar to that of the IEEE 693-1997 and requires that the equipment maintain structural integrity during and after testing and continue to function.

The document also discusses in detail the requirement on a test strong motion time history and TRS. The test time history shall have a duration of 30 ± 4 sec, with the non-stationary characteristic synthesized by an input signal build-hold-decay envelope of 5 sec, 15 sec, and 10 sec, respectively. The TRS shall be calculated at 5% damping, and shall envelop the RRS based on the maximum-one-third-octave bandwidth resolution over the frequency range of 1–33 Hz, or up to the shake table limits. If the resonant frequency of the testing equipment is higher than

5 Hz, the TRS is required to envelop the RRS only down to 3.5 Hz. When resonance phenomena exist below 5 Hz, the RRS shall envelop the RRS only down to 70% of the lowest frequency of resonance.

It is recommended that the TRS be computed with maximum-one-sixth-octave bandwidth resolution. At the latter resolution, the TRS should not exceed the RRS by more than 30% over the amplified frequency range (from 1.3–8.3 Hz), and a point of the TRS may fall below the RRS by 10% or less provided the adjacent one-sixth-octave points are at least equal to the RRS.

2.3.3 International Electrotechnical Commission Standard (IEC-1999)

The international standard IEC60068-2-57 (IEC, 1999), referred to here as “IEC-1999,” outlines methods and standards for environmental testing of electrical equipment, including the testing

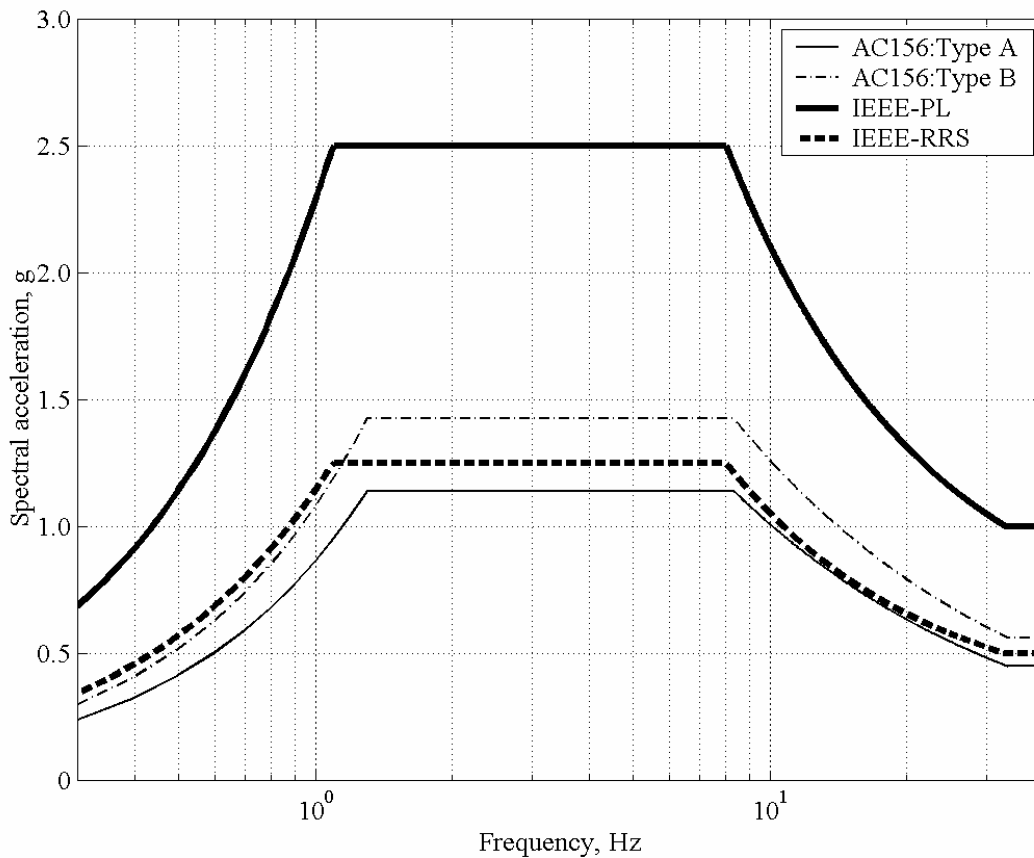


Fig. 2.9 AC 156 RRS for various zones vs. high IEEE RRS and high IEEE PL for 5% damping

procedure for seismic applications. It extends the general requirements on seismic testing described in a separate standard, IEC 68-3-3 (IEC, 1991).

The seismic test response spectrum in the IEC-1999 is assumed as site independent; in other words, that the spectrum envelops all possible cases of soil condition at the site, distance from a possible source, and possible magnitude. The required response spectra depends only on a zero period acceleration (ZPA) of the location where the equipment is intended to be mounted, and a critical damping value for the equipment. ZPA is equal to a peak floor acceleration that is a product of several factors: those of PGA for the site and amplification factor due to elevated mounting. The PGA is limited to 0.5g for strong and very strong earthquakes.

The test frequency range according to the IEC-1999 shall be from 1–35 Hz for seismic applications, whereas in the case of equipment with a natural frequency below 1 Hz, the suggested frequency range is 0.1–35 Hz. Electrical equipment can have a natural frequency lower than 1 Hz; therefore, the last frequency range was used for producing plots of the IEC-1999 spectra for seismic applications. The required response spectrum for seismic qualification is specified for 2%, 5%, and 10% damping. In log-log scale the RRS consists of straight lines representing ramp-up, plateau, and ramp-down.

Analytical formulation of the IEC-1999 spectra is slightly different from the corresponding one for the IEEE PL and is as follows for 5% damping:

$$S_a = \begin{cases} (f/1.6)^{2.33} & 0 < f < 1.6 \text{ Hz}, \\ 3.0 & 1.6 \text{ Hz} \leq f \leq 11.7 \text{ Hz}, \\ (11.7/f)^{1.58} & 11.7 \text{ Hz} \leq f \leq 23.3 \text{ Hz}. \end{cases} \quad (2.6)$$

Both spectra have a plateau with maximum spectral values and two ramps with increasing and decreasing spectral acceleration. Compared with the IEEE, these ramps (in the case of the IEC-1999) are governed by the exponential relationship between the spectral acceleration and the frequency. The IEC-1999 plateau starts from 1.6 Hz and ends at 11.7 Hz. The IEC-1999 response spectra is equal to PGA for frequencies higher than 23.3 Hz, whereas the IEEE spectra is equal to PGA for frequencies higher than 33 Hz. Figure 2.10 presents the IEEE RRS and the IEC-1999 spectra (for ground level mounting, when the IEC amplification factor is equal to 1) for 2% and 5% damping. According to the IEC-1999, the maximum value of spectral acceleration has to be three times that of ZPA for a 5% damping ratio and 5 times that of PGA for a 2% damping ratio. The IEC-1999 spectra in Figure 2.10 are plotted for the ZPA taken as

0.5g, which is an ultimate case for ground level mounting. The IEEE spectra completely envelop the IEC-1999 for almost all natural frequencies (with minor exception around 11 Hz for 2% damping). The IEC-1999 spectra are lower in the low-frequency range compared with the IEEE spectra.

The acceptance criteria for qualification testing in accordance with IEC-1999 are specified in the IEC 68-3-3 document (IEC, 1991) and consist of three levels of qualification criteria depending on the importance of the equipment or structure. The most demanding criterion calls for no malfunction either during or after the test. The least demanding criterion requires that the equipment withstand an earthquake with no major structural damage (no replacement or repair), although some malfunction during the testing can occur if repairable after completion of qualification testing. The acceptance criteria are somewhat close to that of IEEE 693-1997 specified for the PL testing.

Based on the discussion above, the following conclusions can be made. The IEC-1999 spectra do not cover the low-frequency range (around 1 Hz) compared to the IEEE spectra. The plateau of the IEC-1999 spectra is relatively wider than the IEEE plateau and shifted toward high frequencies. The IEEE PL spectra envelop the IEC-1999 spectra anchored at 0.5g; therefore, the IEEE spectra represent a more conservative design approach.

For developing a time history, a tolerance zone for test response spectra is 50% above the RRS and 0% below the RRS, although justifiable single-point dips below and peaks above the tolerance zone may be acceptable if such points do not coincide with the resonant frequency. The tolerance of the test response spectra shall be checked at least in 1/12 octave bands for damping lower or equal to 2% (assumed as 2% for the specimen) and 1/6 octave bands for damping between 2% and 10% (assumed as 5% for the specimen). The 5% damping is a general case for the standard.

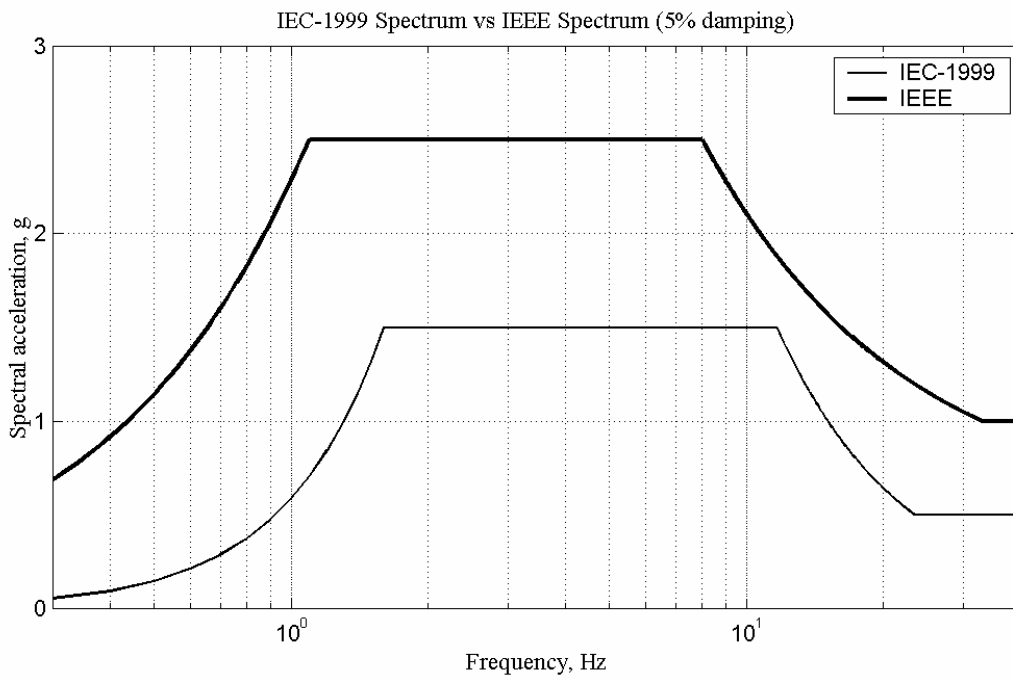
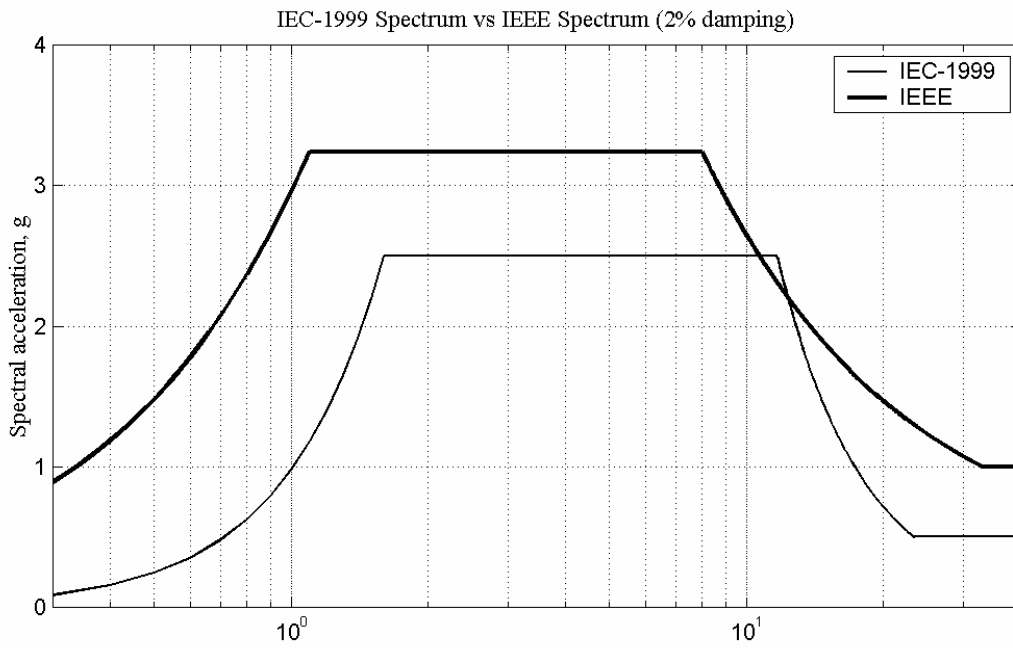


Fig. 2.10 IBC-1999 response spectra vs. IEEE high qualification RRS

2.4 SUMMARY AND CONCLUSIONS

A summary on the design and required response spectra from building codes and various regulating documents is presented in Table 2.2. In general, the IEEE test spectra represent a more conservative design approach than that from the following documents: (1) IBC-2000, (2) UBC-1997, (3) AC156, (4) GR-63-CORE, and (4) IEC-1999 requirements. Depending on a design PGA value for SSE, the design spectra from the RG-1.60 can be more conservative than the IEEE spectra: the IEEE high PL spectrum at 2% damping envelops the RG-1.60 spectrum only if the SSE design PGA is less than 0.9g.

Acceptance criteria specified by various regulatory documents for qualification testing of equipment are quite close to each other and to the IEEE acceptance criterion. The approximate equivalency of the acceptance criteria for qualification testing of various equipment (AC156 and GR-63-CORE) supports the previously stated conclusion that the IEEE qualification testing represents a more conservative approach.

Table 2.2 Summary of design and required response spectra and requirements of test time history from various regulatory documents

		IEEE 693 1997	AC156	IEC-1999	GR-63	RG-1.60	UBC-1997	IBC-2000
Design Spectrum or RRS	Damping, %	2	5	2,5,10	2	0.5,2,5,7,10	5	5
	Site-Dependency	NO	YES	NO	NO	NO	YES	YES
	Amplification factor	2	1.6	2 ⁷	Included	NA	NA	NA
	Frequency range, Hz	0.333	0.1–33.3	0.1–35	0.3–50	0.25–33		
	Plateau range, Hz	1.1–8.0	1.3–8.3	1.6–11.7 ³⁾	2.0–5.0 ⁴	2.5–9.0	Varies	Varies
	Spectral acceleration at plateau, in fractions of PGA	3.24	2.5 (at 5%)	5.0 (at 2%)	3.13 (Zone 4)	2.9 ¹ (at 5%)	2.5	2.5
Input Time History	Duration, sec	20	26–34	5–10	32	NA	NA	NA
	High-peaks count ($\geq 70\%$)	NA	NA	3–20	NA	NA	NA	NA
	Strong part to duration ratio, %	NA	NA	25,50,75	NA	NA	NA	NA
TRS	Tolerance above RRS, %	NA	30	50 ²	30	NA	NA	NA
	Tolerance below RRS, %	NA	10 ⁵	0 ²	0	10 ⁶	NA	NA
	Tolerance range, Hz	NA	1.3–8.3	Not specified	1.0–7.0	NA	NA	NA
	Tolerance resolution, octave bands	NA	1/6	1/12(2%),1/6(5%)	1/6(2%)	~1/8	NA	NA
	Meets or exceeds range, Hz	1/T–33	0.7/T(or 3.5)–33	Not specified	1.0–50.0	Not specified	NA	NA
	Meets or exceeds resolution, octave	NA	1/3	Not specified	1/6(2%)	NA	NA	NA

Notes:

¹ The plateau has some slope and varies from 3.13–2.61; average value is presented.

² Individual points outside of tolerance zone can be acceptable provided such points do not coincide with the resonant frequency.

³ Plateau start frequency is taken as 2.0 Hz if resonant frequency is more than 1 Hz.

⁴ For Zone 4 (in case of Zone 3 the range is from 1.0 to 5.0 Hz and for Zones 1 and 2 the range is from 0.6–5.0 Hz).

⁵ Individual points up to 10% below the RRS can be acceptable provided the adjacent 1/6 octave points are at least equal to the RRS.

⁶ No more than 5 points of the spectra obtained from the time history should fall, and no more than 10% below the design spectra.

⁷ For very flexible supporting structure the amplification factor is taken as 3.

3 Study of Ground Motions and Record Selection for Spectral Matching

This chapter presents a study of 35 strong motion time histories recorded during 18 earthquakes in the United States and abroad. Based on a number of parameters, the best candidate for further modification in the spectral matching procedure is selected from the records. Specific characteristics of the earthquakes that have occurred in eastern and central North America are summarized also. The latter discussion is based on analysis of five strong motion records and the comparison of IBC-2000 design spectra for these regions with the IEEE spectra.

3.1 CRITERIA USED TO SELECT STRONG MOTION RECORD

The study examined strong motion records available from the PEER Strong Motion Database (<http://peer.berkeley.edu/smcat/>) and the COSMOS strong motion database (<http://www.cosmos-eq.org>). The databases have information on the site conditions and the soil type for the instrument locations. A set of 35 strong motion records was selected for a detailed examination. The decision on which strong motion record to consider was made based on several criteria. First, the record had to consist of three time histories in three orthogonal directions. Secondly, the location of the instrument needed to be at the ground level or under the ground (e.g., a tunnel) and installed for obtaining free-field ground motion, or the instrumentation installed in the first level of a lightweight structure. In addition to these two criteria, the strong motion history should satisfy certain parameter limits: peak ground acceleration, peak ground velocity, earthquake magnitude, distance from source, and site soil properties. Table 3.1 presents the list of the ground motion records examined, and Table 3.2 lists the parameters of the strong motion time histories.

3.1.1 Earthquake Magnitude and Distance of Site from Source

The acceleration records from a total 18 earthquakes were studied. The smallest value of the earthquake magnitude was limited to 5.7, which corresponds to the 1979 Coyote Lake earthquake.

Table 3.1 Strong motion records selected for consideration

No.	Earthquake	Date	Station	Vertical	Horiz1	Horiz2
1	Cape Mendocino, CA	4/25/92	89324 Rio Dell Overpass	RIO-UP	RIO270	RIO360
2	Cape Mendocino, CA	4/25/92	89156 Petrolia	PET-UP	PET000	PET090
3	Chi-Chi, Taiwan	9/20/99	TCU079	TCU079-V	TCU079-N	TCU079-W
4	Coyote Lake, CA	8/6/79	57382 Gilroy Array #4	G04-UP	G04270	G04360
5	Coyote Lake, CA	8/6/79	47381 Gilroy Array #3	G03-UP	G03050	G03140
6	Düzce, Turkey	11/12/99	Düzce	DZC-UP	DZC180	DZC270
7	Düzce, Turkey	11/12/99	1062 Lamont	1062-V	1062-N	1062-E
8	Duval, WA	5/3/96	Station 2199	sma-1.vol_2.5131a, b, and c		
9	Imperial Valley, CA	5/19/40	117 El Centro Array #9	I-ELC-UP	I-ELC180	I-ELC270
10	Imperial Valley, CA	10/15/79	6619 SAHOP Casa Flores	H-SHP-UP	H-SHP000	H-SHP270
11	Imperial Valley, CA	10/15/79	6616 Aeropuerto Mexicali	H-AEP-UP	H-AEP045	H-AEP315
12	Imperial Valley, CA	10/15/79	955 El Centro Array #4	H-E04-UP	H-E04140	H-E04230
13	Kern County, CA	7/21/52	1095 Taft Lincoln School	TAF-UP	TAF111	TAF021
14	Kobe, Japan	1/16/95	0 Nishi-Akashi	NIS-UP	NIS000	NIS090
15	Kocaeli, Turkey	8/17/99	Yarmica	YPT-UP	YPT060	YPT330
16	Kocaeli, Turkey	8/17/99	Düzce	DZC-UPK	DZC180K	DZC270K
17	Kocaeli, Turkey	8/17/99	Bursa Tofas	BUR-UP	BUR000	BUR090
18	Landers, CA	6/28/92	22170 Joshua Tree	JOS-UP	JOS000	JOS090
19	Landers, CA	6/28/92	23559 Barstow	BRS-UP	BRS000	BRS090
20	Loma Prieta, CA	10/18/89	13 BRAN	BRN-UP	BRN000	BRN090
21	Loma Prieta, CA	10/18/89	57476 Gilroy-Historic Bldg.	GOF-UP	GOF090	GOF180
22	Loma Prieta, CA	10/18/89	47125 Capitola	CAP-UP	CAP000	CAP090
23	Loma Prieta, CA	10/18/89	47380 Gilroy Array #2	G02-UP	G02000	G02090
24	Nahanni, Canada	12/23/85	6097 Site 1	S1-UP	S1010	S1280
25	Nisqually, WA	2/28/01	Olympia, WSDOT Test Lab	20010228_1.corrected.0730b_a		
26	Northridge, CA	1/17/94	24087 Arleta-Nordhoff FS	ARL-UP	ARL090	ARL360
27	Northridge, CA	1/17/94	24279 Newhall - Fire Sta	NWH-UP	NWH090	NWH360
28	Northridge, CA	1/17/94	74 Sylmar - Converter Sta	SCS-UP	SCS052	SCS142
29	Northridge, CA	1/17/94	24389 LA - Century City	CCN-UP	CCN090	CCN360
30	Parkfield, CA	6/28/66	1015 Cholame #8	C08DWN	C08050	C08320
31	Parkfield, CA	6/28/66	1016 Cholame #12	C12DWN	C12050	C12320

Table 3.1 continued

32	Parkfield, CA	6/28/66	1014 Cholame #5	C05DWN	C05085	C05355
33	Tabas, Iran	9/16/78	9101 Tabas	TAB-UP	TAB-TR	TAB-LN
34	Victoria, Mexico	6/9/80	6604 Cerro Prieto	CPE-UP	CPE045	CPE315
35	Victoria, Mexico	6/9/80	6621 Chihuahua	CHIDWN	CHI102	CHI192

Note: Records 8 and 25 are taken from the COSMOS database; all others are from the PEER database.

Table 3.2 Parameters of strong motion time histories

No.	Earthquake	M	D, km	Site*	Location
1	Cape Mendocino, CA	7.1	18.5	C	1 story lightweight, instrumentation at lowest level
2	Cape Mendocino, CA	7.1	9.5	D	Free-field
3	Chi-Chi, Taiwan	7.6	10.0	1	NA
4	Coyote Lake, CA	5.7	4.5	D	1 story lightweight, instrumentation at lowest level
5	Coyote Lake, CA	5.7	6.0	D	Free-field
6	Düzce, Turkey	7.1	8.2	D	1 story lightweight, instrumentation at lowest level
7	Düzce, Turkey	7.1	13.3	B	Free-field
8	Duval, WA	6.0	14.2	A	NA
9	Imperial Valley, CA	7.0	8.3	D	5+ story heavy construction, instrumentation below ground
10	Imperial Valley, CA	6.5	11.1	C	Free-field
11	Imperial Valley, CA	6.5	8.5	D	Free-field
12	Imperial Valley, CA	6.5	4.2	D	Free-field
13	Kern County, CA	7.4	41.0	D	Under ground
14	Kobe, Japan	6.9	11.1	E	NA
15	Kocaeli, Turkey	7.4	2.6	D	2-4 story lightweight, instrumentation at lowest level
16	Kocaeli, Turkey	7.4	12.7	D	1 story lightweight, instrumentation at lowest level
17	Kocaeli, Turkey	7.4	62.7	D	Free-field
18	Landers, CA	7.3	11.6	C	1 story lightweight, instrumentation at lowest level
19	Landers, CA	7.3	36.1	D	Free-field
20	Loma Prieta, CA	6.9	10.3	A	NA
21	Loma Prieta, CA	6.9	12.7	D	2-4 story lightweight, instrumentation at lowest level
22	Loma Prieta, CA	6.9	14.5	C	1 story lightweight, instrumentation at lowest level
23	Loma Prieta, CA	6.9	12.7	D	Free-field
24	Nahanni, Canada	6.9	7.0	A	NA
25	Nisqually, WA	6.8	18.3	NA	Free-field
26	Northridge, CA	6.7	9.2	D	1 story lightweight, instrumentation at lowest level
27	Northridge, CA	6.7	7.1	D	1 story lightweight, instrumentation at lowest level
28	Northridge, CA	6.7	6.2	D	NA
29	Northridge, CA	6.7	25.7	D	Free-field

Table 3.2 continued

30	Parkfield, CA	6.1	9.2	B	1 story lightweight, instrumentation at lowest level
31	Parkfield, CA	6.1	14.7	B	Free-field
32	Parkfield, CA	6.1	5.3	C	Free-field
33	Tabas, Iran	7.4	3.0	C	1 story lightweight, instrumentation at lowest level
34	Victoria, Mexico	6.1	34.8	A	NA
35	Victoria, Mexico	6.1	36.6	D	NA

(^o) Geomatrix site classification; see Table 3.3.

The Chi-Chi, Taiwan (1999) time history was recorded during the 7.6 magnitude earthquake; that magnitude was the largest considered in this study.

The distance of the recording site from the source ranged from 1.6–39.2 mi (2.6–62.7 km). A scatter plot of the magnitude-distance pairs for the strong ground motion records is shown in Figure 3.1. Eighty-two percent of the acceleration records obtained were from locations within 12.5 mi (20 km) from the source. About one half of the records obtained were from sites with epicentral distances of less than or equal to 6.3 mi (10 km), and about 15% of the records were from sites with epicentral distances equal to or less than 3.1 mi (5 km). Two thirds of the records were obtained at sites within 12.5 mi (20 km) from the source and during earthquakes with magnitude 6.5 or greater. About 17% of the records are from earthquakes with magnitude 7.0 and greater and with epicentral distances of less than or equal to 6.3 mi (10 km).

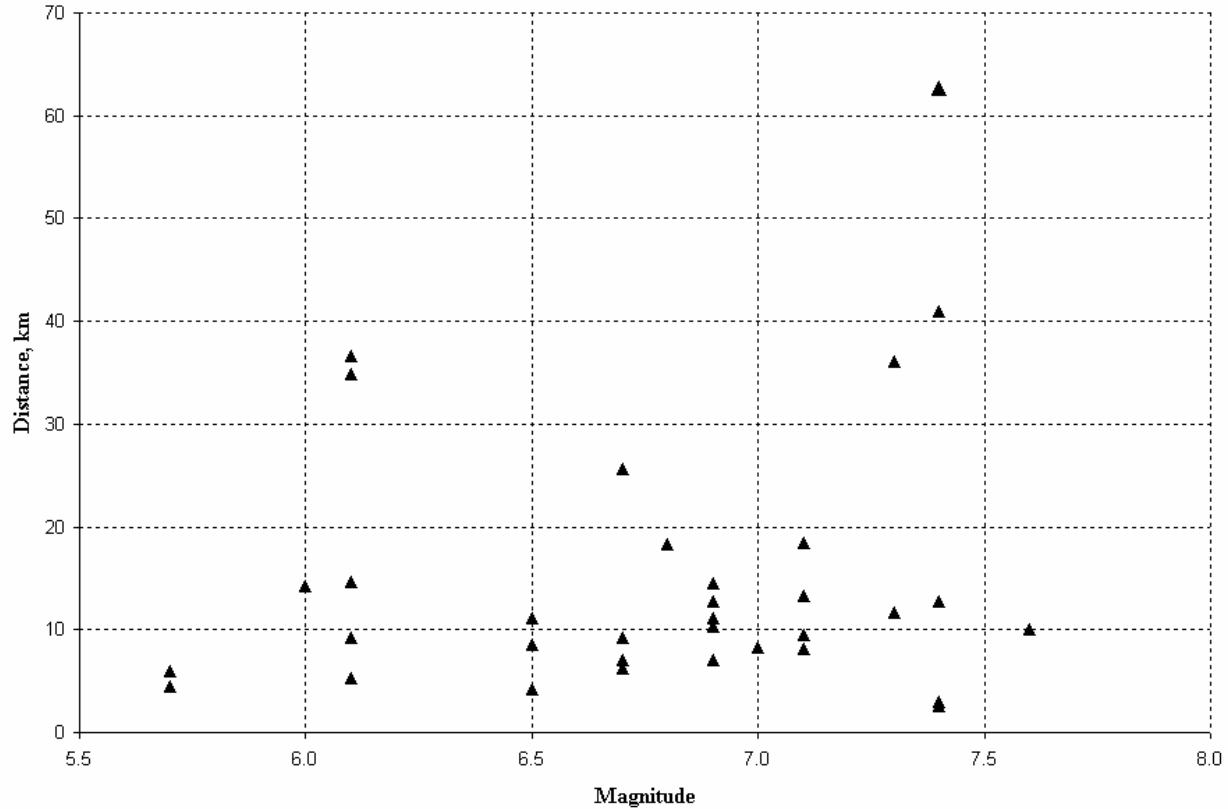


Fig. 3.1 Magnitude vs. distance distribution

3.1.2 Peak Ground Motion Parameters

The range of the peak ground acceleration (PGA) of the strong motion records included in the set was from 0.1–1.1g in the horizontal direction. The plots of the vertical and the maximum horizontal PGA are shown in Figure 3.2 (the largest PGA in one of two horizontal directions was used). The maximum PGA among the records corresponds to the strong motion from the Nahanni, Canada, earthquake of 1985: 2.1g in the vertical direction and 1.1g in the horizontal direction. Two other peaks in the PGA plots of 0.90g and 0.85g are for records from the 1994 Northridge, California, earthquake and the 1978 Tabas, Iran, earthquake, respectively. The histogram of the PGA distribution in the set of the strong motions is presented in Figure 3.3. The plot shows the percentage of the strong motions within a particular PGA range in the set. About two thirds of the records have PGA higher than 0.3g. The average PGA for the whole set of the studied strong motions was 0.41g in the horizontal direction and 0.31g in the vertical direction. Several records with low PGA (Records 17, 19, and 31) were included in the set in order to complete the set with a free-field motion record for a particular earthquake.

For the selected records, the peak ground velocity (PGV) varied from 1.8 in./sec (0.05 m/sec) to 47.8 in./sec (1.21 m/sec) in the horizontal direction with an average 17.3 in./sec (0.44 m/sec). The PGV's maxima of 46.3 in./sec (1.18 m/sec) and 47.8 in./sec (1.21 m/sec) correspond to the records from the Northridge and Tabas earthquakes, respectively. The plots of the vertical and the maximum horizontal PGV are presented in Figure 3.4, and Figure 3.5 shows the horizontal PGV distribution. About 70% of the records have PGV equal to or higher than 10 in./sec (0.25 m/sec).

3.1.3 Site Classification and Instrument Location

The study primarily examined strong motion records for soil types C and D in the Geomatrix classification except for five records (Records 3, 8, 20, 24 and 34), which were obtained at the site with a rock-like soil. The soil property at the site for almost all records is the Geomatrix classification shown in Table 3.3, except for Record 3 of the Chi-Chi, Taiwan, earthquake, which has the Central Weather Bureau classification. The percentage of the specific site property in the set of the ground motions is as follows: site E — 3%, site D — 54%, site C — 17%, and the remaining 26% of the set were obtained from sites A and B. The scatter plot of site classification versus distance from the source is shown in Figure 3.6. About 60% of the records were obtained at epicentral distances less than or equal to 12.5 mi (20 km) and at sites with soil types C, D, and E.

The instrument locations are presented in Table 3.2. Thirty-four percent of the time histories were recorded at the first level of a lightweight construction. About 40% of the time histories represent free-field records. The list was expanded by the records extensively used in the past or by those in active current use for various types of analysis and testing.

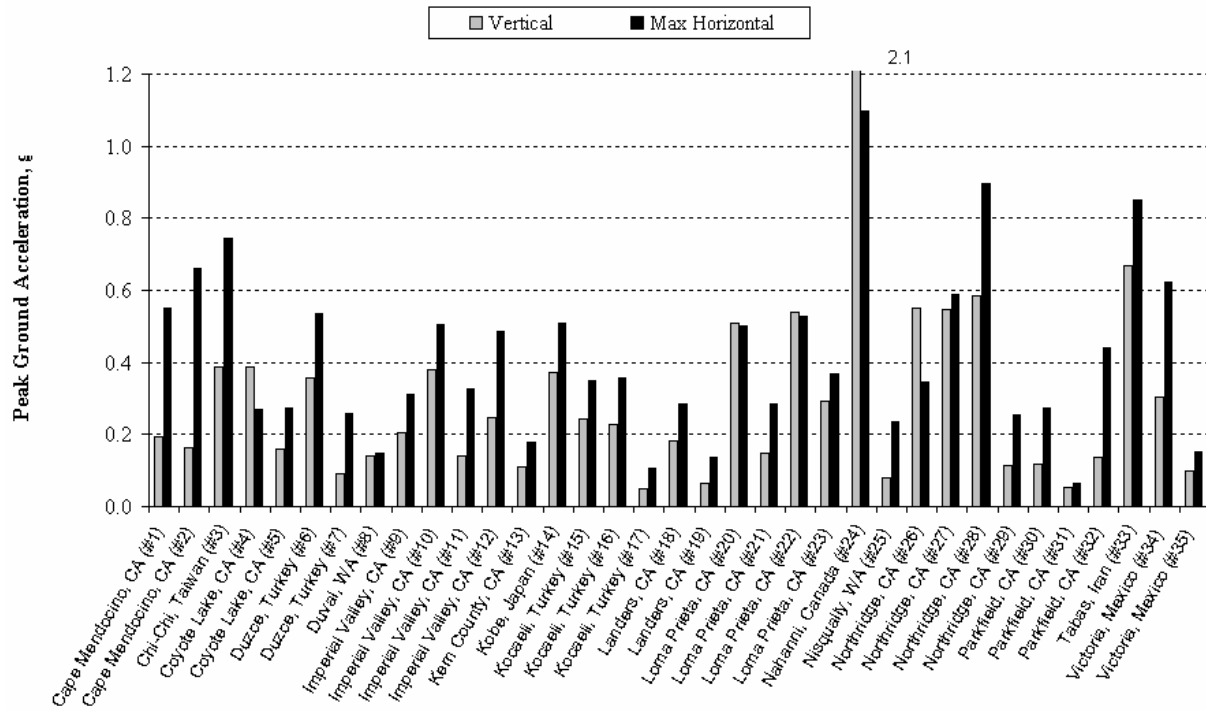


Fig. 3.2 Peak ground accelerations for all records

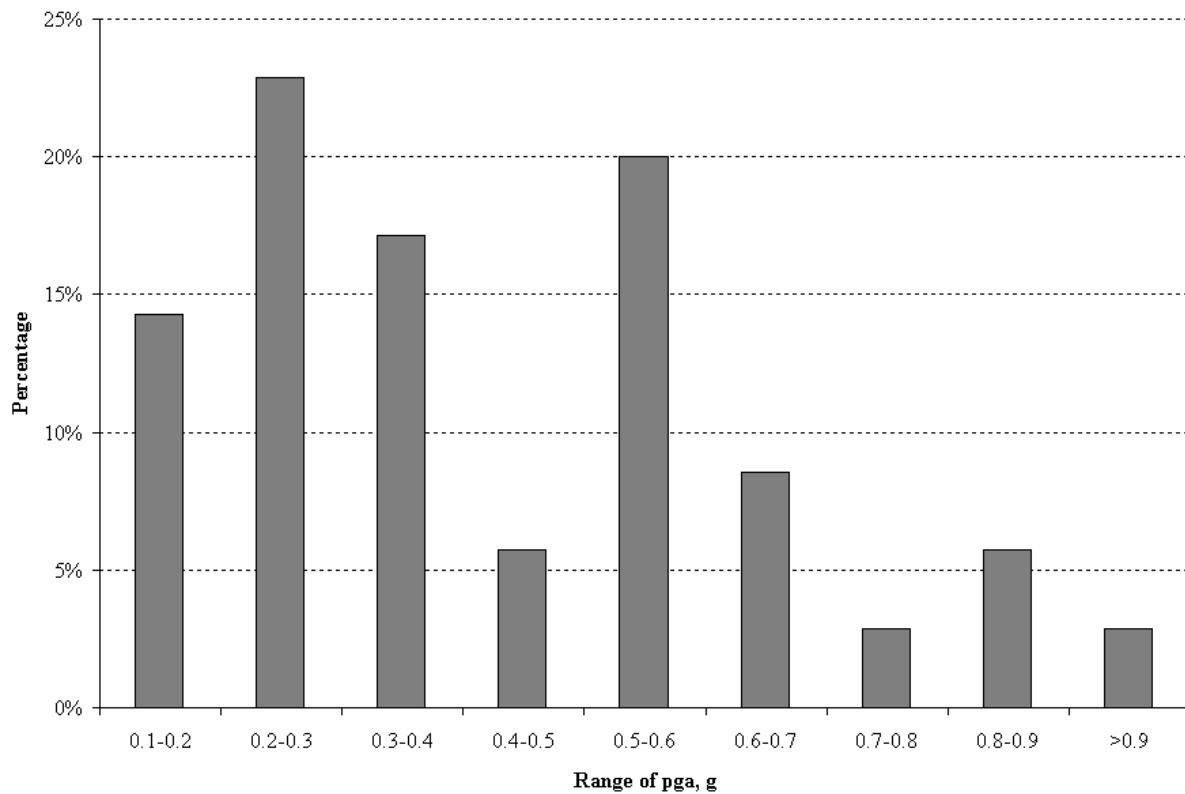


Fig. 3.3 Distribution of peak ground accelerations

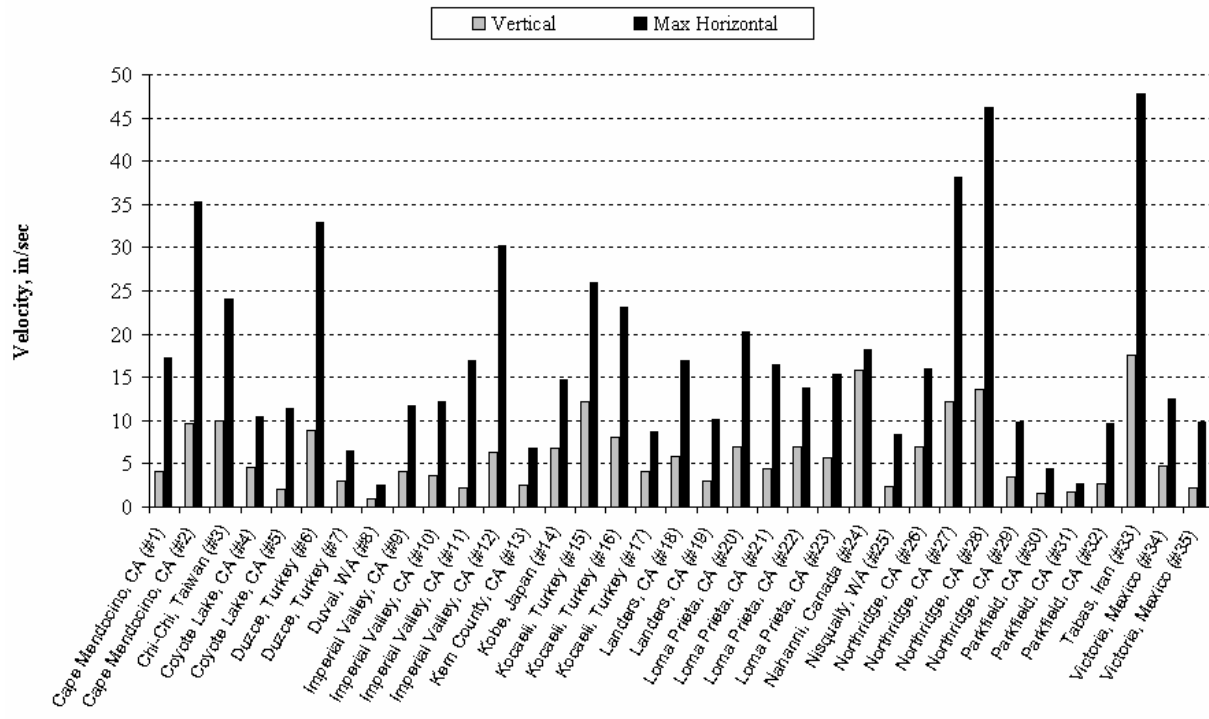


Fig. 3.4 Peak ground velocities for all selected records

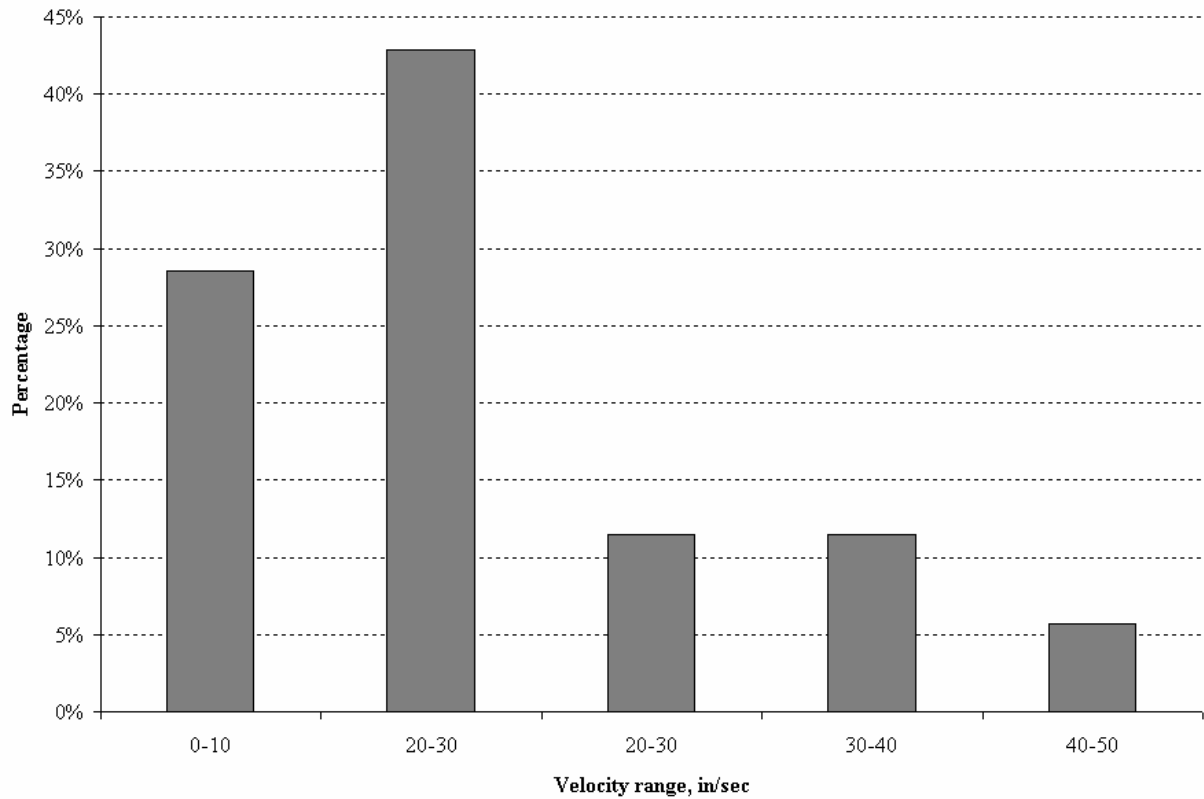


Fig. 3.5 Distribution of peak ground velocity

Table 3.3 Geomatrix classification of geotechnical subsurface characteristics

Type	Site Name	Description of Instrument Site
A	Rock	Rock (vs. > 600 mps) or < 5m of soil over rock
B	Shallow (stiff) soil	Soil profile up to 20m thick overlying rock
C	Deep narrow soil	Soil profile at least 20m thick overlying rock, in a narrow canyon or valley no more than several km wide
D	Deep broad soil	Soil profile at least 20m thick overlying rock, in a broad valley
E	Soft deep soil	Deep soil profile with average vs. < 150 mps

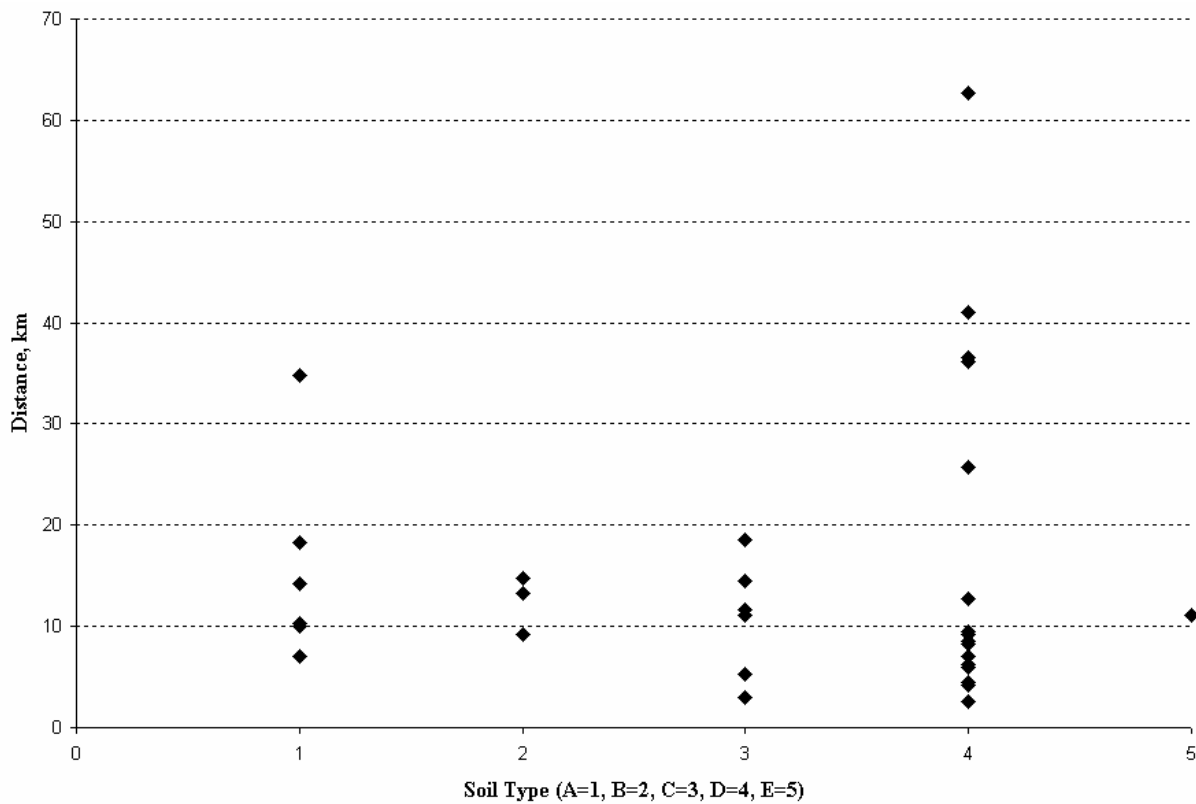


Fig. 3.6 Soil vs. epicentral distance distribution for all selected records

3.2 SUMMARY OF KEY COMPUTED PARAMETERS AND INDICES

Several key parameters and indices introduced and discussed in Appendix A of the study were computed for each strong motion record. This section presents a summary on the key parameters and indices. The summary reveals a range of parameters and indices of actual accelerograms and

sets the corresponding limits and targets for earthquake-like test input time histories for qualification testing by means of an earthquake simulator.

3.2.1 Number of Cycles Histogram

To examine this issue, the number of cycles in the accelerogram was calculated for each record. A rain-flow cycle counting procedure was used in the study that is defined in Appendix A and presented in greater detail in Appendix B. The maximum, the mean, and the mean-plus-one deviation for the cycle counts are shown in Figure 3.7. The histogram presents the number of cycles (vertical axis) for a range of magnitude normalized to PGA (horizontal axis). The magnitude varies up to 5% within the range, and the right edge is excluded from the range.

The number of cycles has the following general trend: the accelerogram carries the largest number of cycles with the lowest magnitude, and the number of cycles rapidly decreases with increasing magnitude. Therefore for the set of the selected accelerograms, the maximum number of cycles decreased from 57 cycles at 0.1–0.15 PGA magnitude range to 1 cycle at 0.95–1.0 PGA range and to 0 cycle at exactly 1.0 PGA magnitude. Figure 3.8 shows the cycle counts with a 25% threshold for each record that is a sum of cycles with magnitude higher than 25% of the PGA.

For all magnitude ranges, the test time history targeted for a qualification test is expected to have the number of cycles greater than the mean for the set and as close as possible to the maximum.

3.2.2 Power Spectral Density

Before the power spectral density (PSD) computation, the records were normalized to 1.0g PGA and the time length of the records was expanded to that of the record with the maximum length. The expanded part of the records was filled with zeros; so all records had the same length in seconds. The frequency content of the strong motion histories varied from a very broad band (e.g., Record 10 in two horizontal directions) to a relatively narrow one (e.g., Record 4 in two horizontal directions).

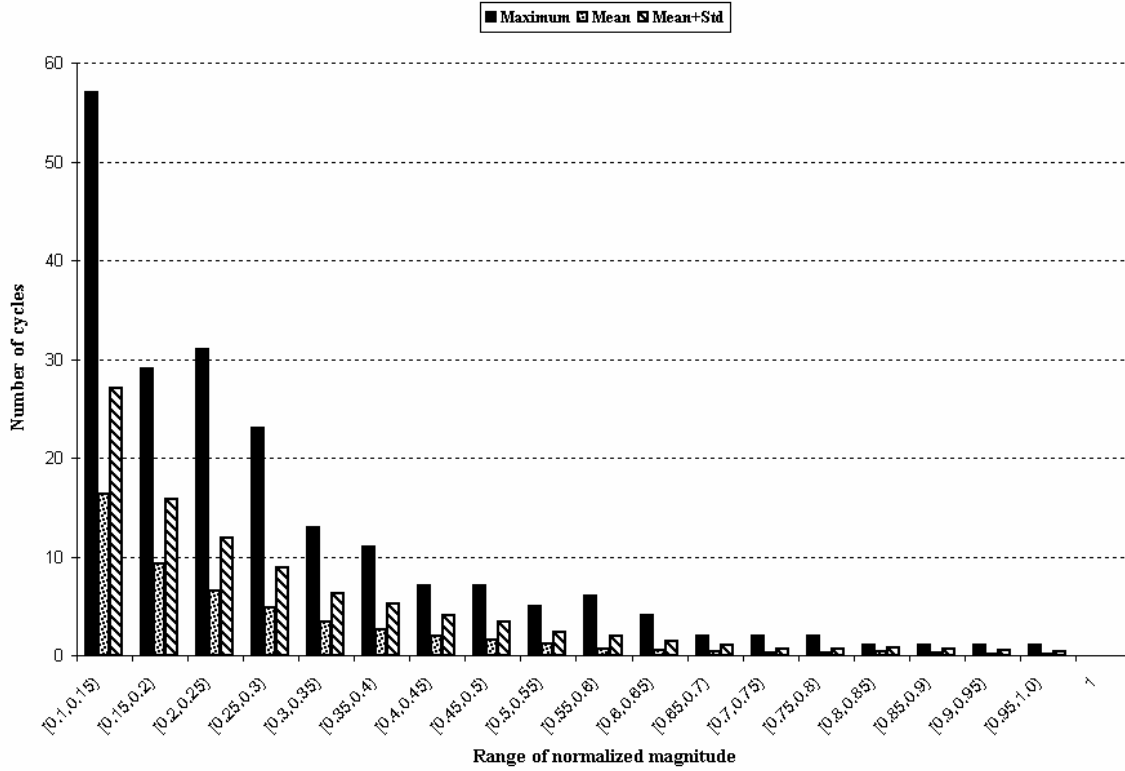


Fig. 3.7 Maximum, mean, and mean-plus-one deviation of cycle counts for all records

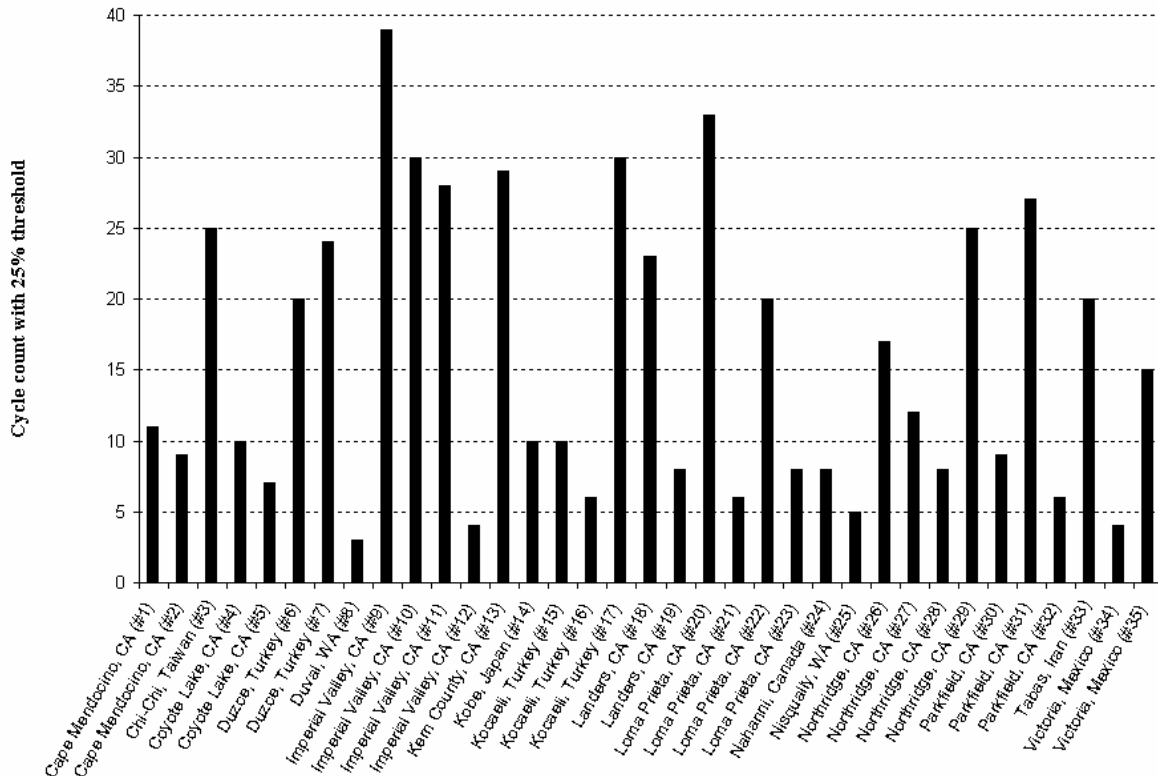


Fig. 3.8 Total cycle counts with 25% maximum magnitude threshold

The mean and the mean-plus-one standard deviation of the PSD for the set are presented in Figure 3.9. The general trend of the mean PSD is as follows: on average the mean PSD starts to decrease after 1.4 Hz and the rate of decay increases after about 5 Hz. The decay rate in the range from 5–20 Hz is close to constant, so on average the mean PSD decays almost linearly in this range.

The time history record targeted for a qualification test is expected to have a broadband power spectral density in order to cover a wide range of frequencies as required by the IEEE 693.

3.2.3 Elastic Response Spectra

The elastic response spectra of normalized records were calculated at 2% critical damping and were compared with the IEEE 693 response spectrum for 1.0g PGA that corresponds to the high seismic Performance Level.

The mean spectrum and the mean-plus-one standard deviation spectrum for the 35 strong motion records are presented in Figure 3.10. The IEEE high PL spectrum completely envelops the mean spectrum for the set. The mean-plus-one deviation spectrum is greater than the IEEE high PL spectrum from about 1.4–6.5 Hz. The mean spectrum decreases in the high-frequency range after about 5 Hz, which corresponds to the corresponding decay zone of the mean PSD (see Fig. 3.9). The mean spectrum increases in the low-frequency range up to 5 Hz and on average, the mean spectrum increases almost linearly in the range from 1.4–5 Hz.

The IEEE 693 spectra are based on the mean of elastic response spectra for a set of strong motions much larger than that considered in the study (Newmark, 1973). Nevertheless, there is a close correlation between the mean spectrum for the set of 35 records and the IEEE spectrum, which demonstrates adequate selection of strong motion records.

3.2.4 Number of Cycles in Response of SDOF System

The number of high-level cycles in the acceleration response of a 2% damped SDOF system due to excitation by the normalized strong motion records was computed. The number of high cycles (with threshold of 70% of maximum magnitude) was calculated for each natural frequency of the SDOF system taken from a certain frequency range that covers the strong part of the IEEE spectrum as defined in Appendix A.

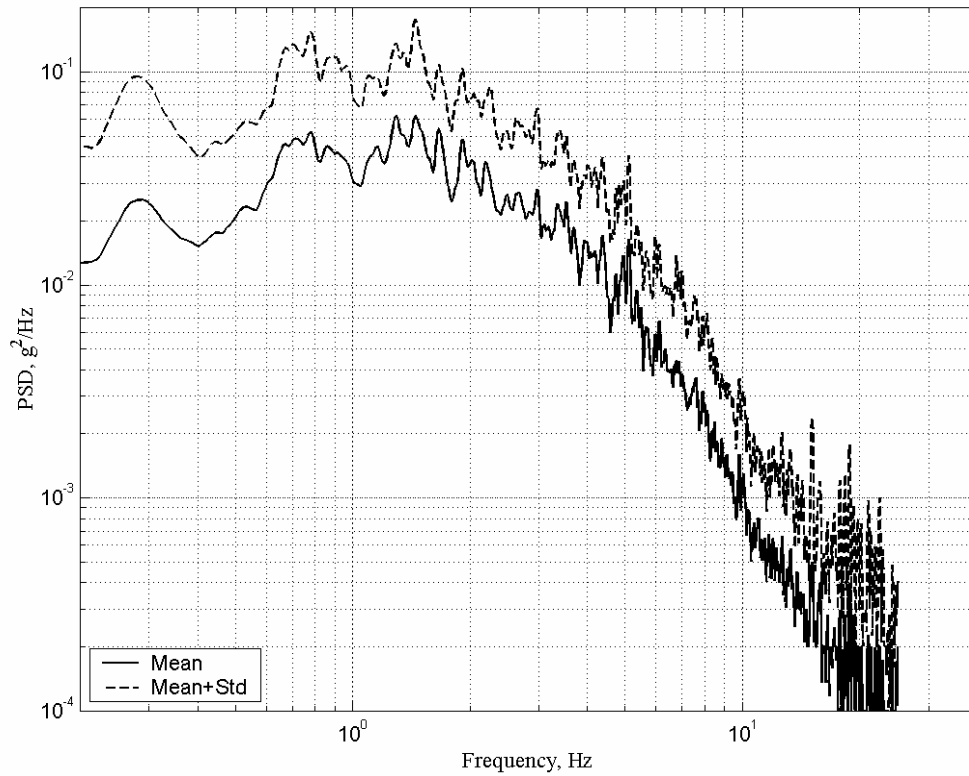


Fig. 3.9 Mean and mean-plus-one deviation PSD for all records

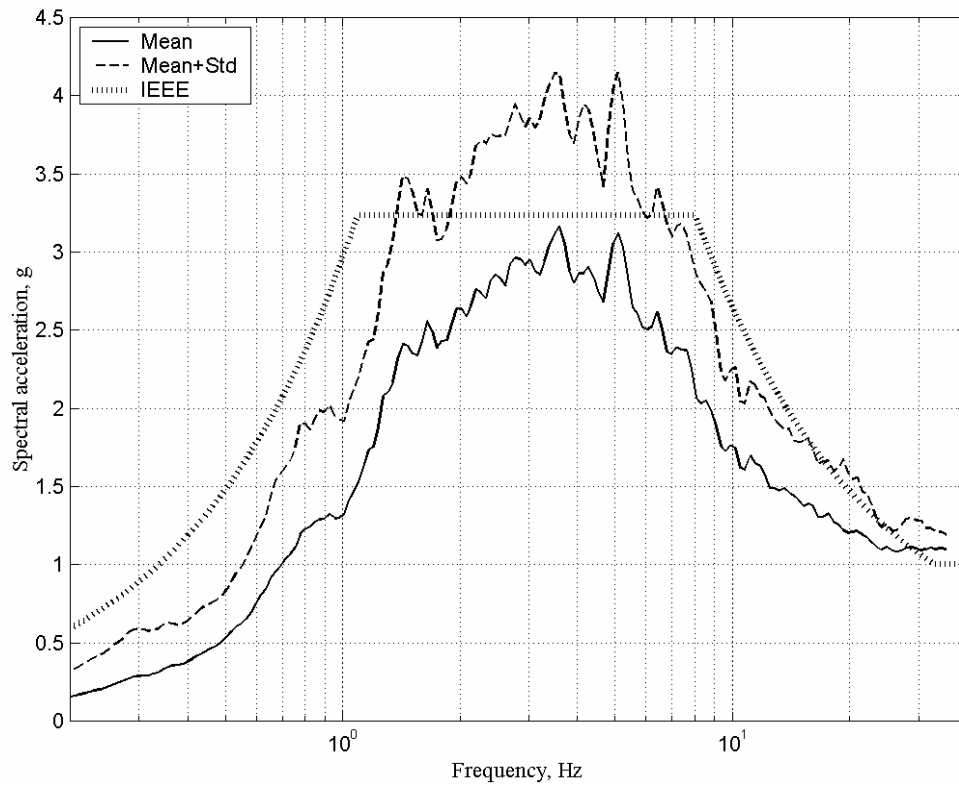


Fig. 3.10 Mean and mean-plus-one deviation spectra for all records

The results for high cycle counts are summarized in Figure 3.11, which shows the mean, the mean-plus-one standard deviation, and the maximum for the set of 35 records. The general trend of the plots is quite similar: all cycle counts increase with increasing frequency, and the relation between cycle count and frequency is close to linear in the log-log scale.

The mean varies from 2 to about 6 cycles, whereas the maximum for the set varies from 6 to 26. The mean of the minimum of cycles was computed as 0.76, reflecting the fact that the majority of strong motion time histories causes at least one cycle with magnitude 70% of maximum or higher in the SDOF system response.

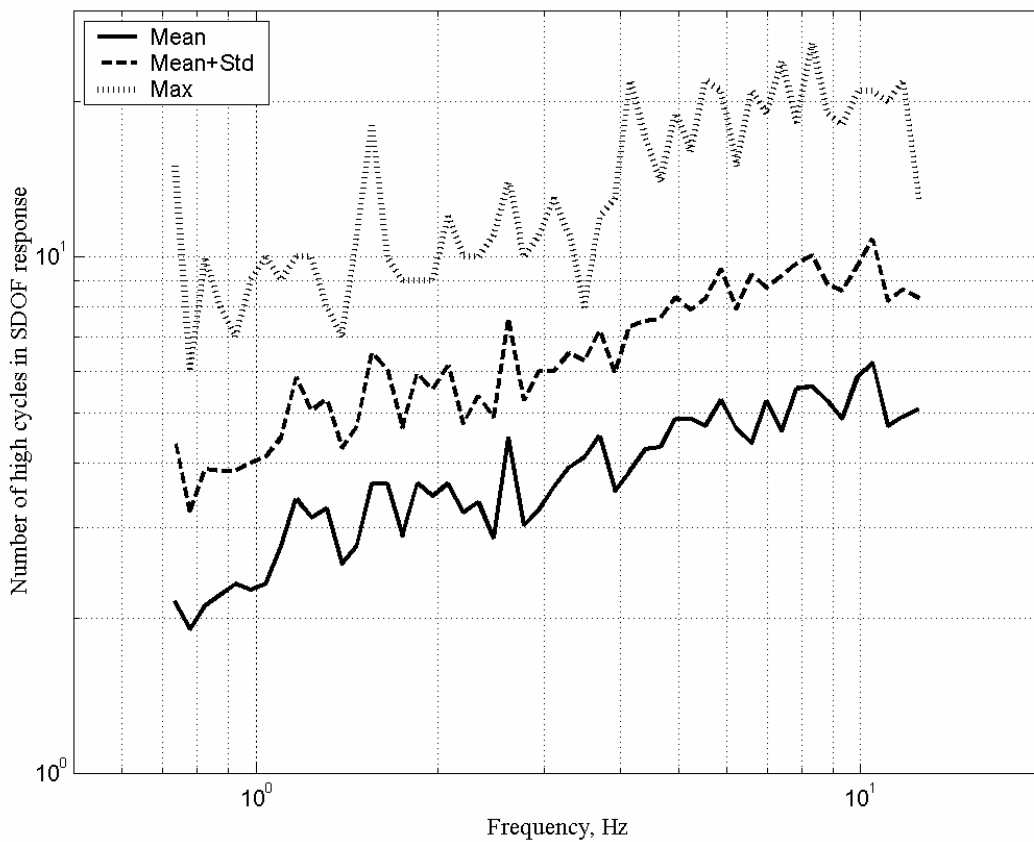


Fig. 3.11 Number of cycles in SDOF response for set of 35 records

3.2.5 Parameters Based on Cumulative Energy

Cumulative energy. A cumulative energy for a strong motion record is defined in Appendix A. Figure 3.12 presents the summary on the total cumulative energy (CE) of the strong motion histories normalized to 1.0 g PGA. For the three components of the ground motions, the mean of the total cumulative energy is close to 1.0 $g^2 \cdot sec$ with the major peaks at Record 17, Record 18, and Record 35 in the vertical and the horizontal direction. As can be seen from Tables 3.1 and 3.2, Record 17 corresponds to the accelerogram measured at a location far away from the source and has a very small PGA (around 0.1g); therefore it is not representative of near-fault ground motions. Record 18 corresponds to the 1992 Landers earthquake, with PGA close to 0.3g in both horizontal directions, and its CE in the vertical and horizontal directions are close. Record 35 represents very uneven distribution of the CE between the vertical and horizontal directions.

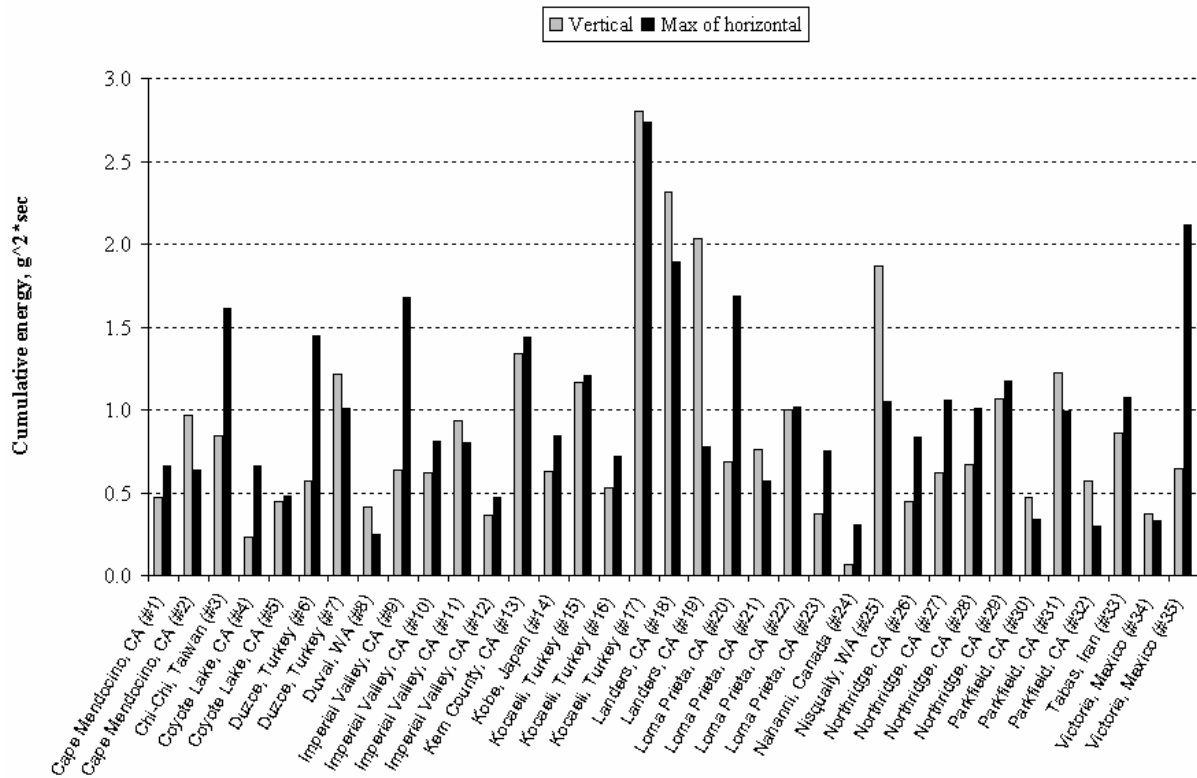


Fig. 3.12 Cumulative energy for all records normalized to 1.0g PGA

Root mean square acceleration (RMS acceleration). The root mean square acceleration is defined in Appendix A, and the RMS accelerations for all records are presented in Figure 3.13. The mean RMS acceleration is 0.16g with maximum value of 0.28g in the horizontal direction. About one half of the records had the RMS acceleration equal to or greater than the mean.

Bracketed duration. The bracketed duration of the strong motion time history is based on the calculation of the cumulative energy and presents time spent to increase the cumulative energy from 5%–95% of its total value. Figure 3.14 presents a summary on the bracketed duration calculated for each time history. The mean duration for the set of all 35 records is about 16 sec for the vertical direction and about 14 sec for the horizontal duration. The IEEE 693-1997 standard (IEEE, 1998) states that the duration of the strong motion time history intended for electrical equipment tests must be at least 20 sec. Only six records have duration (for all three components) longer than or equal to 20 sec: Records 3, 9, 13, 17, 18, and 31, so the choice of a strong motion for the test strong motion time history has to be limited to these 6 records.

Strong part to duration ratio. One more parameter related to the duration characteristics of the accelerogram, namely the duration of the strong part, was calculated in the study. The duration of the strong part is defined in Appendix A of the study and presents time spent to accumulate from 25% to 75% of the total cumulative energy. The value of this parameter is always less than the bracketed duration. The ratio of these two time parameters was introduced as a ratio of the strong part duration to the bracketed duration (referred to below as the “strong part to duration ratio”). The ratio represents the relative duration of the strong part for a strong motion time history and is presented in Figure 3.15. On average, this ratio is about 31% for the whole set of the time histories. Record 18 has the largest value for this ratio, 63% for the horizontal direction and 71% for the vertical direction. Records 6 and 7 also have large values for the ratio (about 55%).

3.2.6 Duration Based on IEEE 693 Definition

The IEEE 693 definition for the bracketed duration is the time range when the accelerogram first reaches 25% of the maximum acceleration to the time when it falls for the last time to 25% of the maximum. Figure 3.16 shows the duration of the records in the IEEE 693 definition. The comparison between the duration based on the cumulative energy calculation and the IEEE 693 definition is presented in Figure 3.17. The plot shows the minimum duration for two horizontal

components and reveals a good consistency between these two definitions of the bracketed duration.

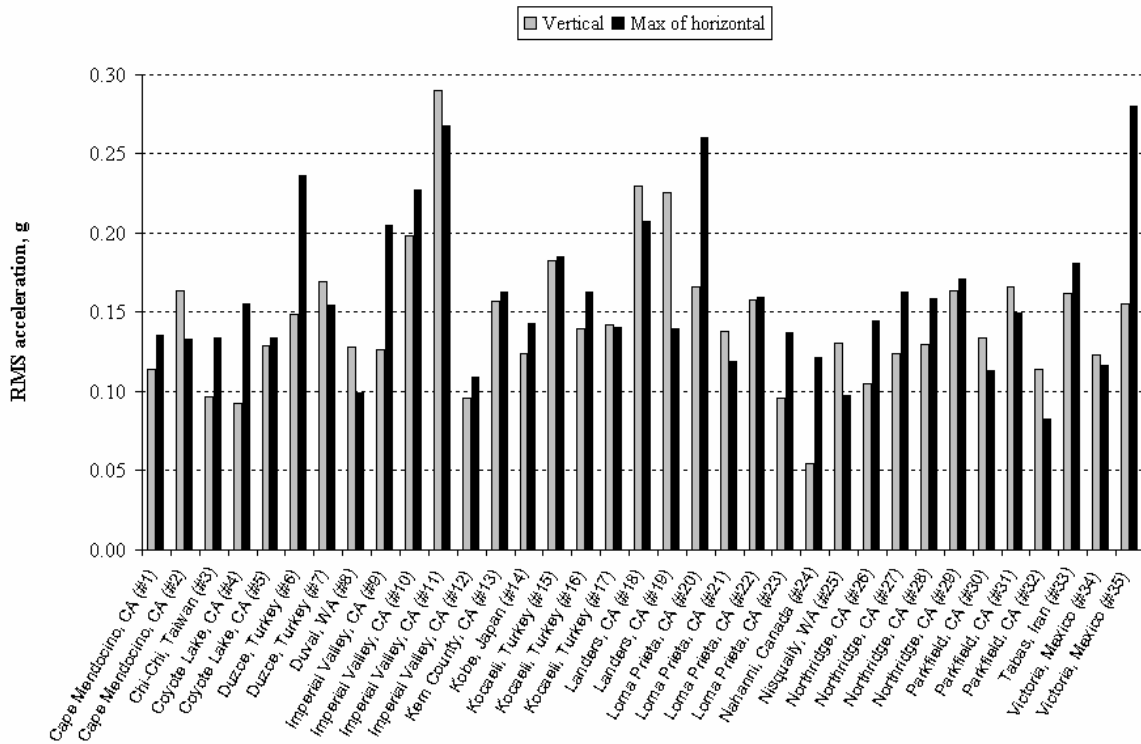


Fig. 3.13 RMS acceleration for all records normalized to 1.0g PGA

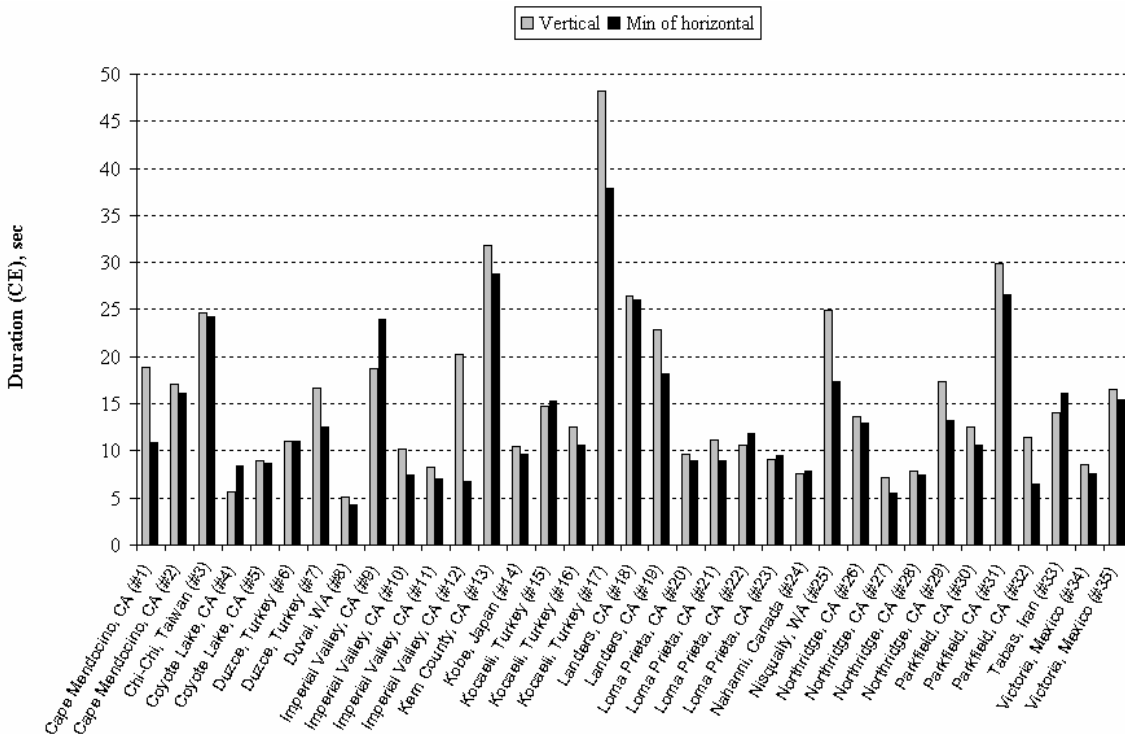


Fig. 3.14 Bracketed duration for all records based on cumulative energy (5%–95%)

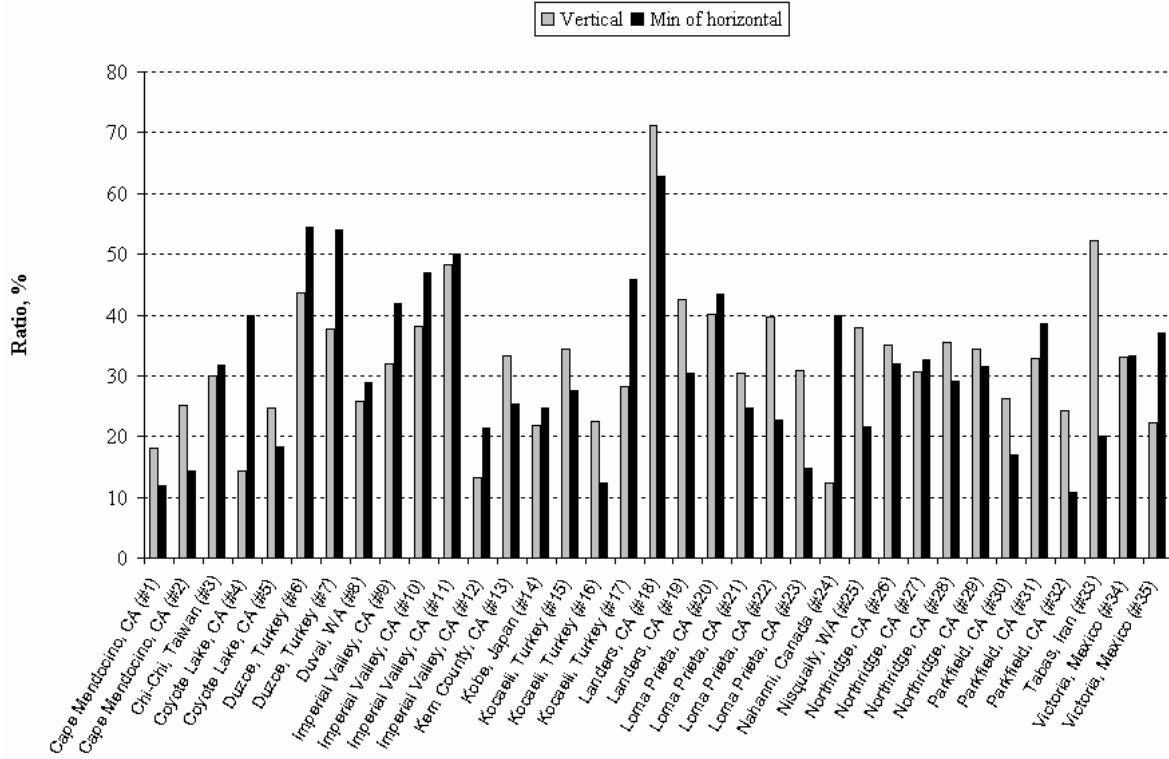


Fig. 3.15 Strong part to bracketed duration ratio for all records based on cumulative energy

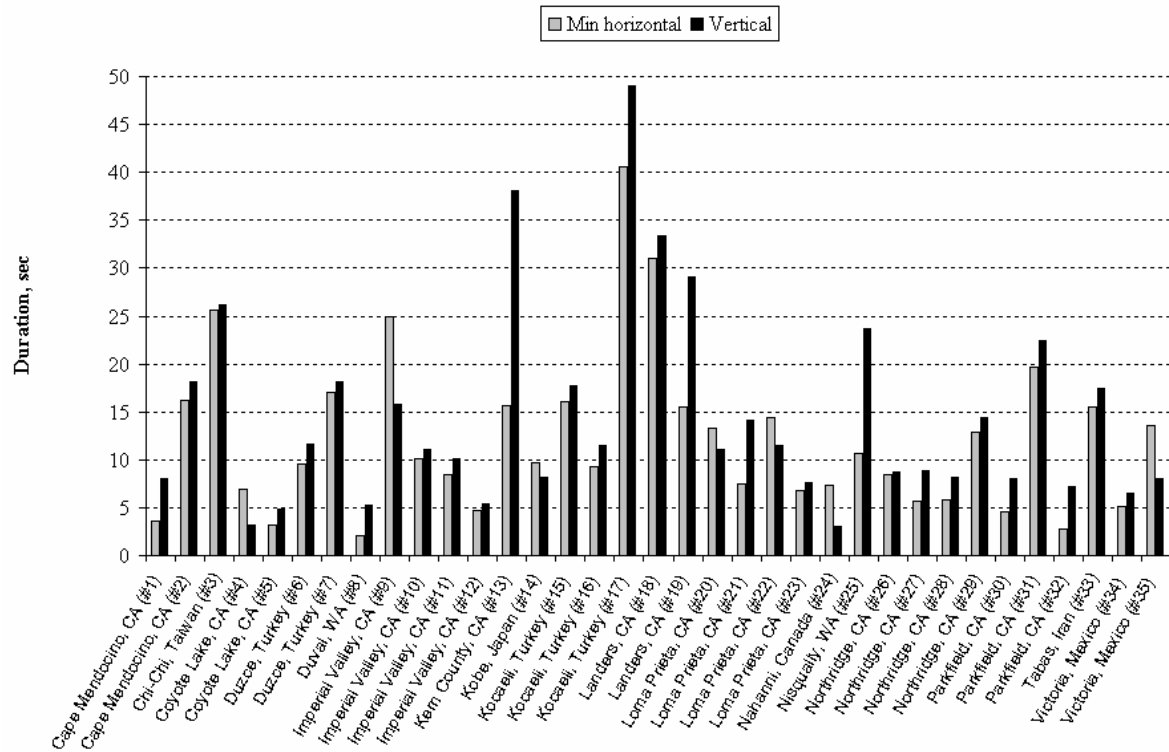


Fig. 3.16 Bracketed duration based on IEEE 693 definition

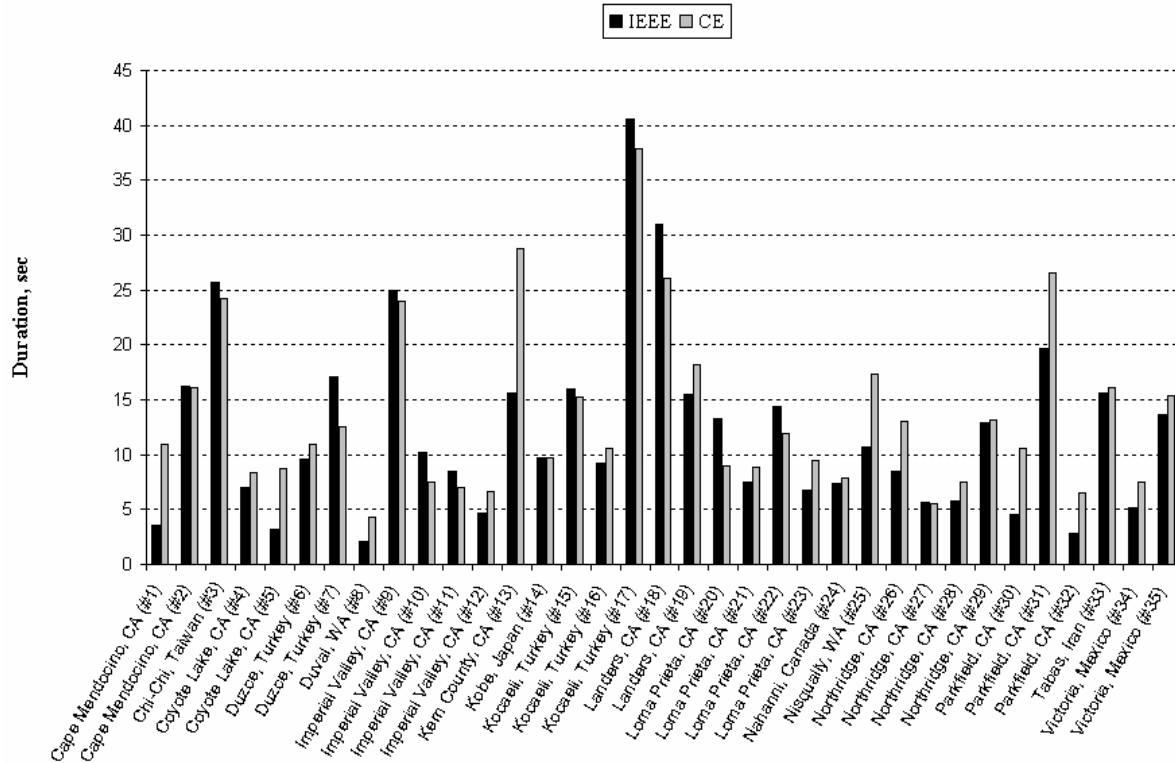


Fig. 3.17 Bracketed durations for cumulative energy (CE) and IEEE 693 definitions

IEEE 693 sets a threshold of 20 sec for the duration of the test time histories. This condition is satisfied in the case of only 4 records: Records 3, 9, 17, and 18. The duration of Records 13 and 31 is less than the threshold duration of 20 sec in one of the horizontal directions.

3.2.7 Cumulative Specific Kinetic Energy

A summary of a kinetic energy study is presented in Figure 3.18, which shows the cumulative specific kinetic energy, CSKE, as defined in Appendix A. CSKE in the vertical direction is generally several times less than that in the corresponding horizontal direction. Since CSKE computation is based on the integration of a velocity time history, the latter result is consistent with the PGV difference for the vertical and the horizontal directions (Fig. 3.3).

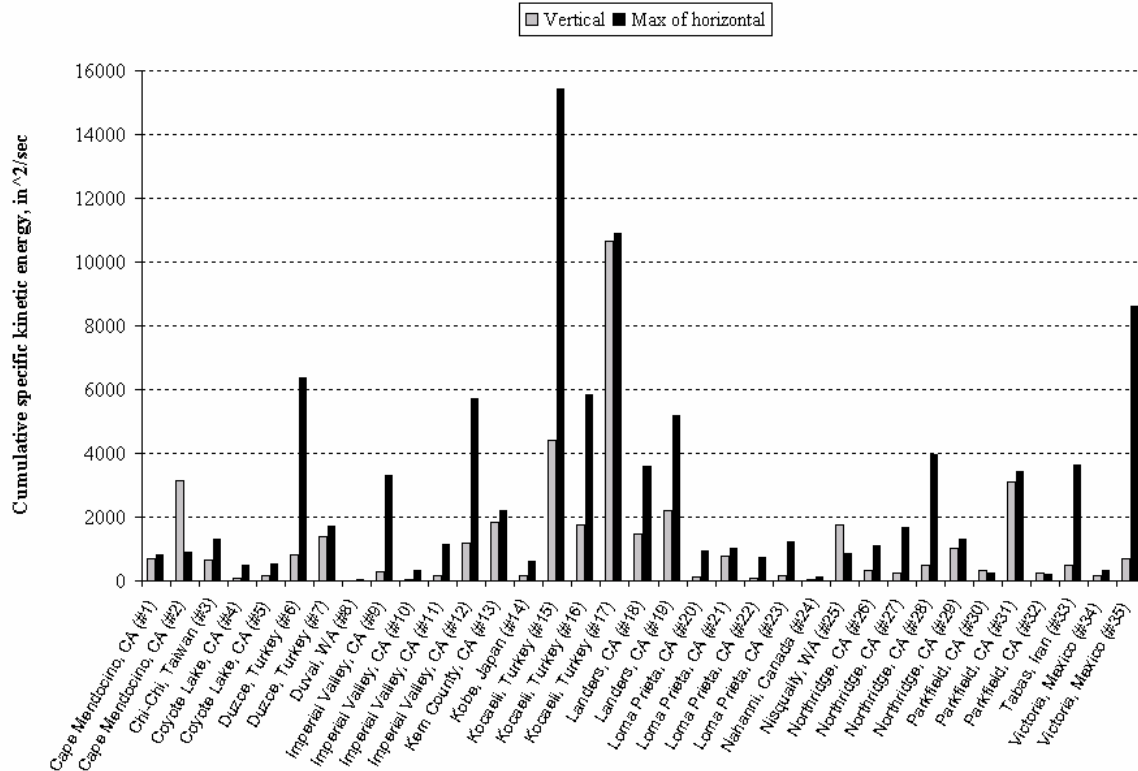


Fig. 3.18 Cumulative specific kinetic energy for normalized accelerograms

3.3 RECORD SELECTION FOR TEST TIME HISTORY AND ITS PARAMETERS

3.3.1 Candidate Selection for Test Time History from 35 Records

The main purpose of examining parameters and characteristics of the strong motion records in Table 3.1 is to select a candidate that would serve as a test time history for seismic qualification testing of electrical equipment. The analysis conducted in the previous section shows that only four strong motion records fully comply with the IEEE requirement on the duration. If the duration of the record is calculated based on the cumulative energy definition, the list of records is increased by two, namely Records 13 and 31. The records with a duration of at least 20 sec in all directions (for both duration definitions) are presented in Table 3.4.

Record 17 can be omitted from further consideration because it represents strong motion recorded far away from the source at 39.2 mi (62.7 km). Record 3 represents the Chi-Chi, Taiwan, earthquake and was recorded at the rock-like site (type 1), so it is not representative of sites with soft soil. Record 13 and Record 31 have low PGA and would require large scaling factors if used.

Table 3.4 List of records with duration longer than 20 sec (IEEE and CE definitions)

No.	Earthquake	D km	Site	PGV		PGA	
				Vertical in./sec	Max Horizontal in./sec	Vertical g	Max Horizontal g
3	Chi-Chi, Taiwan	10.0	1	10.0	24.1	0.39	0.74
9	Imperial Valley	8.3	D	4.2	11.7	0.21	0.31
13	Kern County	41.0	D	2.6	6.9	0.11	0.18
17	Kocaeli, Turkey	62.7	D	4.1	8.8	0.05	0.11
18	Landers, CA	11.6	C	5.9	17.0	0.18	0.28
31	Parkfield	14.7	B	1.8	2.7	0.05	0.06

The two remaining records from Table 3.4 are the 1940 Imperial Valley El Centro record, extensively used in the past for seismic analysis and testing, and the 1992 Landers record from the Joshua Tree station. The Landers record has several advantages compared with the El Centro record. The Landers record has about 50% greater PGV (17.0 in./sec) than the El Centro record (11.7 in./sec), and the strong part to duration ratio for the Landers record is about 60%, whereas in the El Centro record, it is about 40%. In addition, the Landers record has greater cumulative specific kinetic energy than the El Centro record (Fig. 3.18), and after scaling to 1.0 g PGA, the Landers record has more total cumulative energy than that of the scaled El Centro record, as shown in Figure 3.12. The El Centro record has more cycle counts than the Landers record, as shown in Figure 3.9; the difference is not significant and this problem can be improved during the record modification procedure (in order to match the IEEE 693 required spectra).

Based on this discussion, the best time history for use in the seismic qualification tests of electrical equipment is the Landers strong motion record (Record 18). The final summary of the parameters of the Landers record is presented in Figure 3.19. The plot shows the relation between the mean and the mean-plus-one standard deviation for each parameter and the corresponding value for the Landers record (all values are computed for the normalized records, except the first two parameters computed for original records). All values are normalized by the corresponding mean calculated for all 35 records. The plot demonstrates that the Landers record is a robust strong motion time history: its parameters are greater than mean for all of the parameters of normalized records, and when a parameter exceeds the mean value, it is close to or exceeds the mean-plus-one standard deviation for the set.

3.3.2 SDOF System Response Parameters and PSD for Landers Record (Record 18)

PSD and spectra. In this section PSD and elastic response spectra for the Landers record are compared with the mean and the mean-plus-one standard deviation for 35 strong motion records. The PSD for the Landers record obtained for the 0 degree direction (Landers000) is presented in Figure 3.20. The frequency content of the Landers000 is richer in the low-frequency range compared to the mean PSD, since it was recorded at soil type C site within 7.5 mi (12 km) from the source. As a result, the spectrum for the Landers000 has higher peaks in the low-frequency range than the mean spectra, although the average of peaks and dips from 0.8–3 Hz is in vicinity of the IEEE spectrum (Fig. 3.21). The Landers000 has low-frequency content in the high-frequency range (the spectrum is lower than the IEEE spectrum starting from 3 Hz); therefore this part of the frequency range has to be enriched during the spectral matching procedure.

The PSD for the Landers record in 90 degree direction (Landers090) is presented in Figure 3.22. The frequency content of Landers090 is also richer in the low-frequency range than the mean PSD and is slightly richer in high frequencies compared with Landers000. On average, the Landers090 spectrum is greater than the mean spectrum up to 1.7 Hz and in the 2.7–4.7 Hz frequency range, as shown in Figure 3.23.

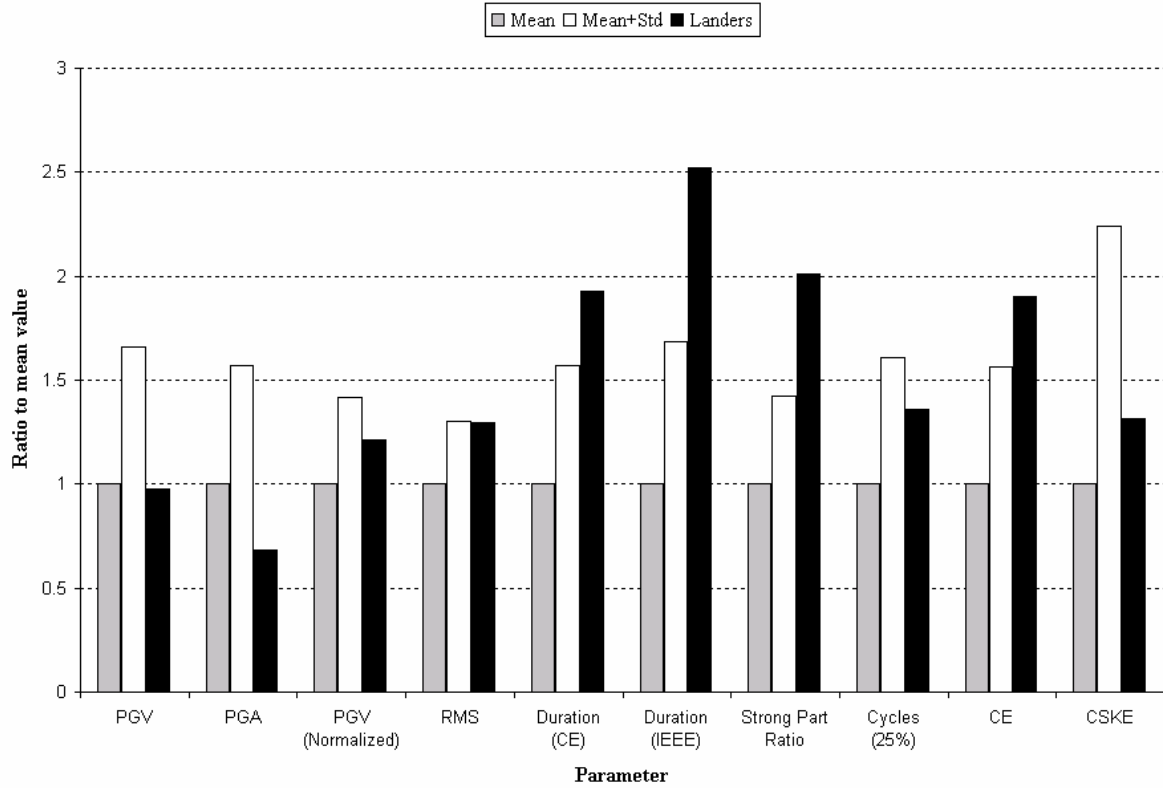


Fig. 3.19 Landers record (Record 18) vs. mean and mean-plus-one standard deviation of the set

Number of high cycles in SDOF response. Cycle number counts with 70% magnitude threshold for Record 18 are plotted in Figure 3.24 and compared with the cycle counts for the set of 35 records. In general they repeat the trend of the mean and the mean-plus-one standard deviation. On average, the Landers record in both directions produces a number of cycles that are greater than the mean and close to the mean-plus-one deviation for the set. For both directions the number of high cycles is limited to one cycle at only three frequencies.

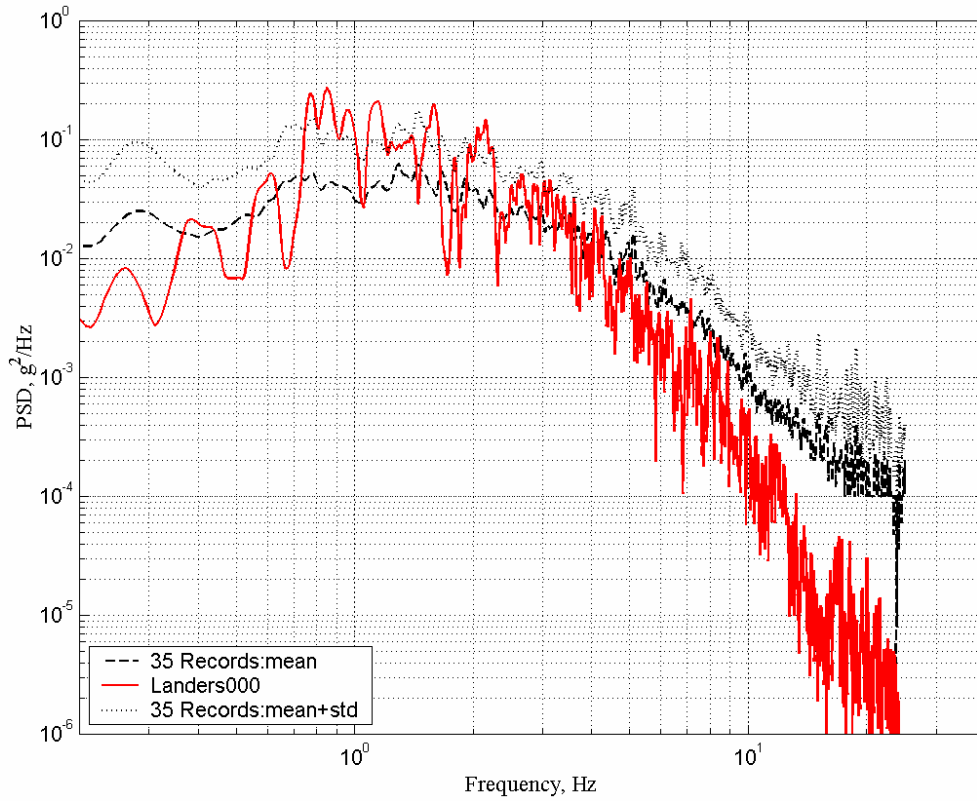


Fig. 3.20 Smoothed PSD of Landers000 vs. mean and mean-plus-one deviation for 35 records

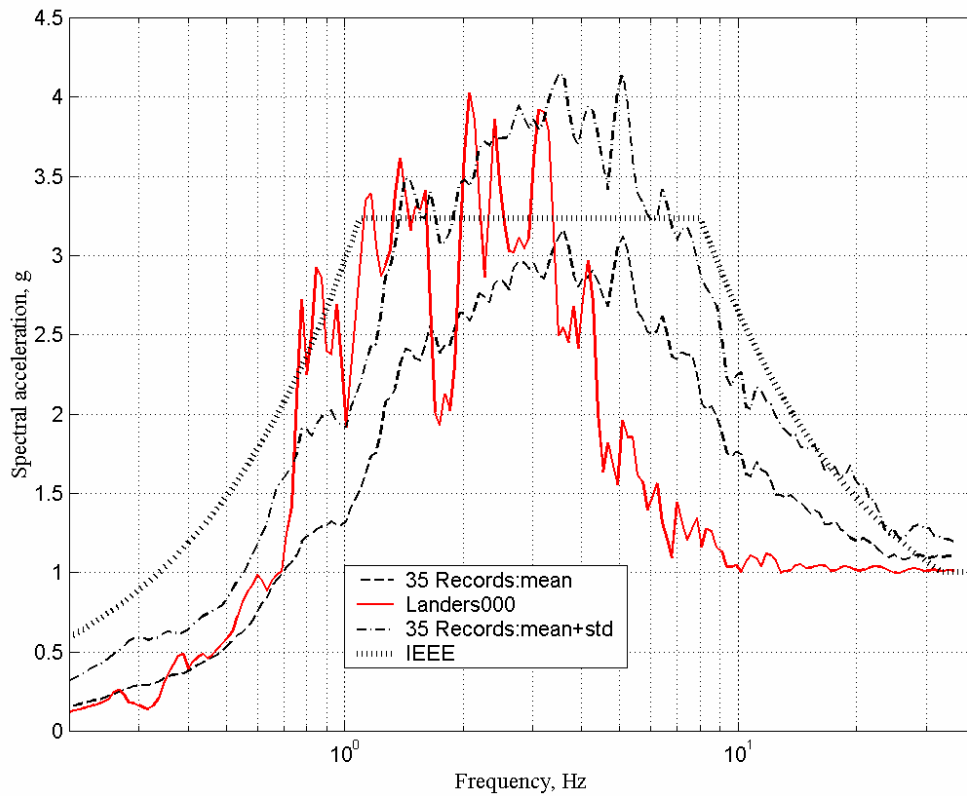


Fig. 3.21 Spectrum of Landers000 vs. mean and mean-plus-one deviation for 35 records

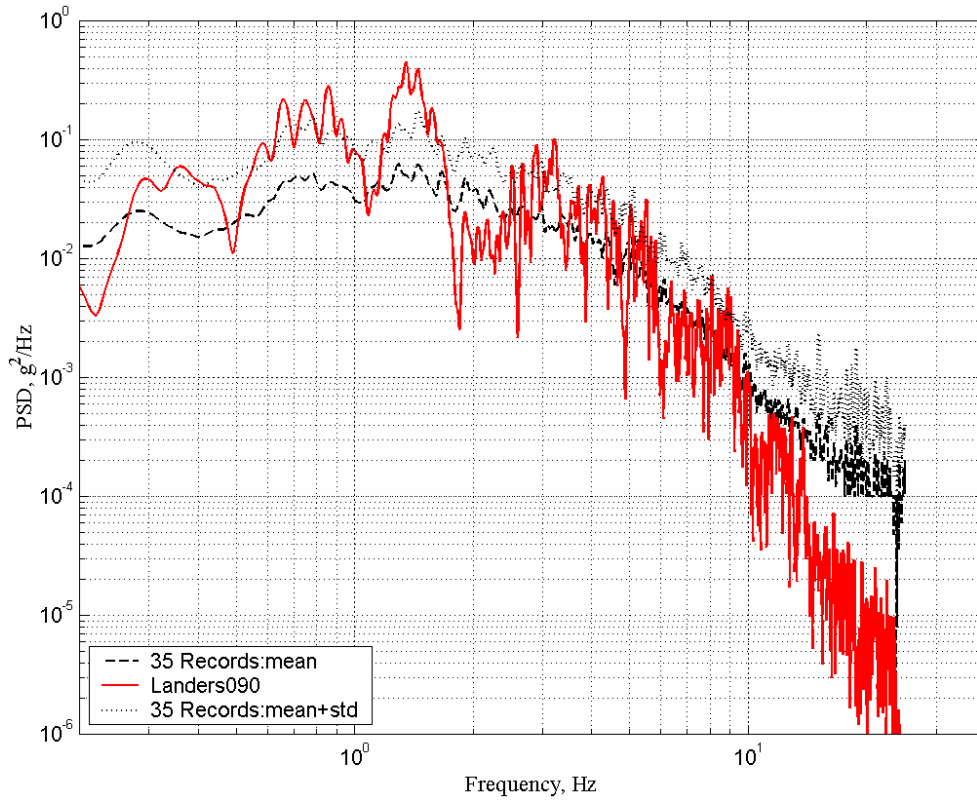


Fig. 3.22 Smoothed PSD of Landers090 vs. mean and mean-plus-one deviation for 35 records

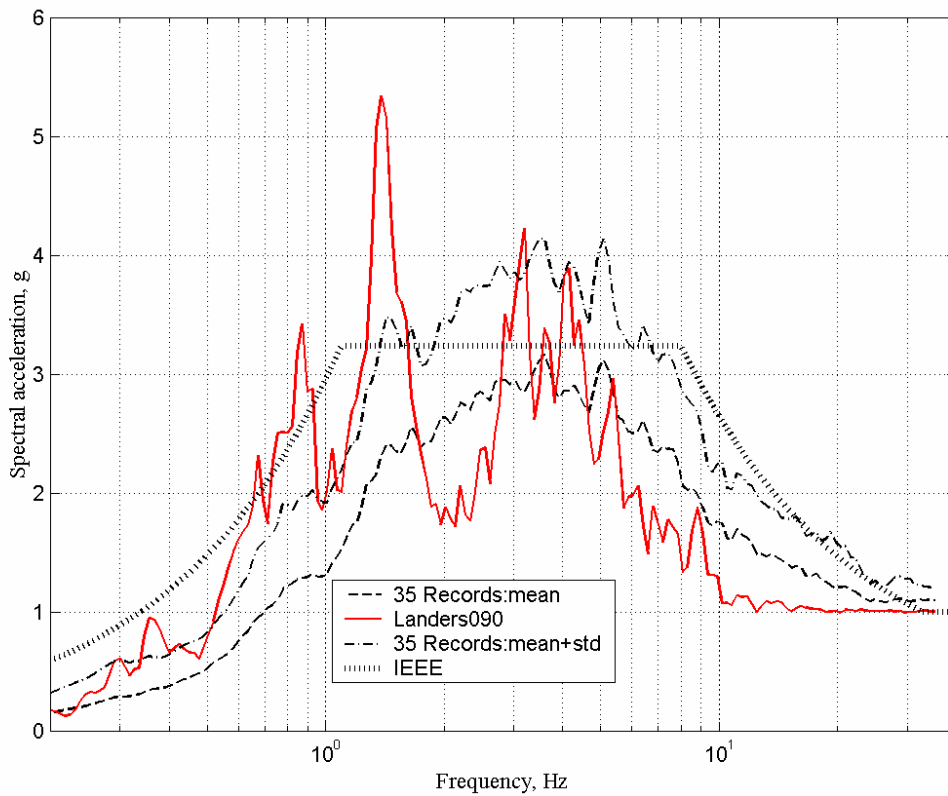


Fig. 3.23 Spectrum of Landers090 vs. mean and mean-plus-one deviation for 35 records

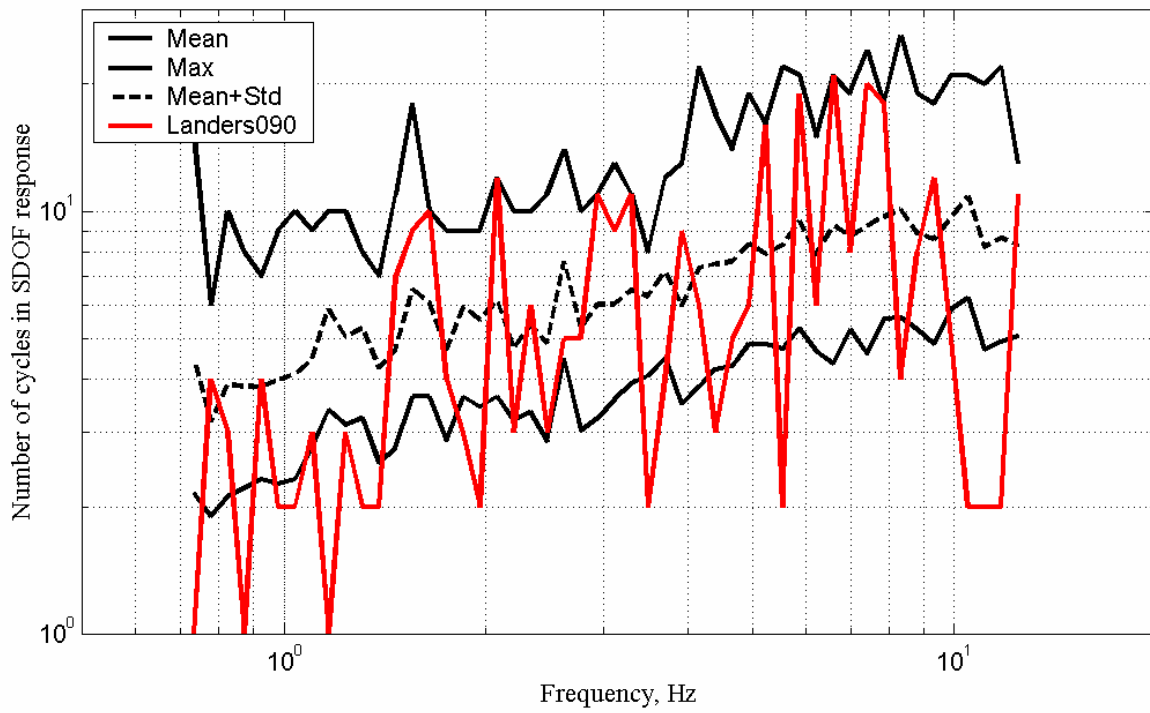
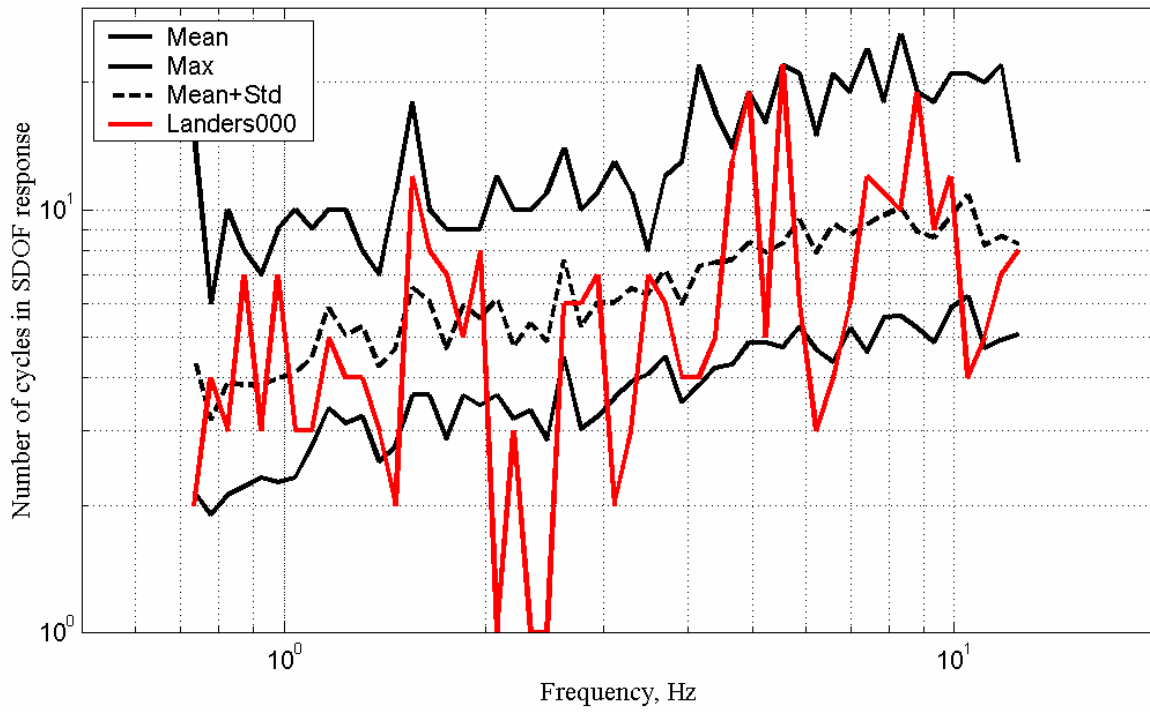


Fig. 3.24 Number of high cycles in SDOF response for Record 18 vs. set of 35 records

3.3.3 Details of Landers Strong Motion Time History (Record 18)

This short section presents information on the 1992 Landers earthquake and the location of Joshua Tree station, since the Landers record was selected as the best candidate for a test time history. The magnitude 7.5 earthquake that occurred near Landers, California, on June 28, 1992, is one of the largest events that occurred in California. Landers is a small town in the Mojave Desert about 43 km north of Palm Springs and 80 km east of San Bernardino. The analysis by the USGS and Caltech (USGS and Caltech, 1992) indicates that the earthquake had a right-lateral strike-slip mechanism. The maximum horizontal offset was reported to be as much as 21 ft. A large set of strong motion time histories was recorded at a number of stations during the earthquake. Extensive faulting was observed during the earthquake along the Camp Rock fault system, which trends northwestward across the Mojave Desert and away from the Joshua Tree station where Record 18 was obtained. The station was the closest the epicenter. The most significant aspect of all records from the Landers earthquake is their long duration caused from the initial earthquake triggering another strong rupture along the Camp Rock fault system.

3.4 SUMMARY AND CONCLUSIONS

Based on the detailed study on the set of 35 strong motion time histories the following conclusions are made. The Joshua Tree acceleration record obtained during the 1992 Landers, California, earthquake represents a robust strong motion time history. The normalized Landers record has several advantages among other strong motions studied: (1) The duration of the Landers record computed for the IEEE and the CE definitions is longer than the 20 sec required by the IEEE 693 standard. (2) The Landers record has the maximum value (among all records studied) for the strong part to duration ratio (about 60%). (3) After scaling to 1.0g PGA, the Landers record has a total cumulative energy that exceeds the mean-plus-one standard deviation of the set. (4) The value of the RMS acceleration for the record is very close to the mean-plus-one standard deviation of the set. (5) The PGV of the normalized Landers record is very close to the mean-plus-one deviation of the set. (6) The number of cycles with 25% threshold in the accelerogram is higher than the mean for the set. (7) The Landers record is a broadband strong motion time history. (8) The number of cycles in the acceleration response of a SDOF system has adequately even distribution in a wide range of the natural frequencies of the system.

As discussed in Appendix C, the analysis based on a study of the low-magnitude earthquakes that occurred in the central and eastern U.S. showed the following: (1) Low-magnitude earthquakes tend to have more high-frequency energy. (2) Earthquakes on rock tend to have more energy in the high-frequency range due to low damping in hard central and eastern rocks. (3) For eastern and central U.S. sites, the IEEE spectral shape is probably too low (high seismic hazard regions, based on current NEHRP estimates). The analysis based on study of MCE spectra at major seismic hazard regions revealed the following conclusions: The IEEE procedure of qualification testing is appropriate for most seismic regions of the U.S. except the central U.S. (CUS). Current hazard estimates provided in NEHRP maps of the CUS indicate that high hazard areas, such as around Memphis, Tennessee, have MCE spectra that exceed the IEEE 693 PL spectra, particularly in the frequency range above 8 Hz. Spectral enveloping of these sites would principally require shifting the plateau of the IEEE 693 spectrum toward the high-frequency side for type A sites, and both frequency-shifting and increasing the spectral acceleration by about 20% for site types B, C, and D. A more detailed discussion is provided in Appendix C. The paucity of strong motion data from central/eastern U.S. earthquakes highlights the need for additional research in order to provide improved estimates of seismic hazards in the region.

4 Development of Response-Spectrum-Compatible Time History

This chapter discusses the advantages and disadvantages of the time domain and frequency domain procedures that are generally used for the development of a response-spectrum-compatible strong motion time history (Preumont, 1978). Due to a number of advantages outlined in the discussion, the time domain procedure was selected as a spectrum matching procedure to develop the IEEE response-spectrum-compatible time history from the Landers (Joshua Tree) record.

Both the time and frequency domain procedures have several implementations available either commercially or in open source. The procedures are discussed in examples of three programs, each representing distinct approaches to a spectrum matching problem. The matching procedure in the time domain is a FORTRAN implementation of the algorithm developed by Abrahamson (Abrahamson, 1996). This chapter discusses two frequency domain procedure programs that are available in an open source. The first one modifies an original earthquake record in the frequency domain and generates a spectrum-compatible time history; the code is written to run in the Matlab environment and was commonly used at the PEER test laboratory. The code can be downloaded from the PEER website presenting all deliverables of the study (http://peer.berkeley.edu/lifelines/Task408_411/Task408.html). The second implementation is a FORTRAN-based program named “SimQke-1” (that can be downloaded from the NISEE website: <http://nisee.berkeley.edu/software/simqke1/>) that generates a synthetic time history, the spectrum of which matches the target spectrum.

4.1 SPECTRUM MATCHING PROCEDURE IN TIME DOMAIN

4.1.1 Description of Time Domain Matching Procedure

Generally, a matching procedure in the frequency domain does not have good convergence properties, particularly for multiple damping spectra. An alternative approach adjusts the reference time history in the time domain by adding wavelets to it. Kaul (Kaul, 1978) proposed a formal optimization procedure for this type of time domain matching that was extended to an algorithm to simultaneously match spectra at multiple damping values developed by Lilhanand and Tseng (Lilhanand and Tseng, 1987 and 1988). One of the main advantages of the time domain procedure is that in most cases it preserves the non-stationary character of the reference time history. The procedure has good convergence properties for several damping values, although it is more complex compared to the frequency domain approach.

A modification to the Lilhanand and Tseng algorithm developed by Abrahamson (Abrahamson, 1996) produces realistic displacement time histories in addition to realistic acceleration and velocity time histories, especially at long periods. The procedure modifies the time history by adding a special type of short duration wavelets to the reference time history. The executable file is called “match.exe”; version 2.2b of the program was used in the study.

4.1.2 Spectral Matching of Landers (Joshua Tree) Record in Time Domain

The original three-component time history recorded at the Joshua Tree station during the Landers 1992 earthquake was scaled to 1.0g PGA for the two horizontal components and up to 0.8g PGA for the vertical component. The time domain matching procedure was used to modify the historic Landers record and match its spectrum to the IEEE high PL spectra at 2% and 5% damping. The PGAs of the modified acceleration time histories in three principal directions are very close to that of the scaled original time history; namely the modified time history has 1.0g PGA in the X direction, 0.99g PGA in the Y direction, and 0.80g PGA in the Z direction. Figures 4.1–4.4 present results of the matching procedure application. Figure 4.1 presents a three-component strong motion time history for the original Landers-Joshua Tree record and three components of the IEEE-compatible time history modified by the time domain procedure.

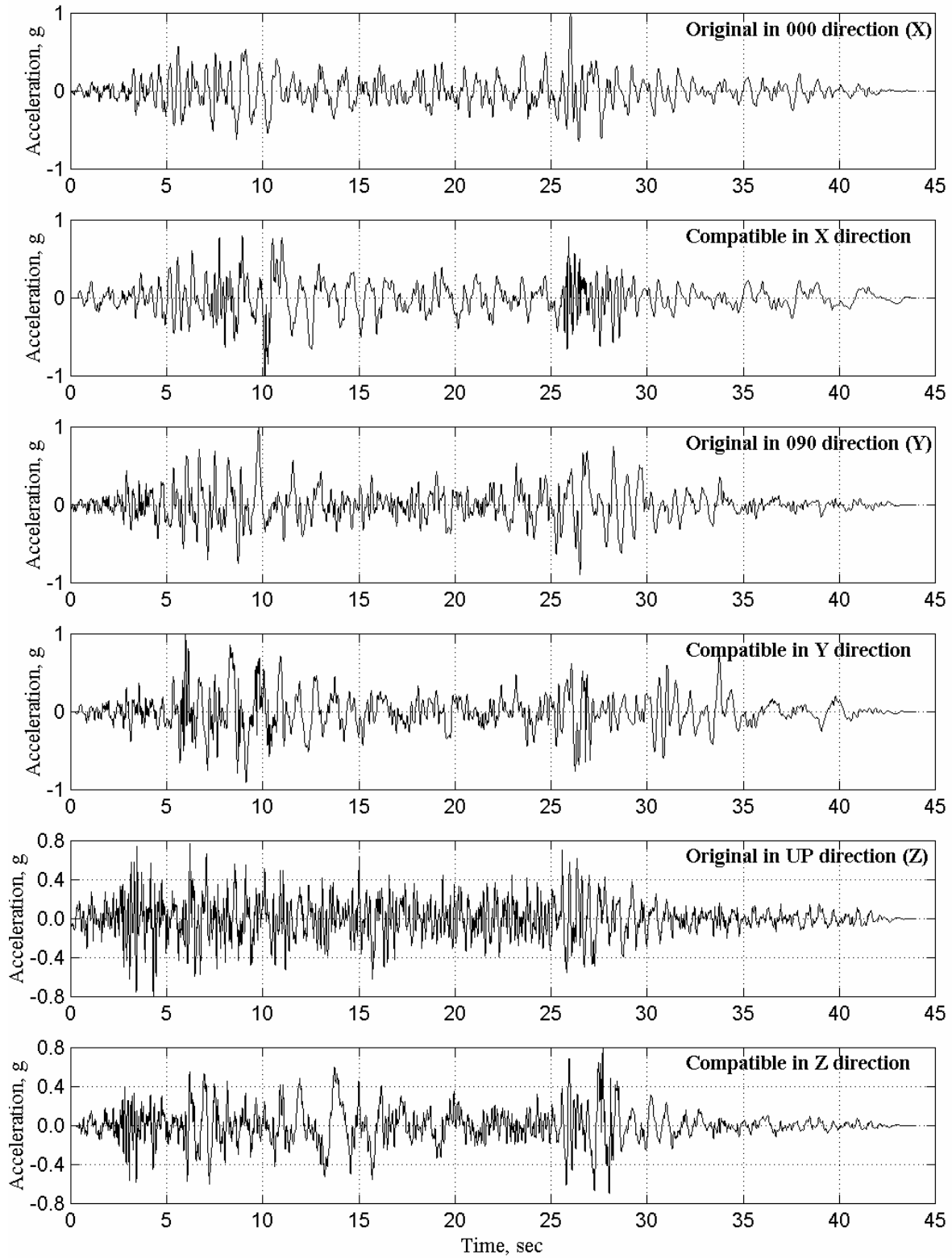


Fig. 4.1 Original and IEEE spectrum-compatible Landers time histories

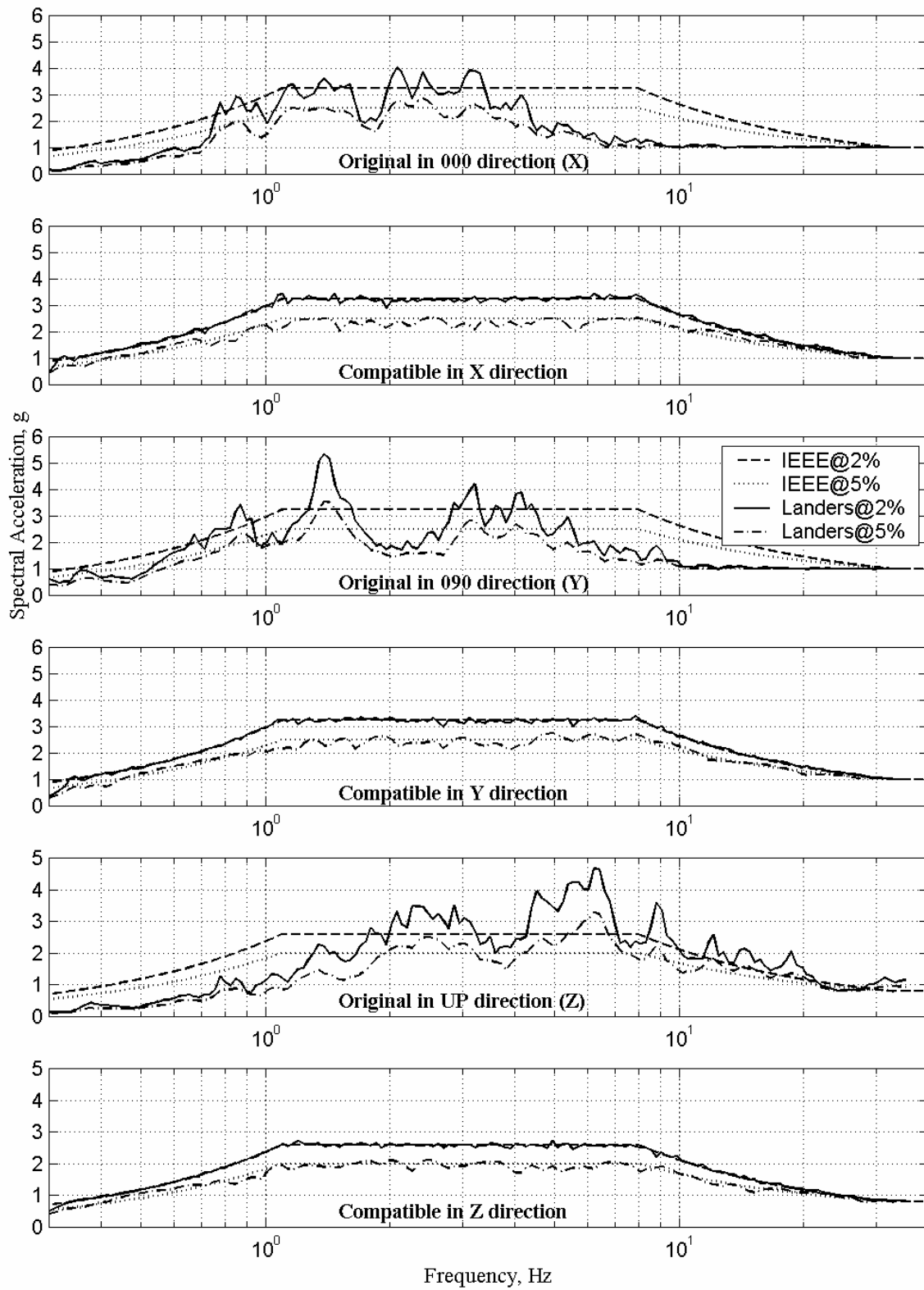


Fig. 4.2 Response spectra for original and IEEE-spectrum-compatible Landers time histories

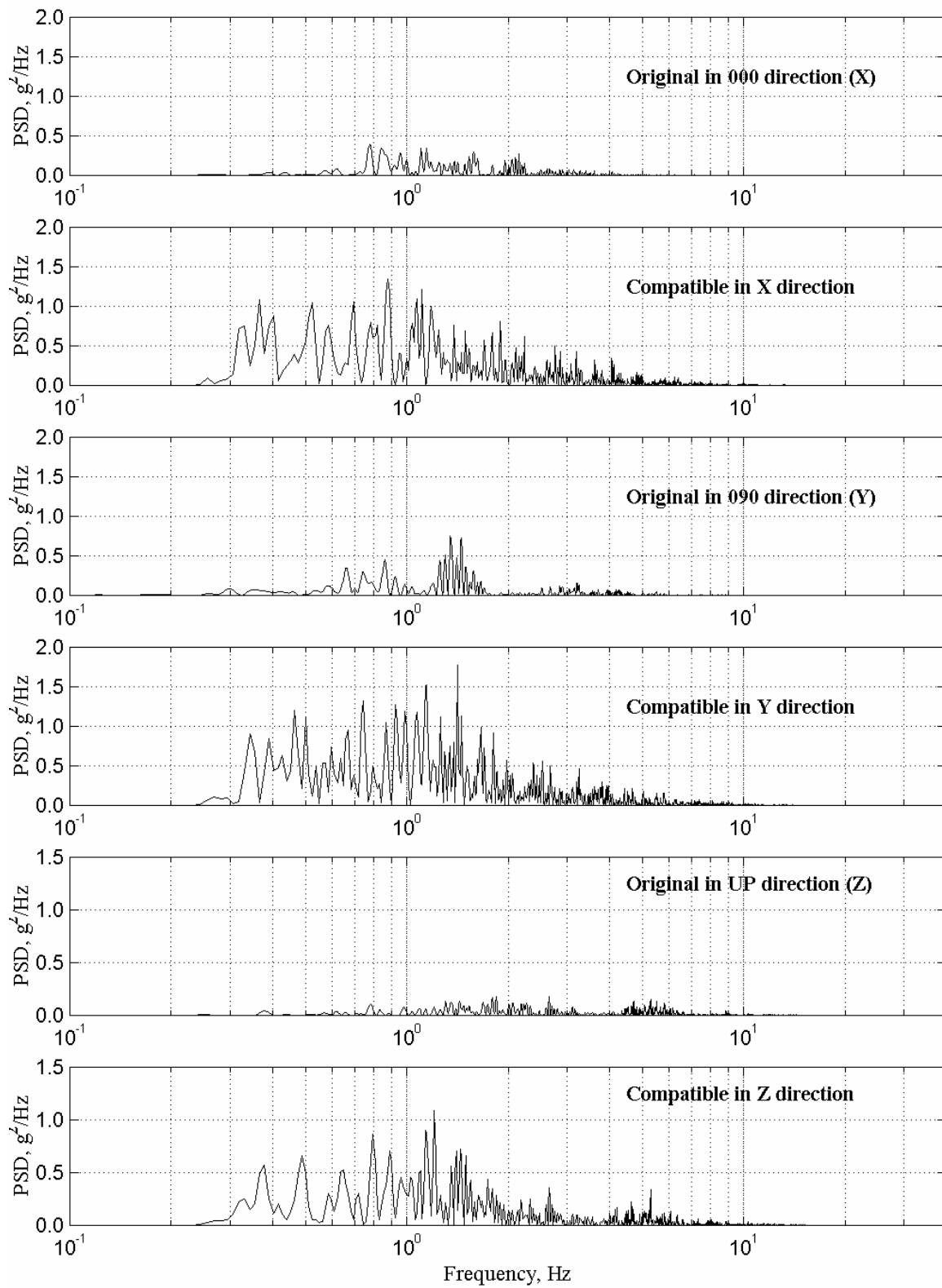


Fig. 4.3 Power spectral density for original and IEEE-compatible Landers time histories

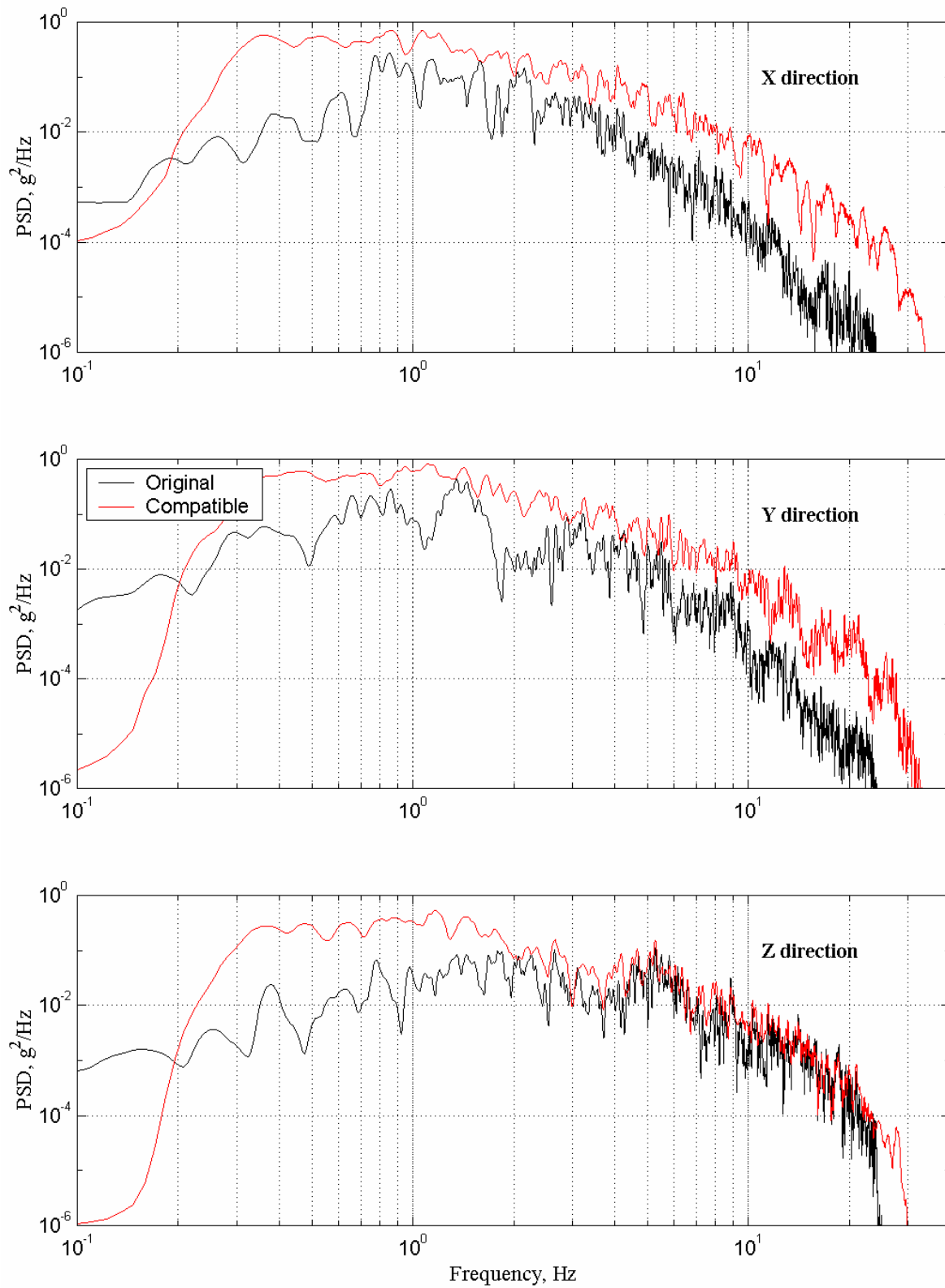


Fig. 4.4 Smoothed PSD for original and IEEE-spectrum-compatible Landers time histories

The elastic response spectra for 2% and 5% damping are presented in Figure 4.2. The response spectra match the target response spectra for both values of critical damping. Figure 4.3 presents a power spectral density of the modified Landers acceleration time history compared with the original one. The frequency content of the modified time history was significantly enriched in the low-frequency and high-frequency ranges for all three components. The magnitude of the power spectral density was increased in a wide range of frequencies also. The log-log plots of smoothed PSD before and after application of the modification procedure are presented in Figure 4.4.

4.2 SPECTRAL MATCHING OF REFERENCE TIME HISTORY IN FREQUENCY DOMAIN

4.2.1 Procedure for Response Fit in Frequency Domain

The procedure aimed at matching a reference strong motion to a target response spectrum in the frequency domain uses the discrete Fourier transforms. In this case the Fourier amplitudes of a reference time history are adjusted based on a ratio between the target response spectrum and that for the reference time history. At this point the adjusted transforms are transformed back to a time domain. To assure zero accelerations at the start and end time step, the inverse Fourier transform of the modified time history is multiplied by a tapering function. The procedure is usually repeated for a specified number of iterations.

The procedure adjusts the Fourier magnitudes of the time history without changing the Fourier phases and, as a result, the modified time history has the same frequency content as the reference time history. Therefore, in a case when the reference time history has a deficit in some range of frequency, this range cannot be enriched as was done for the matching procedure in the time domain. Another disadvantage of the procedure is that it does not have good convergence for multiple damping spectra. The time history matched to a target response spectrum for one damping generally produces a significant misfit between the target and the time history response spectrum for another damping.

4.2.2 Spectral Matching Results for Response Fit in Frequency Domain

The Landers time history recorded at the Joshua Tree station was chosen to demonstrate the performance of the response fit procedure. The reference time history was matched by the procedure at a critical damping of 2%. Figure 4.5 presents the original and the modified acceleration time histories. The phase angles of the vibrations were preserved and only magnitudes were changed.

Figure 4.6 shows the elastic response spectra before and after the procedure application. The plots show close matching only for one critical damping, of 2%. The plot of the elastic response spectrum for the time history calculated for 5% damping shows a significant misfit relative to the target response spectrum for all three components.

Because the procedure adjusts only magnitudes of Fourier transforms without changing the phase angles, there is very limited change or no change at all in the frequency content of the modified signal, as shown in Figure 4.7. The changes are made for the magnitudes of the Fourier transforms only, including some amplification of the transform magnitudes in the high-frequency range as shown in these plots. This increase of the high-frequency oscillations can be observed in the time history plots in Figure 4.5. The smoothed PSD plots in log-log scale before and after the procedure application are shown in Figure 4.8.

4.3 SYNTHETIC ACCELEROGRAM MATCHING TARGET SPECTRA (SimQke)

4.3.1 General Description of Procedure for Generating Synthetic Time Histories

SimQke-1 generates statistically independent accelerograms, performs a baseline correlation on the generated motions to ensure zero final ground velocity, and calculates response spectra. The program was developed by Vanmarcke and others (Vanmarcke, 1976; Gasparini, 1976). The later modifications were performed by T. Blake for the PC DOS version in 1990.

The program generates a synthetic time history, which response spectra match, or which are compatible with a set of specified smooth response spectra. The basis for the spectrum-compatible time history generation is the relationship between the response spectrum values for specified damping and the “expected” Fourier amplitudes of the ground motion. The time history is synthesized by superimposing sinusoidal components with pseudo-random phase angles and

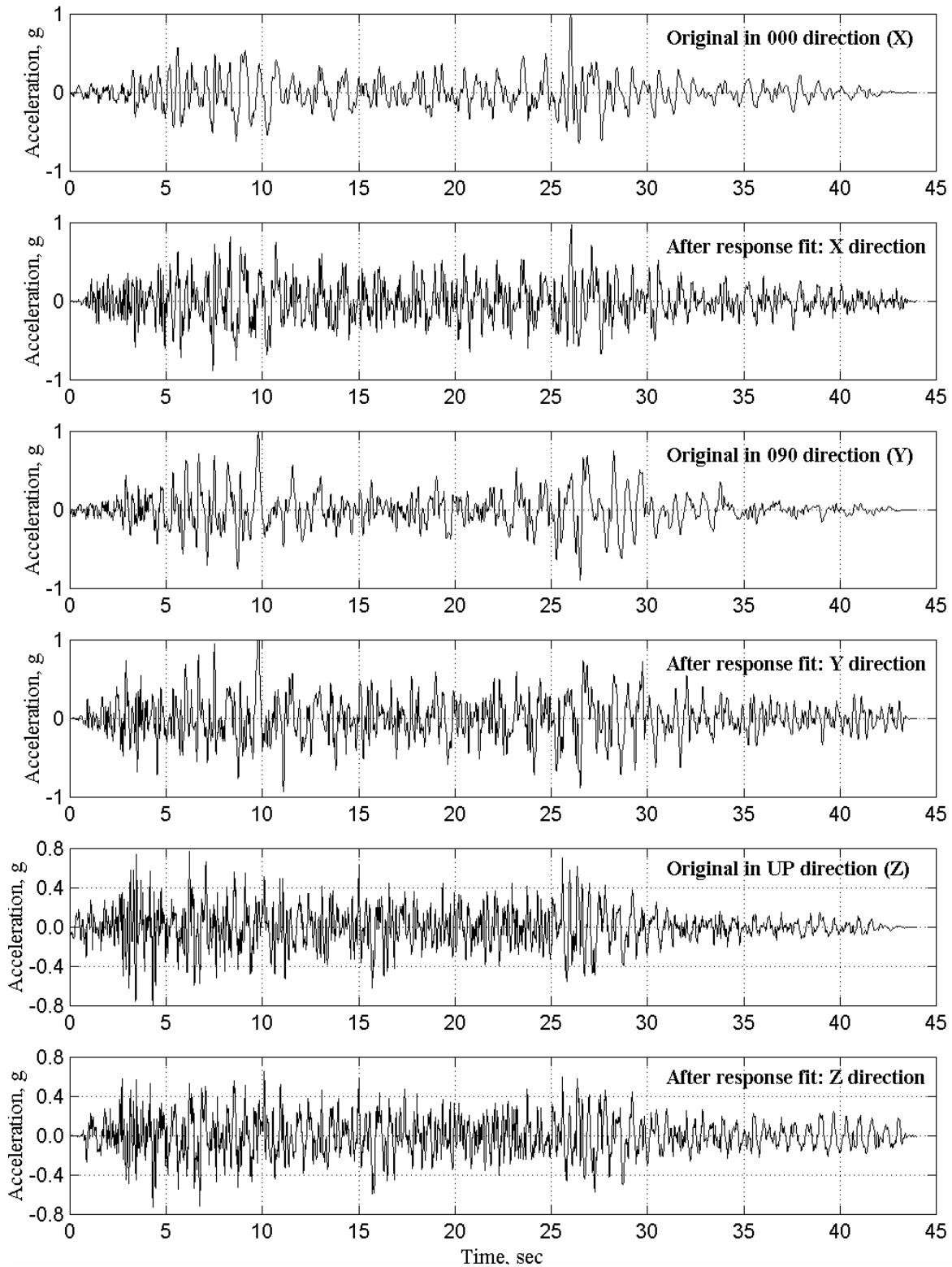


Fig. 4.5 Original and IEEE-compatible (frequency domain) Landers time histories

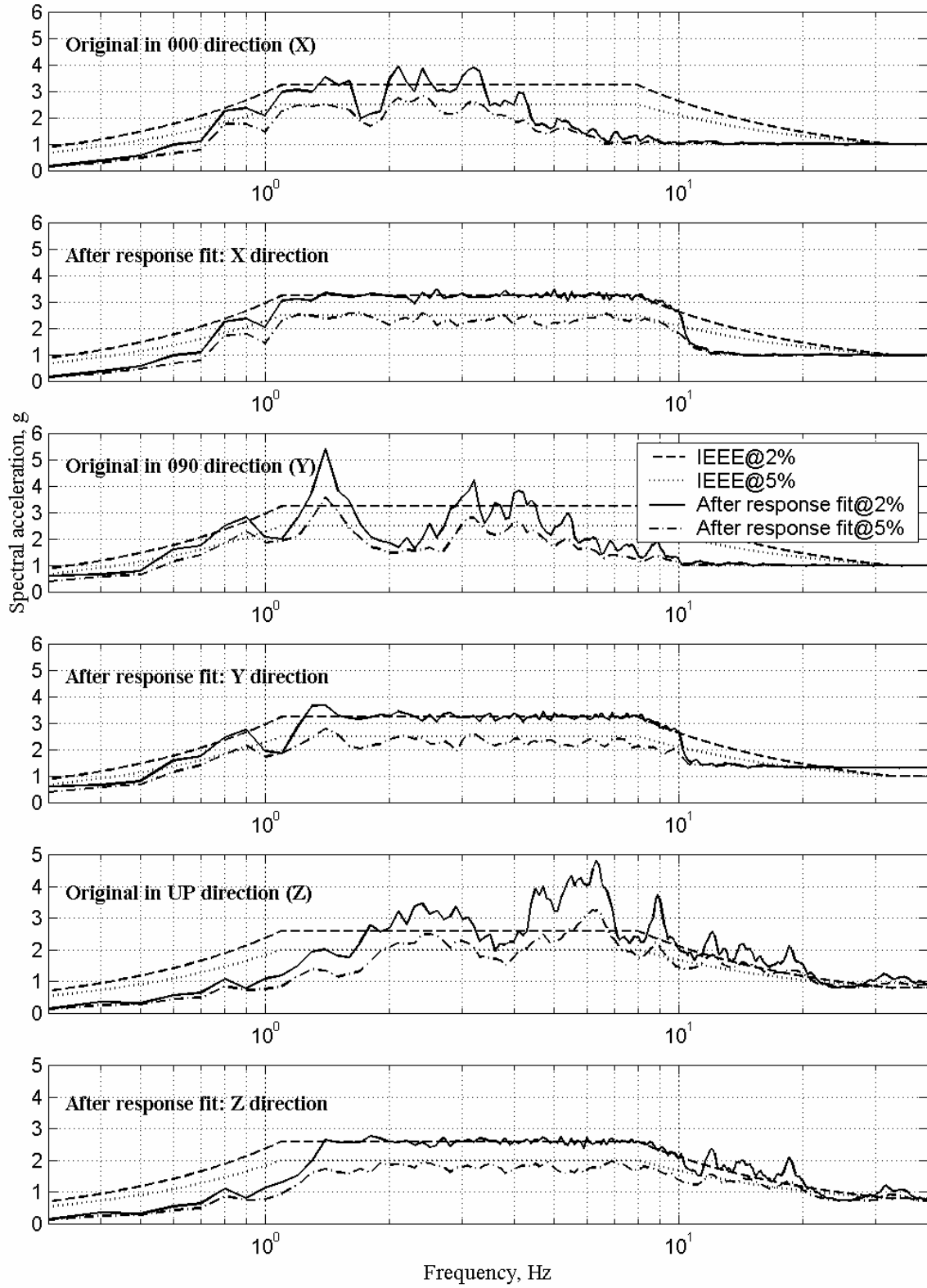


Fig. 4.6 Spectra for original and IEEE-compatible (frequency domain) Landers time histories

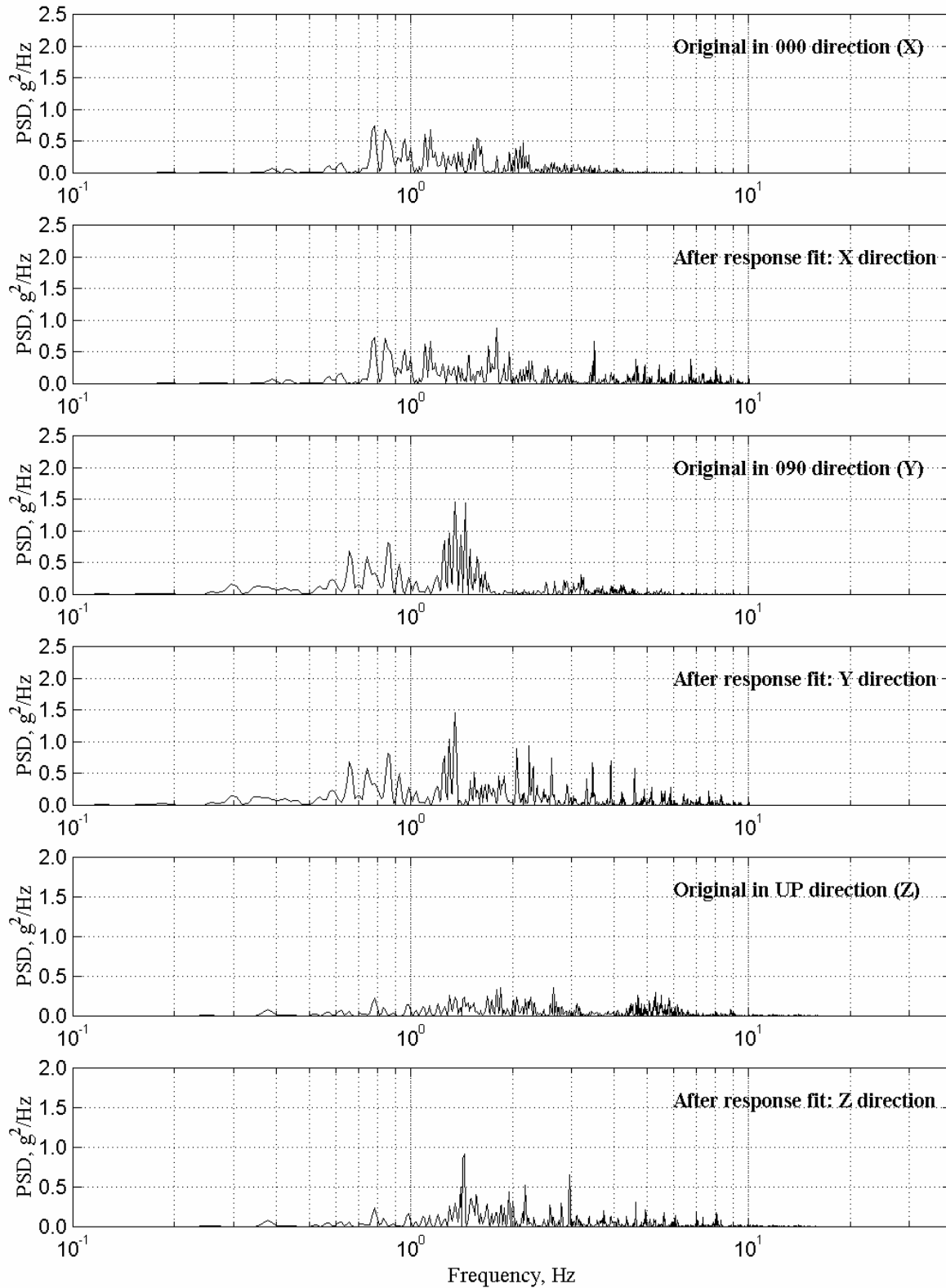


Fig. 4.7 PSD for original and IEEE-compatible (frequency domain) Landers signals

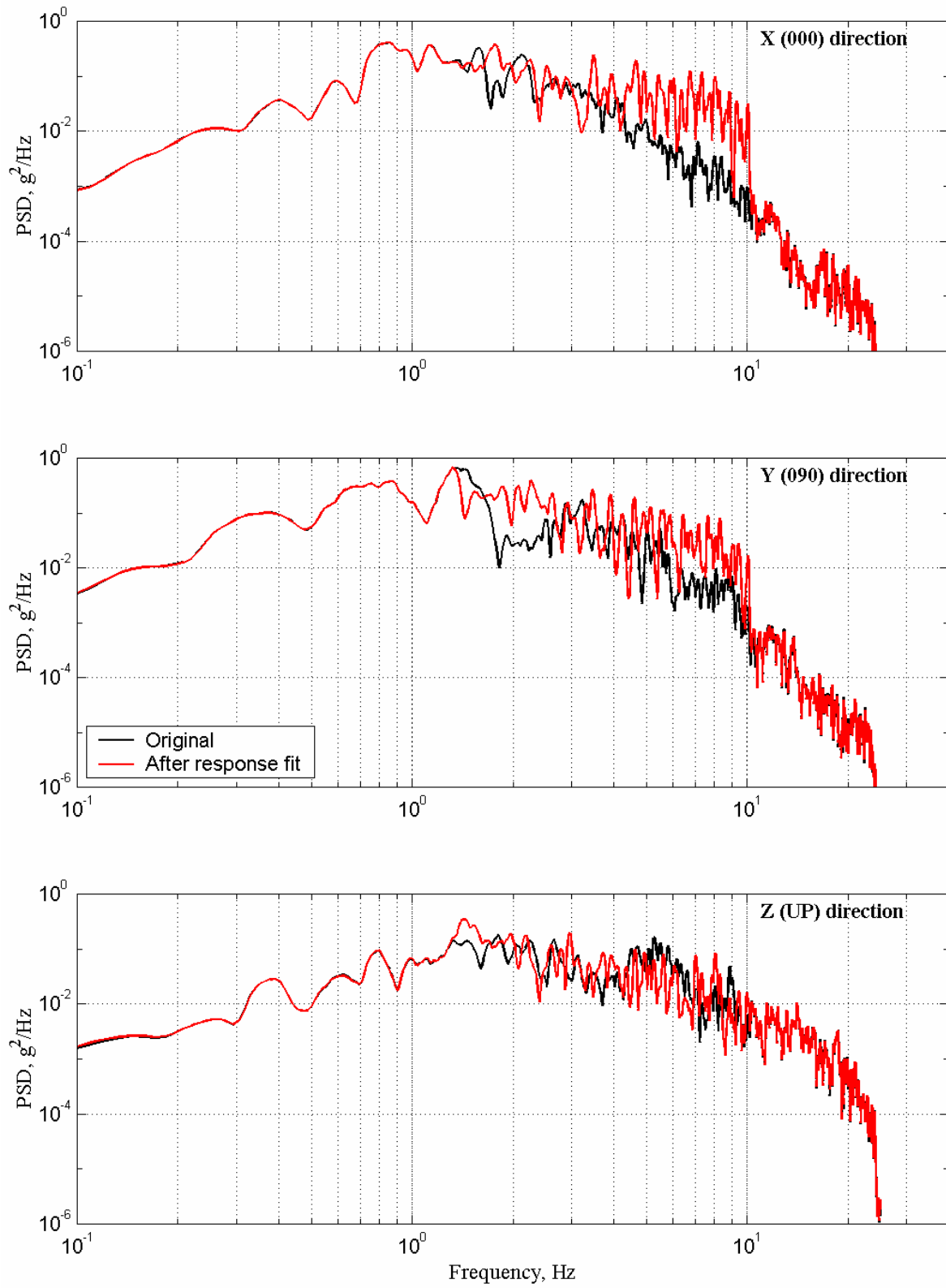


Fig. 4.8 Smoothed PSD for original and IEEE-compatible (frequency domain) Landers signals

by multiplying the resulting stationary trace by a user-specified function representing the variation of ground motion intensity with time (a tapered function). The program SimQke-1 adjusts, by iteration, the ordinates of the spectral density function to improve the agreement between computed and target response spectra.

4.3.2 Results for Synthetic Generation of Strong Motion Time History

Figure 4.9 presents a summary of the results for a synthetic strong motion time history generated by SimQke-1. The top plot shows the time history that obviously has a stationary character because it consists only of harmonics tapered at the beginning and end of the signal. The frequency content of the time history is evenly distributed over the duration of the signal, whereas in the case of an historic record, such as the Landers (Joshua Tree) record, this distribution would be strongly time dependent (compare the top plots of Figs. 4.1 and 4.9).

The middle plot in Figure 4.9 presents the elastic response for the signal versus the IEEE spectra at 2% and 5% damping. The signal was generated to be IEEE spectrum compatible at 2% damping; therefore, it matches the corresponding IEEE spectrum at this damping. The spectra misfit is much greater than that for the spectrum obtained by the time domain matching procedure (Fig. 4.2). As discussed previously, this is a general problem of all procedures based on frequency domain matching. The bottom plot in Figure 4.9 shows that the generated synthetic signal has a rich frequency content in a broad range of frequencies.

4.4 COMPARISON OF FREQUENCY CONTENT FOR TIME HISTORIES MODIFIED BY MATCHING PROCEDURES

4.4.1 PSD Comparison

A comparison between PSD plots for the IEEE-compatible time histories produced by matching procedures is presented in Figure 4.10. All PSD plots (except the plot for the mean of 35 historic strong motion time histories) were smoothed by averaging over seven frequencies. The comparison is focused only on discussion of the modified time histories in the X direction. The PSD for the synthetic signal generated by SimQke-1 is, in general, greater than all other PSD plots from the other matching procedures. The time domain matching procedure produces a time history in which the PSD is somewhat close to the PSD of the synthetic record and has the same

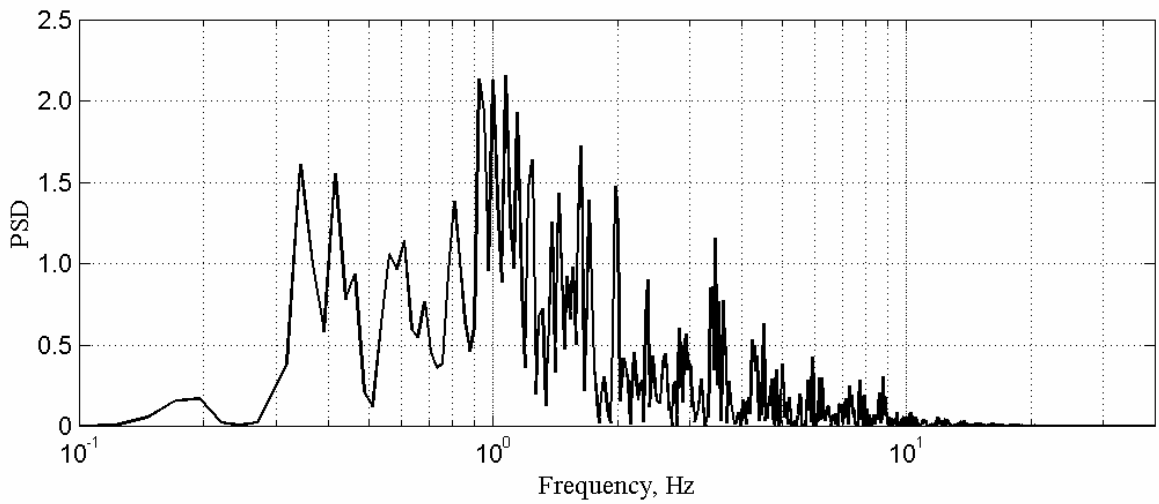
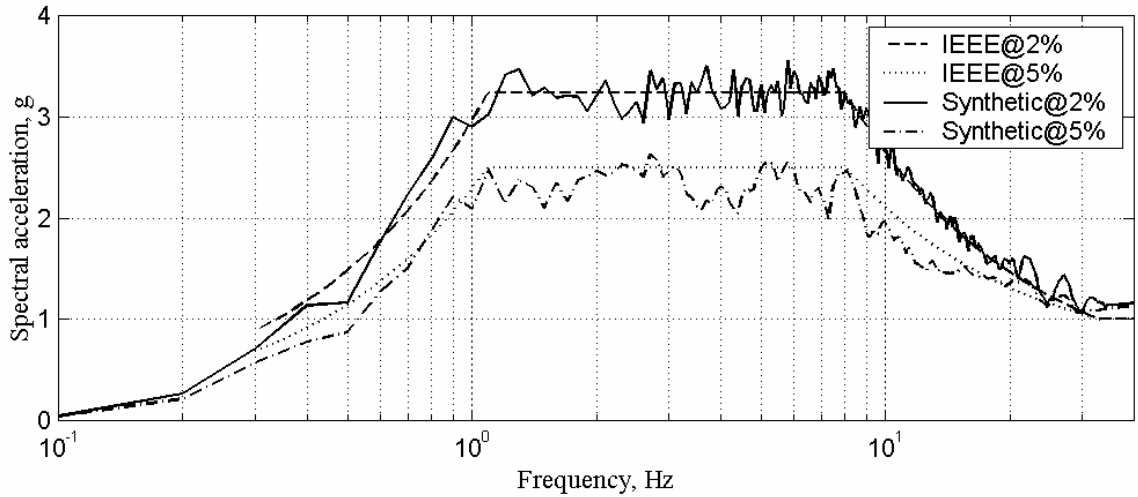
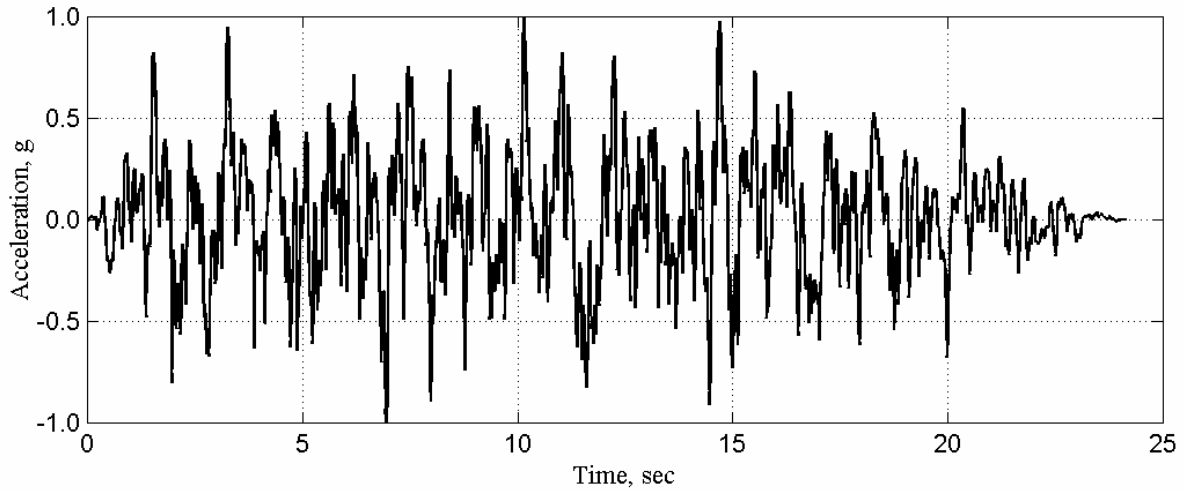


Fig. 4.9 Synthetic strong motion time history generated by means of SimQke-1

trend of even amplitude attenuation in the high-frequency range. In contrast to these two procedures, the response fit procedure produces a time history in which the PSD has quite a large variation from its mean and does not evenly decay in the high-frequency range.

4.4.2 Time-Dependent Frequency Analysis (Spectrogram)

A time-dependent frequency analysis or spectrogram is a useful tool to understand how the frequency content of a record changes over its duration. Figure 4.11a presents a spectrogram for the historic Landers record in the 0 degree direction (X component), whereas Figure 4.11b presents the spectrogram for the IEEE-compatible time history by using the time domain procedure. The spectrogram for the IEEE-compatible time history modified by the frequency domain procedure is shown in Figure 4.11c, and last, the spectrogram for a synthetically generated time history is plotted in Figure 4.11d. The plot colors depend upon the magnitude's modulus of the Fourier transforms and corresponds to dark red when the modulus reaches the maximum.

The earthquake record (Fig. 4.11a) is non-stationary because its frequency content strongly depends on time. The record's frequency content is broader at the beginning of the signal and becomes narrower toward the end of the time history where the content mostly consists of frequencies below 10 Hz, which would be expected for the accelerogram recorded in the forward-directivity zone near the fault.

The IEEE-compatible strong motion time history preserves this non-stationary behavior of the historic strong motion and adds short duration wavelets to match the IEEE spectra, as shown in Figure 4.11b. The wavelets with short duration were added to the reference time history at optimal times, so the spectrogram is strongly time dependent. The wavelets were added at multiple locations along the duration of the time history with a noticeable concentration around 10 sec and 25 sec that are related to locations of two different peaks in the acceleration time history of the reference record. The deficiency of the original Landers record in the high-frequency range was fixed by these high-frequency wavelets.

The frequency response procedure also delivers a time history in which the frequency content is less dependent on time (Fig. 4.11c), a common problem for all frequency domain trend of even amplitude attenuation in the high-frequency range. In contrast to these two procedures, the response fit procedures. The same problem was encountered for the synthetically generated

time history that consists of harmonics tapered at the beginning and end of the signal in order to simulate an earthquake record. Therefore the frequency content changes insignificantly over duration of the time history, as shown in Figure 4.11d.

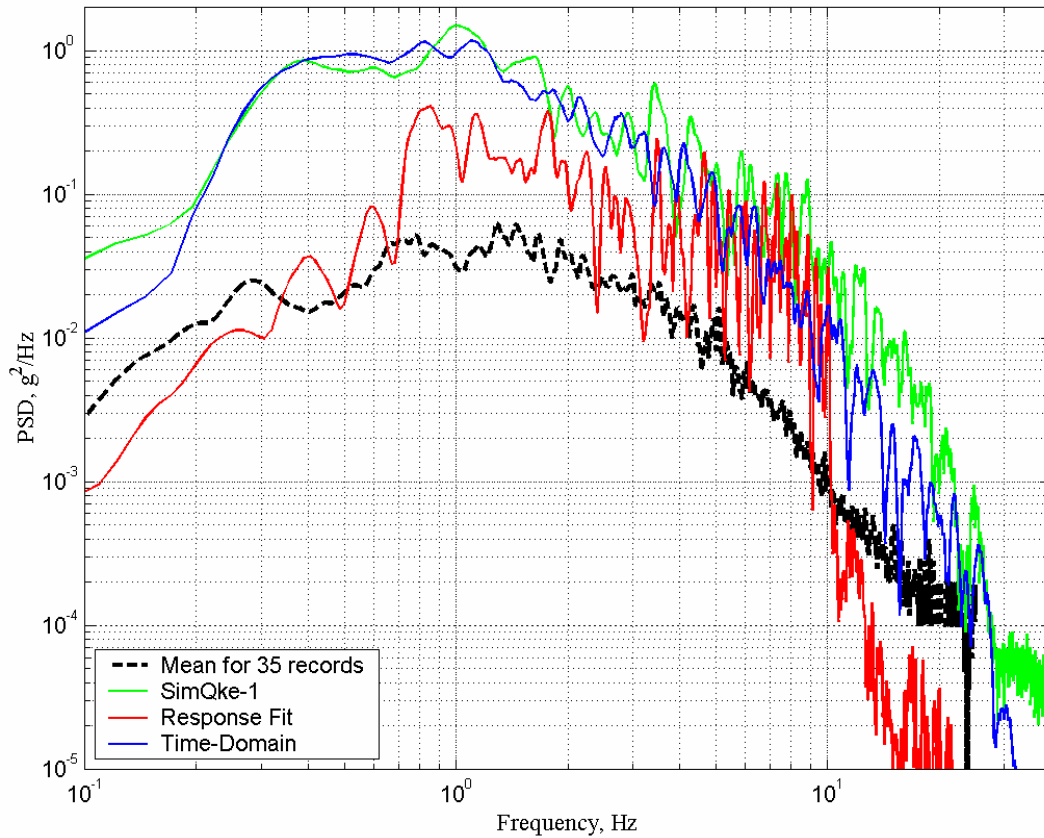


Fig. 4.10 Smoothed PSD for IEEE-compatible time histories generated by various matching procedures (X direction)

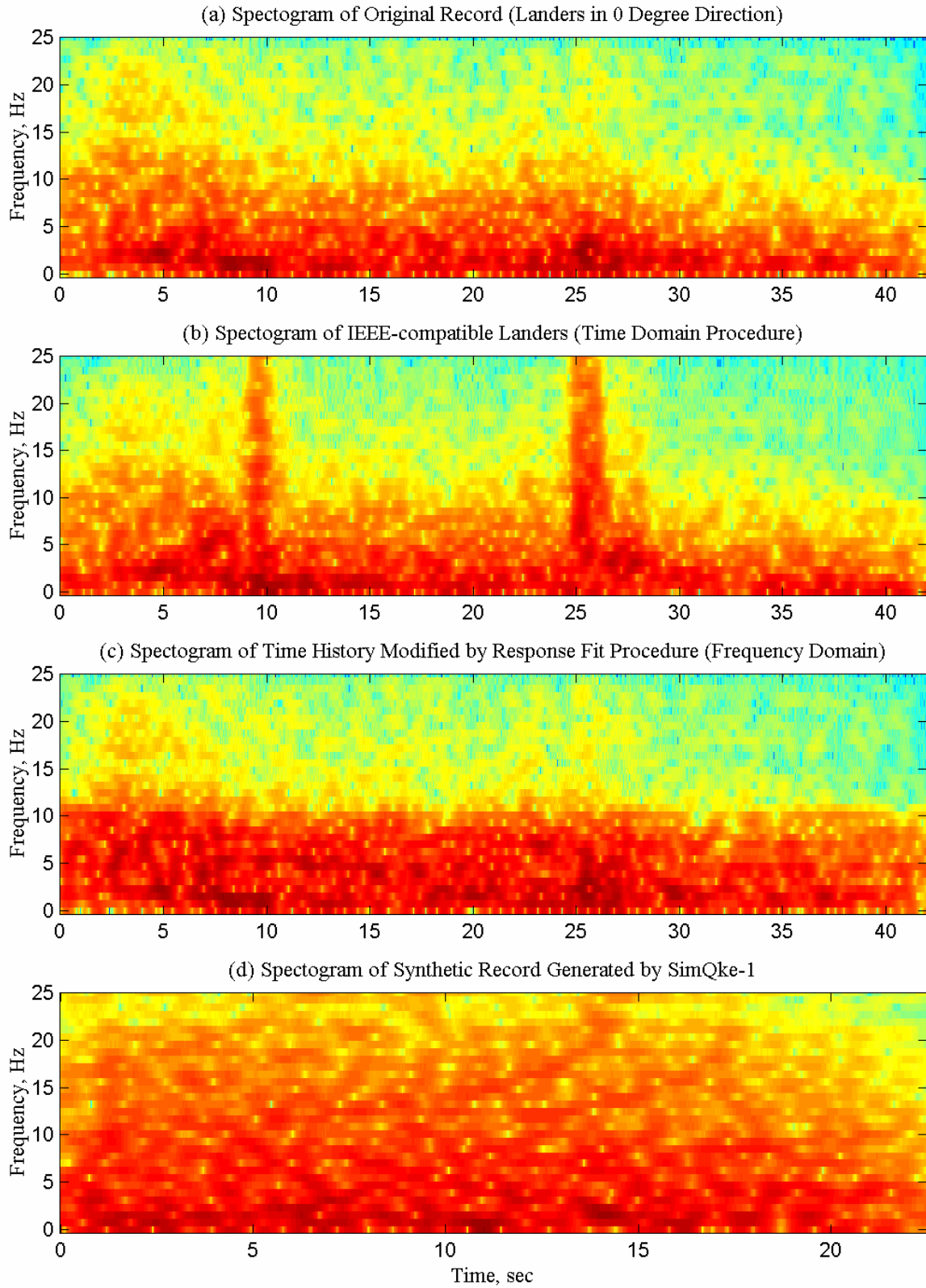


Fig. 4.11 Time-dependent frequency content of synthetic, reference, and IEEE-compatible signals (X direction)

4.5 CONCLUSIONS

The advantages of the time domain matching procedure and the IEEE-compatible Landers test time history are as follows. First, the modifications introduced do not alter the non-stationary character of a reference historic record. Second, the target spectrum can be matched with low deviation from it at several damping values. Third, the power spectral density of the signal is evenly enriched in a wide frequency range and is strongly time dependent, which is characteristic of an actual strong motion record.

In contrast to the time domain procedure, the frequency domain matching procedure can introduce an undesirable high-frequency noise in the time history. The time history matched to the target spectrum at one damping can significantly misfit the target response spectrum for another damping. The power spectral density is not as even as that for the time history produced by the time domain method.

Although the synthetically generated signal has a rich frequency content, its strongly stationary characteristic is opposite that of an actual record. Thus, the frequency content of the synthetic time history changes insignificantly over its duration. The spectrum of the synthetic time history mostly matches the target spectrum only at one damping, and the spectra misfit is not as small as that for the time domain matching procedure.

Based on this analysis of response spectrum matching procedures, the IEEE-response-spectra-compatible time history using the time domain matching procedure is recommended for qualification testing of electrical substation equipment. The IEEE-compatible strong motion time history modified from the Landers historic record is also called TestQke4IEEE in the report. It can be accessed and downloaded from the Internet via a website of the West Coast Subcommittee of the IEEE 693 at <http://www.westcoastsubcommittee.com/ieee693/spectra/spectrums.htm> or from the PEER's website at http://peer.berkeley.edu/lifelines/Task408_411/Task408.html.

5 Input Time Histories for Earthquake Simulators

This chapter presents information on existing and planned earthquake simulators in the U.S. A filtering procedure needed to modify the IEEE-compatible time history that will accommodate the limitations of the simulators is also discussed. Two versions of an input time history for the EERC earthquake simulator filtered from the IEEE-compatible Landers (TestQke4IEEE) are presented. The chapter presents characteristics of the IEEE-compatible Landers time history (TestQke4IEEE) in comparison with other input time histories for earthquake simulators used in qualification testing of electrical substation equipment.

5.1 MAJOR EXISTING AND FUTURE U.S. EARTHQUAKE SIMULATORS

According to the IEEE 693 standard (IEEE, 1998), a seismic qualification test on electrical equipment shall be conducted with a random time history strong motion on an earthquake simulator. Each earthquake simulator, or “shake table,” has specific limitations on performance. The capacity of the shake table usually includes limitations on the number of degrees of freedom of the simulator, a maximum payload, a maximum displacement stroke in available test directions, a maximum velocity and acceleration of loading, a maximum geometric size for the specimen, and the test frequency range.

The list of major existing earthquake simulators in the U.S. is presented in Table 5.1. The table expands a similar list presented in the report on Task 410 under the PEER/PG&E Lifelines Project (Nigbor and Kallinikidou, 2002) and shows an additional parameter for the vertical clearance above the shake table platform. The value in the brackets presents the clearance above the earthquake simulator platform up to a crane hook. The parameter limits the maximum height of the electrical equipment intended for seismic qualification testing.

In late 1999, the National Science Foundation (NSF) launched a major new research initiative known as the “George E. Brown, Jr. Network for Earthquake Engineering Simulation (NEES).” This ten-year program, with capital outlays in excess of \$80 million will significantly transform the ability of the U.S. to carry out earthquake engineering research and to obtain information vital to developing improved methods for reducing the nation’s vulnerability to catastrophic earthquakes. The NEES equipment sites will be operated as shared-use facilities, and NEES will be implemented as a network-enabled collaboration.

Table 5.1 Existing major earthquake simulators in the U.S.

Institution	Payload (metric ton)	Size (m x m)	DOFs	Frequency range (Hz)	Max stroke (m)	Max velocity (m/s)	Clearance above table (m)
ANDI (Astro Nuclear/Dynamics, Inc., Pennsylvania)	5	3x3(hex)	6	NA	0.10	1.27	NA
EERC, University of California, Berkeley, California	63.5	6.1x6.1	6	0-15	0.127	0.76	11.5 (9.6)
State University of New York at Buffalo, New York	50	3.7x3.7	5	0.1-50	0.15	0.76	6.6 (NA)
University of California, San Diego, California	32.7	3.0x4.9	1	1-50	0.152	1.0	11.6 (10.6)
University of Nevada at Reno, Nevada	45	4.3x4.5	2	0.1-30	0.3	1.0	10.0 (8.2)
University of Illinois at Urbana- Campaign, Illinois	4.5	3.7x3.7	1	0.1-50	0.05	0.38	NA
CERL (U.S. Army, Civil Engineering Research Laboratory, Illinois)	54	3.6x3.6	3	0.1-60	0.3	1.3	11.2 (NA)
Wyle Laboratories, Alabama	27	6.1x6.1	2	0-100	0.152	0.89	NA

Under the NEES program, experimental facilities with earthquake simulators will be significantly upgraded or built at three universities: the State University of New York at Buffalo, the University of Nevada, Reno, and the University of California, San Diego. Table 5.2 presents a summary of the capacities of the planned NEES earthquake simulators.

Table 5.2 Future NEES earthquake simulators in the U.S.

Institution	Total payload (metric ton)	Size (m x m)	Number of tables	DOFs	Frequency range (Hz)	Max stroke (m)	Max velocity (m/s)	Clearance above table (m)	Max distance between tables (m)
State University of New York at Buffalo, New York	2x50	3.7x3.7	2	6	0.1-50	0.15	1.25/0.5	NA	30.0
University of Nevada at Reno, Nevada	3x45	4.3x4.5	3	2	0.1-30	0.3	1.0	10.0 (8.2)	36.5
University of California, San Diego, California	2000	7.6x12.2	1	1	1-20	0.75	1.8	No limit	NA

5.1.1 Examples of Existing Earthquake Simulator Facilities

Earthquake Simulation Laboratory at EERC, UC Berkeley. The central feature of the laboratory is the 20 ft x 20 ft (6.1 m x 6.1 m) earthquake simulator. The earthquake simulator is programmed to reproduce any waveform including any earthquake record within the capacities of force, velocity, displacement, and frequency of the system. It may be used to subject structures weighing up to 140,000 lbs (63.5 tons) to horizontal accelerations of 1.5g. An MTS controller performs the primary control of the shake table and provides a closed-loop control of motion on translation and rotation about three principal axes: a vertical axis and two horizontal ones. The controller is designed so that each of these six degrees of freedom can be programmed individually to run concurrently. The maximum stroke is 5.0 in. (0.127 m) in the horizontal direction and 2.0 in. (0.051 m) in the vertical. The maximum velocity of the earthquake simulator is 30 in./sec (0.76 m/sec) for lightweight testing models. Models of up to 38 ft (11.5 m) in height can be tested on the shake table.

The earthquake simulator is located in a 40 ft (12 m) high x 60 ft (18 m) wide x 120 ft (36m) long building, which is a separate, specially designed structure. The building is serviced by a 22,500 lbs (10-ton) bridge crane and has an adequate amount of space for test specimen assembly and instrumentation indoors, which simplifies the final erecting of equipment for testing on the shake table.

CERL. The original biaxial “shaker,” which began operating at CERL in Champaign, Illinois, in 1972, was funded under the Safeguard anti-ballistic missile program as part of a test facility for designing Safeguard ground support structures. The simulator therefore offered high-frequency, high-acceleration capabilities that were not available elsewhere.

The \$5 million earthquake simulator upgrade came as a result of the 1994 National Earthquake Hazards Reduction Program Act requiring federal agencies to develop inventories of their owned or leased buildings that are vulnerable to earthquakes and to provide cost estimates for reducing risks. After a two-year project to upgrade the CERL biaxial shaking table, the Triaxial Earthquake and Shock Simulator (TESS) came online and performed its first seismic test. Adding motion in the third axis allowed TESS to provide full six-degrees-of-freedom testing. This brought about more realistic modeling of seismic events and helps CERL researchers assess with higher accuracy the vulnerability of military, public, and private facilities to earthquakes.

TESS is the first mid-size capacity triaxial shake table being used in the U.S. It can subject scale model structures weighing up to 120,000 lbs (54 tons) to earthquake simulations. The Construction Engineering Research Laboratory (CERL) has performed both seismic and shock qualification testing of critical equipment on TESS.

Wyle. Wyle, located in El Segundo, California, provides compliance testing to nearly all major standards, including the IEEE and many other domestic and international requirements. Wyle is one of the commercial laboratories providing many testing services in various fields, including seismic qualification. Among the services the company offers is seismic testing using triaxial and biaxial electrohydraulic systems capable of simulating any possible earthquake for specimens weighing up to 60,000 lbs (27 tons).

ANDI. Seismic shake table technology was strongly influenced by experimental work in the 1960s and 1970s at the Westinghouse seismic testing facilities in Large, Pennsylvania. This facility eventually installed several pioneering shake tables and shock testing machines, and was where many of the concepts for the industry seismic test standards (IEEE-344) were developed and verified. In 1992 Astro Nuclear/Dynamics, Inc. (ANDI) purchased the test facilities and has continued to offer equipment qualification and dedication services to the nuclear industry, as well as to upgrade the test facilities.

As part of this upgrade, a five-ton capacity independent triaxial shake table (model R-6), data acquisition system, and digital chatter monitoring system were constructed. This

independent triaxial system supplements the existing biaxial tables at ANDI. The R-6 is capable of peak-to-peak displacements in excess of 8 in. (0.20 m), peak input velocity of 50 in./sec (1.25 m/sec), and peak acceleration (ZPA) of 2–4g's, depending on the test specimen weight. Peak spectral accelerations of 15g can be achieved on 5% response spectra. The top of the simulator platform is in the shape of a hexagon, 10 ft (3 m) across the flats.

5.1.2 Future Upgrades of Earthquake Simulator Facilities

Structural Engineering and Earthquake Simulation Laboratory (SEESL) at the State University of New York at Buffalo. Under the NEES program, the existing 14 ft x 14 ft (3.6 m x 3.6 m), 110,000 lbs (50 ton) shake table will be upgraded from 5 degrees of freedom (DOF) to 6 DOF by adding a transverse DOF. A new high-performance shake table with the same characteristics will be constructed.

An earthquake simulator system will consist of two high-performance, six-degrees-of-freedom shake tables, which can be repositioned from being directly adjacent to positions up to 100 ft (30 m) apart (center to center). Together, the tables can test specimens of up to 220,000 lbs (100 tons) and as long as 120 ft (36 m), and subject them to fully in-phase or uncorrelated dynamic excitations.

Nominal performance specifications for continuous uniaxial sinusoidal motion with a nominal 44,000 lb (20 ton) rigid specimen for each shake table are as follows. The table will be capable of developing a maximum stroke of 6 in. (0.15 m) in two horizontal directions and 3 in. (0.075 m) in the vertical direction. The peak velocity can reach 50 in./sec (1.25 m/sec) in both horizontal directions and 20 in./sec (0.50 m) in the vertical. The maximum acceleration can be as high as 1.15g for all three principal directions, with a 44,000 lb (20 ton) specimen on the table. The upgrade project also includes a new 89,000 lb (40 ton) crane to move specimens and their components onto and off the tables.

Large-Scale Structures Laboratory (LSSL) at the University of Nevada, Reno. The NEES upgrade converts the two existing tables from uniaxial to biaxial motion, and includes the installation of a third biaxial table. Manufactured by MTS, each table measures 17 ft x 17.7 ft (4.35 m x 4.50 m). Each table has a stroke of ± 12 in. (0.3 m), and can reach a peak velocity of 40 in./sec (1 m/sec) and an acceleration of ± 1 g under the full 100,000 lb (45 ton) payload in both

directions. All three shake tables will be relocatable with the same characteristics in both directions.

Together the three tables can host specimens of up to 300,000 lbs (135 tons) in total weight, and can be separated a minimum distance of about 30 ft (9 m) up to a maximum of 122 ft (36.5 m), center to center. Each table may be operated (1) independently of the other two tables, (2) in-phase with the other two tables, thus forming a single large table, or (3) differentially, with the other two tables for the simulation of spatial variation effects in earthquake ground motions.

The test and assembly are serviced by two 50,000 lbs (22 ton) overhead cranes with a clear height of 36.7 ft (11 m).

Large high-performance (LHP) outdoor shake table site at the University of California, San Diego (UCSD). This outdoor shake table will be a 25 ft x 40 ft (7.6 m x 12.2 m) single-degree-of-freedom earthquake simulator. The table will have a peak horizontal velocity of 70 in./sec (1.8 m/s), a maximum stroke of ± 30 in. (0.75 m), a maximum gravity (vertical) payload of 4.4 million lbs (2,000 tons), a maximum overturning moment of 37 million lb-ft (5,000 ton-m), a force capacity of actuators of 1.5 million lbs (680 tons), and a frequency bandwidth from 0–20 Hz.

The facility will be the only outdoor shake table in the U.S. and will enable large full-scale testing of structural systems and soil-foundation-structure interaction that cannot be readily extrapolated from testing at smaller scale, or under quasi-static or pseudo-dynamic test conditions, as well as testing large-scale systems to observe their response under near-source ground motion. The LHP outdoor shake table will be located about 10 miles (16 km) from the UCSD campus at the UCSD Camp Elliott field site. This site will allow room for multiple test specimens to be constructed and instrumented before placement on the shake table. A 40,000 lbs (17.7 ton) rough terrain crane will be provided at Camp Elliott for loading, unloading, and construction purposes.

5.2 IEEE-COMPATIBLE LANDERS AND FILTERING PROCEDURES TO ACCOMMODATE SIMULATOR CAPACITY

5.2.1 Properties of IEEE-Compatible Landers (TestQke4IEEE)

The IEEE-compatible Landers strong motion time history (TestQke4IEEE) was defined in the previous chapter. The spectra for IEEE-compatible Landers matches the IEEE spectra at

relatively high-frequency resolution, as presented in Figures 5.1a and b, which show the spectrum plots for 1/24 octave frequency bands. As do any elastic response spectra computed for a historic strong motion time history, the spectra of the IEEE-compatible Landers have many peaks and valleys. Maximum deviations from the IEEE spectra for 2% and 5% damping are presented in Table 5.3. The best match between the IEEE-compatible Landers spectra and the IEEE spectra is obtained for 2% damping as recommended by the IEEE 693 standard (IEEE, 1998). For instance, the signal in the X direction produces spectral accelerations that are only up to 10% below and 6% above the spectral plateau in the 1.1–8 Hz frequency range. The match between the IEEE-compatible Landers spectra and the IEEE spectra is slightly better for signals in the Y and Z directions, as shown in Table 5.3. For 2% damping the spectra for IEEE-compatible Landers do not fall below 10% and do not exceed 9% above the target response spectrum in all three principal directions and in a wide frequency range from 0.45–33.0 Hz (at 1/24 octave frequency resolution).

Therefore, the spectra for the IEEE-compatible Landers (TestQke4IEEE) at 2% damping have low deviation from the IEEE spectrum: the peaks are not higher than 15% above the IEEE spectrum and the spectrum dips do not fall below -15% of the target. Thus the spectra of the IEEE-compatible Landers are located within the 30% tolerance zone, as shown in Figure 5.1a. The spectra of the IEEE-compatible Landers at 5% damping also match the target spectrum, although the deviation is not as good as for 2% damping. Nevertheless, almost all spectral acceleration points from the 5% spectra are located inside the specified tolerance zone of 30%, as shown in Figure 5.1b.

Figure 5.2 presents the acceleration time histories for the IEEE-compatible Landers in three principal directions. As discussed before, the time histories were delivered from the historic Landers strong motion time histories by adding short duration wavelets. The modification preserved the non-stationary character and the general trend of the reference Landers history with the addition of two high-acceleration pulses. The first pulse is concentrated around the 10 sec mark, whereas the second starts at about the 25 sec mark. The peak ground accelerations in three principal directions for the IEEE-compatible Landers are presented in Table 5.4.

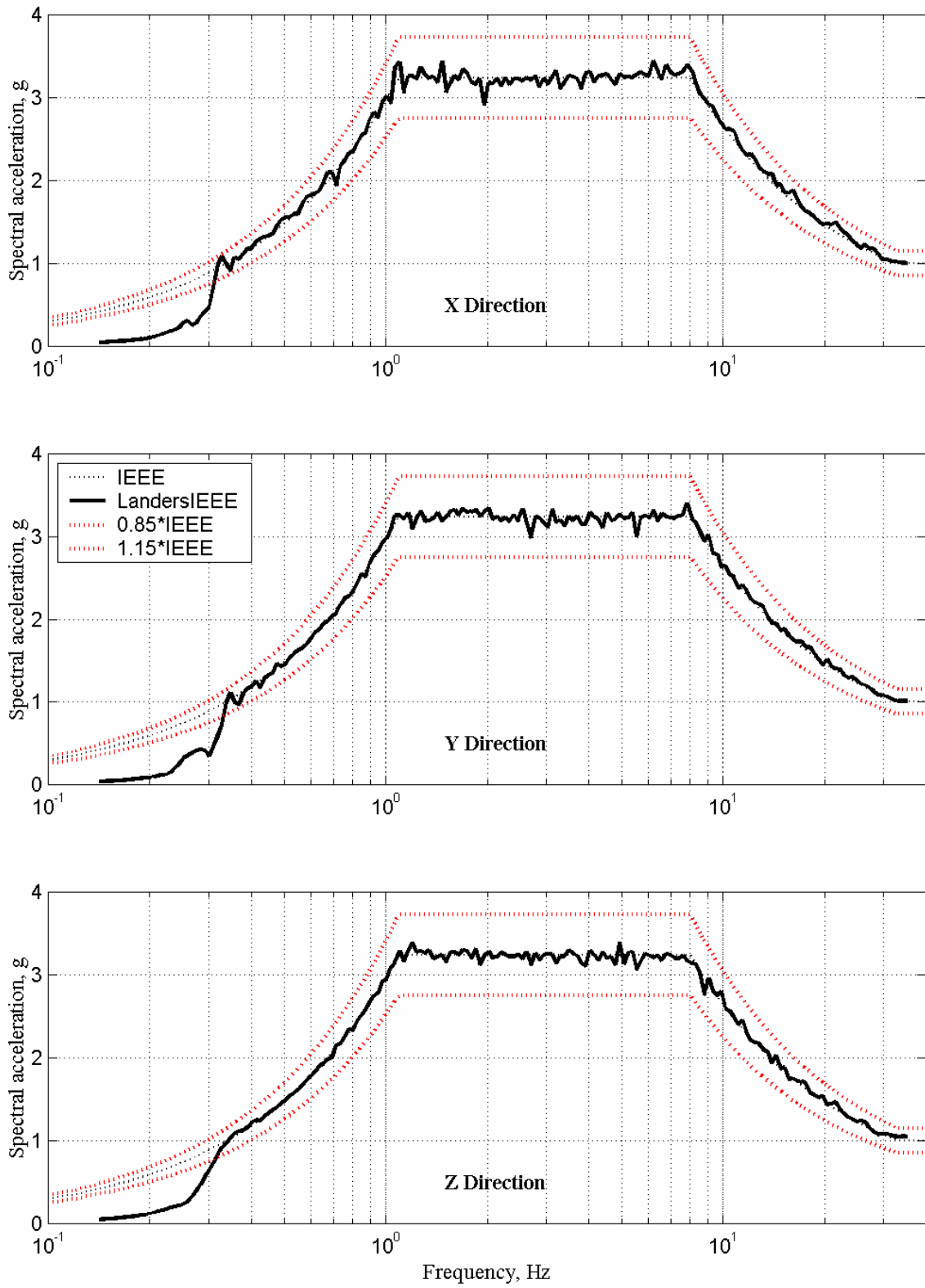


Fig. 5.1a Tolerance zone for IEEE-compatible Landers at 2% damping (1/24 octave resolution)

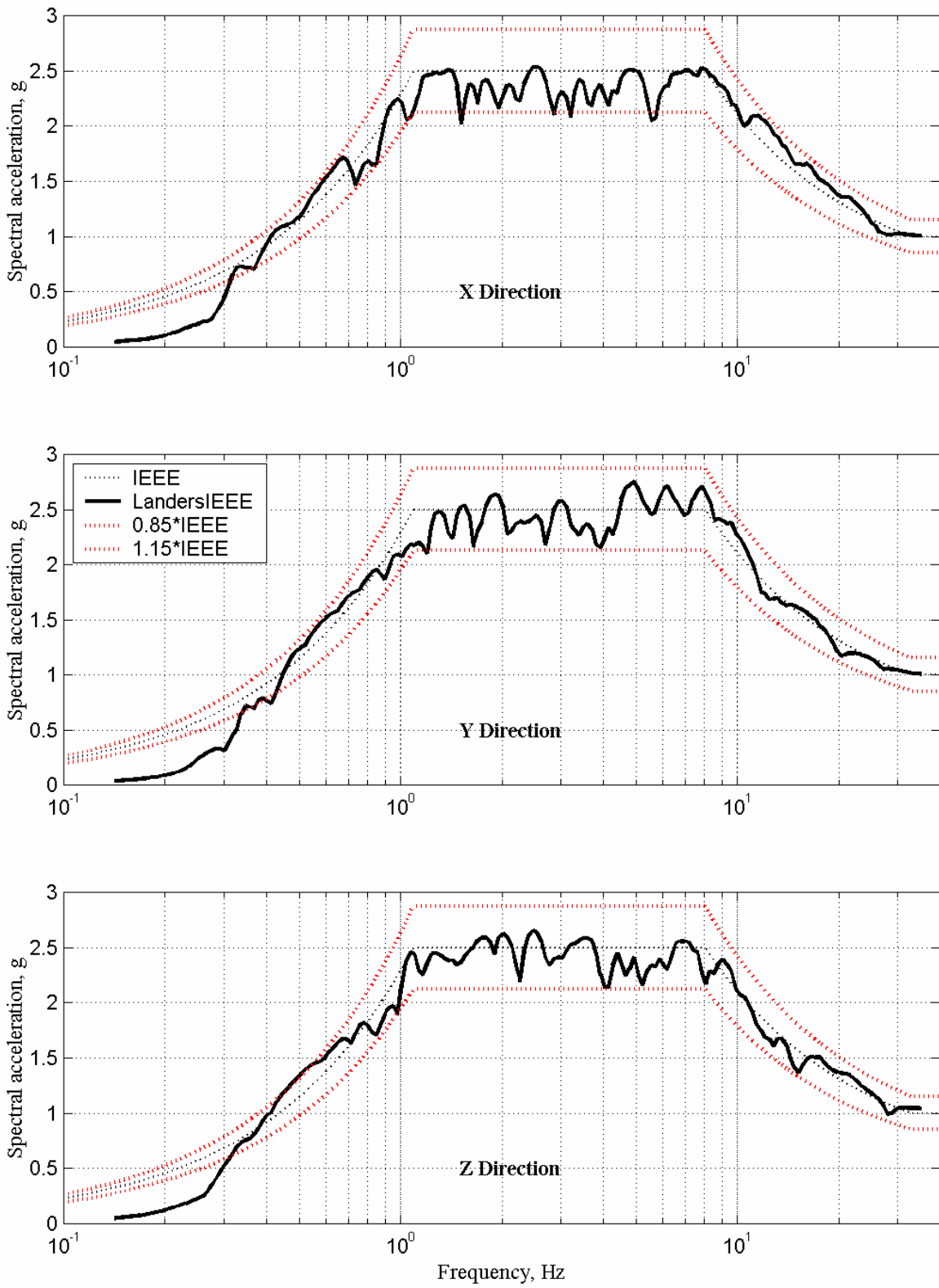


Fig. 5.1b Tolerance zone for IEEE-compatible Landers at 5% damping (1/24 octave resolution)

The velocity and displacement time histories for the IEEE-compatible Landers are shown in Figures 5.3 and 5.4. They reflect the same general trend of the historic Landers time history with the two additional pulses. The peak ground velocities and the peak ground displacements are presented in Table 5.4.

Table 5.3 Deviation of IEEE-compatible Landers from IEEE spectra (in percents at 1/24 octave frequency resolution)

		Frequency Range, Hz		
Damping	Direction	0.45 < f < 1.1	1.1 ≤ f ≤ 8.0	8.0 < f < 33.0
2%	Dips in X	-8%	-10%	-3%
	Peaks in X	7%	6%	8%
	Dips in Y	-3%	-8%	-2%
	Peaks in Y	4%	5%	5%
	Dips in Z	-2%	-6%	-7%
	Peaks in Z	2%	5%	6%
5%	Dips in X	-15%	-19%	-7%
	Peaks in X	12%	2%	12%
	Dips in Y	-11%	-16%	-10%
	Peaks in Y	11%	10%	10%
	Dips in Z	-16%	-14%	-13%
	Peaks in Z	17%	6%	7%

The IEEE-compatible Landers cannot be used as an input signal in most earthquake simulators because its peak values exceed the capacity limits of the simulators. For instance, the peak ground velocity and the peak ground displacement are as high as 74.1 in./sec (1.88 m/sec) and 17.6 in. (0.45 m), correspondingly. Factoring all components of the IEEE-compatible Landers by 0.5 produces a time history suitable for qualification testing at high RRS level (IEEE, 1998). The scaled three-component time history would have 37.1 in./sec (0.94 m) and 8.9 in. (0.23 m) for the peak ground velocity and the peak ground displacement, correspondingly. But even this scaled-down time history can serve as an input signal on a limited number of earthquake simulators. There are only two simulators from Table 5.1 that can accommodate these peaks. Therefore for the majority of earthquake simulators, the IEEE-compatible Landers has to be filtered in order to deliver the input signal that accommodates the capacities of the simulators. Less filtering would be required for the new high-performance shake table being developed under the NEES program.

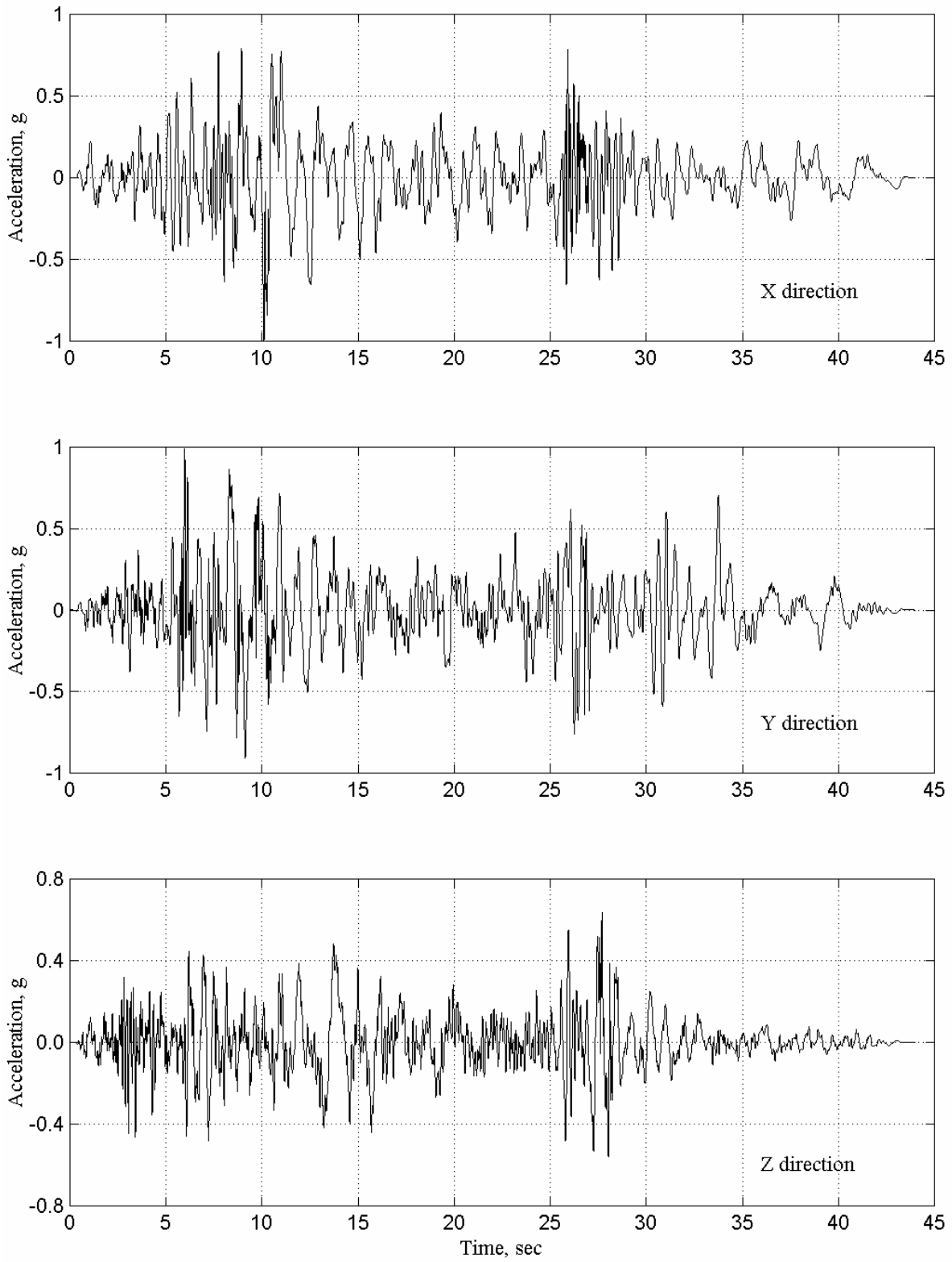


Fig. 5.2 Acceleration time histories in three principal directions for IEEE-compatible Landers

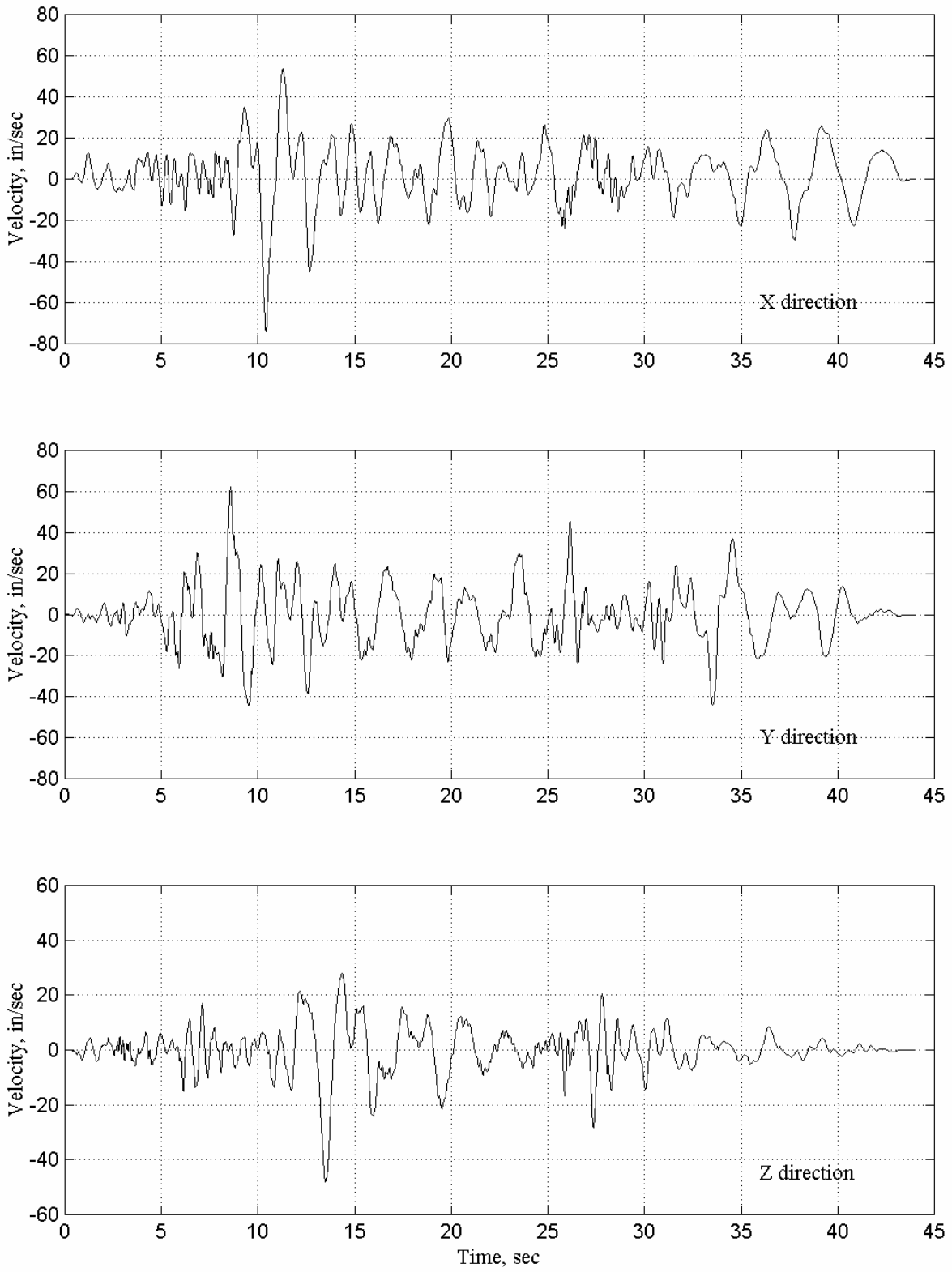


Fig. 5.3 Velocity time histories in three principal directions for IEEE-compatible Landers

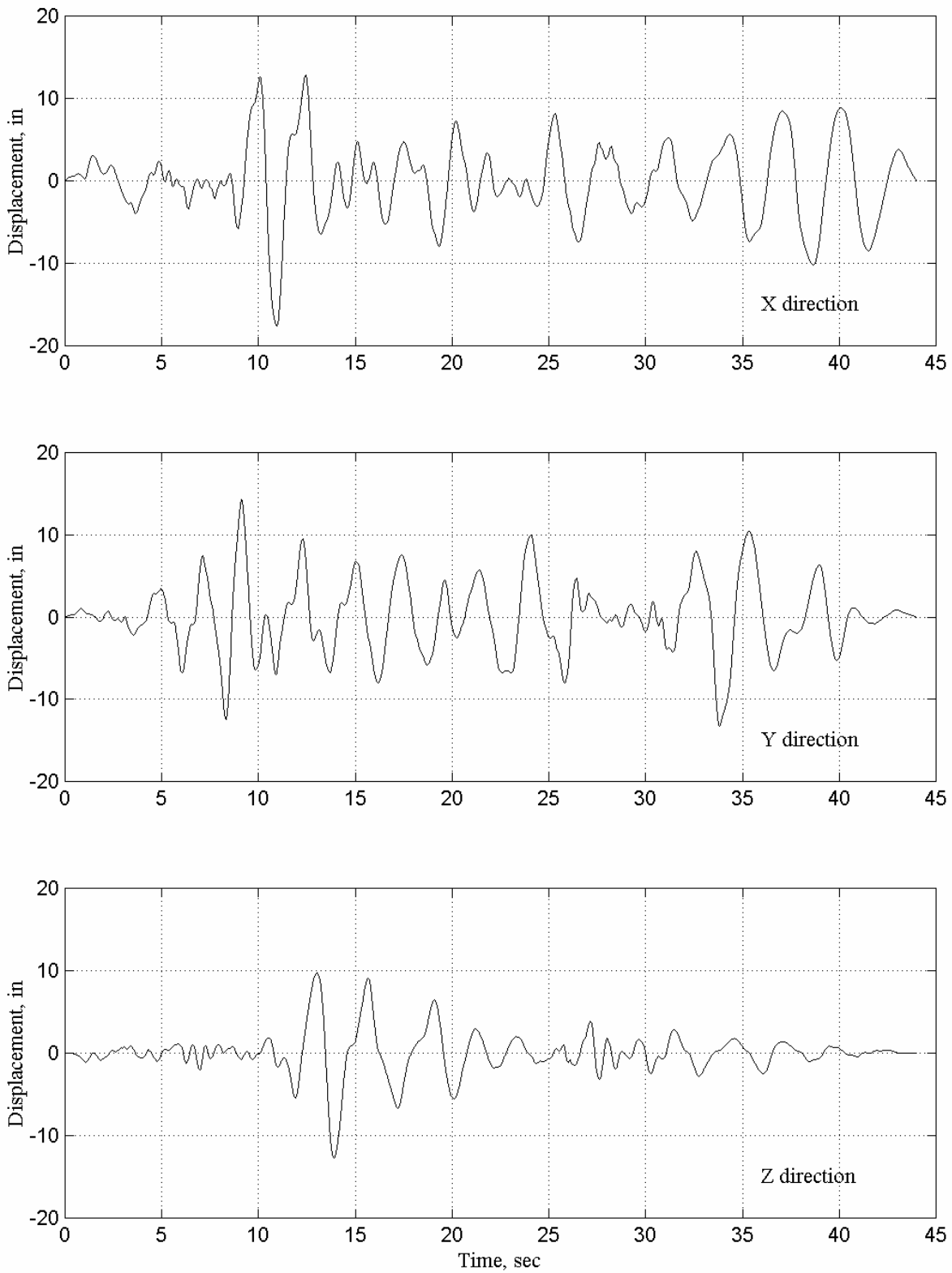


Fig. 5.4 Displacement time histories in three principal directions for IEEE-compatible Landers

Table 5.4 Peak values for IEEE-compatible Landers, Tabas1, and Tabas2

Signal	Direction	PGA g	PGV in./sec	PGD in.
Landers	X	1.00	74.1	17.6
	Y	0.99	62.1	14.2
	Z	0.80	60.0	16.0
Tabas-1	X	0.94	28.8	12.3
	Y	0.93	29.4	15.7
	Z	0.80	39.7	10.4
Tabas-2	X	0.97	74.4	28.3
	Y	1.07	93.7	42.4
	Z	0.67	65.7	17.9

5.2.2 Filtering Procedure Used for EERC Earthquake Simulator

The filtering procedure used in the study is based on band-pass filtering in the frequency domain. The Matlab environment code of the procedure was developed by Don Clyde of EERC, University of California, Berkeley, and the script can be downloaded from the PEER website that contains all deliverables of the study: http://peer.berkeley.edu/lifelines/Task408_411/Task408.html. The program requires several input parameters: the acceleration data, the time increment, the band filter, and a string of the acceleration file name. The band-pass filter consists of a high-pass filter and a low-pass filter. The high-pass filter has a cut-off frequency that presents the threshold frequency in the low-frequency zone, whereas the cut-off frequency for the low-pass filter presents the threshold frequency in the high-frequency zone. The magnitude versus frequency relationship for the filter has a trapezoidal form: the magnitude is zero up to the cut-off frequency of the high-pass filter, linearly increases up to unity at the corner frequency of the filter, remains constant up to the corner frequency of the low-pass filter, and linearly decreases to zero at the cut-off frequency of the low-pass filter. Therefore, the band-pass filter passes the signal with no changes in the frequency range between the high-pass filter and low-pass filter corners.

The acceleration time history is transferred into the frequency domain by the fast Fourier transform. Figure 5.5 shows a graphical presentation of the filtering procedure. The top plot presents the original acceleration time history with the modulus of the fast Fourier amplitude on the next plot. The third plot presents the trapezoidal filter of the procedure. A product of the filter amplitude and the Fourier amplitude (that consists of real and imaginary parts) of the time

history produces the Fourier transform amplitude of the final signal; its modulus is shown on the second plot from the bottom. The reverse fast Fourier transform procedure produces the time history of the final signal presented in the last plot at the bottom.

As can be seen from the plots, the final signal and the original time history are quite different and even have different PGA: 1.0g in the case of the original time history and 0.94g for the final signal. This difference in the filtered signal PGA and the target PGA can be reduced by scaling up the pre-filtered IEEE-compatible time history, which is also desirable to achieve the requirement for enveloping the required response spectra.

5.2.3 Filtering Procedure Developed at MTS

Over the years, the MTS corporation has developed a very extensive and integrated software program called Seismic Test Execution (STEX) that manages signal generation, data acquisition, data analysis, data files, and test operation of MTS earthquake simulators. Earthquake signals may be modified from a menu of filters with various editing and scaling functions. The STEX program allows for a choice of digital filters such as Butterworth, and spectrum smoothing (Hanning). Earthquake signals can be modified to conform to a target response spectrum by iterative scaling of the Fourier spectrum. The earthquake and target response spectra are compared and the differences used to determine the scaling of the Fourier spectrum. This method results in stationary waves being added or subtracted to the original signal. The same approach can be further applied to compensate for nonlinear responses in the earthquake simulator in which the resulting motion of the simulator is modified to become the new signal.

Developments in recent years of high-speed digital processors have resulted in large advances in the use of digital control for improved performance in earthquake simulators. Brad Thoen of MTS has used adaptive inverse control and online iteration methods to improve the responses of both new and old earthquake simulators (Nowak et al., 2000; Filiatrault et al., 2000). One of the advantages of the adaptive control method over the modification of the input signal by scaling the Fourier spectrum is that it would not result in stationary waves being added to the output motion.

5.2.4 Two Sample Input Signals Filtered from IEEE-Compatible Landers

A test facility can use its own filtering procedure or use the procedure discussed above and supplied in the deliverables of the study. In order to demonstrate the specifics of the filtering results and to offer a filtered input signal for an earthquake simulator that would be available for immediate use at several simulators in the U.S., two input signals filtered from the IEEE-compatible Landers (TestQke4IEEE) were delivered in the study. The sample input signals were filtered for use at the PEER earthquake simulator and are discussed below.

The IEEE 693 document (IEEE, 1998) establishes two options for qualification testing at high level. The first option requires that the test response spectrum should envelop the IEEE RRS anchored at 0.5g PGA. The second option is PL testing, so the test response spectrum should envelop the IEEE PL spectrum anchored at 1.0g PGA. Two sample versions of the input time histories (or signals) for earthquake simulator reflect these two options for qualification testing and are named a “LandersRRS” and “LandersPL.” The three-component LandersRRS is intended for the high seismic qualification testing by means of the high RRS approach anchored at 0.5g PGA, whereas LandersPL (that also consists of three components) is intended for use during high PL qualification testing at 1.0g PGA. They were developed to accommodate the limitations of the EERC earthquake simulator and were aimed at using the least filtering possible in order to preserve a broadband character of the time histories. These sample versions were filtered from the IEEE-compatible Landers time history (TestQke4IEEE); the scale factor (to accommodate the PGA drop during filtering procedure), the band-pass filter parameters, and the peak values of the input signals are presented in Table 5.5.

Figure 5.6 presents elastic response spectra computed with 1/24 octave frequency resolution for the LandersRRS at 2% and 5% damping. For wide-frequency ranges (from 0.6–33 Hz for two horizontal directions and from 0.8–33 Hz for the vertical direction) the response spectra are located within a 30% tolerance zone above the IEEE spectrum at 2% damping with no dips below the target response spectra. Although the spectra at 5% damping have several isolated dips (valleys) below the IEEE response spectrum, the deviation from the IEEE spectrum is relatively small.

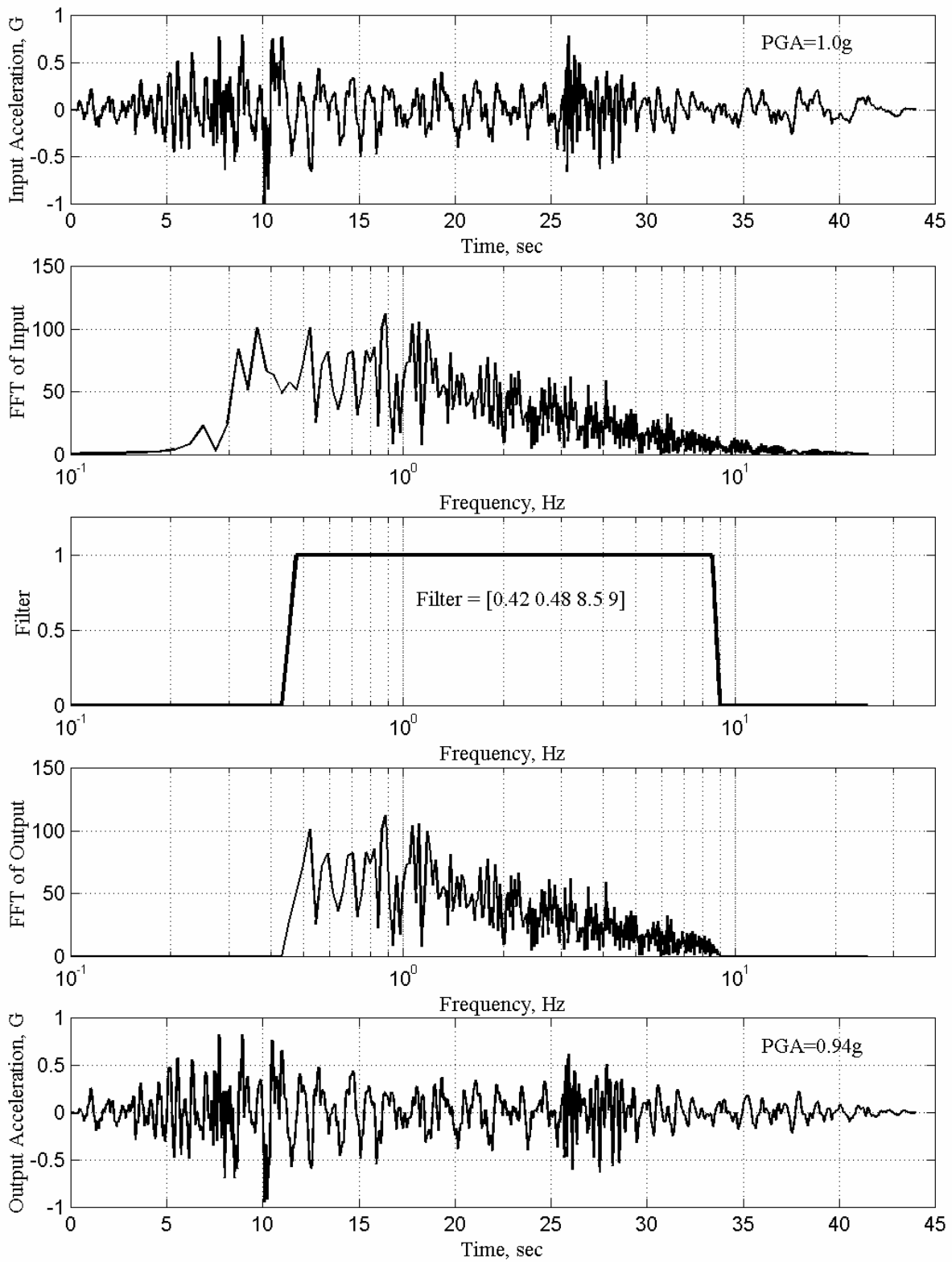


Fig. 5.5 Steps of filtering procedure (from top to bottom)

The elastic response spectra for LandersPL are presented in Figure 5.7. The isolated valleys in the spectra below the target response spectrum are not deeper than 5% and are concentrated in the low-frequency range (below 1.3 Hz for the two horizontal directions and below 2.1 Hz in the vertical direction). Most of the spectral accelerations are located within the 30% tolerance zone above the IEEE spectrum at 2% damping. In addition to these dips in low frequency, the spectra at 5% damping have several isolated valleys below the IEEE response spectrum.

Table 5.5 Filtering parameters and peak values for sample versions

Signal	Direction	Scale factor	Band-pass filter	PGA g	PGV in./sec	PGD in.
LandersRRS	X	0.585	[0.48 0.50 33 34]	0.53	30.3	4.7
	Y	0.575	[0.48 0.50 33 34]	0.51	26.8	4.9
	Z	0.47	[0.74 0.76 33 34]	0.43	16.7	2.0
LandersPL	X	1.20	[0.92 0.95 33 34]	0.88	29.0	3.2
	Y	1.20	[0.94 0.96 33 34]	1.10	30.0	3.4
	Z	0.96	[1.22 1.23 33 34]	0.86	22.6	2.0

The filtering procedure performed to deliver a high PL test signal often produces valleys in response spectra close to the cut frequency of the high-pass filter. This phenomenon was observed for the VERTEQII record in 1/12 octave resolution (see discussion in Chapter 2), for the CERL input signal developed for high PL qualification testing, and for the IEEE-compatible Landers filtered for high PL testing (LandersPL). The valleys are not related to any particular filtering procedure because all of these input signals were developed at different laboratories and used completely different filtering procedures. The valleys in the response spectra of the input signal are undesirable, especially when they occur at frequencies close to the natural frequency of testing equipment. The high RRS testing requires less filtering; therefore the filtered signal produces a theoretical spectrum that does not fall below the RRS spectrum (as shown for the case of LandersRRS). Therefore to achieve adequate conservatism and avoid these dips in the spectrum for high PL, the RRS option can be considered as the only appropriate approach for qualification testing of electrical equipment with a low natural frequency.

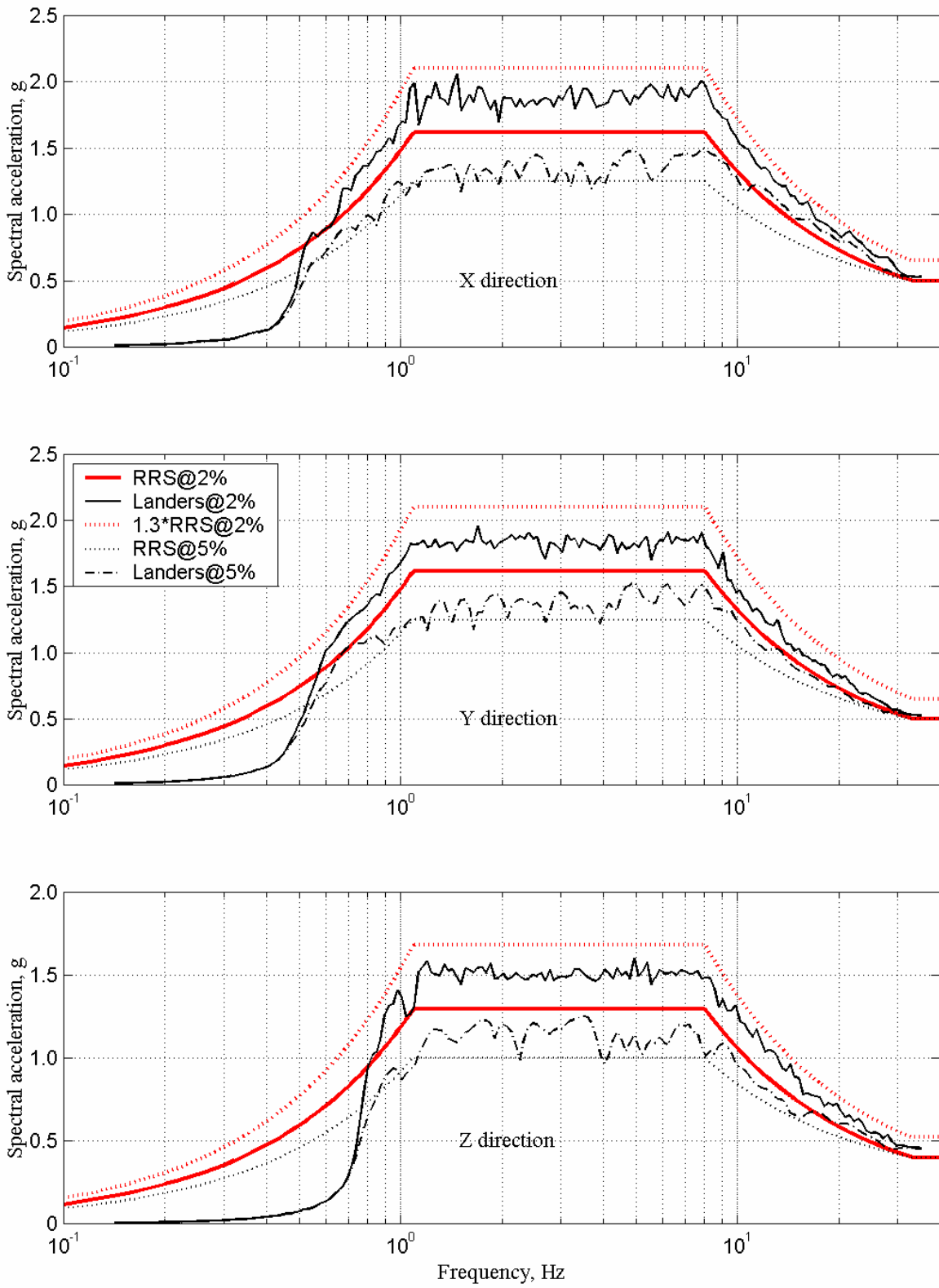


Fig. 5.6 Landers RRS designed for use in high RRS qualification test

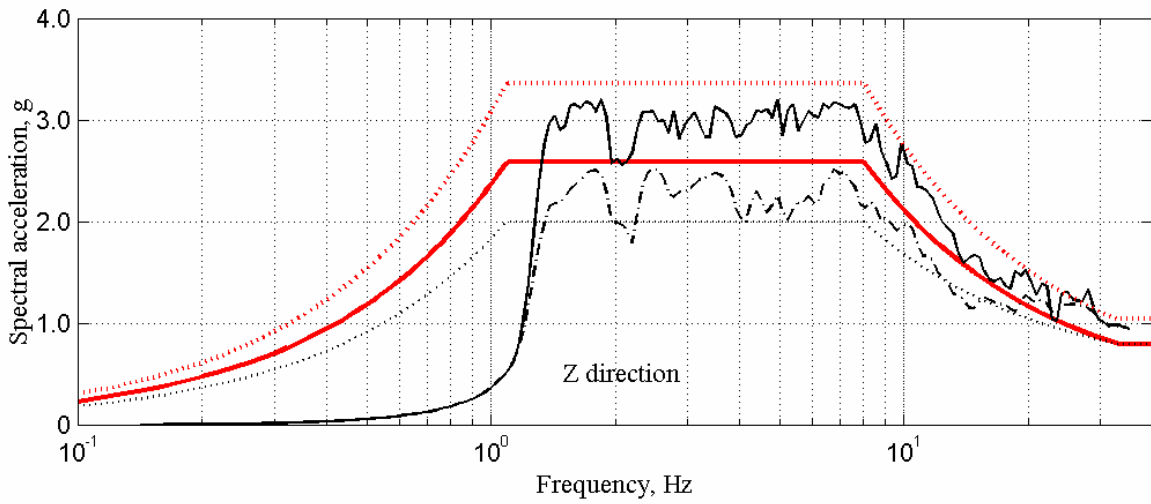
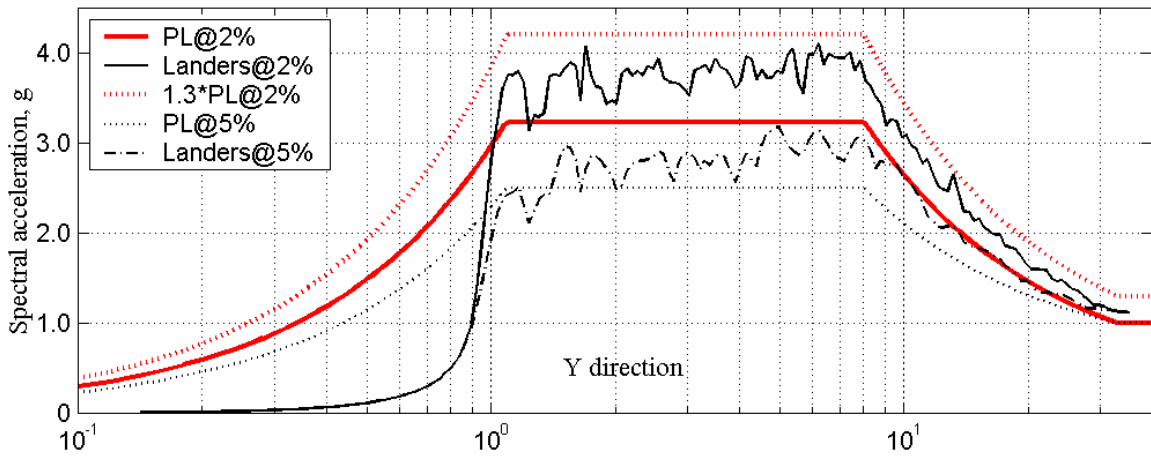
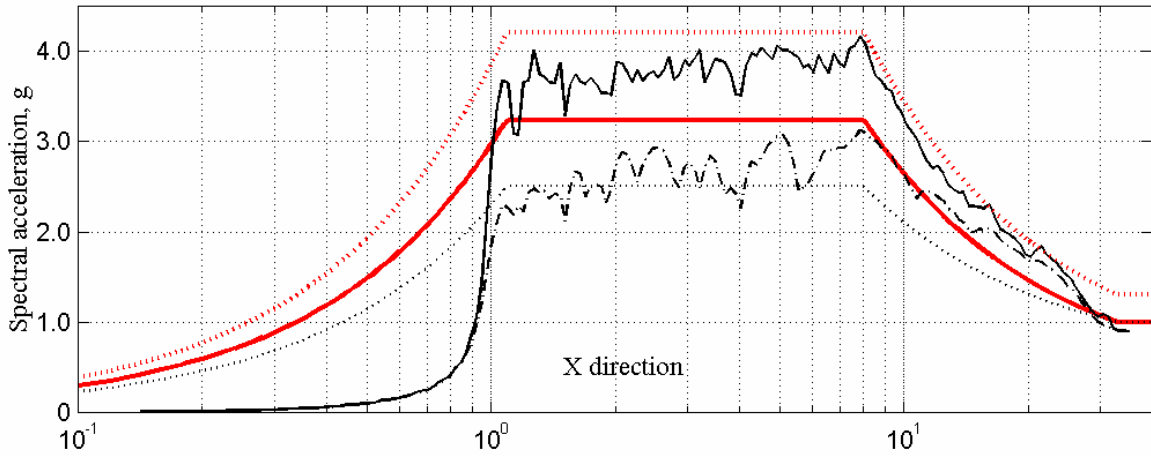


Fig. 5.7 Landers PL proposed for use in high PL qualification test

5.3 PROPOSED SIGNAL VS. STRONG MOTION SIGNALS CURRENTLY IN USE

5.3.1 Tabas-1 and Tabas-2 Time Histories (EERC, UC Berkeley)

A number of qualification tests on electrical equipment were performed with two input signals (Gilani et al., 1999; Gilani et al., 2000) by PEER on the EERC simulator. The signals were developed from the three-component strong motion time history of near-field earthquake motions recorded during the 1978 Tabas, Iran, earthquake. Each signal envelopes the IEEE spectra only in a certain frequency range: Tabas-1 in the high-frequency range (above 3 Hz) and Tabas-2 in the low-frequency range (below 4 Hz). It was assumed that two separate tests with two narrow band signals would be equivalent to one test with broadband signal, and the qualification tests were conducted by means of these two signals. Figures 5.8 and 5.9 present the power spectral density and the elastic response spectra for these input signals.

Unlike the IEEE-compatible Landers spectra, the elastic response spectra for Tabas-1 and Tabas-2 do not fit inside of the 30% tolerance strip around the IEEE spectrum. The spectral acceleration dips and peaks relative to the target response spectrum exceed the -15% and $+15\%$ thresholds, respectively, for all three components and for both input signals. For the same frequency resolution ($1/24$ octave bands), the spectra based on the IEEE-compatible Landers have significantly better correlation with the target IEEE response spectrum.

5.3.2 Synthetic Strong Motion History Used at CERL

The CERL laboratory usually performs the seismic qualification tests using a synthetic strong motion time history that was developed at the laboratory. The test signal is aimed to envelop the IEEE spectra and to accommodate the limitations of the test simulator at the laboratory. Figure 5.10 shows the time history; the power spectral density and the elastic response spectra for the strong motion signal are presented in Figure 5.11.

The acceleration time history for the CERL test signal was assembled from harmonics; therefore its components in three principal directions have a stationary character opposite to the IEEE-compatible Landers (compare Fig. 5.11 to Fig. 5.2). The CERL is a filtered signal that accommodates the limitations of the CERL earthquake simulator; therefore it has to fit inside of the tolerance zone above the IEEE spectrum at 2% damping. The elastic response spectra for the CERL test signal exceed the 30% tolerance zone above the target IEEE spectrum only at several

individual points for two horizontal directions: maximum 6% dip at 1.7 Hz for the X direction and maximum 2% peak at 2.1 Hz in the Y direction. The spectrum fits perfectly inside of the 30% tolerance strip for the vertical direction. The correlation between the IEEE spectrum and the CERL spectra is not as good for 5% damping.

5.3.3 Summary of Key Parameters

This section presents a comparison between the current IEEE-compatible test signals and the IEEE-compatible Landers. All records are taken with no modifications, so they are not filtered (except the CERL record that was supplied in a pre-filtered form with a high-pass filter at about 1 Hz).

Peak values. Peak ground acceleration, peak ground velocity, and peak ground displacement are very important parameters for assessing the necessity of filtering a test signal to be used as an input strong motion for a particular earthquake simulator. The peak values of the test time histories are presented in Table 5.4. The frequency content of the IEEE-compatible Landers and Tabas-2 includes the low-frequency range; therefore the signals produce high velocities and displacements. Because of the capacity limitations of the major earthquake simulators in the U.S. and abroad, the signal should be filtered to remove the low-frequency oscillations from the frequency content of the signals. The CERL laboratory supplied the CERL signal in a filtered form so it could be used at many earthquake simulators (similar to the CERL capacities) without modification.

Frequency content. The frequency contents in the form of smoothed power spectral densities (PSD) of all test signals are presented in Figure 5.12 and are plotted against the mean PSD for the set of 35 historic strong motions. In general, the PSD for the IEEE-compatible Landers is lower than the PSD for the CERL signal in the high-frequency range starting from about 1.5Hz. Tabas-1 modified from a historic record and intended for testing in the high-frequency zone also produces a PSD that tends to be lower than the CERL PSD. Therefore the phenomenon is most likely related to the stationary character of the CERL signal. The general trend of the PSD for the IEEE-compatible Landers in respect to the Tabas test signals is as follows: it is always higher than the PSD for Tabas-1 (created for tests in the low-frequency range) and slightly lower than the PSD for Tabas-2 in the high-frequency range starting from

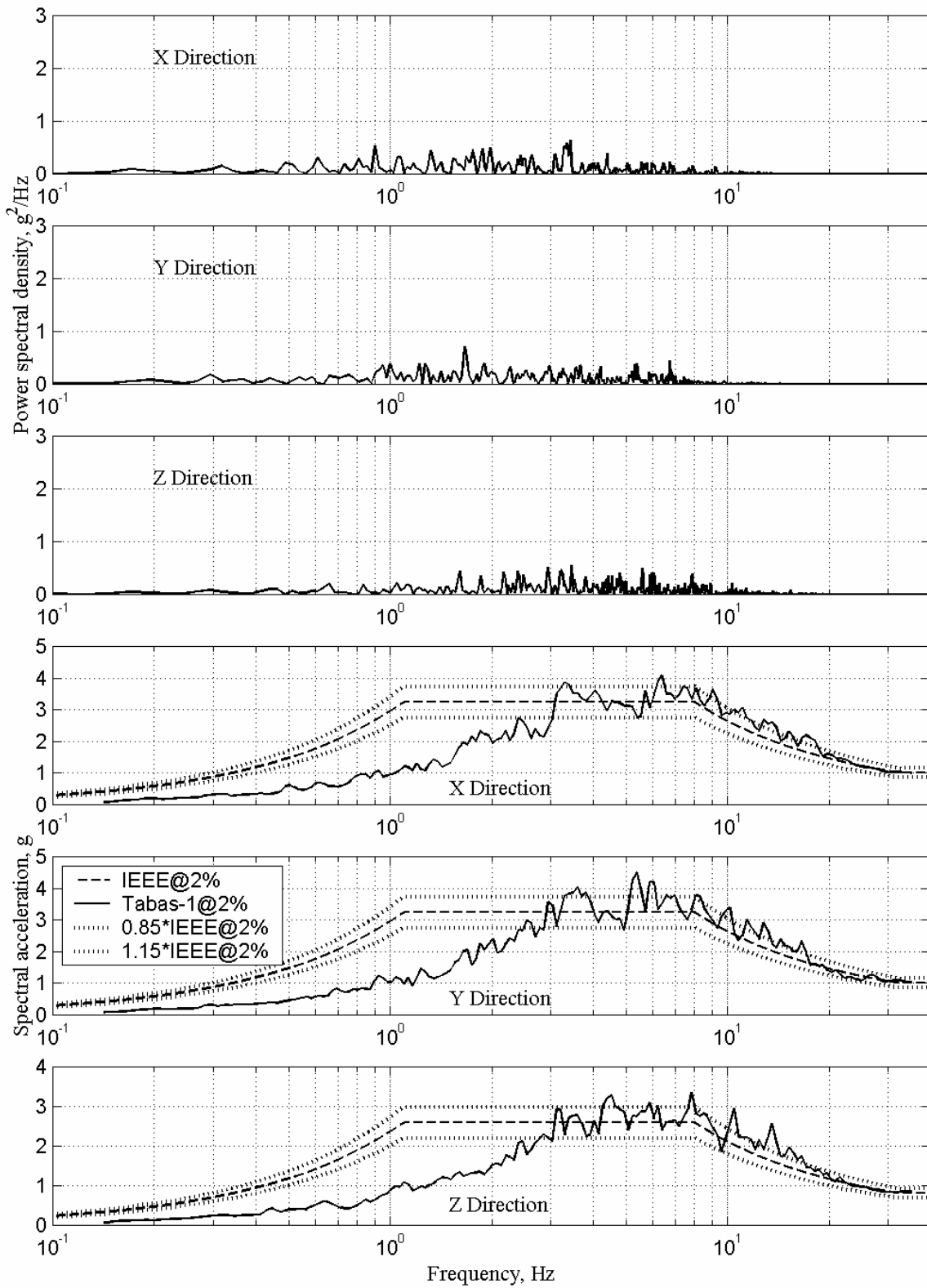


Fig. 5.8 PSD and elastic response spectra for Tabas-1

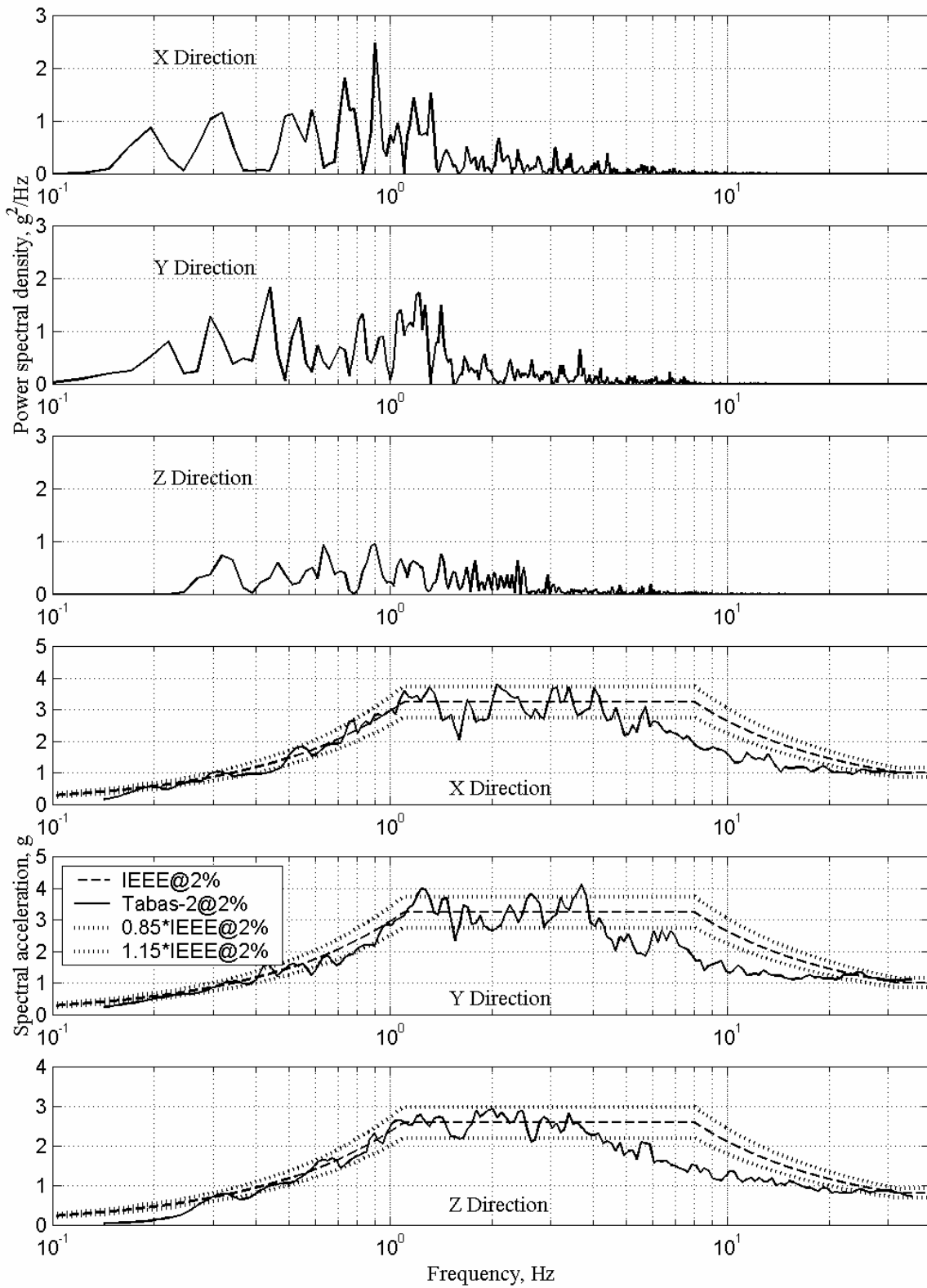


Fig. 5.9 PSD and elastic response spectra for Tabas-2

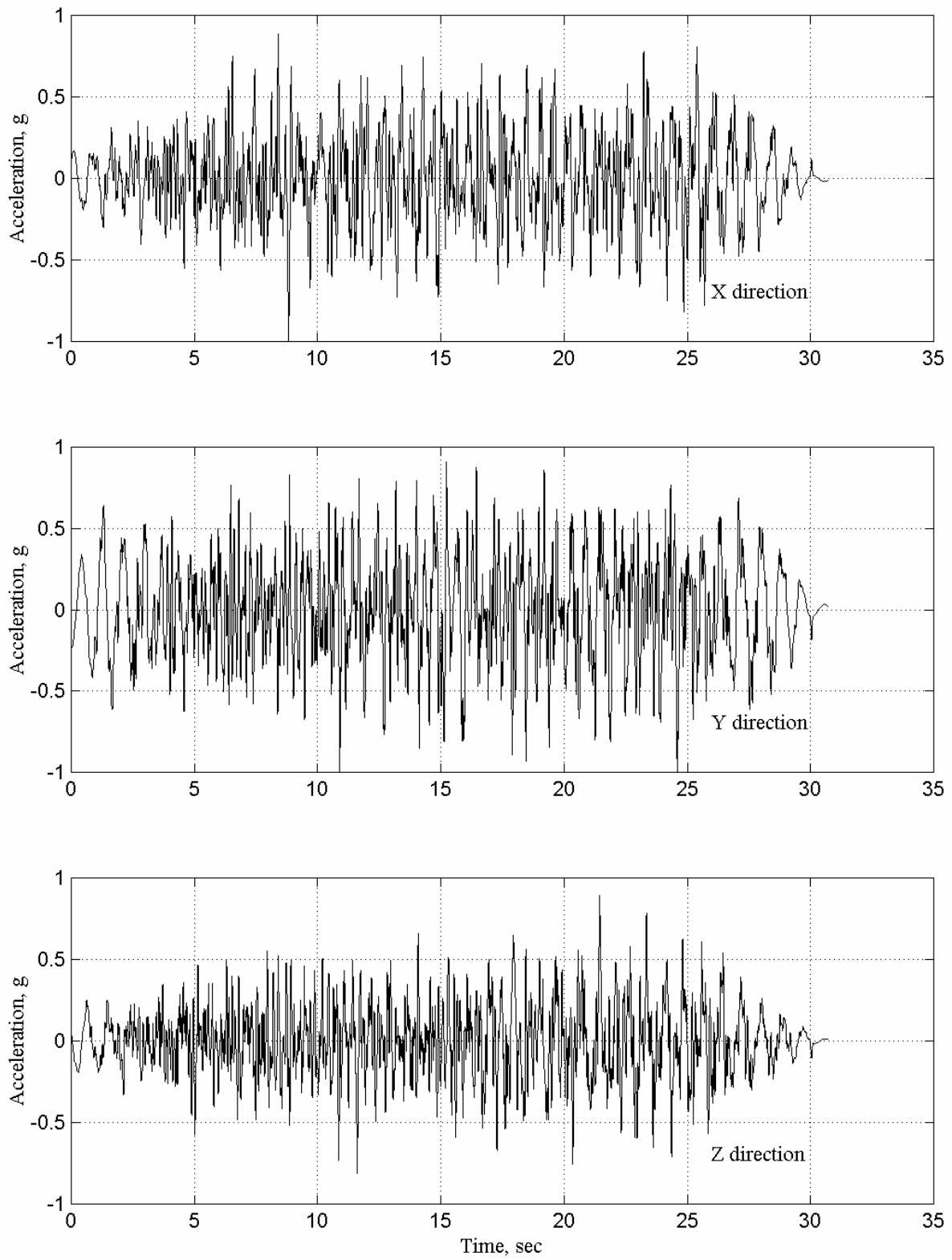


Fig. 5.10 Acceleration time history for CERL synthetic strong motion

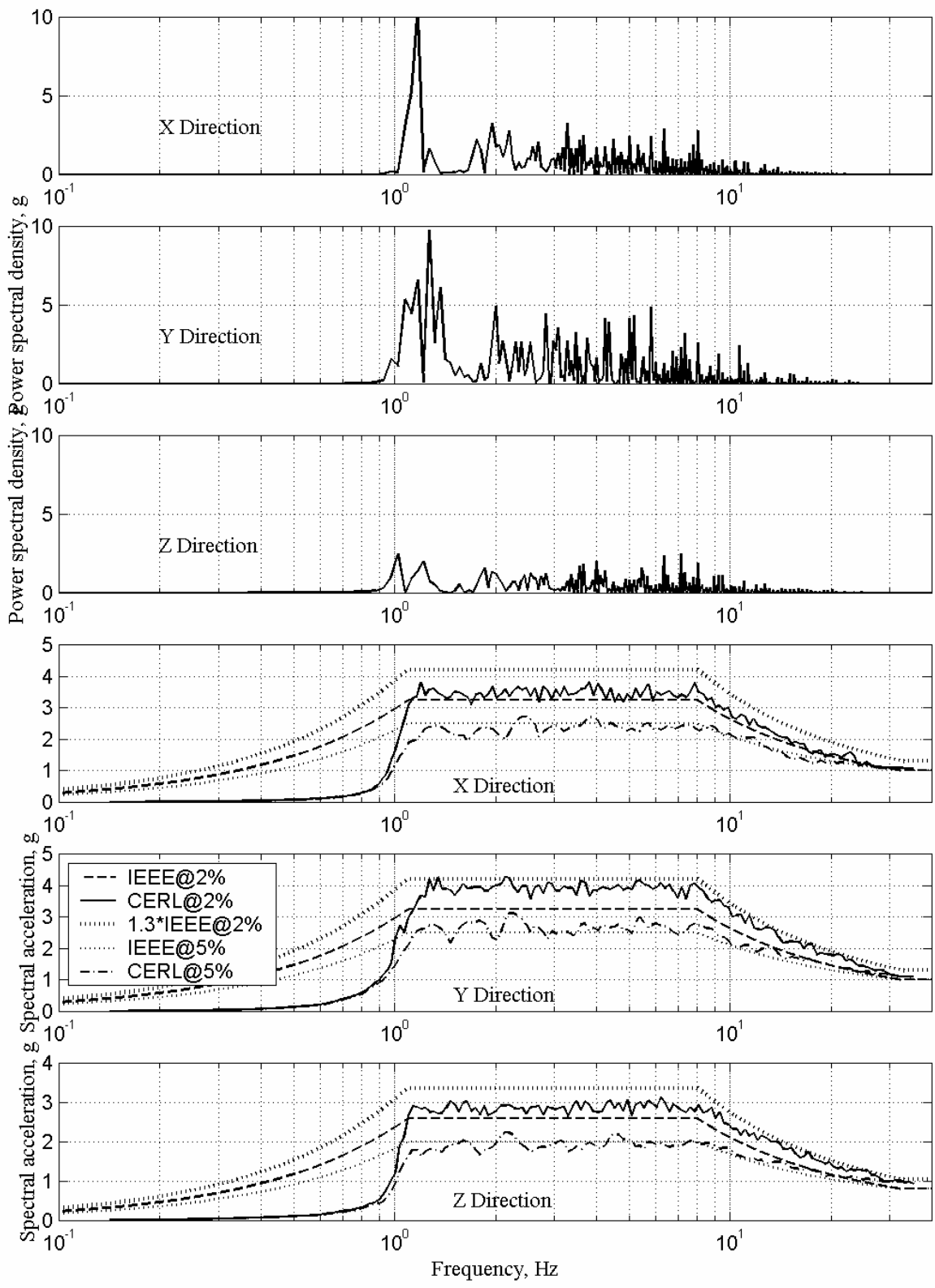


Fig. 5.11 PSD and spectra CERL synthetic strong motion

about 5Hz.

Cycle counts. The final result of the cycle counting procedure is a histogram that represents the number of cycles' distribution over various magnitude ranges. Figure 5.13 shows the histogram for a number of acceleration cycles with a 25% threshold, so all cycles with magnitude higher than 25% of the PGA are presented here. The IEEE-compatible Landers always has a greater number of cycles than the mean of the set of 35 records studied in Chapter 4. It is closer to the maximum cycle number computed for the set of 35 records than all other test records except the CERL strong motion time history. This synthetically generated record (CERL) consists of many harmonics that introduce a higher number of cycles at any magnitude range. After the 35% magnitude range, the cycle number becomes even greater than the maximum for the set studied earlier in Chapter 4. As a result, the total number of cycles with magnitude greater than 25% of the PGA is more than twice greater for the CERL signal compared to the IEEE-compatible Landers (98 cycles against 44, respectively). This fact can lead to unnecessary overtesting of electrical equipment during a qualification test. Unlike the CERL signal, the IEEE-compatible Landers carries a realistic number of acceleration cycles (in the acceleration time history) at all magnitude ranges, and the number of cycles becomes very close to the maximum for the set at high (the most dangerous for brittle equipment) magnitudes. Tabas-1 and Tabas-2 have a fewer number of cycles at any magnitude range.

Cycle counts in SDOF system response. The results of a cycle count in the response of the SDOF system to the input signal is presented in Figures 5.14–5.17. Only high-level cycles were counted, namely the total number of cycles with 70% of the maximum acceleration magnitude for the selected natural frequency and damping of the SDOF system were computed. In general, the number of high cycles in the SDOF system response due to the IEEE-compatible Landers relatively closely represents the mean trend for the set of 35 records, as shown in Figure 5.14. It varies from 1–9 for the X direction and from 1–14 for the Y. It is noteworthy that the high cycle plots for the IEEE-compatible Landers have only 4 isolated dips to one cycle count for both principal directions. A similar trend of close variation around the mean count is observed for Tabas-1 and Tabas-2, shown in Figures 5.15–5.16, and is definitely related to the non-stationary character of the signals. Unlike the IEEE-compatible Landers, the high cycle count is limited to one cycle at many natural frequencies, namely 9 dips to one cycle count for the X direction and 11 for the Y.

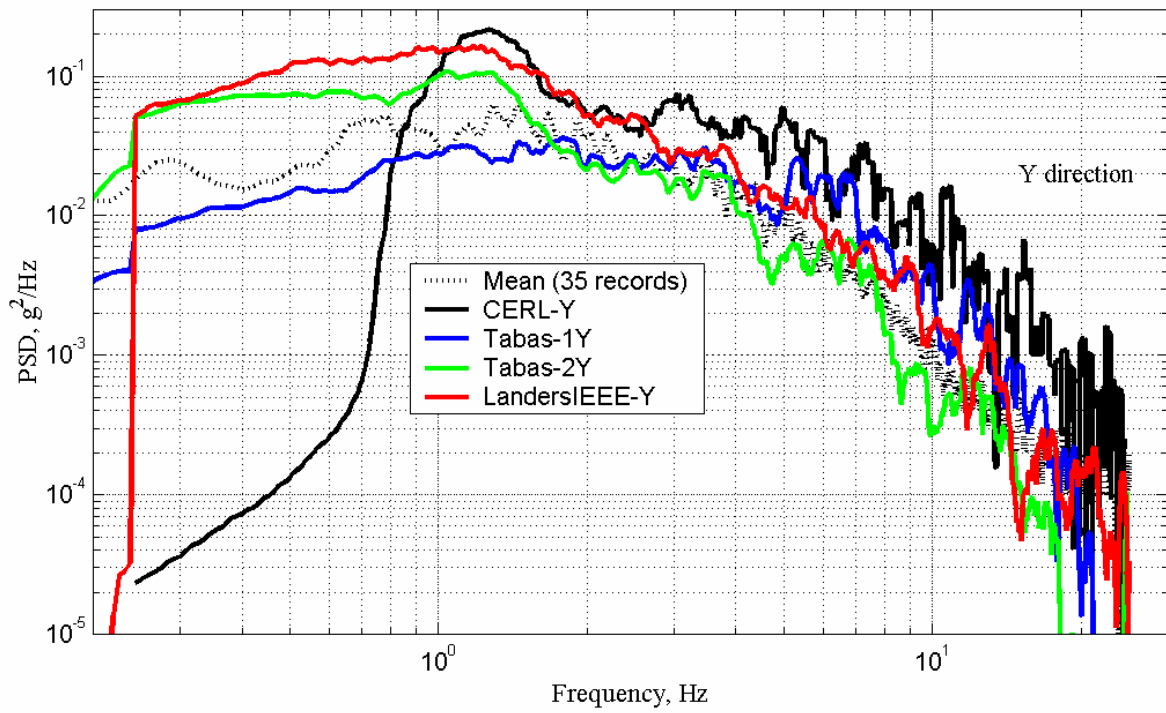
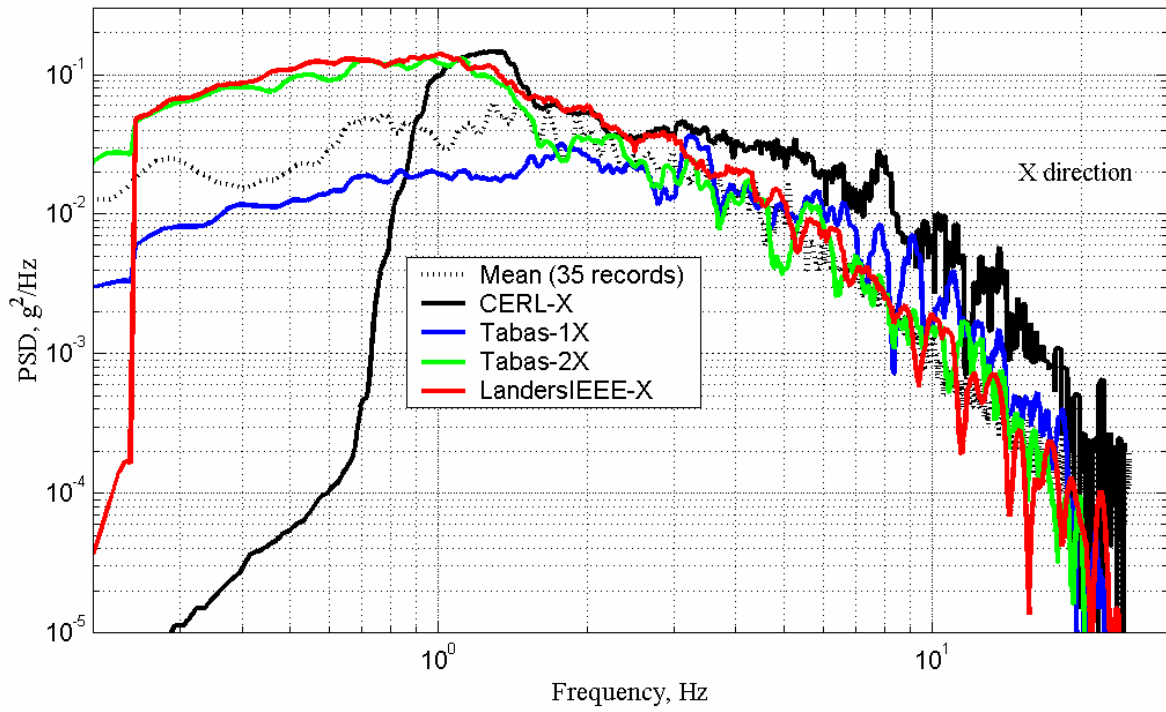


Fig. 5.12 Smoothed PSD for test signals vs. mean of set of 35 strong motions

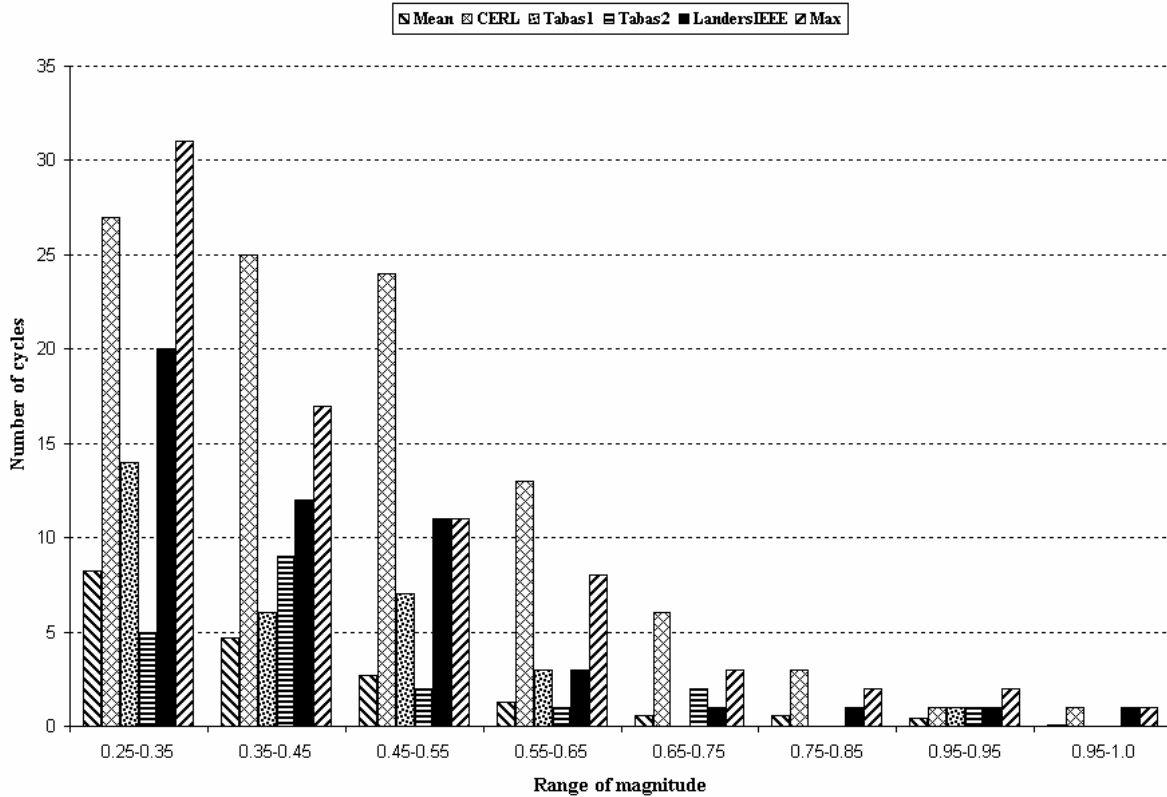


Fig. 5.13 Cycle count results for IEEE-compatible test signals

The CERL signal produces a significantly different result (Fig. 5.17): the number of high cycles in the SDOF system response is much higher than the mean for the set. Furthermore, it exceeds the maximum value for the set: 46 cycles in the X direction and 42 cycles in the Y. The maximum number of the high cycles for the set did not exceed 26 cycles, and the mean count was limited by about 6 cycles. The result confirms the previous conclusion based on analysis of cycles in the input acceleration time history: use of the synthetically generated CERL signal in a qualification testing can lead to overtesting of electrical equipment.

Cumulative energy. The cumulative energy computed for each test record is presented in Figure 5.18. The dark columns represent the mean (on the left) and the maximum (on the right) for the set of 35 records. The IEEE-compatible Landers has almost the same values of the cumulative energy in two horizontal directions as the CERL has. The Tabas-1 and Tabas-2 does not impose as much cumulative energy as the CERL and the IEEE-compatible Landers do: the values are about twice less for the Tabas test signals. The cumulative energy for the Y-direction of the IEEE-compatible Landers is greater than the energy for the X-direction.

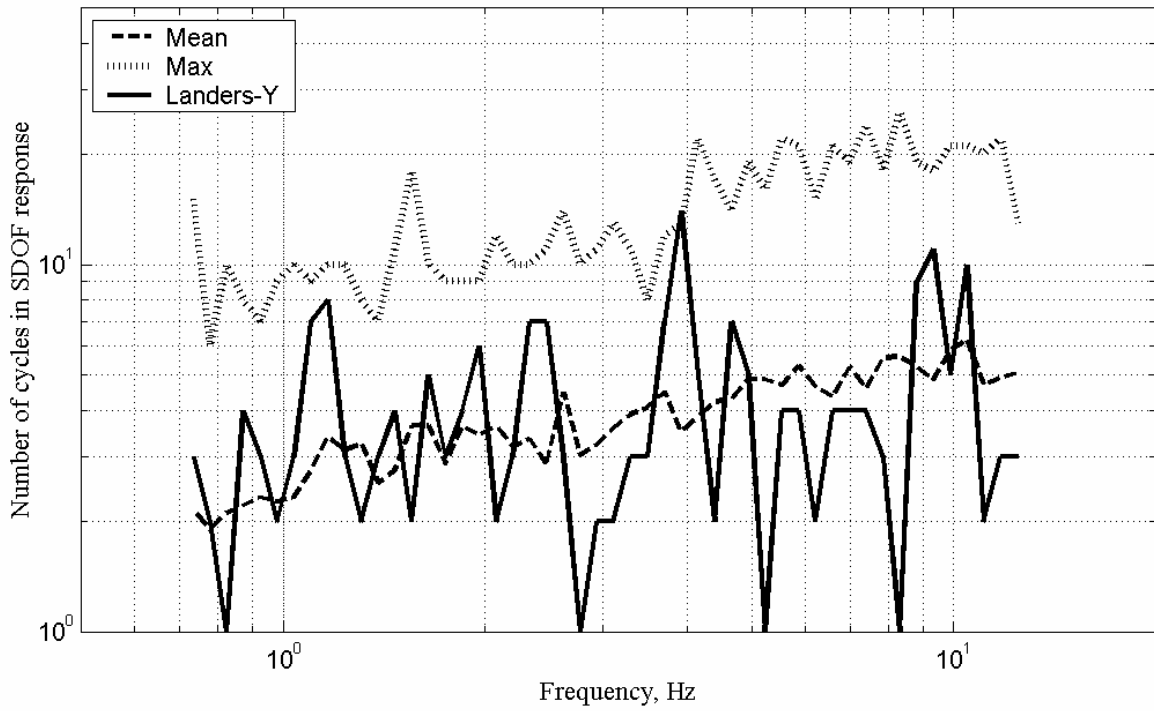
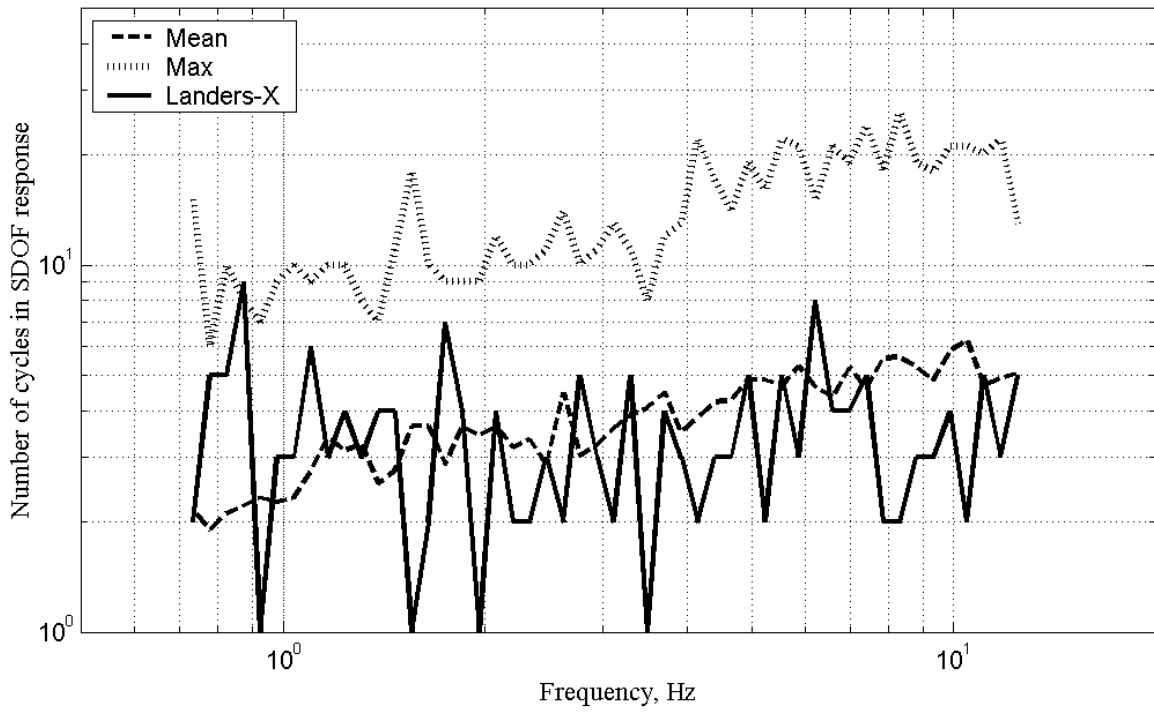


Fig. 5.14 Number of high-level cycles in SDOF system response for IEEE-compatible Landers

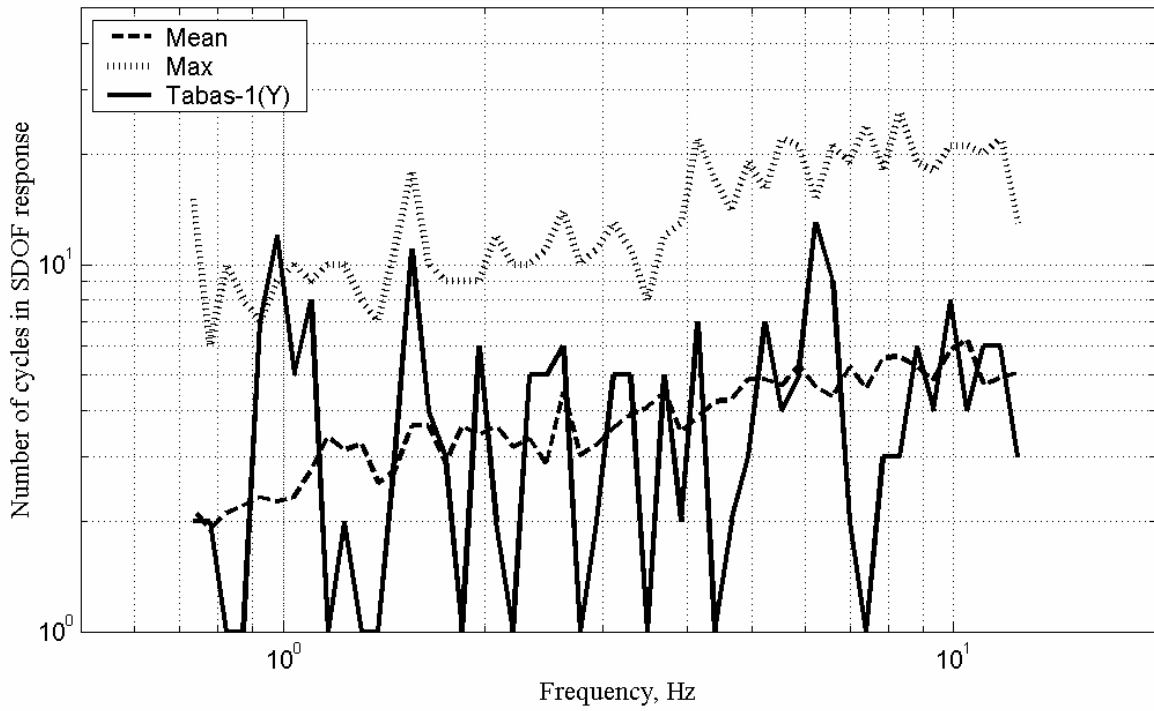
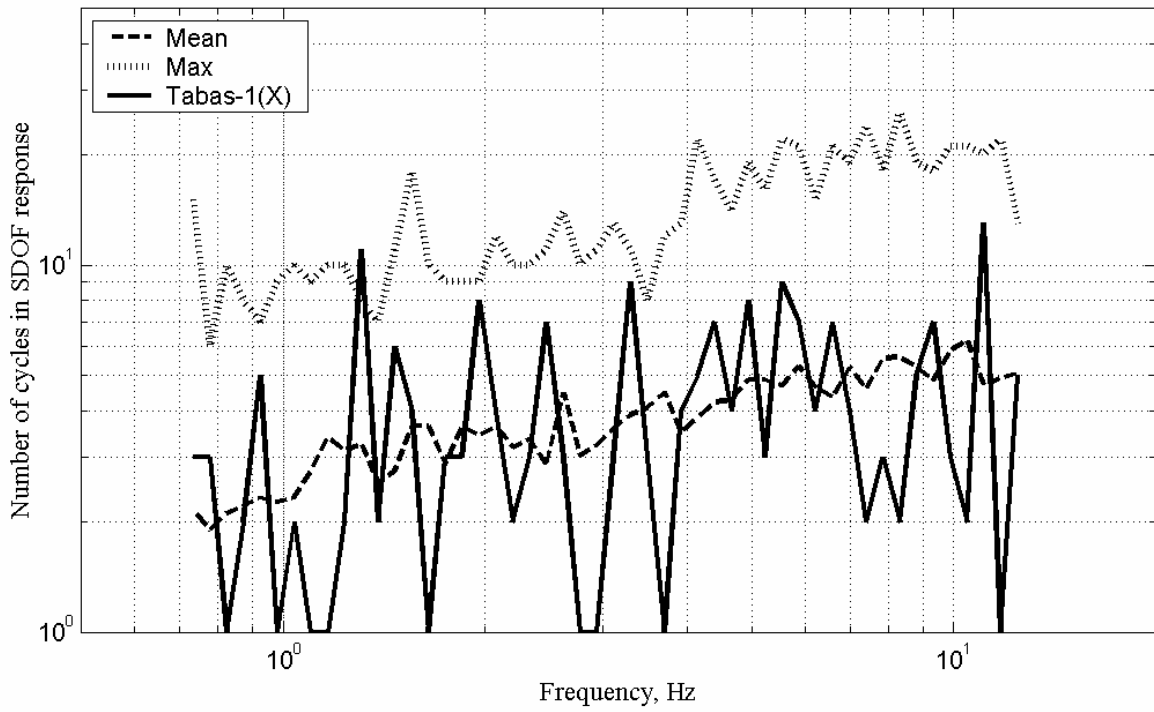


Fig. 5.15 Number of high-level cycles in SDOF system response for Tabas-1

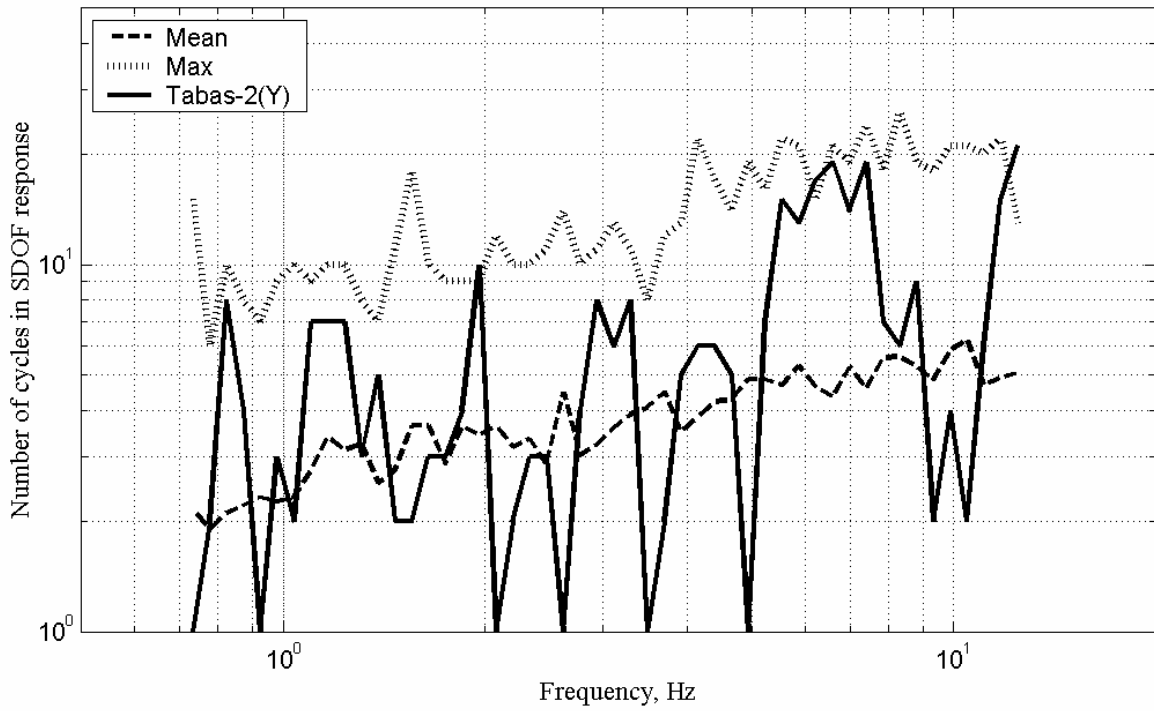
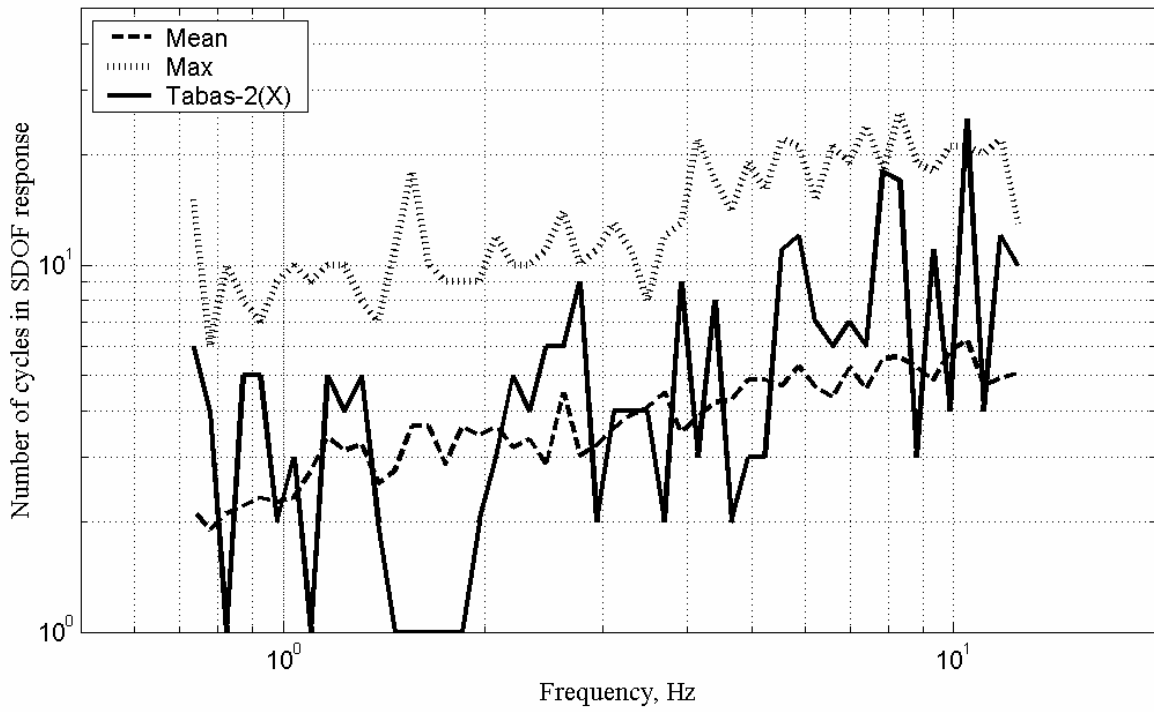


Fig. 5.16 Number of high-level cycles in SDOF system response for Tabas-2

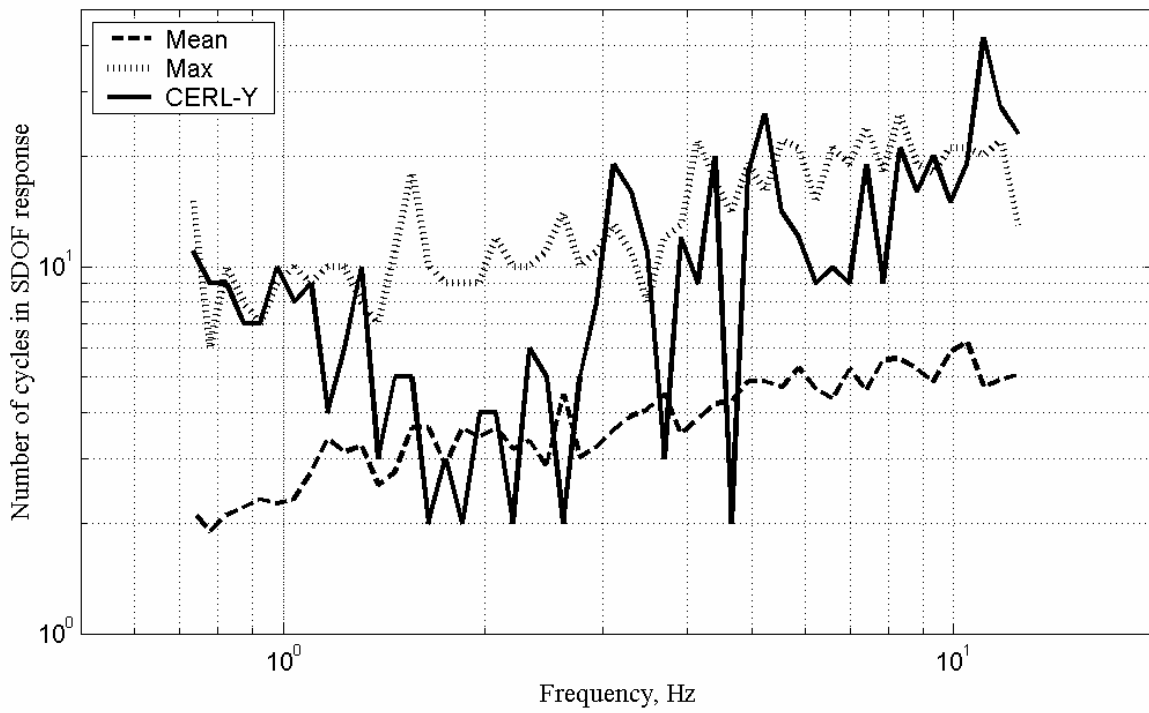
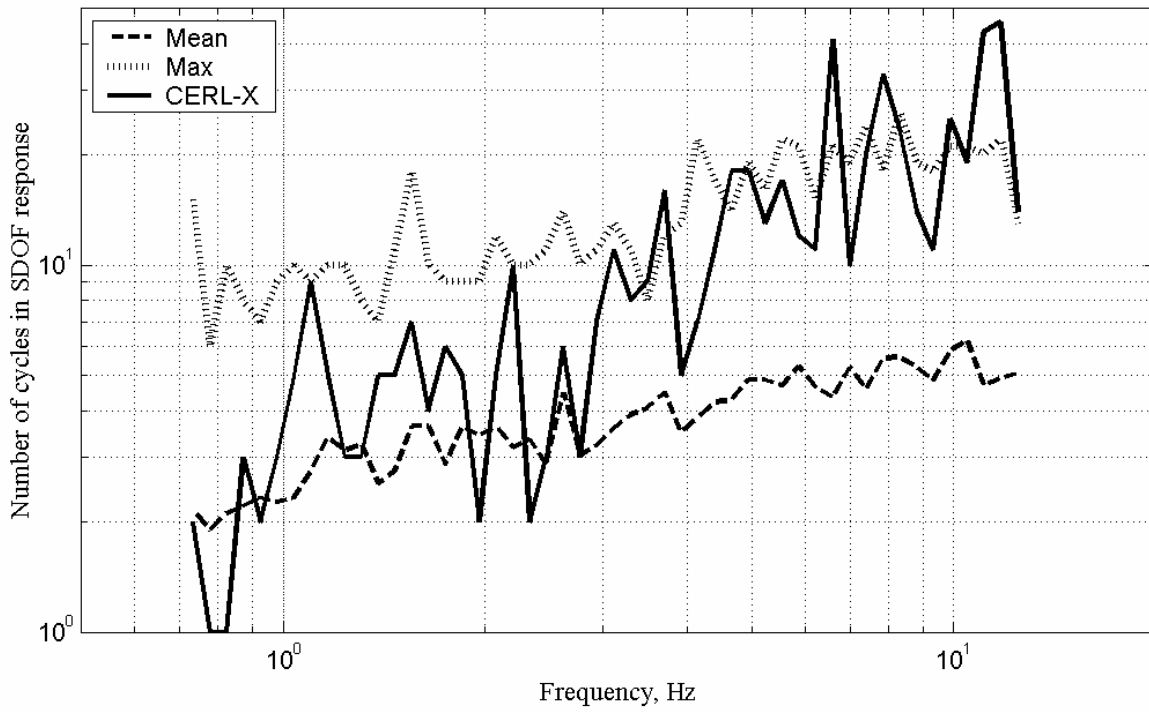


Fig. 5.17 Number of high-level cycles in SDOF system response for IEEE-compatible CERL

Duration. The bracketed duration based on cumulative energy is presented in Figure 5.19. The IEEE-compatible Landers has longer than 20 sec duration for both horizontal directions as required by the IEEE 693 standard. The CERL signal also overpasses the 20 sec threshold, although it has slightly shorter duration than the IEEE-compatible Landers. The Tabas test signals have duration less than 20 sec because they were designed for joint and consecutive use in a qualification testing.

Strong part to duration ratio. Figure 5.20 shows the strong part to duration ratio introduced earlier and based on the definition of cumulative energy. As discussed in Chapter 4, the ratio for the Landers record was the greatest among all records from the set of 35 historic strong motions. This characteristic of the Landers signal is preserved in the IEEE-compatible Landers, so it has the maximum strong part to duration ratio of the other test signals. The CERL signal has a ratio close to the IEEE-compatible Landers, but slightly lower. The ratio for the Tabas test signals is almost twice lower than that for the IEEE-compatible Landers.

Cumulative specific kinetic energy. The cumulative specific kinetic energy (CSKE) represents how much kinetic energy per unit of mass is imposed on equipment by an earthquake simulator over the duration of the input signal, as presented in Figure 5.21. The value of CSKE strongly depends on the number of cycles with low frequency and their magnitude in the velocity time history for the signal. The IEEE-compatible Landers is a broadband time history that includes a number of oscillations with frequencies in a wide range including low frequencies; therefore, the CSKE of the time history is one of the greatest ones.

Tabas-2 was designed for a qualification testing in the range of low frequencies (below 4 Hz) including extremely low frequencies; therefore the CSKE of the test signal is slightly greater than that for the IEEE-compatible Landers. Tabas-1 was intended for testing at high frequencies (higher than 3 Hz); therefore CSKE is much lower than for the Tabas-2 than that for the IEEE-compatible Landers. The CERL test signal is a filtered time history with a high-pass filter at around 1 Hz. This fact explains relatively low CSKE for this synthetically generated test signal.

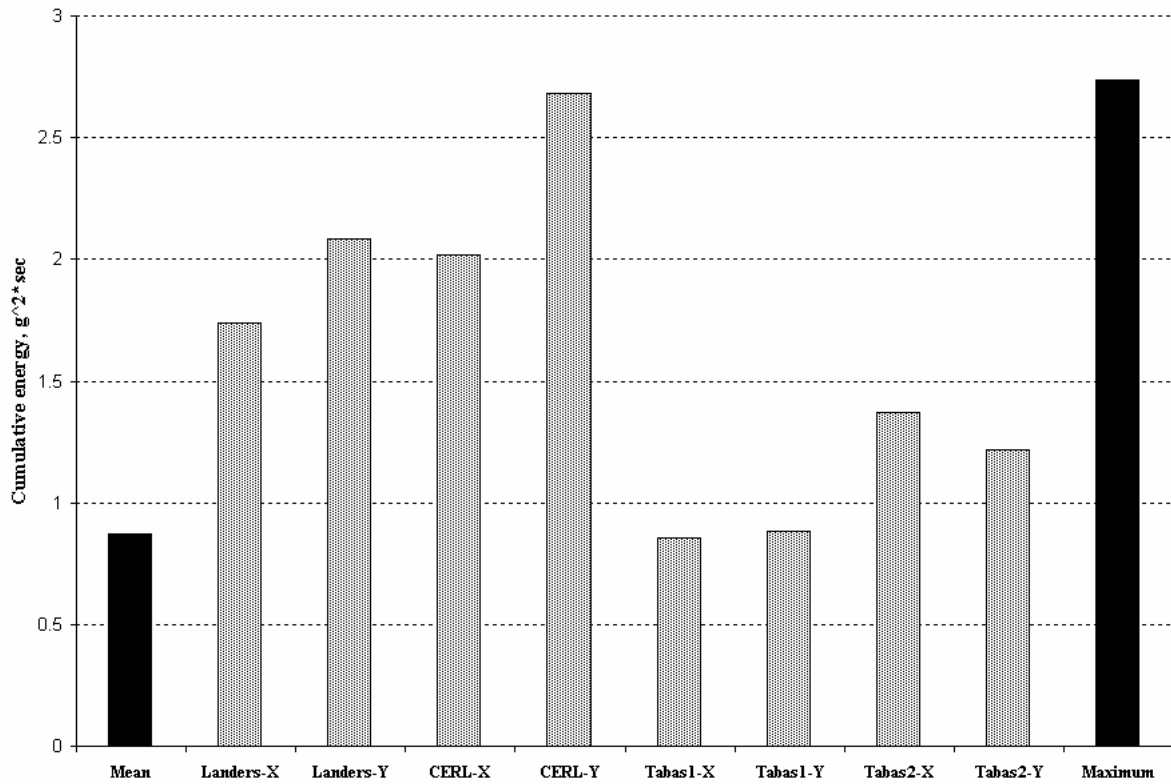


Fig. 5.18 Cumulative energy for IEEE-compatible test signals

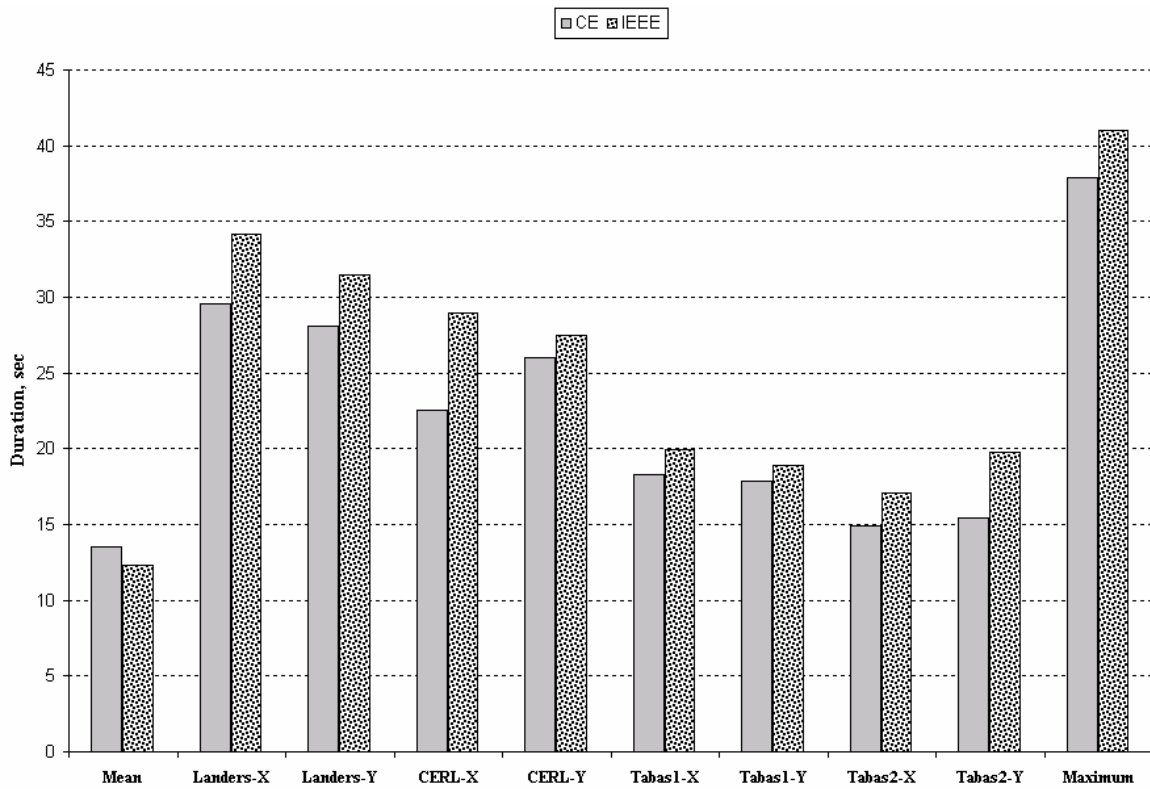


Fig. 5.19 Duration of IEEE-compatible Landers signals

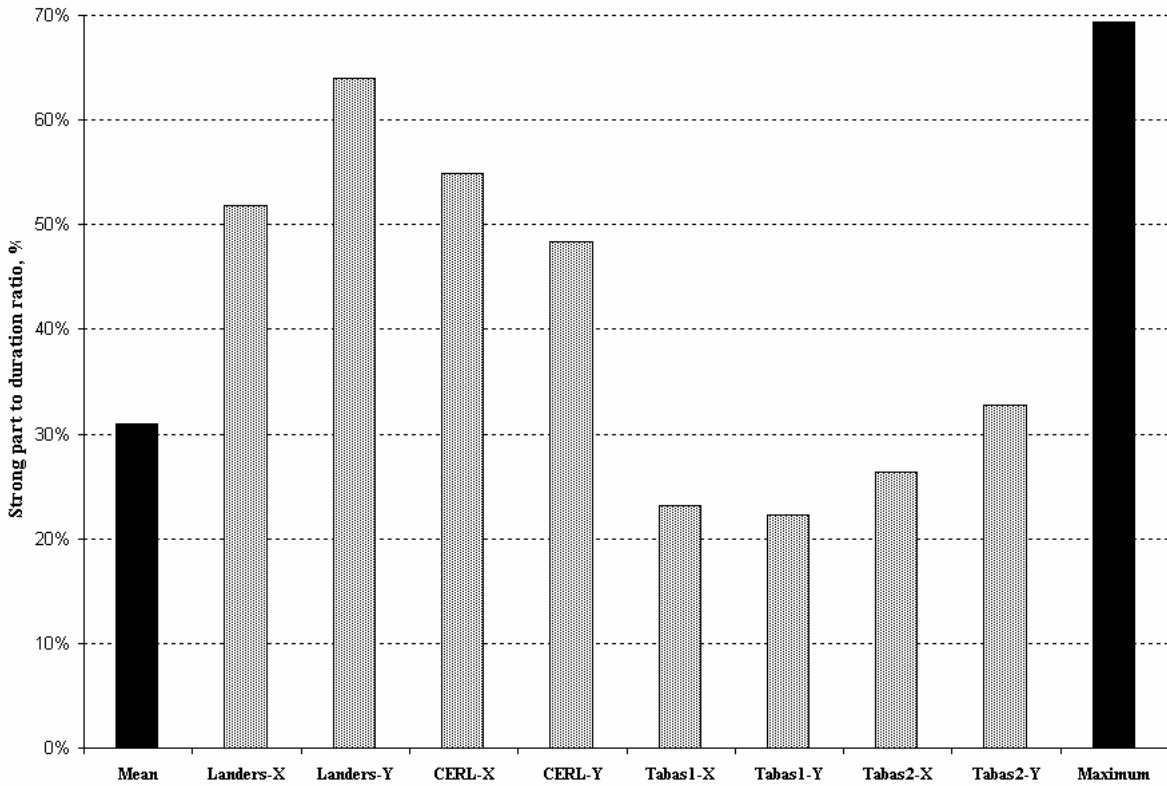


Fig. 5.20 Strong part to duration ratio for test signals

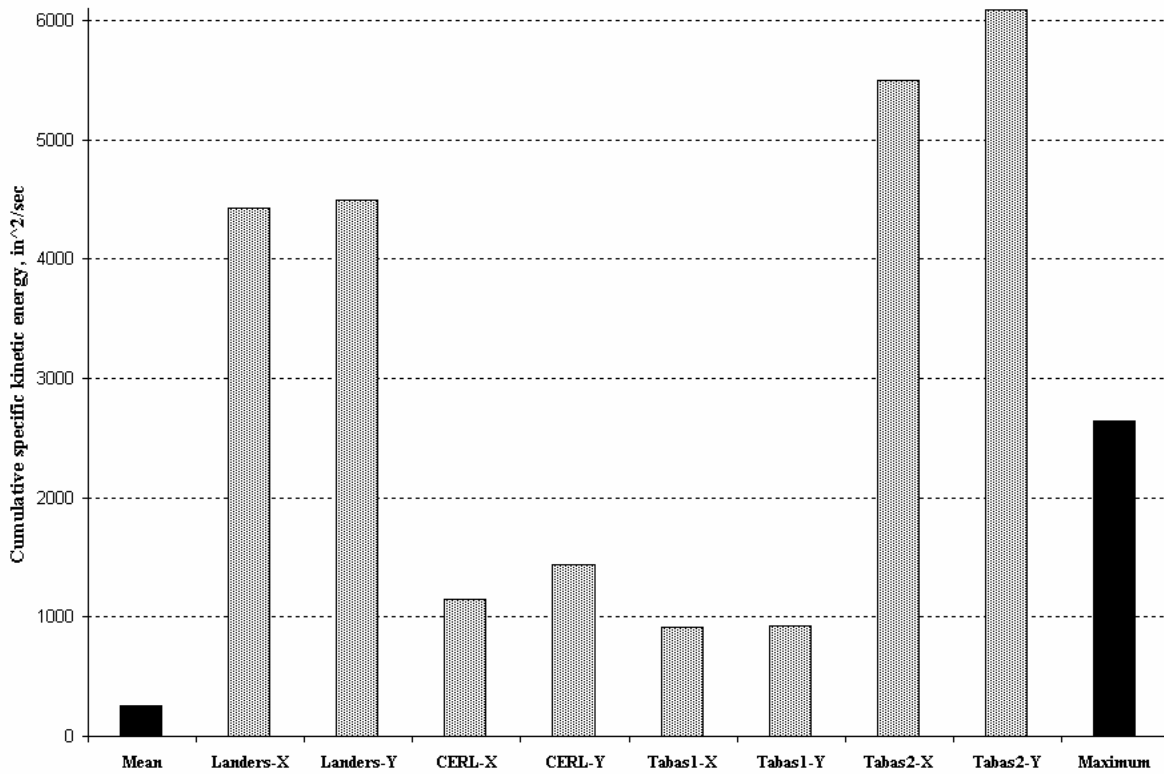


Fig. 5.21 Cumulative specific kinetic energy for IEEE-compatible signals

5.3.4 Conclusions

The discussion above reveals the following main conclusions. The IEEE-compatible Landers (TestQke4IEEE) is a robust strong motion time history that can be used for qualification testing in accordance with the IEEE 693 standard (IEEE, 1998). The main advantages of the IEEE-compatible Landers are formulated as follows:

- the spectra of the time history fit inside of the 30% tolerance zone around the target IEEE response spectrum (at 2% damping) at 1/24 octave frequency resolution. The spectral accelerations at 5% damping are also in the specified 30% tolerance zone except at several individual points.
- the strong motion time history satisfies the 20 sec duration requirement of the IEEE 693 standard. The duration of the time history is longer than the duration of the CERL, Tabas-1, and Tabas-2 (when the last two are considered separately).
- the IEEE-compatible Landers represents a broadband record, in which frequency content is time dependent.
- a non-stationary random behavior of the reference historic record is preserved during the IEEE spectrum procedure conducted in the time domain.
- the IEEE-compatible Landers has the greatest strong part to duration ratio among all studied historic ground motion records and among the test signals studied.
- the cumulative energy of the IEEE-compatible Landers is very close to that of the CERL signal that is the highest among the test signals.
- the number of high-level cycles in the SDOF system response for the IEEE-compatible Landers is in good correlation with the mean for the set of 35 records. It produces at least one cycle for all frequencies and the high cycle count is equal to one cycle only at 4 isolated frequencies. In contrast to the IEEE-compatible Landers, the CERL test signal can cause overtesting of equipment because the latter causes about twice more high cycles in the SDOF response than the former. A similar conclusion is made for the number of cycles imposed by the acceleration time history. The CERL signal imposes an excessive number of cycles that are higher than the maximum for the historic time histories, whereas the number of cycles for the IEEE-compatible Landers is greater than mean and less than the maximum for the set.

- the IEEE-compatible Landers imposes almost as much cumulative specific kinetic energy on electrical equipment as the Tabas-2 does (maximum cumulative specific kinetic energy for test signals studied was observed for Tabas-2).

6 Recommended Requirements for Qualification Testing of Electrical Equipment

This chapter presents recommended requirements for a strong motion time history intended for use in qualification testing of electrical substation by means of an earthquake simulator. Although the study provides the recommended strong motion time history, a user has an option to create a user-specific input signal that would comply with the requirements.

6.1 ANALYSIS FOR TOLERANCE ESTIMATION AND FILTERING LIMITS

The recommended requirements for qualification testing of electrical equipment are summarized in detail in the next section based on the presented analysis.. The analysis focuses on three issues: frequency resolution for TRS verification against the RRS, tolerance zone above the IEEE spectrum, and limitations on a stop frequency in a high-pass filter.

6.1.1 Frequency Resolution for TRS Verification against RRS

A frequency resolution is one of the key requirements for TRS verification against the RRS procedure and is described in detail in most regulatory documents for qualification testing. The IEC-1999 (IEC, 1999) standard specifies 1/12 octave resolution for the 2% damped RRS and 1/6 octave resolution for the 5% damped RRS. The requirements for non-structural component testing described in the AC-156 document (ICBO ES, 2000) also call for 1/6 octave frequency resolution for a general case of a 5% damped system. In general, an elastic response spectrum plotted for a 5% SDOF system is smoother than the corresponding spectrum computed for the system at 2% damping; therefore the reduction in the frequency resolution for a 5% damped system is justified and reasonable.

Supplemental recommendations (U.S. Nuclear Regulatory Commission, 1980) to the RG-1.60 (USASC, 1973) that regulate the seismic design of nuclear power plants recommend a frequency resolution close to 1/8 octave, namely each frequency within 10% of the previous one. Bargiglia et al. (1991) serves as an example of qualification testing of electrical equipment where the frequency resolution of 1/12 octave was used to verify the TRS against the RRS.

Based on the discussion above, the frequency resolution for TRS verification against the RRS is recommended as at least 1/12 octave for a general case of a 2% damped system.

6.1.2 Tolerance Zone Estimation

Tolerance between the TRS and the RRS is another important characteristic in qualification testing; its correct selection could help to avoid unnecessary overtesting or undesired undertesting of electrical equipment. The recommendation on tolerance selection is based on a statistical analysis of 35 strong motion time histories discussed in detail in previous chapters.

Tolerance between TRS and RRS. A mean and a standard deviation for spectra of 35 historic records were computed for two values of critical damping, 2% and 5%, as shown in the bottom plot of Figure 6.1. A relative deviation, defined as the ratio of a standard deviation to a mean at each natural frequency from the range corresponding to the strong part of the IEEE spectrum, was calculated for two damping values and presented in the top plot. The mean for the relative standard deviation was computed as 36% for 2% damping and 30% for 5% damping in this frequency range.

The tolerance of 30% for 5% damped systems is consistent with the corresponding requirement for non-structural component testing described in the AC156 (ICBO ES, 2000) document. A 50% tolerance zone prescribed by the IEC-1999 (IEC, 1999) for various values of critical damping seems to be too conservative and could lead to significant overtesting of equipment.

Therefore, based on average spectra deviation from the mean for historic strong motion records, it is proposed that the tolerance zone above the IEEE spectrum at 2% damping be set as 40%. In other words, the test response spectra (TRS) computed from accelerations recorded at the platform of the earthquake simulator should not exceed 140% of the IEEE spectrum in the

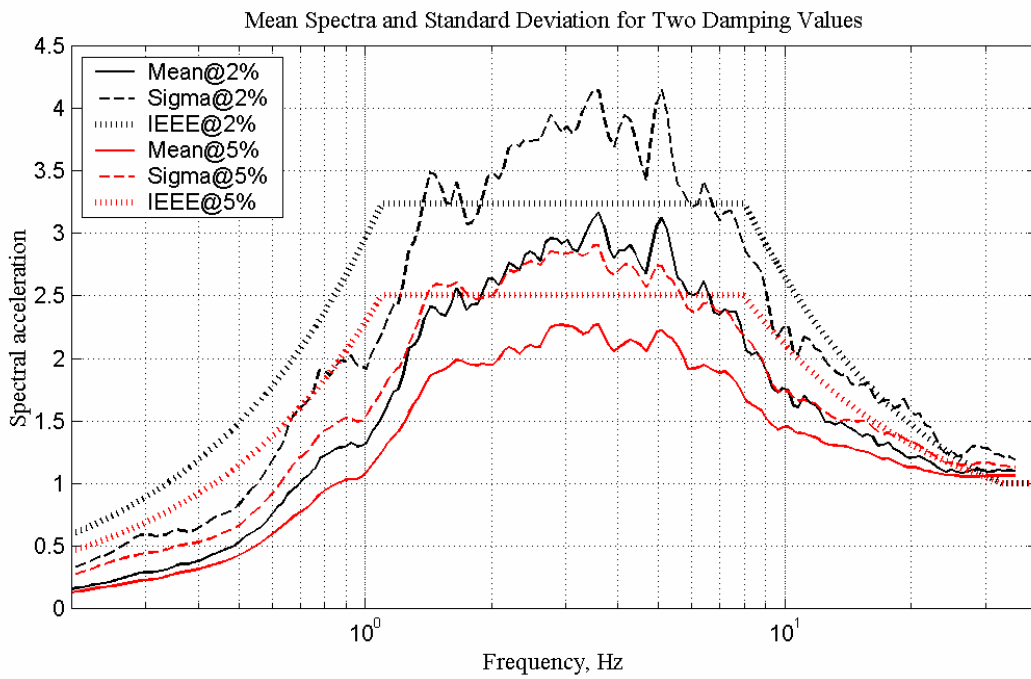
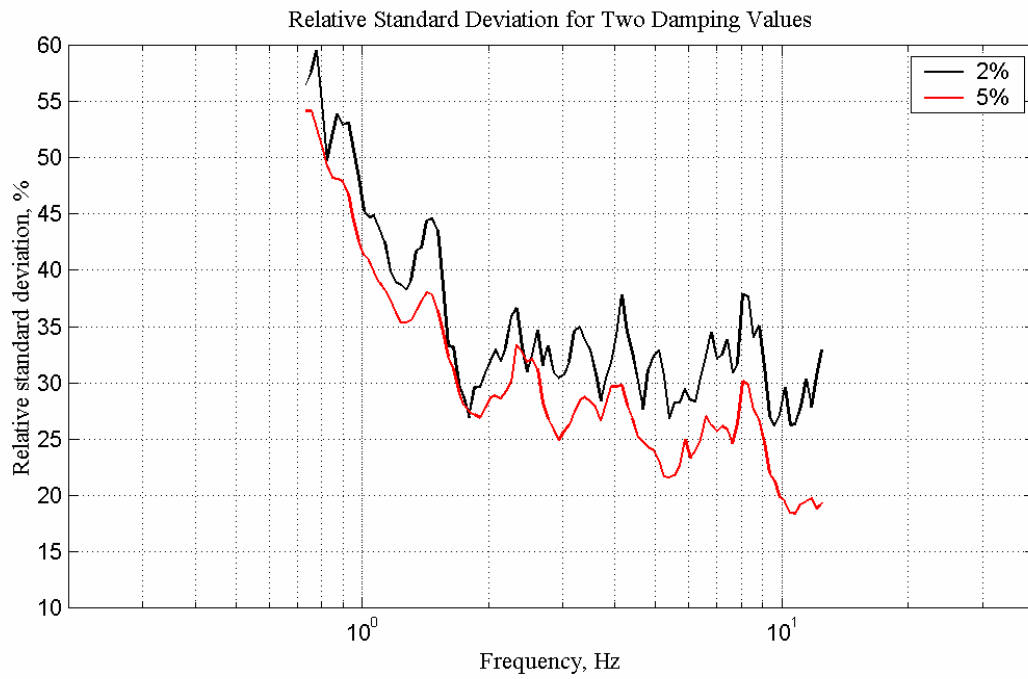


Fig. 6.1 Tolerance analysis conducted for 35 historic strong motion time histories

1/12 octave frequency resolution. Individual points of the TRS up to 10% below the IEEE spectrum can be acceptable provided that the adjacent 1/12 octave points are at least equal to the IEEE spectrum.

Tolerance between theoretical RS and RRS. In order to provide some tolerance for an earthquake simulator performance and accommodate the 40% tolerance zone for TRS above the IEEE spectrum, some recommendations should be followed for generation of the test strong motion time history. The elastic response spectrum computed for the test input strong motion filtered from the IEEE-compatible signal is called here “a theoretical response spectrum.” It is recommended that the theoretical response spectrum does not at any point exceed more than 30% above the RRS and does not fall below 5% of the RRS at individual points for 1/12 octave frequency resolution. The filtering procedure can introduce a significant change in the theoretical response spectrum; therefore, the IEEE-compatible time history should be closely matched to the IEEE target spectrum with at most $\pm 10\%$ variation from the target spectrum in at least 1/24 octave frequency resolution.

6.1.3 Analysis of Limits of Natural Frequency Based on Variation of Stop Frequency of High-Pass Filter

A filtering procedure generally introduces a significant change in the strong motion time history that can lead to a response variation of the SDOF system impacted by it. The limit on a stop filter in a high-pass filter in relation to a natural frequency of a testing system that would minimize the response variation of the system due to filtering is discussed in this section.

The impact of a filtering procedure on the parameters of the SDOF system response was studied based on using the IEEE-compatible Landers in the X direction. The filtering procedure used throughout the study is discussed in great detail in Chapter 5. The signal was filtered with various stop frequencies (f_s) of the high-pass filter and with a constant difference of 0.03 Hz between a corner (f_c) and the stop frequencies. The parameters for the low-pass filter remained the same: 33 Hz for the corner frequency and 34 Hz for the stop frequency. The stop frequency varied from 0.92 Hz (the test strong motion recommended for PL testing at simulators with a capacity similar to that of EERC) to 2.52 Hz with a 0.1 Hz increment. The input and output acceleration time histories were not normalized before or after imposing on the SDOF system, so their peak values were preserved. The peak ground displacement (PGD), peak ground velocity

(PGV), and peak ground acceleration (PGA) for each filtered version is presented in Table 6.1. The plots of peak values divided by the corresponding peak value for the signal filtered at the 0.92 Hz stop frequency are presented in Figure 6.2. The PGA changes insignificantly with variation of the stop frequency, whereas a dramatic change occurs in the peak ground velocity and displacement. The PGV drops to about 40% and the PGD drops to about 20% of that at 0.92 Hz stop frequency. This represents a general strategy of any filtering procedure that consists of preserving the PGA (to be able to test an equipment at a certain severity level) and reducing PGV and PGD to accommodate simulator capacity.

Impact of filtering on number of high cycles in SDOF system response. The number of high acceleration cycles in a SDOF system response was calculated as follows. The acceleration cycle was included into a count only if its magnitude was greater than 70% of that for the IEEE plateau value (for spectrum anchored at 1.0g) and was computed only for 2% damped systems. In other words, the number of high cycles represents a count of cycles with amplitudes within limits of the strong part of the IEEE spectrum anchored at 1.0g PGA.

Table 6.1 Peak values for filtered versions of the IEEE-compatible Landers record

No.	Stop frequency: f_s , Hz	Corner frequency: f_c , Hz	PGD, in.	PGV, in./sec	PGA, g
1	0.92	0.95	3.15	29.0	0.88
2	1.02	1.05	2.45	23.7	0.9
3	1.12	1.15	3.12	26.9	1.03
4	1.22	1.25	2.36	24.1	0.93
5	1.32	1.35	1.73	19.5	0.98
6	1.42	1.45	1.38	17.3	0.9
7	1.52	1.55	1.11	16.4	0.89
8	1.62	1.65	1.06	14.8	0.86
9	1.72	1.75	1.03	15.1	0.89
10	1.82	1.85	0.96	14.4	0.86
11	1.92	1.95	0.97	15.3	0.88
12	2.02	2.05	0.93	14.2	0.87
13	2.12	2.15	0.73	12.5	0.89
14	2.22	2.25	0.6	10.7	0.84
15	2.32	2.35	0.55	10.3	0.86
16	2.42	2.45	0.47	10.5	0.85
17	2.52	2.55	0.50	9.9	0.86

Typical results for high cycle counts computed for several filtered signals are presented in Figure 6.3. The number of high cycles in a SDOF system response varies from one filtered version to another, but is close to the corresponding value of the least filtered version at natural frequencies far enough from the stop frequency of the high-pass filter. The differences between the counts for the initial signal with the least filtering (stop frequency at 0.92 Hz) and all others plotted in 1/12 octave resolution are presented in Figures 6.4 and 6.5. The difference between cycle counts, also called “a relative count of high cycles,” is within ± 2 cycles for natural frequencies far enough from the stop frequency of the high-pass filter and for most of the stop frequencies. The ± 2 cycles tolerance is located between two dashed green lines in Figures 6.4 and 6.5. It is worth noting that dips below -2 cycles tolerance would be acceptable because they would show that the filtered signal cases have more cycles in the SDOF system response than the initial one. At the same time, peaks more than $+2$ cycles above the tolerance zone would be not acceptable because they would show that the filtered signal produced fewer high cycles in the SDOF system response, in this sense weaker than the initial signal.

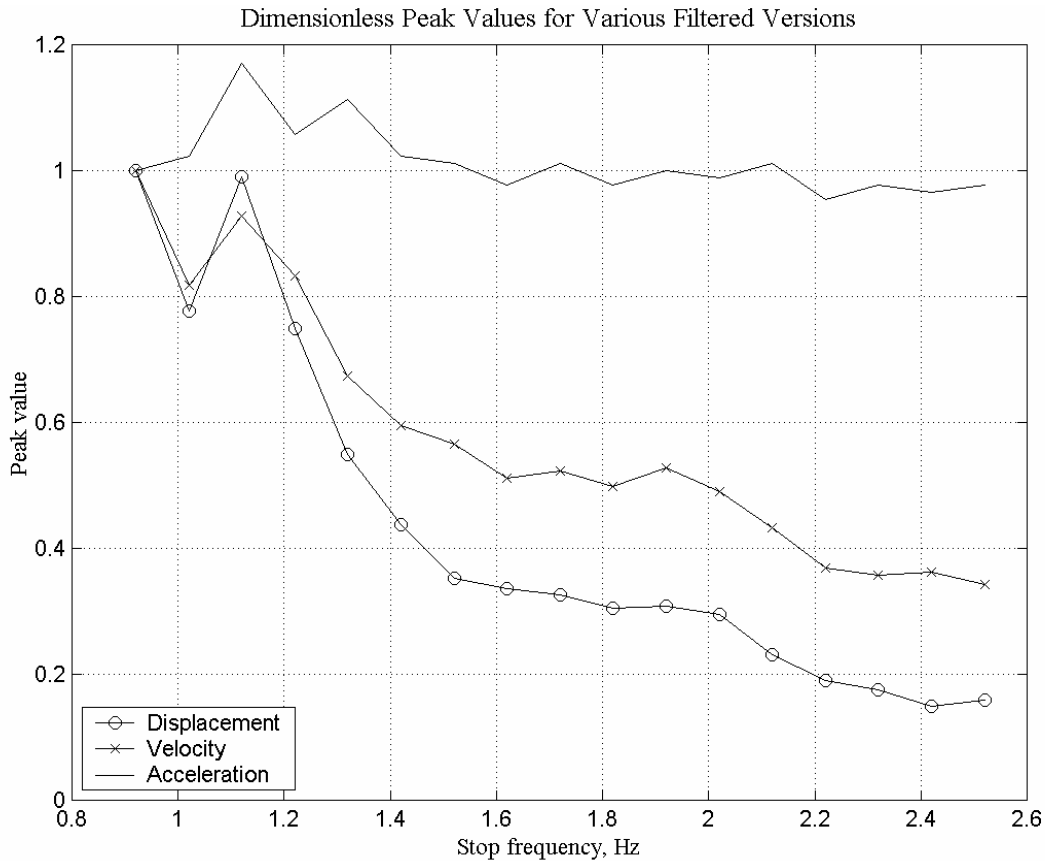


Fig. 6.2 Normalized peak values for all filtered versions

The analysis presented in the figures demonstrates that the response of a SDOF system with a natural frequency that is greater than 1/0.7 times the stop frequency of the high-pass filter will be insignificantly affected by the filtering procedure. Therefore an acceptable limit for a stop frequency in the high-pass filter should be not higher than 70% of the natural frequency of the electrical equipment.

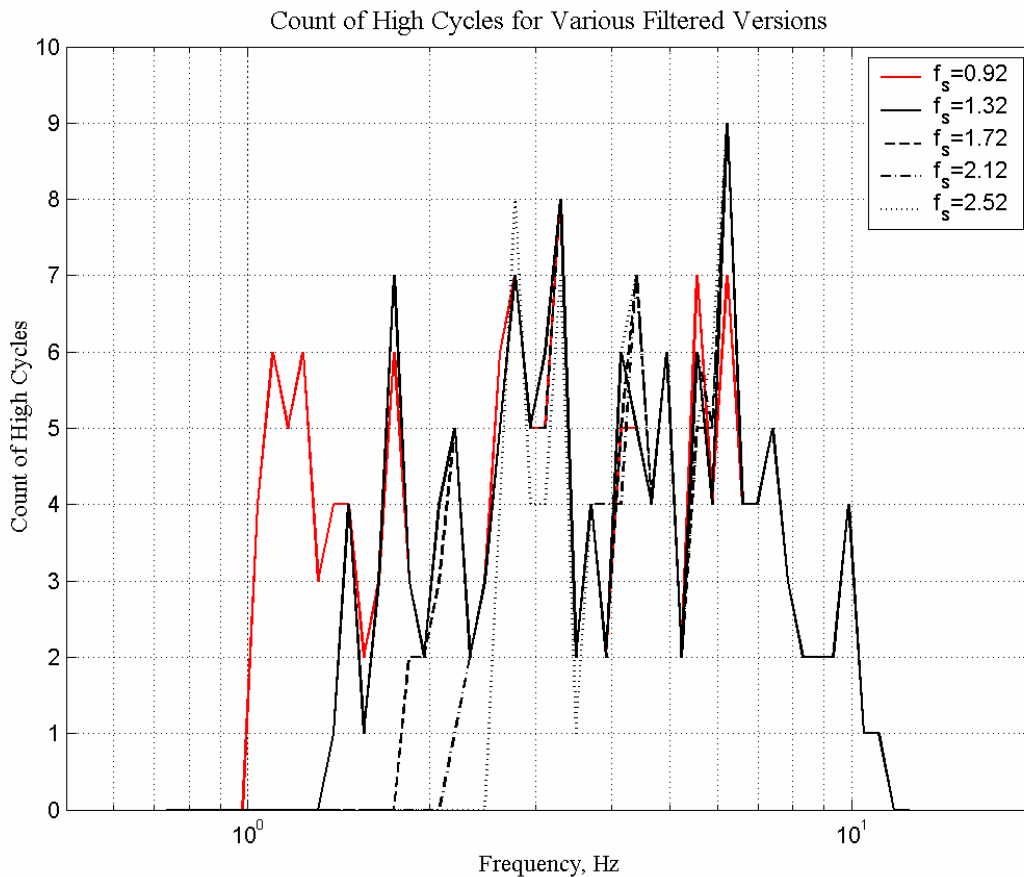


Fig. 6.3 Count of high cycles for various filtered versions

Impact of filtering on elastic response spectra. The impact of filtering on elastic response spectra was studied for the same set of filtered strong motions presented in Table 6.1. Elastic response spectra for several filtered versions are presented in Figure 6.6, where they are plotted at 1/12 octave frequency resolution against the IEEE high PL spectrum anchored at 1.0g PGA. These response spectra comply with the recommendation for the tolerance of the theoretical response spectrum; namely, they fit inside the -5% to +30% tolerance zone for the

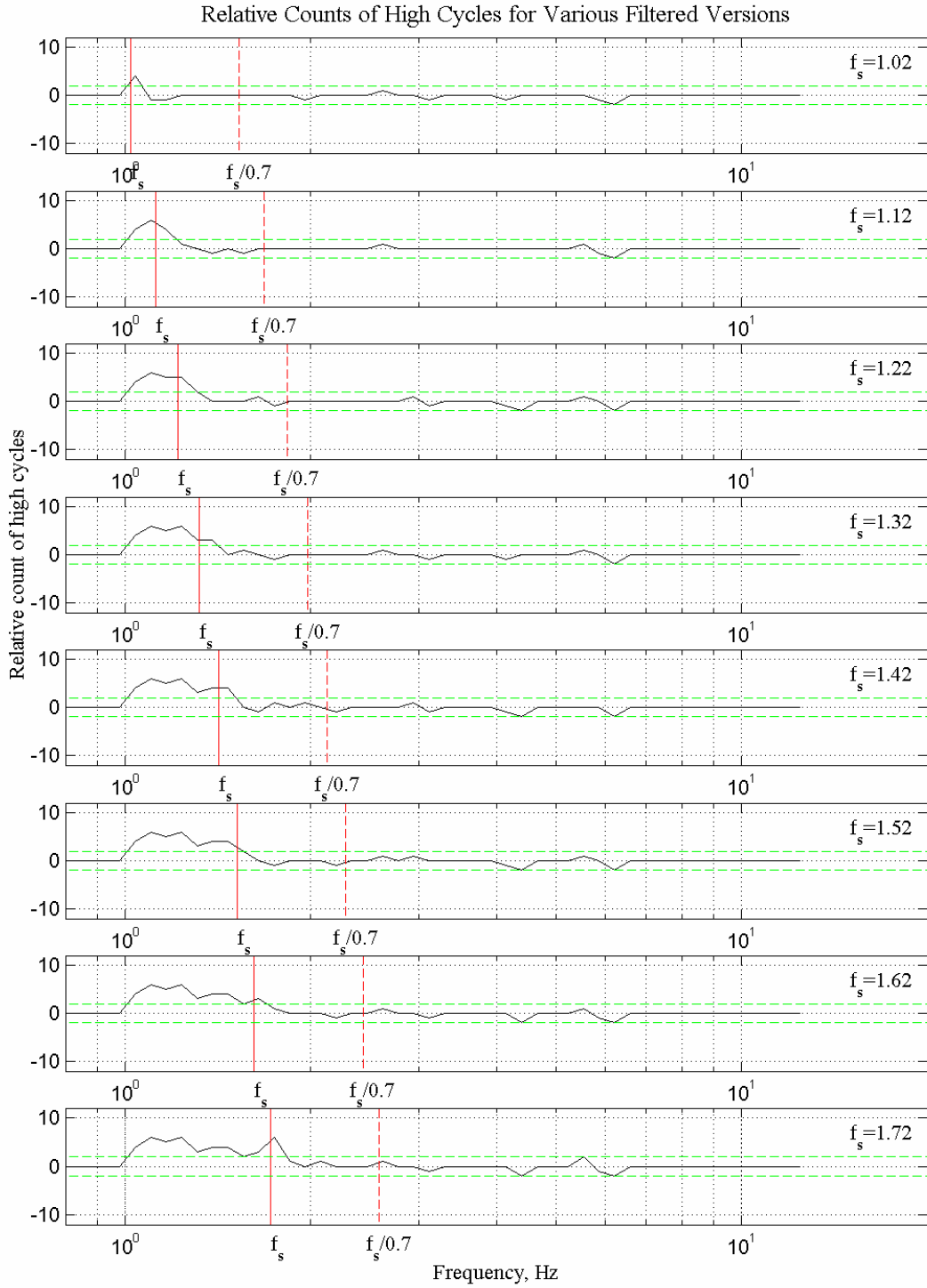


Fig. 6.4 Difference in cycle counts at 1/12 octave resolution: part 1

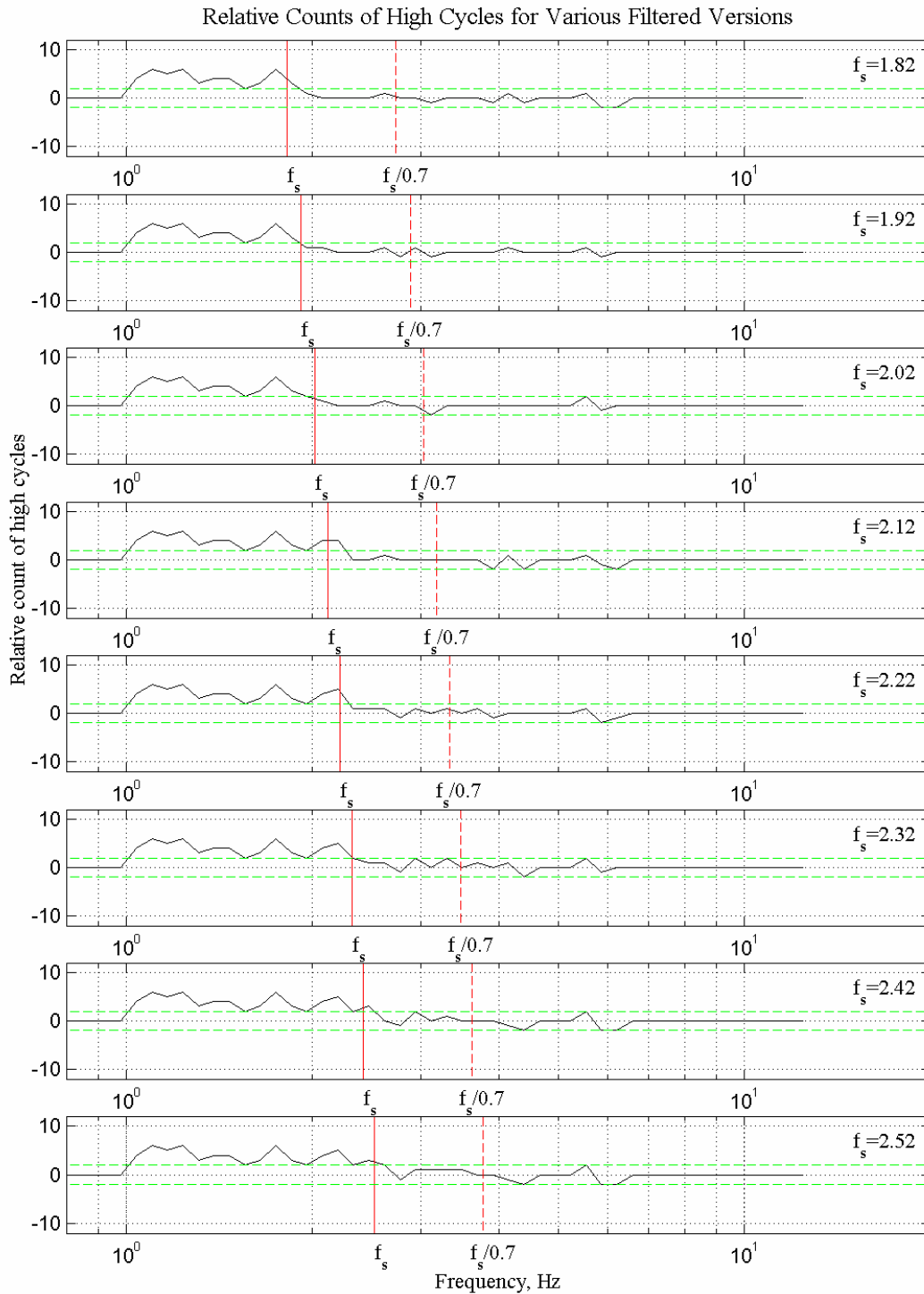


Fig. 6.5 Difference in cycle counts at 1/12 octave resolution: part 2

required frequency resolution. The valleys below the IEEE spectrum are less than 5% and limited to only one individual point at 1/12 octave frequency resolution.

Spectra differences between the least filtered signal (the initial one recommended for testing at PL level at the EERC simulator) and each other signal normalized to the plateau value of the IEEE spectrum are presented in Figures 6.7 and 6.8.

The normalized differences between spectra are within $\pm 10\%$ for the natural frequencies far enough from the stop frequency of the high-pass filter and for the majority of the stop frequencies. The $\pm 10\%$ cycles tolerance is located between two dashed green lines in Figures 6.7 and 6.8. It should be noted that dips below the -10% tolerance line (as can be seen in the case of the 1.52 Hz and 1.62 Hz stop frequencies) are acceptable because they show that the filtered signal causes higher spectral acceleration than the initial one. At the same time, peaks more than $+10\%$ above the tolerance zone would be not acceptable because they would show that the filtered signal develops less spectral acceleration; in this sense it is weaker than the initial signal.

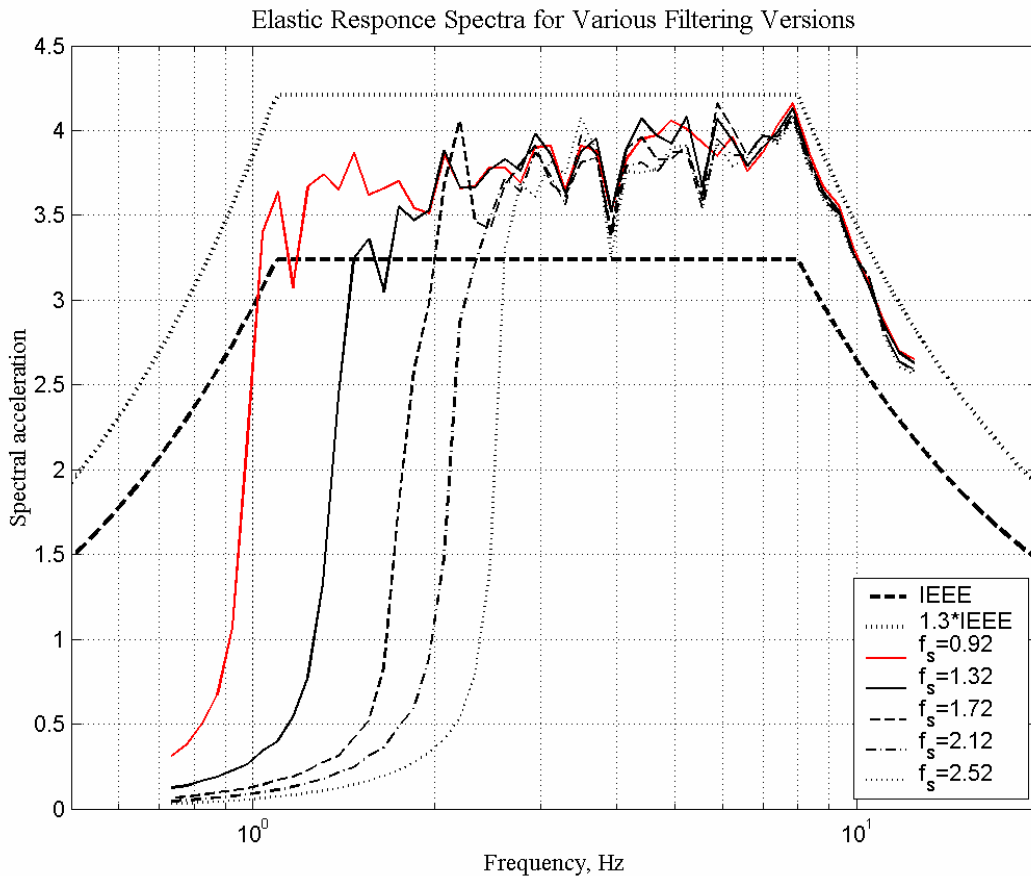


Fig. 6.6 Elastic response spectra computed for various filtered versions

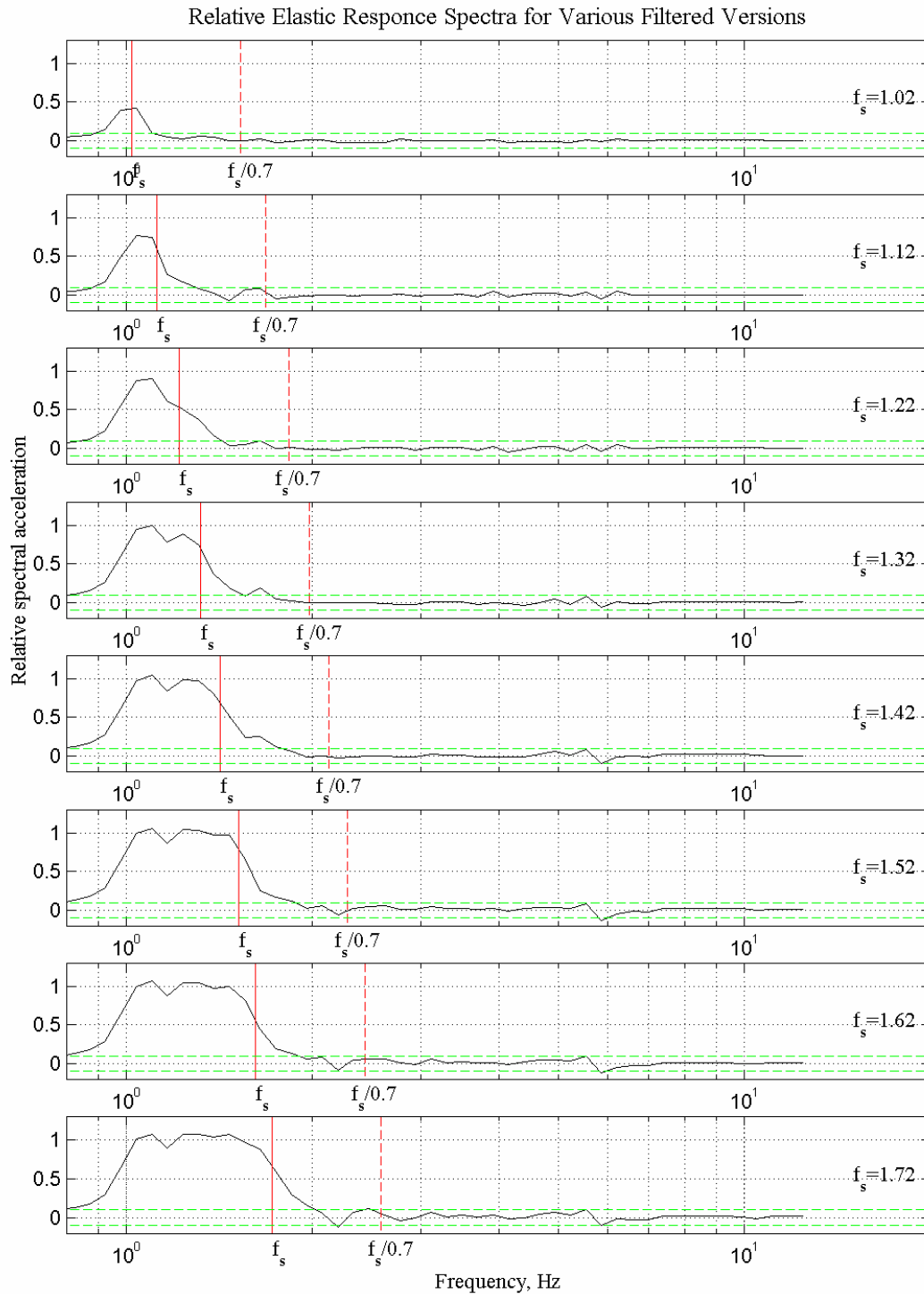


Fig. 6.7 Normalized difference in elastic response spectra: part 1

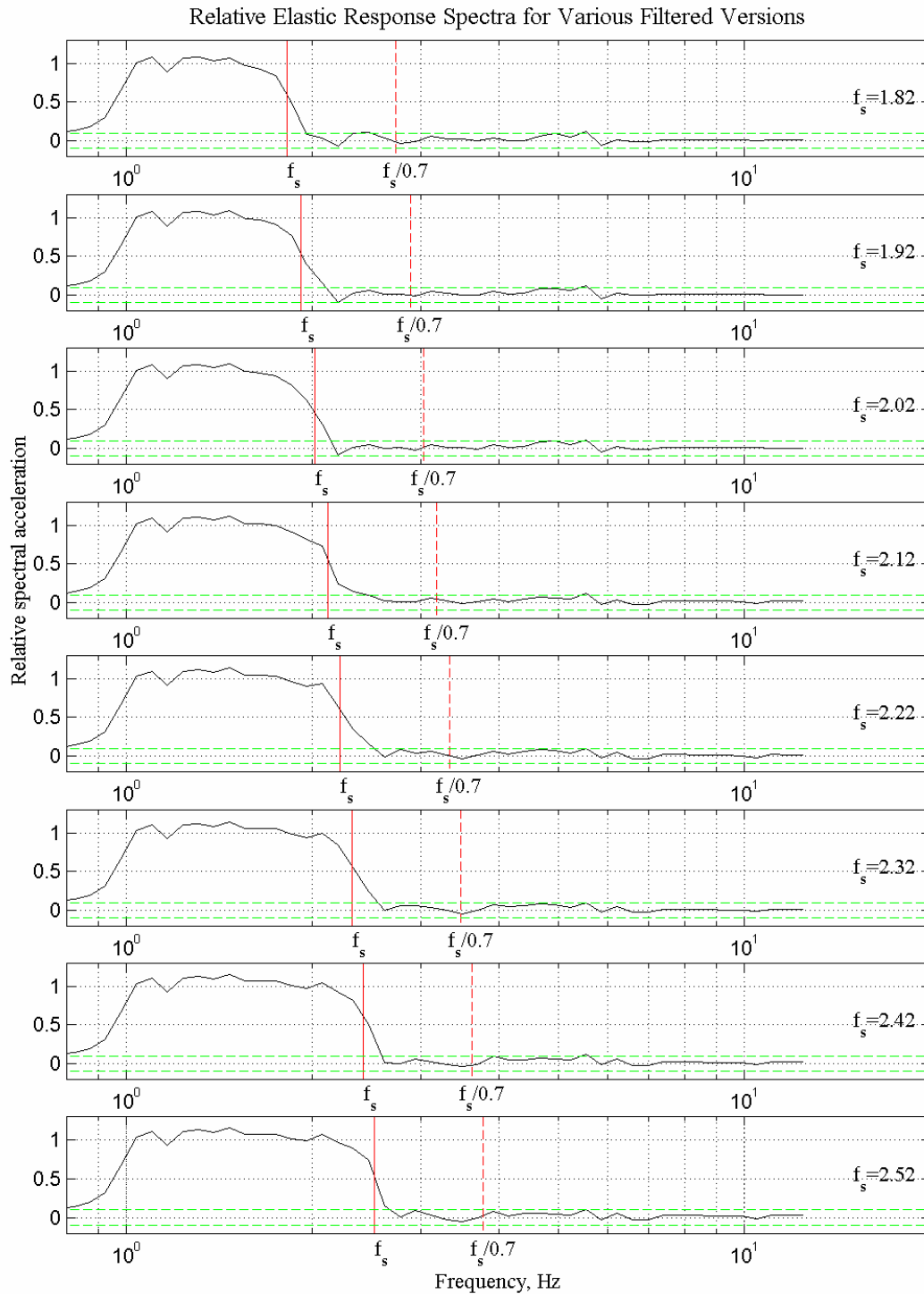


Fig. 6.8 Normalized difference in elastic response spectra: part 2

The analysis demonstrates that the response spectra of a SDOF system with a natural frequency higher than $1/0.7$ times the stop frequency of the high-pass filter will be insignificantly affected by the filtering procedure that confirms a similar result for high cycle counts. Therefore an acceptable limit for a stop frequency in the high-pass filter is recommended to have not higher than 70% of the natural frequency of the electrical equipment.

6.2 TEST SIGNAL REQUIREMENTS FOR ELECTRICAL EQUIPMENT

Based on previous discussion and analysis, the following section presents recommendations on qualification testing of electrical equipment by means of time history testing on an earthquake simulator. The discussion here is also based on recommendations and requirements taken from related codes, standards, and regulatory documents.

The study developed the IEEE-compatible strong motion time history that was modified from a recorded strong motion time history to match the IEEE spectra with a low mismatch. The study also provides a filtering procedure to develop a test signal from the IEEE-compatible time history that would accommodate the capacity of a particular earthquake simulator. The IEEE-compatible strong motion time history and its sample versions (filtered for use at the EERC simulator) comply with the recommendations on qualification testing of electrical equipment developed in the study and summarized below. The use of the prescribed time history is optional and can be replaced with another signal closely matched to the IEEE spectra that complies with all recommendations for qualification testing.

A system with 2% critical damping is a general case for qualification testing of electrical equipment.

6.2.1 Requirements on Generation of Alternative IEEE-Compatible Signal

The IEEE-compatible signal can be modified from a recorded strong motion time history or it can be synthetically generated. The matching procedure shall be conducted with at least $1/24$ octave frequency resolution with the maximum mismatch between the spectra of $\pm 10\%$ at $1/24$ octave. The IEEE-compatible Landers record was matched to the IEEE spectra at about $1/30$ octave frequency resolution (for two damping values of 2% and 5% with emphasis on better

correlation with 2% target spectrum) and the mismatch between spectra at 2% damping does not exceed $\pm 10\%$ at 1/24 octave frequency resolution.

The frequency resolution for verification of the response spectrum of the IEEE-compatible signal and the RRS is recommended to be set as 1/24 octave, which gives about 200 points in the frequency range from 0.15–35 Hz (corner frequency of the IEEE plateau of 1.1 Hz is among these points):

$$f_i = 0.1375 * 2^{(i/24)} \quad (i = 1, \dots, 192). \quad (7.1)$$

6.2.2 Filtering Procedure and Theoretical Response Spectrum of Filtered Signal

The filtering procedure adopted in the study uses a combined high-pass and low-pass filter that has a trapezoidal shape in the frequency domain. The IEEE-compatible signal shall be scaled up before filtering (in order to envelop the IEEE-spectrum) and the procedure then applied. The resultant signal shall produce an elastic response spectrum that is within a -5% to $+30\%$ tolerance zone from the IEEE spectrum at the 1/12 octave frequency resolution. Spectrum valleys below the target by -5% can be acceptable only at individual points provided that the adjacent 1/12 octave points are at least equal to the RRS.

Based on this information and the analysis above, the frequency resolution for verification of theoretical RS against the RRS is recommended to be set as 1/12 octave, which gives about 100 points in the frequency range from 0.15–35 Hz (corner frequency of the IEEE plateau of 1.1 Hz is among these points):

$$f_i = 0.1375 * 2^{(i/12)} \quad (i = 1, \dots, 96). \quad (7.2)$$

A stop frequency of the high-pass filter used in the filtering procedure should be less than 70% of the natural frequency of equipment intended for qualification testing by means of the filtered time history.

Two filtered versions of the IEEE-compatible Landers (intended for use at the EERC simulator) comply with the recommendations for filtered signals specified above and are available for downloading.

6.2.3 Tolerance and Frequency Resolution for TRS

Although the theoretical response spectrum for a filtered signal shall fit in the -5% to $+30\%$ tolerance zone, this tolerance may be not enough for test response spectra computed for accelerations recorded at a simulator platform. Therefore, the tolerance between TRS and the RRS shall be increased as described below.

Although the GR-63 (Telecordia, 2002) document requires plotting TRS against the RRS at $1/6$ octave resolution for 2% damping, other documents suggest using a resolution of $1/12$ octave at this damping in order to verify the mismatch between these two spectra. Regulatory Guide 1.60 (USASC, 1973) calls for $1/10$ octave frequency resolution. The detailed information obtained from codes, standards, and other regulatory documents was presented earlier in Table 2.2. The low-frequency resolution of $1/6$ octave is mostly recommended for 5% damping when the TRS plots are significantly smoother than in the case of 2% damped spectra. A number of qualification tests conducted by others (Bargiglia et al., 1991) also used $1/12$ octave resolution to compare the TRS and the RRS at 2% damping.

Therefore it is recommended that the TRS should meet or exceed the IEEE RRS at the $1/12$ octave frequency resolution described by Eq. 7.2.

Another important aspect of TRS is a tolerance zone above the RRS that was specified in three documents among all the codes and standards studied. In two cases, the tolerance zone was set at 30% above the RRS (Telcordia, 2002, for 2% damped and ICBO ES, 2000, for 5% damped), and the third established a 50% tolerance zone above the RRS (IEC, 1999). In order to avoid unnecessary overtesting during qualification tests, the study recommends the 40% tolerance zone at 2% critical damping, which is a general case for electrical equipment. TRS valleys up to -10% are acceptable only at individual points provided that the adjacent $1/12$ octave points are at least equal to the RRS.

6.2.4 Number of Cycles with High Amplitude in SDOF System Response

In addition to other requirements specified in the IEEE 693 standard (IEC, 1999), it is recommended that the input strong motion be checked for the number of high-amplitude cycles in the SDOF system response. This parameter was defined earlier and discussed in detail in

Chapter 6; a similar parameter, named count of “high-peaks” is specified in the IEC-1999 standard.

The comprehensive study on a set of 35 historic strong motions showed that the maximum for a high cycle count varies from 6–26 in a wide range of frequencies (computed from a SDOF system response with fixed damping of 2%). The mean of the high cycle counts for the set varied from about 2–6 cycles. Therefore in order to avoid unnecessary overtesting and undesired undertesting, it is recommended to limit the cycle count to this range of cycles, although several individual dips to one high cycle count in the count frequency plots are acceptable. The IEC-1999 (IEC, 1999) standard calls for 3–20 “high peaks” in input strong motion for seismic testing. It is noteworthy that three “high peaks” with the same range would produce one cycle according to the ASTM definition (ASTM, 1997). It should also be noted that the cycle count is generally significantly larger for synthetic input signals generated from a series of harmonics as demonstrated earlier in the example of the CERL input signal.

Most of the time histories caused at least one high cycle in the SDOF response. Therefore, the lower limit for the number of high cycles is at least one cycle at any natural frequency of the SDOF system at 2% critical damping when the cycle count is plotted in the 1/12 octave frequency resolution for the frequency range corresponding to the strong part of the spectrum.

6.2.5 Strong Motion Duration

The IEEE 693 standard (IEC, 1999) requires an input signal that is at least 20 sec long. The requirement does take into account a duration of strong vibrations. The strong part ratio parameter introduced in the study and expressed as a strong part to duration ratio can be used for this purpose. The statistical study on the set of 35 historic strong motions showed that this ratio can vary from about 10%–60% for the horizontal direction. The mean of the set was about 30%. To avoid undertesting during qualification testing, requiring at least 30% for the strong part ratio is recommended.

7 Summary and Conclusions

The main objectives of the theoretical research and the IEEE-compatible time history modified from a recorded accelerogram were achieved. The reference time history was selected based on analyses of a number of parameters and indices from a large set of strong motion records. A time domain matching procedure was used in the development of the IEEE-compatible time history. The time history is recommended for seismic qualification testing of electrical substation equipment in accordance with the IEEE 693 procedure. All major achievements and recommendations for generating the procedures of the test time history and seismic qualification are summarized in this chapter.

7.1 STUDY OF STRONG MOTION RECORDS AND MATCHING PROCEDURES

7.1.1 Study of Strong Motion Time Histories

Based on the detailed study on the set of 35 strong motion time histories, the following conclusions are made. The Joshua Tree acceleration record obtained during the 1992 Landers, California, earthquake represents a robust strong motion time history. The normalized Landers record has several advantages over other strong motions studied as follows:

- The duration of the Landers record computed for the IEEE and the CE definitions is longer than 20 sec as required by the IEEE 693 standard.
- The Landers record has the maximum value (among all records studied) for the strong part to duration ratio (about 60%).
- After scaling to 1.0g PGA, the Landers record has total cumulative energy that exceeds the mean-plus-one standard deviation of the set.
- The value of the RMS acceleration for the record is very close to the mean-plus-one standard deviation of the set.

- The PGV of the normalized Landers record is very close to the mean-plus-one deviation of the set.

- The number of cycles with a 25% threshold in the accelerogram is higher than the mean for the set.

- The Landers record is a broadband strong motion time history.

- The number of high cycles in the acceleration response of a SDOF system has adequate even distribution in a wide range of the natural frequencies of the system.

The analysis based on a study of low-magnitude earthquakes that occurred in the central and eastern U.S. showed the following characteristics:

- Low-magnitude earthquakes tend to have more high-frequency energy,

- Earthquakes on rock tend to have more energy in the high-frequency range due to low damping in central and eastern hard rocks, and

- For eastern and central U.S. sites, the IEEE spectral shape is probably too low (high seismic hazard regions, based on current NEHRP estimates).

Analysis based on a study of MCE spectra at major seismic hazard regions revealed the following conclusions:

- The IEEE procedure of qualification testing is appropriate for most seismic regions of the U.S. except the central U.S. (CUS).

- Current hazard estimates provided in NEHRP maps of the CUS indicate that high hazard areas, such as Memphis, Tennessee, have MCE spectra that exceed the IEEE 693 PL spectra, particularly in the frequency range above 8 Hz. Spectral enveloping of these sites would principally require shifting the plateau of the IEEE 693 spectrum toward the high-frequency side for type A sites, and would require both frequency-shifting and increasing the spectral acceleration by about 20% for site types B, C, and D.

- The paucity of strong motion data from central/eastern U.S. earthquakes highlights the need for additional research to provide improved estimates of the seismic hazards in these regions.

7.1.2 Study of Spectrum Matching Procedures

The advantages of the time domain matching procedure and the IEEE-compatible Landers test time history generated are as follows:

- The modifications introduced do not alter the non-stationary character of a reference historic record.
- The target spectrum can be matched with low deviation from it at several damping values.
- The power spectral density of the signal is evenly enriched in the wide frequency range and is strongly time dependent, which is characteristic of an actual strong motion record.

The disadvantages of the frequency domain matching procedure and the synthetically generated time histories are as follows.

- The frequency domain matching procedure can introduce an undesirable high-frequency noise in the time history.
- The time history matched to the target spectrum at one damping can significantly misfit the target response spectrum for another damping.
- The power spectral density for a signal produced by the frequency domain procedure is not as even as that for the time history produced by the time domain method.
- The synthetically generated signal has a strong stationary character opposite to that of an actual strong ground motion record.
- The time history produced by a frequency domain procedure and a synthetically generated time history can impose an excessive number of cycles on equipment.

Based on this analysis of response spectrum matching procedures, the time history procedure was used in the development of the IEEE-response-spectra-compatible time history.

7.2 SUMMARY AND CONCLUSIONS FOR RECOMMENDED INPUT SIGNAL

The input signal (time history for qualification testing) developed in the study satisfies all requirements specified in this chapter. Additionally, it has a number of other advantageous properties summarized below.

7.2.1 Properties of Recommended Input Signal

The IEEE-compatible Landers (TestQke4IEEE) is a robust strong motion time history that can be used for qualification testing in accordance with the IEEE 693 standard. The main advantages of the test record are as follows.

- The spectra of the strong motion time history fits inside a $\pm 10\%$ tolerance zone around the target IEEE response spectrum (at 2% damping) at a 1/24 octave frequency resolution. The spectra adequately closely match the IEEE spectrum for 5% damping.

- The test strong motion time history satisfies the 20 sec duration requirement of the IEEE 693 standard. The duration of the signal is longer than the duration of the CERL, Tabas-1, and Tabas-2 (when the last two are considered separately).

- The IEEE-compatible Landers represents a broadband record consisting of oscillations with frequencies from the wide frequency range specified by the standard.

- The non-stationary random behavior of the reference historic record is preserved during the target spectrum matching procedure conducted in the time domain.

- The IEEE-compatible Landers has the highest strong part to duration ratio among all the historic ground motion records studied and among the test signals in current use.

- The cumulative energy of the IEEE-compatible Landers is very close to the CE of the CERL signal, which is the highest among test signals in current use.

- The number of high-level cycles in the SDOF system response under the impact of the IEEE-compatible Landers correlates well with the mean for the set of 35 records, despite the CERL signal that can cause overtesting of equipment due to the extremely high number of these cycles. A similar conclusion is made for the number of cycles imposed by the acceleration time history. The CERL signal imposes an excessive number of cycles higher than the maximum value for the historic time histories, whereas the number of cycles for the IEEE-compatible Landers is greater than mean and less than the maximum for the set.

- The IEEE-compatible Landers imposes as much total kinetic energy on electrical equipment as the Tabas-2 (the maximum total kinetic energy for test signals is observed for Tabas-2).

7.2.2 Summary of Recommended Requirements for Qualification Testing

Based on the previous analysis and discussion, the following requirements for a test signal intended for qualification testing of electrical equipment are recommended. It should be noted that the IEEE-compatible Landers and two sample versions for testing at the EERC simulator comply with all requirements presented below (except the TRS requirement that depends on the performance of a particular shake table).

- The IEEE-compatible signal can be modified from a historic strong motion time history or can be synthetically generated. The matching procedure shall be conducted with at least 1/24 octave frequency resolution with the maximum mismatch between the spectra of $\pm 10\%$ at 1/24 octave.

- The signal filtered from the IEEE-compatible time history shall produce an elastic response spectrum that is within the -5% to $+30\%$ tolerance zone from the IEEE spectrum at 1/12 octave frequency resolution. Spectrum dips up to -5% can be acceptable only at individual points, provided that the adjacent 1/12 octave points are at least equal to the RRS.

- The theoretical input motion record used for testing may be high-pass filtered at frequencies less than or equal to 70% of the lowest frequency of the test article, but not higher than 2 Hz.

- To avoid unnecessary overtesting and undesired undertesting during qualification tests, the study recommends the 40% tolerance zone for TRS above the IEEE spectrum at 2% critical damping, in general for electrical equipment. TRS dips up to -10% can be acceptable only at individual points, provided that the adjacent 1/12 octave points are at least equal to the RRS.

- The maximum number of high cycles in a SDOF system response should be about 26 cycles, the maximum for the set of 35 historic strong motion records used in the study. The high cycle counts for the majority of natural frequencies should be higher than 2. The lower limit for the number of high cycles is one cycle at 2% critical damping when the cycle count is verified in the 1/12 octave frequency resolution for the frequency range corresponding to the strong part of the spectrum. The number of dips to 1 high cycle in count-frequency plots should be limited.

- To avoid undertesting during the qualification test, it is recommended that the requirement for the strong part ratio be at least 30%; this number represents the mean for the set of 35 historic records.

7.3 RECOMMENDATIONS FOR IEEE 693 QUALIFICATION PROCEDURE

Based on detailed analysis, the study recommends that certain requirements summarized in Appendix D be included in the new version of IEEE 693. The input signal developed in the study satisfies all requirements specified in this chapter.

7.3.1 Prescribed IEEE-Compatible Landers

The IEEE-compatible Landers is a robust strong motion time history that was created by means of an earthquake simulator for qualification testing in accordance with the IEEE 693 standard. The strong motion time history is proposed for inclusion in the new version of the IEEE 693 document as a prescribed time history for shake table testing.

7.3.2 Requirements on Generation and Filtering Procedure

The recommendations developed in the study and summarized in Appendix D are recommended for inclusion in the new version of the IEEE 693 standard for generation and filtering of the IEEE-compatible time history.

7.3.3 Limitations of RRS Prescribed by IEEE 693 in Central and Eastern U.S.

The IEEE 693 document specifies a RRS that was based upon historic strong motions that may not be representative of large earthquakes at rock sites in the central and eastern U.S. and southeastern Canada. While users of the standard should be aware of this discrepancy, its effects are somewhat mitigated by the fact that large earthquakes in this region of North America have a very low frequency of occurrence. In addition, exceedances of the currently specified IEEE 693 spectra occur at high frequencies, which are likely to be less damaging to electrical substation equipment. High seismic hazards and the scarcity of data from historic earthquakes suggest that

additional research is needed to better define the seismic hazard in this region. A more detailed discussion of these issues is provided in Appendix C.

References

- Abrahamson, N. 1996. Non-Stationary Response Spectral Matching. Non-published paper.
- Arias, A. 1969. *A Measure of Earthquake Intensity in Seismic Design for Nuclear Power Plants*. Ed. By R. Hansen. Cambridge: Massachusetts Institute of Technology.
- ASCE. 2003. *Minimum Design Loads for Buildings and Other Structures*. ASCE Standard No. 7-02. Reston. Virginia: American Society of Civil Engineers.
- ASTM, 1986. ASTM E1049 - 85. (Reapproved 1997) '*Standard Practices for Cycle Counting in Fatigue Analysis*'. American Society for Testing and Materials, Annual Book of ASTM Standards, Section 3: Metals Test Methods and Analytical Procedures, Vol. 03.01-Metals-Mechanical Testing; Elevated and Low-Temperature Tests, ASTM, Philadelphia, 1986, pp. 836-848.
- Bannantine, J.A., Comer, J.J., and Handrock J.L., "*Fundamentals of Metal Fatigue Analysis*", Prentice Hall: Englewood Cliffs, New Jersey 07632. 1990.
- Bargiglia A., Salvetti M., Vallino M. An in-progress experience on seismic qualification of gas-insulated substations. Paper presented at the IEEE seminar on Power Delivery, San Diego, California, 1991).
- Bolt, B. A. 1969. Duration of Strong Motion, *Proceedings of 4th World Conference Earthquake Engineering*, 1304-1314, Santiago, Chile.
- BSSC. 1997. *NEHRP Recommended Provisions for Seismic Regulations for New Buildings and Other Structures*. Part 1: Provisions (FEMA 302). Washington, D.C.: Building Seismic Safety Council.
- Chang, J.B. "Round-Robin Crack Growth Predictions on Center-Cracked Tension Specimens under Random Spectrum Loading", *Methods and Models for Predicting Fatigue Crack*

- Growth under Random Loading*. ASTM STP 748, American Society for Testing and Materials, 1981, pp. 3-40.
- CSMIP Strong-Motion Records from the Landers, California Earthquake of June 28, 1992. California Department of Conservation. Division of Mines and Geology. Office of Strong Motion Studies. Report OSMS 92-09.
- Dobry, R., Idriss, I.M., and Ng, E. 1978. Duration Characteristics of Horizontal Components of Strong Motion Earthquake Records. *Bulletin of the Seismological Society of America*, 68(5): 1487-1520.
- Downing, S.D., and Socie D.F., “*Simplified Rainflow Counting Algorithms*”, Int. J. Fatigue, Vol. 4, No. 1, 1982, pp. 31-40.
- ETSI. 2003. ETSI EN 300 019-1-3 v2.1.1: *Environmental Engineering (EE); Environmental Conditions and Environmental Tests for Telecommunications Equipment; Part 1-3: Classification of Environmental Conditions; Stationary Use at Weatherprotected Locations*. European Telecommunications Standards Institute: France.
- Filiatrault A., Kremmidas S., Seible F., Allan J. Clark A. J., Nowak R., and Thoen B.K. 2000. *Upgrade of first generation uniaxial seismic simulation system with second generation real-time three-variable digital control system*. Proceedings of the 12th World Conference on Earthquake Engineering January 30-February 4, Auckland, New Zealand.
- Filiatrault, A 2002. *Elements of Earthquake Engineering and Structural Dynamics*. Second Edition: Polytechnic International Press.
- Frenkel A.D., Mueller C.S., Barnhard T.P., Leyendecker E.V., Wesson R.L., Harmsen S.C., Klein F.W, Perkins D.M., Dickman N.C., Hanson S.L., and Hopper M.G. 2000. USGS National Seismic Hazard Maps. Earthquake Spectra. Vol.16. No.1. P.1-19.
- Gasparini, D.A., and E.H. Vanmarcke. 1976. *Simulated Earthquake Motions Compatible With Prescribed Response Spectra*. Department of Civil Engineering, Research Report R76-4, Massachusetts Institute of Technology, Cambridge, Massachusetts, January.
- Gilani, A.S.J., Whittaker, A.S., Fenves, G., Fujisaki, E. 1999. *Seismic Evaluation and Retrofit of 230-kV Porcelain Transformer Bushings*. PEER, UC Berkeley Report 1999/14.

- Gilani, A.S.J., Whittaker, A.S., Fenves, G., Chen, C.H., Ho H., Fujisaki, E. 2000. *Seismic Evaluation and Analysis of 230-kV Disconnect Switches*. PEER, UC Berkeley Report 2000/06.
- <http://nisee.berkeley.edu/software/simqke1/> (PEER's web-site for SimQke's download).
- http://peer.berkeley.edu/lifelines/Task408_411/Task408.html (the Internet address for all deliverables of the study that includes Matlab code for response fit procedure in frequency domain [D. Clyde]).
- <http://www.westcoastsubcommittee.com/ieee693/spectra/spectrums.htm> (IEEE West Coast Subcommittee's web-site from which the IEEE-compatible Landers can be downloaded).
- ICBO. 1997. *Uniform Building Code –1997*. Vol. 2: Structural Engineering Design Provisions. Whittier, C.A.: International Conference of Building Officials.
- ICBO ES. 2000. *Acceptance Criteria for Seismic Qualification Testing of Nonstructural Components, AC156*. California: ICBO ES.
- ICC. 2000. *International Building Code – 2000*.
- IEC. 1991. International Electrotechnical Commission: *IEC 60068-3-3 Environmental Testing, Part 3: Guidance: Seismic Test Methods for Equipments*. First Edition. Geneva, Switzerland.
- IEC. 1999. International Electrotechnical Commission: *IEC60068-2-57 Environmental Testing, Part 2-57: Tests - Test Ff: Vibration - Time-history method*. Second Edition. Geneva, Switzerland.
- IEEE, 1998. IEEE Standard 693-1997. 1997. *Recommended Practices for Seismic Design of Substations*. Piscataway, N.J.: IEEE Standards Department.
- IEEE Standard 693-2004. 2004. *IEEE Recommended Practice for Seismic Design of Substations*. Draft.
- Leyendecker E.V., Hunt R.J., Frenkel A.D., and Rukstales K.S. 2000. Development of Maximum Considered Earthquake Ground Motion Maps. *Earthquake Spectra*. Vol.16. No.1. P.21-40.
- Lilhanang, K. and W.S.Tseng. 1987. Generation of Synthetic Time Histories Compatible with Multiple-Damping Response Spectra. *SmiRT-9*. Lausanne, K2/10.

- Lilhanang, K. and W.S.Tseng. 1988. Development and Application of Realistic Earthquake Time Histories Compatible with Multiple Damping Response Spectra, *9th World Conf. Earth. Engin.*. Tokyo, Japan, Vol. II, pp. 819-824.
- Kaul, M.K. 1978. Spectrum-Consistent Time-History Generation. *ASCE J. Eng. Mech.* EM4, 781-788.
- Kennedy, R.P. 2004. Personal communication with Anshel Schiff regarding development of input motion requirements for the Nuclear Regulatory Commission, RPK Structural Mechanics Consulting.
- Naeim, F. and Anderson J.C. 1996. Design Classification of Horizontal and Vertical Earthquake Ground Motion (1933-1994). *A Report to the U.S. Geological Survey (USGS). JAMA Report No. 7738.68-96.*: J.A. Martin and Associates, Inc.
- Newmark, N.M., J. A. Blume, and K. K. Kapur. 1973. Design Response Spectra for Nuclear Power Plants. *ASCE Structural Engineering Meeting*. San Francisco, April 1973.
- Nigbor R.L. and E. Kallinikidou. *Evaluation of Large Scale Seismic Testing Methods for Electrical Substation Systems*. PEER/PG&E Lifelines Project 410 (Draft 31 May 2002).
- Nowak R. F., Kusner D. A., Larson R.L., and Thoen B.K. 2000. *Utilizing modern digital signal processing for improvement of large scale shaking table performance*. Proceedings of the 12th World Conference on Earthquake Engineering January 30-February 4, Auckland, New Zealand.
- Matsuishi and T. Endo, “*Fatigue of Metals Subjected to Varying Stress*”, paper presented to Japan Society of Mechanical Engineers, Fukuoka, Japan, March 1968.
- Miner, M.A., “*Cumulative Damage in Fatigue*”, *Trans. ASME, Journal of Applied Mechanics*, Vol. 67, Sept. 1945, pp. A159-A164.
- Page, R.A., Boore, D.M., Loyner, W.M., and Caulter, H.W. 1972. Ground Motion Values for Use in the Seismic Design of the Trans-Alaska Pipeline System, USGS, Circular 672.
- Palmgren, A., “*Durability of Ball Bearings*”, *ZVDI*, Vol.68, No. 14, 1924, pp. 339-341.
- Pantraki F.D., “*Low Cycle Fatigue Behavior of High-Strength and Ordinary Reinforcing Steels*”, State University of New York at Buffalo, December 1991.
- Preumont, A. 1978. The Generation of Spectrum Compatible Accelerograms for the Design of Nuclear Power Plants. *Earth. Eng. Struct. Dyn.* 12, pp.481-497.

- Stephens, R.I., Fatemi, A., Stephens, R.R., and Fuchs, H.O., “*Metal Fatigue in Engineering*”, Wiley Interscience, New York, 2001.
- Takhirov, S., Fenves, G., Fujisaki E., Clyde D. 2005. “Seismic Qualification Testing and Analysis of a 500 kV Disconnect Switch.” PEER Report 2004/08. Berkeley, Calif.: Pacific Earthquake Engineering Research Center, University of California.
- The MathWorks, Inc., 2001. Matlab: Language of Technical Computing. Release 12.1.
- Telcordia Technologies, Inc., 2002. *NEBS Requirements: Physical Protection. GR-63-CORE. Issue 2.* Chester, NJ: Telecordia Technologies, Inc.
- Vanmarcke, E.H. 1976. Structural Response to Earthquakes. Chapter 8 in *Seismic Risk and Engineering Decisions*. Edited by C. Lomitz and E. Rosenblueth, published by Elsevier Publishing Co., Amsterdam.
- USASC. 1973. *Design Response Spectra for Seismic Design of Nuclear Power Plants. Regulatory Guide 1.60.* Revision 1. Washington D.C.: Directorate of Regulatory Standards.
- US Nuclear Regulatory Commission. 1980. NUREG-0800: *Standard Review Plan for the Review of Safety Analysis Reports for Nuclear Power Plants. SRP Section 3.7.1 Seismic Design Parameters.* (1st Edition) November 1975, (2nd Edition) March 1980, (3rd Edition) July 1981.
- US Nuclear Regulatory Commission, 1996. Amendments to 10 CFR Parts 50,52, and 100, and Issuance of a New Appendix S to Part 50. May 24, 1996.

Appendix A Parameters of Strong Motion Records and Response Indices

Appendix A presents definitions and discussions of parameters and indices used to characterize the strong motion records. The parameters and the indices are used to describe the severity of the earthquake records and are divided into two groups. The first group consists of parameters obtained directly from the recorded strong motion data, the second of parameters and indices obtained by passing the recorded data through a single-degree-of-freedom (SDOF) system and by manipulating the system response. Therefore, the former group includes ground motion parameters, whereas the latter group includes spectra and other response indices delivered from SDOF system analysis.

A.1 PARAMETERS OF STRONG MOTION RECORD

This section discusses parameters delivered directly from an acceleration time history by means of simple manipulations. The parameters include peak values for acceleration and velocity, durations, cumulative energy, and cycle count.

A.1.1 Peak Values of Ground Motion

Peak ground acceleration. One of the most commonly used parameters to describe the strong motion record is peak ground acceleration (PGA). The PGA is calculated as a maximum of absolute value of the acceleration. The value of PGA can be presented as a number with dimensions of the acceleration in any particular measuring system or as a fraction of g , where g is an acceleration due to gravity, that is 386.4 in./sec^2 (9.81 m/sec^2).

Peak ground velocity. Peak ground velocity (PGV) is another important parameter commonly used to characterize a strong motion record. A strong motion record usually

represents an acceleration time history recorded at a particular location; therefore, the determination of the velocity time history involves some data manipulation. The acceleration time history has to be numerically integrated over the time, and the absolute maximum of the delivered velocity time history yields the PGV. Depending on the selected measuring system, the PGV can be presented in in./sec (m/sec).

A.1.2 Cumulative Energy or Arias Intensity and Related Parameters

Cumulative energy. For engineering purposes, the cumulative energy of a strong motion record, CE , is defined as the area under the squared acceleration record, and represents a measure of intensity of the record:

$$CE = \int_0^t a(\tau)^2 d\tau,$$

where $a(\tau)$ is a time history of the acceleration and t is a length (measured in seconds) of the strong motion record.

The cumulative energy is a very important parameter commonly used to calculate other parameters of a strong motion record, e.g., Arias intensity, root mean square acceleration, and duration parameters. For instance, the cumulative energy is proportional to a measure of intensity of a strong motion, Arias intensity (Arias, 1969), I_A :

$$I_A = \pi CE / g.$$

It is worth noting that a plot of cumulative energy computed for a strong motion record has a specific feature that distinguishes it from a synthetically generated time history consisting of harmonics. The cumulative energy for the earthquake strong motion is very irregular over the duration of the record, whereas the cumulative energy of the stationary time history has a steady, close to linear increase over the time, as shown in Figure A.1, which presents the Joshua Tree record (in the 0 direction: Landers000) obtained during the 1992 Landers, California, earthquake and the synthetically generated CERL time history (X direction) for qualification testing.

Depending on the selected measuring system, the cumulative energy can be presented in in.²/sec³ (m²/sec³) or simply in g² sec.

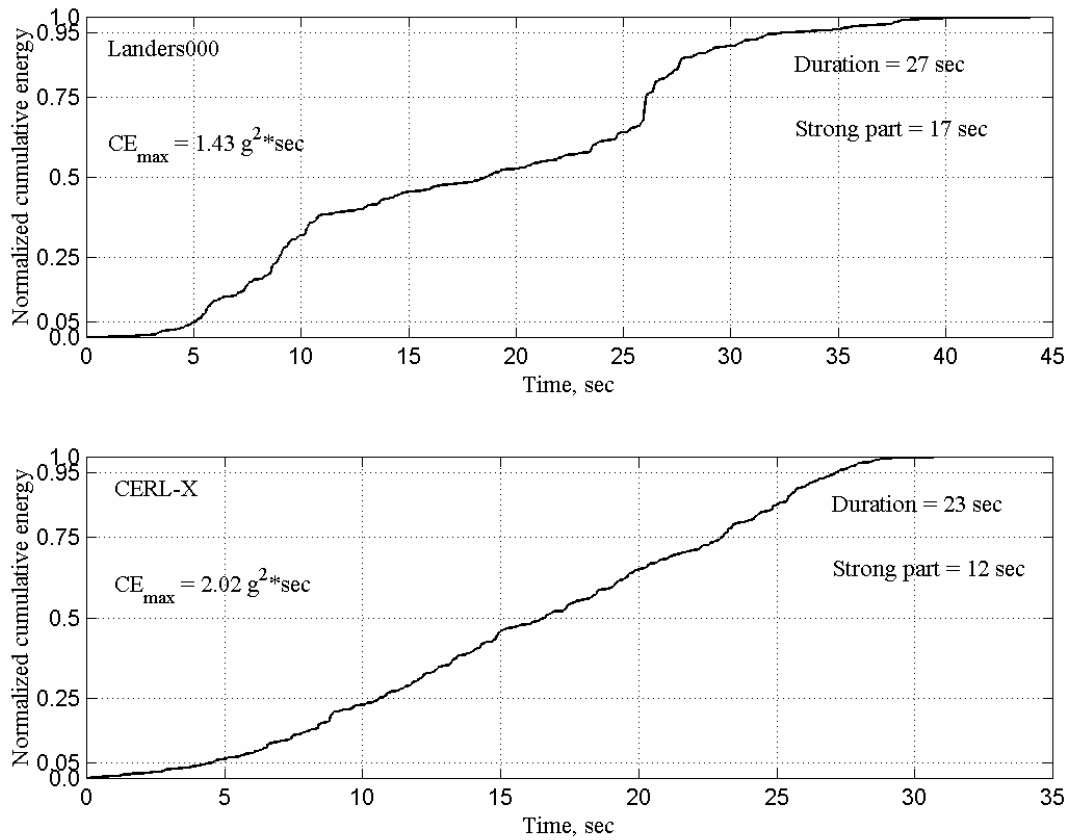


Fig. A.1 Example of CE computation: difference between general trends of CE for actual record (Landers000) and synthetically generated (CERL in X direction) time history

Root mean square acceleration. The computed cumulative energy can be used in calculating the parameter of a strong motion record known as the “root mean square” (RMS) acceleration a_{RMS} , commonly used to characterize amplitude of the accelerogram (Filiatrault, 2002):

$$a_{RMS} = \sqrt{CE/t}$$

In contrast to the peak ground acceleration (PGA), the RMS acceleration takes into account the complete ground motion time history and is a factored mean amplitude for the entire accelerogram. The RMS acceleration is usually presented in fractions of g.

Duration based on CE. A method to calculate a duration of a strong motion record based on using the cumulative energy or Arias intensity was proposed by Dobry, Idriss, and Ng (Dobry et al., 1978). The method defines the duration as the time interval required to accumulate

between 5% and 95% of the accelerogram's maximum cumulative energy. For CE normalized to the maximum value, these threshold values correspond to 0.05 and 0.95 and are presented by horizontal dashed lines in Figure A.1.

Strong part duration based on CE. Another parameter for measuring the duration of a strong motion part of an accelerogram, or “strong part duration,” is introduced as follows. This duration is defined as the time interval required to accumulate between 25%–75% of the maximum cumulative energy. For CE normalized to the maximum value, these threshold values correspond to 0.25 and 0.75, respectively, and are represented by the horizontal dashed lines in Figure A.1. The ratio of the strong part duration to the duration of the strong motion history expressed by percent can serve as an important parameter to measure the intensity of the record. The ratio is extensively used in the study.

The term “duration of strong part” is also used in the IEC-1999 international standard (IEC, 1999), although it is defined quite differently: the duration is taken as the length of the strong motion record in seconds, and the definition of the strong part duration coincides with the IEEE definition of the duration presented below.

A.1.3 Bracketed Duration

In the IEEE 693 standard the bracketed duration is defined as the time interval between the first and the last occurrences of accelerations equal to or larger than 25% of the maximum value of the acceleration. Bracketed durations based on this IEEE definition, and based on the cumulative energy were extensively used in the study.

The other existing definition of the bracketed duration is a time interval between the first and last occurrences of accelerations equal to or larger than 0.05g (Bolt, 1969; Page et al., 1972). The comprehensive study conducted on a large database of strong motion records by Naeim and Anderson (Naeim et al., 1996) showed that the bracketed duration based on the last definition is not effective for classification of strong motion records. The duration calculated with 0.05g threshold can produce a result that overestimates the engineering significance of the bracketed duration. The bracketed duration was calculated (Naeim et al., 1996) with various thresholds, namely 0.05g, 0.10g, and 0.30g; the analysis showed that low-level ground vibrations could produce a long duration based on a 0.05g threshold, whereas an actual duration of strong motion vibrations is much shorter.

A.1.4 Cycle Counting Procedure (ASTM)

In order to classify the strong motion in terms of fatigue analysis, a cycle counting procedure is used. The procedure is based on the commonly used ASTM procedure, called the “simplified rain flow cycle counting procedure.” A detailed description of the procedure and some notes on fracture mechanics are presented in Appendix B. As a result, the cycle counting procedure yields a histogram of cycle counts for the magnitude range of the cycles. The procedure counts the cycles of the accelerogram in order to deliver a number of cycles in the excitation’s acceleration imposed on equipment during testing.

A.1.5 Power Spectral Density

Another important parameter of the strong motion record is a power spectral density (PSD). This parameter is commonly used to obtain information on the frequency distribution of the energy contained in the accelerogram. The power spectral density presents how the modulus of the fast Fourier transform of the strong motion depends on frequency, or period. For records normalized to 1.0g PGA, the PSD is presented in g^2/Hz .

A.2 RESPONSE INDICES BASED ON ELASTIC SDOF SYSTEM ANALYSIS

A.2.1 Spectral Displacement, Velocity, and Acceleration

As previously mentioned, the second group of parameters and indices are based on analysis of a single-degree-of-freedom system impacted by a particular strong motion signal. The spectral relative displacement, denoted usually as ***SD***, is the most important index and is usually presented as an elastic response spectrum. The spectrum is the plot of the maximum response displacement of the SDOF system to a specified earthquake strong motion plotted as a function of the system’s natural frequency or period for a particular critical damping of the system. The index presents the maximum value of the displacement relative to the displacement of the ground; therefore it has the term “relative” in its definition. For simplicity of further discussion, this term is omitted for all spectral indices.

Spectral pseudo-velocity. Electrical equipment has a relatively low damping value, usually below 10% of critical damping. In this case it can be assumed (with some acceptable

accuracy) that the maximum response velocity of the SDOF system is equal to spectral relative pseudo-velocity defined as the product of the natural frequency of the system, ω , and the spectral relative displacement:

$$S_V = \omega S_D .$$

For simplicity, the spectral relative pseudo-velocity is referred to below as “spectral velocity.”

Spectral pseudo-acceleration. Based on the same assumption of low damping, the spectral relative pseudo-acceleration, S_A , is defined as a product of the spectral relative velocity and the natural frequency of the system:

$$S_A = \omega S_V, \text{ or } S_A = \omega^2 S_D .$$

This index is the most commonly used spectral quantity to characterize the possible impact of the particular strong motion signal to the structure. For simplicity the spectral relative pseudo-acceleration is referred to below as “spectral acceleration.”

The IEEE 693 specifications (IEEE, 1998) present several levels for the required response acceleration spectra for various PGAs. All strong motion records in the report are normalized to their PGA in order to have the same PGA equal to 1.0g for all records; this PGA corresponds to IEEE required response spectra at Performance Level.

Frequency resolution in spectral acceleration plot (spectrum). Chopra (Chopra, 1995) summarizes the properties of spectral accelerations of a linear SDOF system excited by a harmonic acceleration. The spectral acceleration of a SDOF system with damping β at resonant frequency is limited only by $1/(2\beta)$ and does not depend on the resonant and excitation frequencies. The shape of the spectrum also depends only on the system’s damping and the ratio of the resonant and excitation frequencies, as shown in the two top plots of Figure A.2. The plots present examples of spectra in 1/24 octave frequency resolution for a 2% damped SDOF system excited by harmonic acceleration with frequencies 1.0 Hz and 4.0 Hz. In case of linear frequency resolution with $\Delta f = 0.01$ Hz increment (two bottom plots of Fig. A.2), the spectra mistakenly seem to have a difference in their shapes because the plots have different resolution in relation to the resonant frequency (the bottom plot). Therefore, any frequency resolution that obeys the law

$$f_{i+1} / f_i = \text{const} \text{ (const} = 2^{1/24} \text{ in case of 1/24 octave),}$$

would correctly represent the spectral shapes and produce the same shapes for spectral accelerations plotted against SDOF system frequency to excitation frequency ratio.

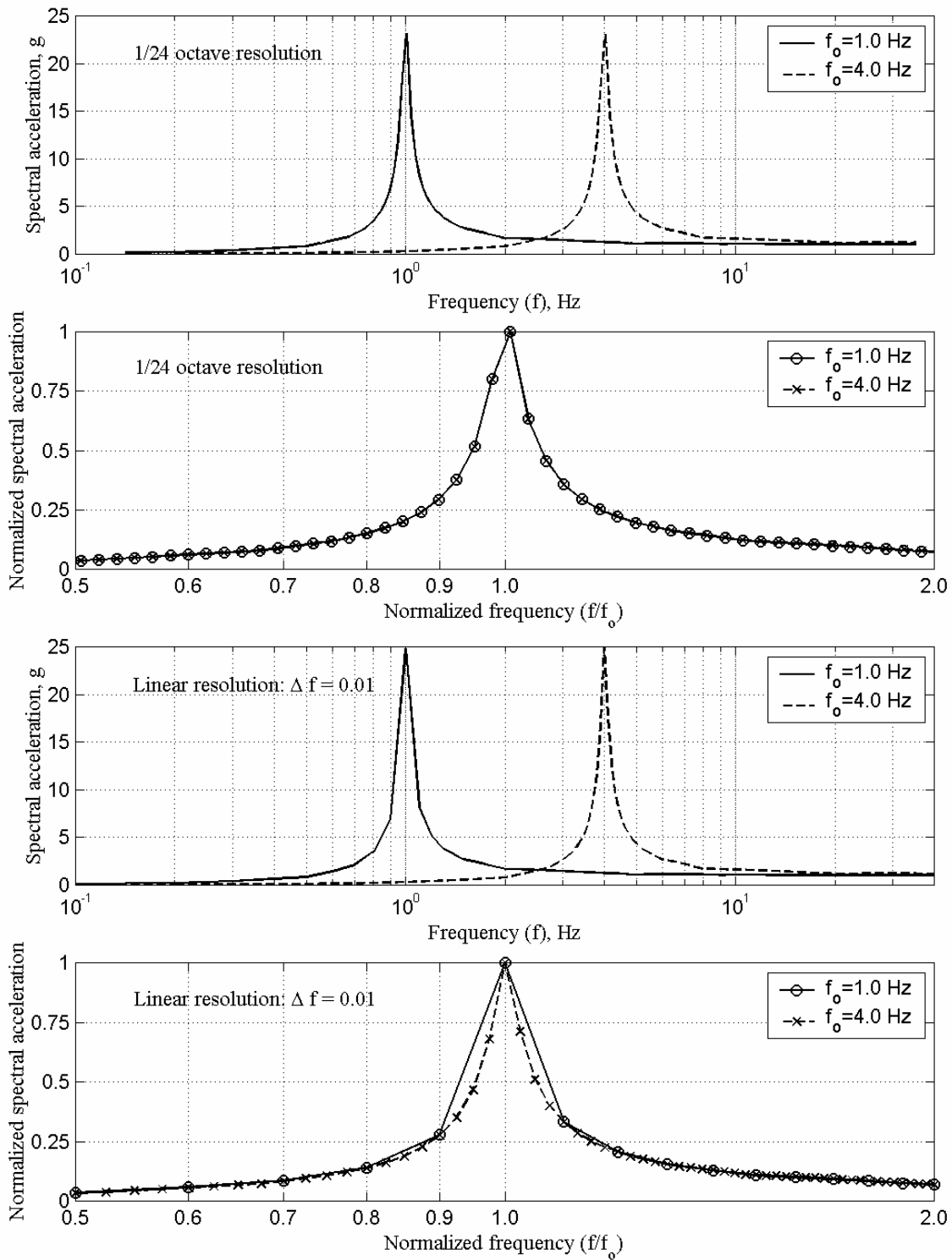


Fig. A.2 Misleading difference in spectral shape for linear vs. 1/24 octave frequency resolutions

A.2.2 Number of Cycles in SDOF Response

In order to rate an intensity of the strong motion time history and its affect on a SDOF system, a new parameter was introduced. The parameter represents the number of high cycles in the acceleration response of the SDOF system plotted against the natural frequency of the system and calculated for a fixed damping value. Only cycles with relatively high magnitude are included in the high cycle count: the study uses a threshold of 70% of the maximum magnitude. The study uses a 2% damping value and calculates the number of high cycles only for frequencies of a strong part of the required response spectrum. The strong part of a required response spectrum (RRS) is a part of the spectrum for which the response acceleration is higher than for the -3 dB bandpass of the RRS (IEC, 1999). In other words it is a part of the spectrum where the spectral accelerations are higher than the plateau value divided by the square root of two. In the case of the IEEE spectrum, the strong part of the spectrum covers frequencies from 0.78–11.78 Hz, as shown in Figure A.3.

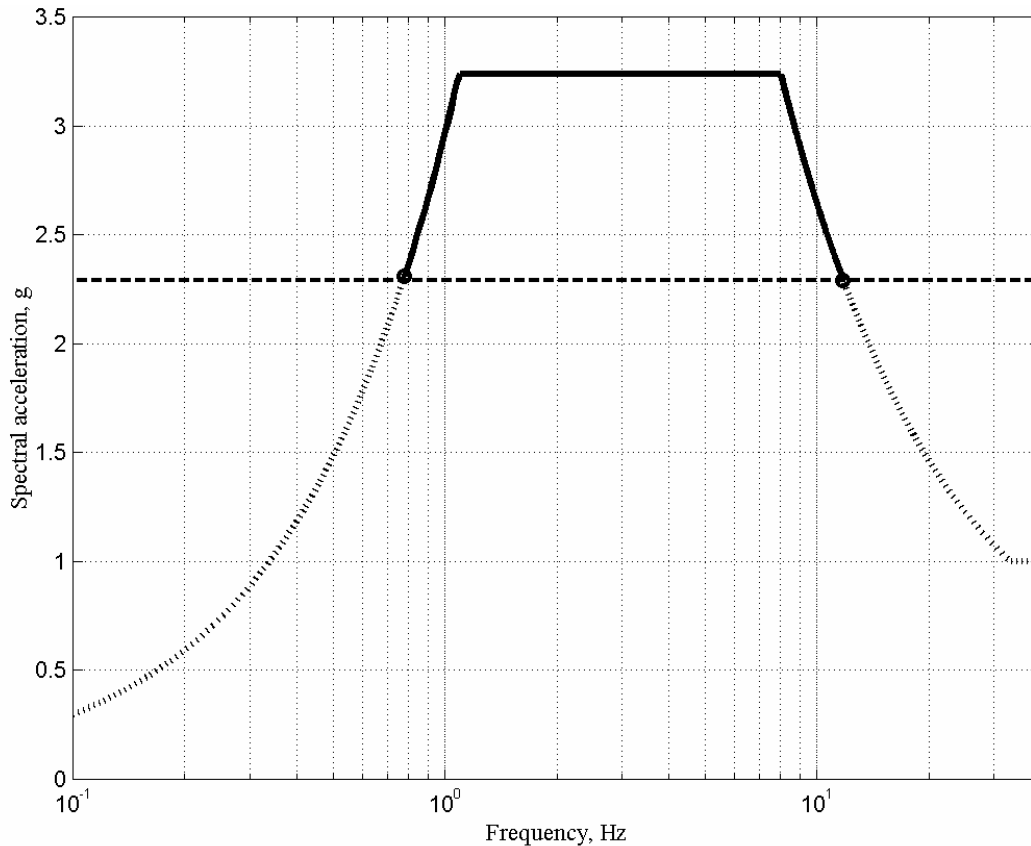


Fig. A.3 Strong part of the IEEE high PL response spectrum (solid line)

A similar parameter, called the “number of high peaks of the response with 70% maximum amplitude threshold,” is used in the international standard (IEC-1999). The standard specifies that the elastic response of a SDOF to the application of a test time history shall result in 3–20 high peaks for a 5% damped system (IEC-1999, section 6.4). The high peak is defined as a positive or a negative maximum deviation (with 70% threshold) from the zero line between two consecutive zero crossing points.

Appendix B Notes on Fracture Mechanics and Cycle-Counting Procedure

This appendix presents information on fracture mechanics that explains the necessity of cycle-counting, and the details of the cycle-counting procedure used in the study.

B.1 STRESS-LIFE DIAGRAMS AND STRAIN-LIFE CURVES

B.1.1 Case of Elastic Deformations

One of the main characteristics of specimen behavior in fatigue is a stress-life diagram, or S - N curve, that plots constant stress amplitude versus number of cycles to failure. This curve delivered from cyclic tests carries important design information and is commonly used in engineering practice to estimate the life of various parts. The analytical expression of the S - N curves for fully elastic deformation is commonly given in the form:

$$N_f = k S^{-b},$$

where b and k are material parameters estimated from test data obtained using identical specimens, N_f is the number of cycles to failure, and S is the stress amplitude at which these cycles were performed.

In structural steel design codes, a stress range threshold S_0 is often used. For stress levels below this threshold, no damage is assumed to occur (and an infinite life is assumed). The S - N relation is then

$$N_f = \{k S^{-b} \text{ when } S > S_0 \text{ and } \infty \text{ when } S \leq S_0\}.$$

It should be noted that the $S-N$ approach does not deal with local physical phenomena within the material. For instance, it does predict when cracking is initiated or starting to propagate, and this curve considers only the total life to fracture.

The stress amplitude S can be expressed through a stress range $\Delta\sigma$ in the following simple way:

$$S = \Delta\sigma/2.$$

The $S-N$ curve can be presented in other formulation using the introduced stress amplitude:

$$\Delta\sigma/2 = \sigma_f (2N_f)^a, \text{ where } a = -1/b \text{ and } \sigma_f = (2k)^{1/b}.$$

B.1.2 Case of Inelastic Deformations

Analysis of experimental data has led to the empirical relations between plastic strain range $\Delta\varepsilon_p$ and the number of cycles to failure N_f . The most well known is the relation independently proposed by Manson and Coffin (Manson and Coffin, 1954):

$$\Delta\varepsilon_p/2 = \varepsilon_f (2N_f)^c,$$

where $\Delta\varepsilon_p/2$ is the plastic strain amplitude, ε_f is the fatigue ductility coefficient, and c is the fatigue ductility exponent. Both these parameters are empirical constants characterizing the fatigue properties of the material.

The total strain amplitude is the sum of the elastic and plastic strain amplitudes, that is,

$$\Delta\varepsilon/2 = \Delta\varepsilon_e/2 + \Delta\varepsilon_p/2,$$

where the elastic strain amplitude is defined as $\Delta\varepsilon_e/2 = \Delta\sigma/(2E)$.

Taking into account the $S-N$ curve representation for elastic deformations, the following representation of an $S-N$ curve for plastic deformations can be obtained:

$$\Delta\varepsilon/2 = \sigma_f (2N_f)^{-1/b}/E + \varepsilon_f (2N_f)^c.$$

Here, E is Young's modulus, σ_f is the fatigue strength coefficient, and b is the fatigue strength exponent. The preceding formula is known as the "strain-life relation" and serves as a tool to estimate the fatigue life in the presence of plastic deformation. It has the advantage of making it possible to describe both low-cycle (high plastic deformation case) and high-cycle fatigue (deformations are fully elastic) within one mathematical scheme.

B.2 MINER'S RULE

B.2.1 Fatigue in Cyclic Loading

Fatigue failure is the result of the cumulative effect of all cycles of a loading history. The term "cumulative damage" refers to the additive effect of the damage caused in general by each individual loading event for a random history, or in particular by each cycle for a constant amplitude history.

One of the first and still very widely used methods for predicting cumulative damage was proposed in 1924 (Palmgren, 1924) for prediction of the ball bearing life and later further developed in 1945 (Miner, 1945) for aircraft fatigue life prediction. This method employs a linear damage law commonly known as "Miner's rule." It utilizes the concept of a damage fraction, D_i , for the i^{th} cycle of loading and may be defined as the fraction of life used up by an event or series of events. These fractions are then added together and failure is assumed to occur when the summation of the damage fractions equals or exceeds 1, i.e.,

$$\sum D_i \geq 1 \quad (1)$$

According to the linear damage rule, the damage fraction D_i at any strain (or stress) amplitude level ε_i (or σ_i) is equal to the cycle ratio n_i / N_{fi} , where n_i is the number of cycles at a strain amplitude ε_i (or σ_i) and N_{fi} is the fatigue life in cycles at the same strain (or stress) amplitude. For example, the damage fraction due one cycle with i^{th} amplitude of loading is $1 / N_{fi}$.

Therefore, according to Miner's rule, the failure occurs when

$$\sum D_i = \sum n_i / N_{fi} \geq \quad (2)$$

The main advantage of this method is its simplicity, but it also has limitations. First, it does not consider the irregularity of historically random events. This shortcoming can be overcome by converting irregular histories into an equivalent sum of cycles of various amplitudes by means of various cycle-counting methods available (Stephens et al., 2001; Bannantine et al., 1990). Second, it does not consider the sequence of loading effects. The sequence of events has a major influence on fatigue life, especially in low-cycle fatigue behavior (Pantraki, 1991). As an example of the events sequence effect, a two-step history can be discussed. This test involves cycles for a certain number of cycles with an initial stress level, which is changed to another stress level on the second step of testing. If the initial stress level is lower than the last, the test is called a “low-high test,” but if the initial stress level is higher than the last, the test is called a “high-low test.” The general trend for two-step tests is that failure of the specimen occurs when cumulative damage equals or exceeds some value that is different from 1, as assumed in Miner’s rule. For high-low tests this value is less than 1, but for low-high tests this value is larger than 1. In other words, Miner’s rule is not conservative for high-low tests.

However, the two-step tests do not relate to many service load histories. Most load histories do not follow a step arrangement and instead are made up from a random distribution of loads of various magnitudes, as usually happens during an earthquake. Tests using random histories with several stress levels show very good correlation with Miner’s rule (Bannantine et al., 1990). Based on these results, Miner’s rule will be used in further consideration to assess the degree of possible damage caused by a strong motion on equipment.

B.2.2 Spectrum Loading versus Constant-Amplitude Fatigue Tests

Generally, loads acting on equipment are very irregular, whereas the *S-N* curve is obtained for a set of tests with constant amplitude cyclic loading. This poses the question of whether these test results can accurately predict the fatigue life of the specimen experiencing random spectrum loading. The answer is very important to the aircraft industry and its millions of daily passengers. Research in this field (Chang, 1981) shows that data from constant amplitude fatigue crack growth tests of center-cracked-tension specimens can be used to predict the fatigue crack growth

lifespan of these specimens when subjected to random load sequences. Because of the specific application to the aircraft industry, the research was conducted for very low-frequency irregular loading (below 0.1 Hz) and for loading peaks and valleys causing only tension in the specimen.

B.3 CYCLE-COUNTING PROCEDURES

Miner's rule uses a number of cycles at a certain level of loading. To predict the life of equipment subjected to a variable load history, it is necessary to reduce the complex history into a number of events with constant amplitude. This process of reducing a complex time history involves what is termed "cycle counting." In the following discussion, two cycle-counting procedures (both based on the rain-flow counting technique) are discussed, and both count cycles in acceleration time histories. In general, these techniques can also be applied to other "loading" parameters, such as stress, torque, moment, load, and so on.

B.3.1 Rain-Flow Cycle-Counting Technique

Proposed by Matsuishi and Endo (Matsuishi and Endo, 1968), the rain-flow cycle-counting technique is the most popular and probably the best method of cycle counting. The first step in implementing this procedure is to draw the strain-time history so that the time axis is oriented vertically, with time increasing downward. Now imagine that the strain history flows from a number of "pagoda roofs." Cycles are defined by the manner in which rain is allowed to "drip" or "fall" down the roofs. A number of rules are imposed on the dripping rain to identify a closed cycle:

- To eliminate the counting of half cycles, the strain history is drawn to begin and end at the strain value of greatest magnitude (either the highest peak or the lowest valley). A flow of rain is begun at each strain reversal in the history and is allowed to flow unless:
 - The rain began at a local maximum point (peak) and falls opposite a local maximum point greater than that from which it came.
 - The rain began at a local minimum point (valley) and falls opposite a local minimum point greater (in magnitude) than that from which it came.
 - The flow of rain encounters a previous rain-flow.

The procedure is simple to perform but should start from either the highest peak or the lowest valley. This procedure is useful for time histories consisting of repeating blocks, so counting the cycles within the blocks and knowing the total number of blocks gives the total number of cycles.

A cycle-counting procedure can be performed manually for simple time histories, but for complex time histories with a lot of irregularities the procedure has to be performed by a computer. At present a number of computer algorithms for rain-flow cycle counting have been developed (Downing and Socie, 1982) that may be easily adapted and implemented in various programming languages. Several such rain-flow cycle-counting algorithms are presented by the American Society for Testing and Materials (ASTM) in the *Annual Book of ASTM Standards* (ASTM, 1986). The Matlab code developed in this study uses a standard algorithm based on the rain-flow cycle-counting idea and developed for an irregular time history.

The implementation procedure consists of two parts. The first part finds peaks and valleys of the loading time history. At this stage the code finds points where the slope of a loading history changes its sign and eliminates points with a zero slope, as shown in a sample in Figure B.1. The zoomed-in view of the same plot is presented in Figure B.2.

At the second stage, a separate Matlab code employs the cycle-counting procedure (defined as “simplified rain-flow counting for repeating histories” in ASTM, 1986). The procedure of cycle counting used in the study was based on a classical technique of the rain-flow counting technique described above. Since the technique is based on using a time history that starts and ends at maximum peak or minimum valley, the irregular time history was modified to meet this criterion. It was assumed that the acceleration time history starts and ends at zero, which is very common for an acceleration strong motion time history.

First, the maximum or the minimum value (the highest peak or the deepest valley) of the acceleration is determined and the signal is divided into two parts: before or after the peak or the valley. Second, these parts are rearranged in a new signal in the following manner: the part after the peak or the valley starts the new signal, and the part representing the old signal before the peak or valley concludes the new signal. Therefore, the new modified signal will start and end with the maximum peak or the minimum valley, as shown in Figure B.3. The classical rain-flow technique defined as “simplified rain-flow counting for repeating histories” in the ASTM manual (ASTM, 1986) adapted from Downing and Socie (Downing and Socie, 1982) was employed throughout the study to compute the number of cycles.

The final result is plotted in the form of a histogram that shows the number of cycles versus absolute value of magnitude normalized by the absolute maximum value of the time history. The magnitude is defined as half of the range for each particular cycle. The final plot for cycle counts presents the number of cycles in a certain range of magnitude that start from 0.1 and increases in 0.1 range increments, as shown in Figure B.4. For instance, a column between 0.3–0.4 magnitude range represents the number of cycles with magnitude varied from 0.3–0.4.

The cycle-counting procedure was compared with a slightly different procedure described in the ASTM standard (ASTM, 1986), in which the code uses a slightly different definition for a cycle: a cycle is defined as a load variation from the minimum to the maximum and then back to the minimum load (or the maximum-minimum-maximum variation). Therefore, if only one part of the variation exists, it is counted as a half cycle. The procedure produces two vectors of cycle counts: one represents the number of half cycles at certain magnitude ranges (absolute value of difference between adjacent peak and valley divided by two), and the second one represents the number of full cycles at the same ranges. Finally, the number of half and full cycles were added for each particular range of magnitude. The final result of the cycle-counting procedure is a histogram that shows the number of cycles at particular magnitude ranges, similar to the histogram for the simplified rain-flow counting procedure.

Each procedure produces close but slightly different results as expected (ASTM, 1986) for the historic El Centro acceleration time history. In the case when a time history starts and ends with maximum peak or minimum valley, these two procedures produce identical counts for the total number of cycles.

The simplified ASTM cycle-counting procedure applied to a sample load history is presented in Figures A.5–A.6. The cycle-counting procedure consists of several steps, and the final cycle count for this sample load history is four cycles with various ranges.

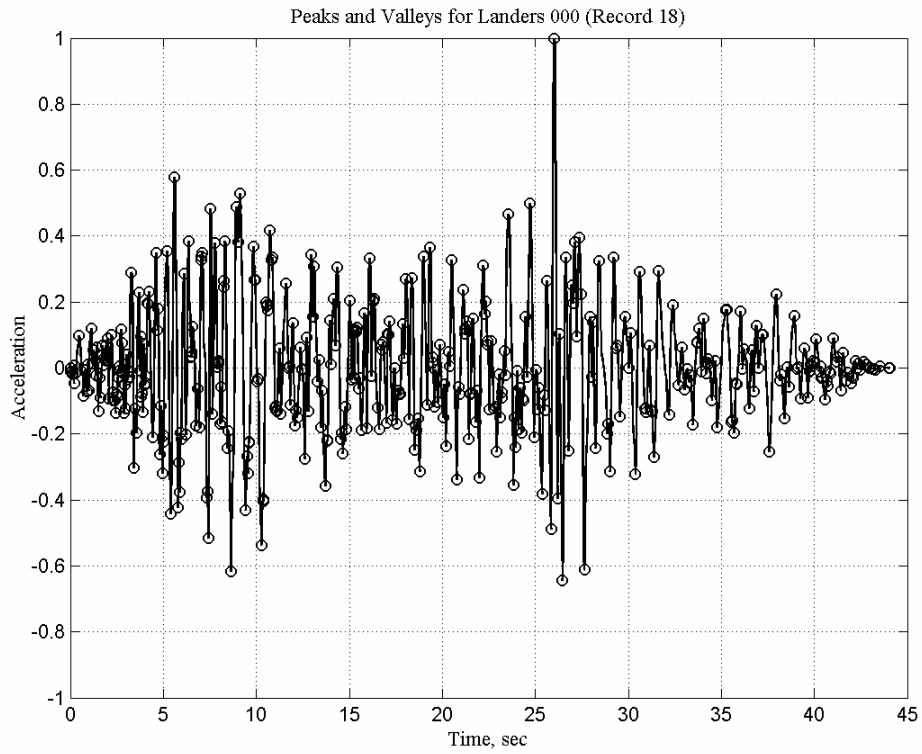


Fig. B.1 Points where slope changes its sign

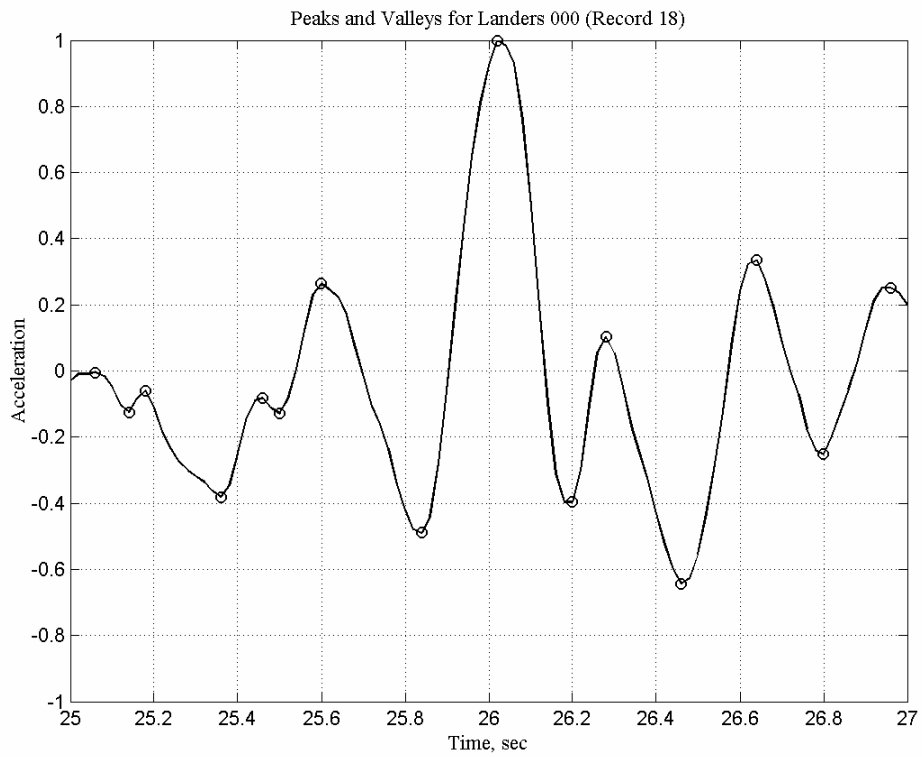


Fig. B.2 Points where slope changes its sign (close view)

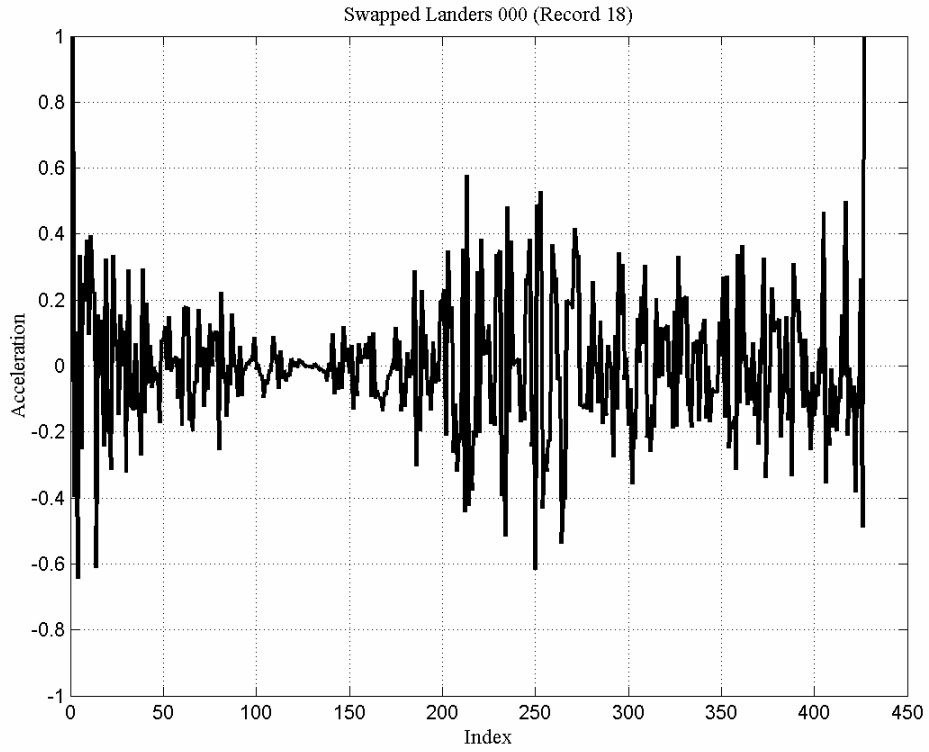


Fig. B.3 Modified Landers000 that starts from and ends at the same maximum value

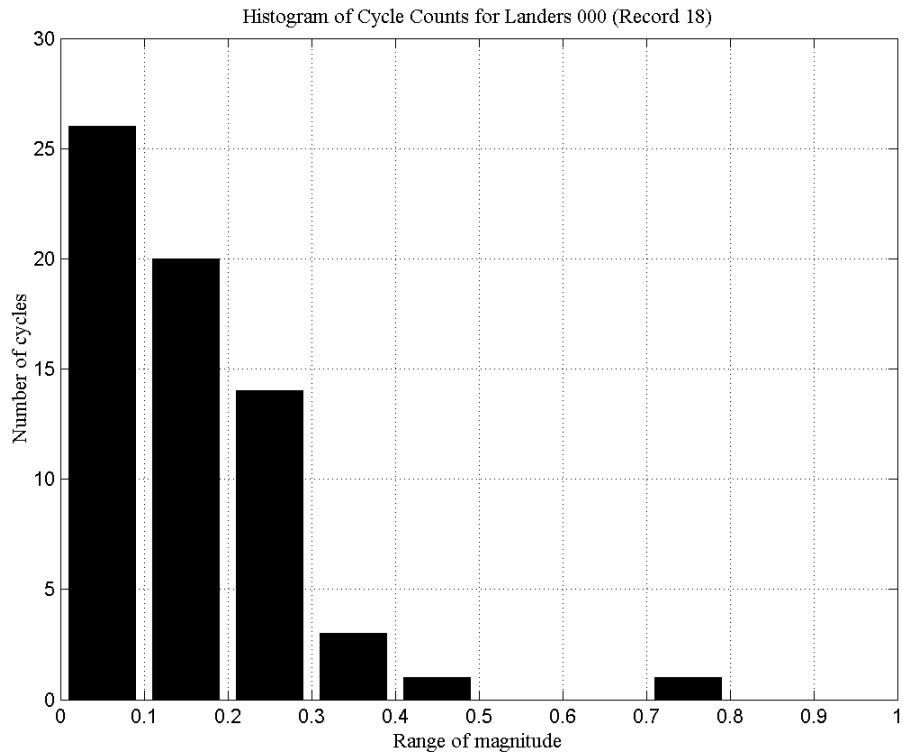
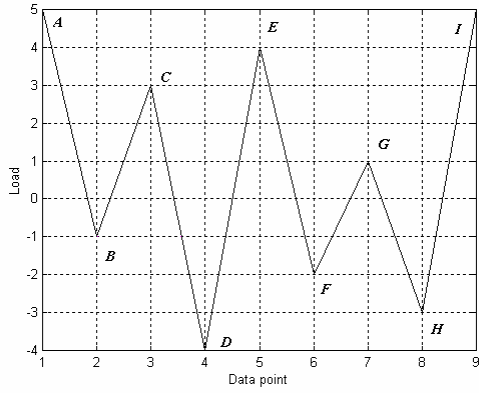
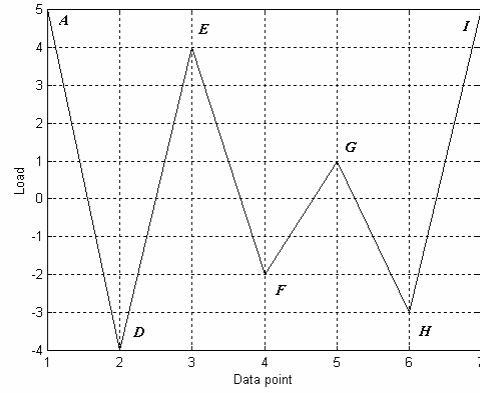


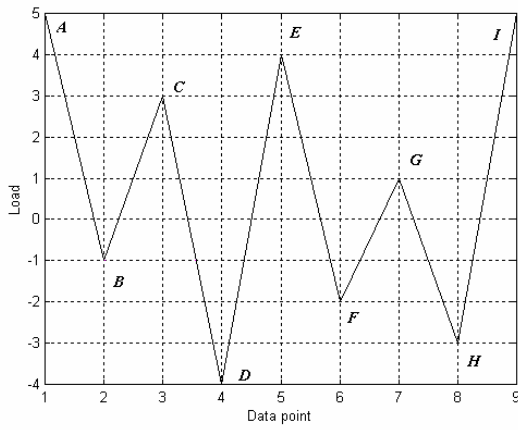
Fig. B.4 Cycle count for Landers000



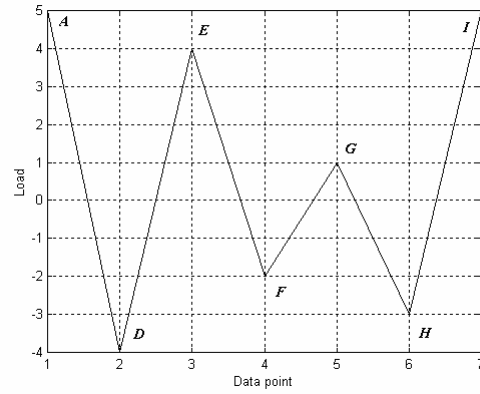
Step 0: Initial stage



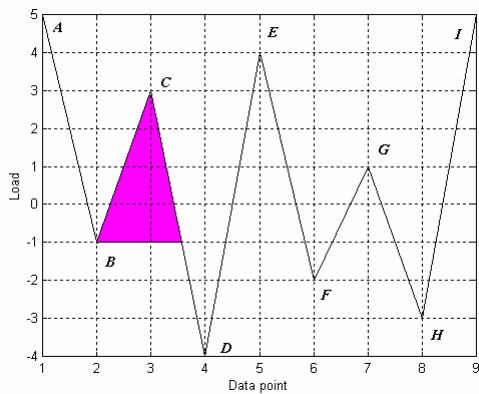
Result plot after step 2.



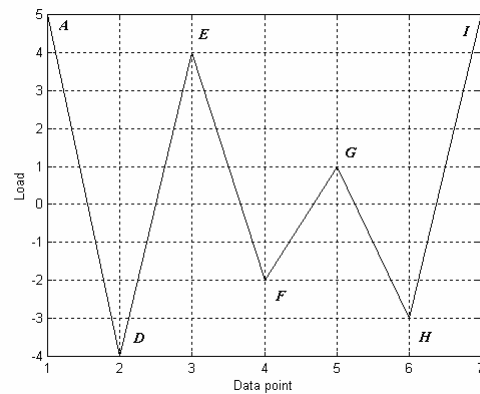
Step 1: $AB > BC$ (no cycles)



Step 3: $DE > EF$ (no cycles)

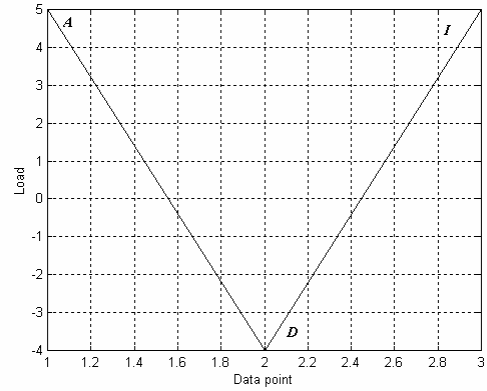
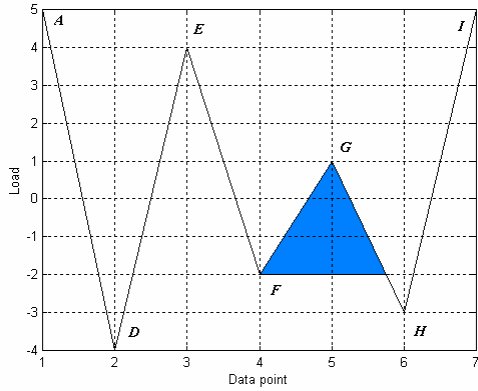


Step 2: $BC \leq CD$ (1 cycle with BC range)

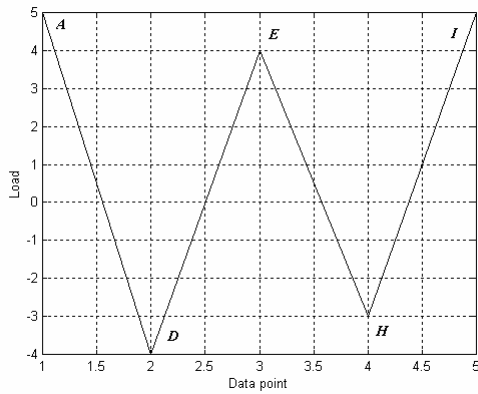


Step 4: $EF > FG$ (no cycles)

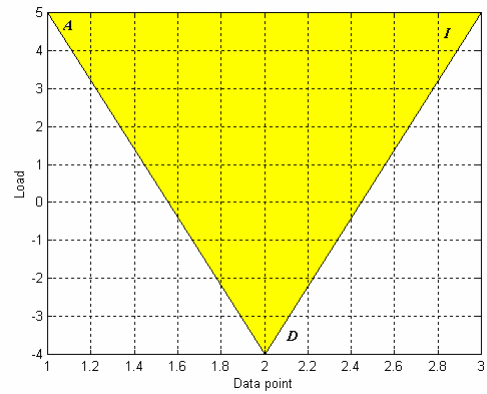
Fig. B.5 First four steps for a sample load history (ASTM simplified procedure)



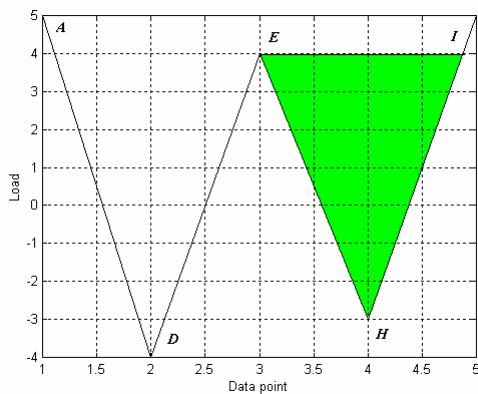
Step 5: Initial stage



Result plot after step 6



Result plot after step 5



Step 7: $AD \leq DI$ (1 cycle with AD range)

Total 4 cycles:

- 1 cycle with range of 4 units (BC)
- 1 cycle with range of 3 units (FG)
- 1 cycle with range of 7 units (EH)
- 1 cycle with range of 9 units (AD)

Step 2: $EH \leq HI$ (1 cycle with EH range)

Step 8: Final results

Fig. B.6 Last steps and final result for a sample load history (ASTM simplified)

Appendix C Examination of Earthquake Records from Eastern and Central North America

This appendix examines earthquakes that have occurred in eastern North America (ENA: the eastern U.S. and the southeastern Canada) and in central North America (CNA: the Central U.S.). The specific characteristics of these earthquakes are discussed in comparison with the western U.S. (WUS) earthquakes. Based on analysis of available strong motion records and current hazard estimates, the limitations on correct representation of the ENA and CNA earthquakes by the IEEE spectrum are discussed.

C.1 STRONG MOTION RECORDS FROM ENA AND CNA EARTHQUAKES

The number of strong motion records for the ENA and CNA earthquakes is very limited; only the strong motion time histories listed in Table C.1 (from five historic events) were examined. The list consists of the records obtained from earthquakes with relatively low magnitude: the average magnitude for the set of 35 strong motions was about 6.8, whereas for these five records it was about 4.7. Records for the 1982 Enola and the 1975 New Madrid earthquakes were obtained from the United States Geological Survey (USGS) website and belong to the National Strong Motion Program (NSMP) database (<http://nsmp.wr.usgs.gov/data.html>), and the remaining three records were downloaded from the COSMOS database (<http://www.cosmos-eq.org>). Soil conditions at the sites are not available in the databases.

Table C.1 Strong motion records from eastern and central North America

No	Earthquake	Date	M	D, km	Station	File names
1	Enola, AK	7/5/82	3.8	0.2	0413 Arkansas swarm	186e13sd.foa,b,c
2	Miramichi, Canada	3/31/82	5.0	5.1	Indian Brook II - Site 4	1982.u.090v02ia,b,c
3	New Hampshire, NH	1/19/82	4.5	10.4	Franklin Falls Dam, NH	1982c019a14ffdoa,b,c
4	New Madrid, MO	6/13/75	4.3	9.0	2240 Northeast Arkansas	164w40nm.roa,b,c
5	Saquenay, Canada	11/25/88	5.8	194.8	Dickey, Maine	1988.u.329x46dc.kya,b,c

C.2 SPECTRA AND PSD COMPARISON FOR WUS SET COMPARED WITH ENA AND CNA SET

The ENA and CNA earthquakes have properties that distinguish them from the WUS earthquakes. One specific detail of the ENA and CNA earthquakes is their frequency content: the content is shifted toward high frequencies compared to the WUS earthquakes.

The PSD and the elastic response spectra for the strong motions from Table C.1 are presented in Figure C.1. They are plotted against the mean plots for the set of 35 strong motion time histories examined in the previous sections. The plots demonstrate the specific character of the ENA and CNA records: the frequency content of the strong motion time histories is concentrated around high frequencies starting with the first peak at about 12 Hz. This phenomenon can clearly be seen from both plots for the PSD and the spectra.

The strong motion energy of ENA and CNA is concentrated in the high-frequency range; therefore the mean spectrum for the ENA and CNA records is higher than the IEEE PL spectrum starting from about 11 Hz (anchored at the same 1.0g PGA).

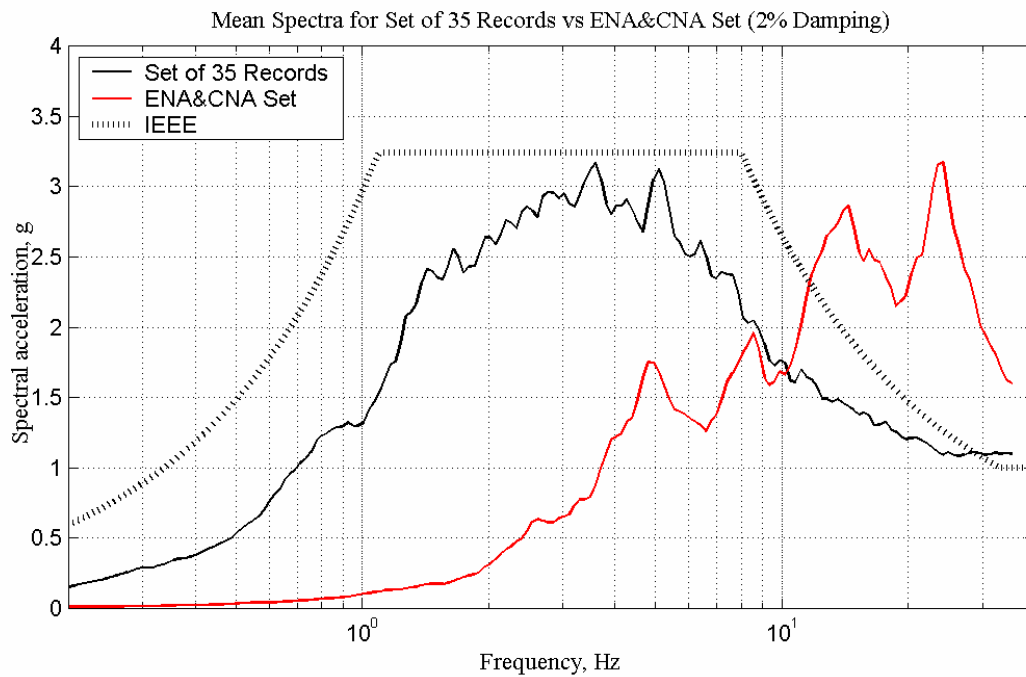
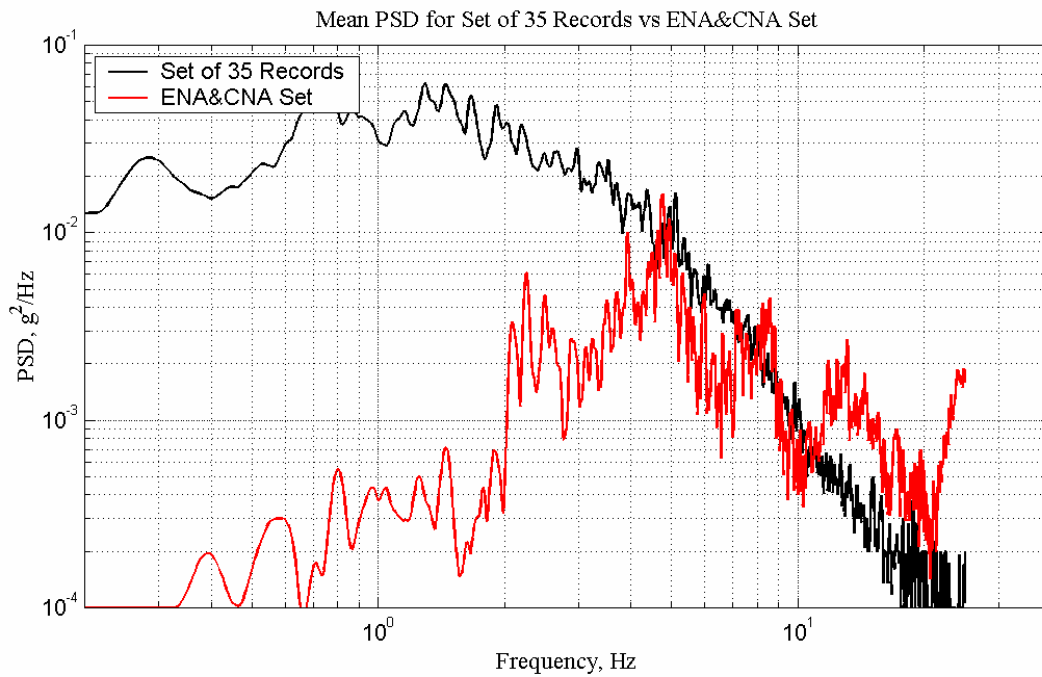


Fig. C.1 Comparison for mean PSD and spectra: set of 35 records and ENA and CNA set

C.3 ENA AND CNA EARTHQUAKES IN RELATION TO BUILDING CODES

C.3.1 Spectra Mean of ENA and CNA Records Anchored to PGA Specified by Building Codes

The UBC-1997 building code (ICBO, 1997) specifies a design earthquake (a design response spectrum depends on this definition) as an earthquake with 10% probability of exceedance in 50 years. Because of the differences in slopes of the seismic hazard curves of the eastern U.S. (EUS) and the western U.S. (WUS) (Leyendecker, et al., 2000), buildings located in these regions would have different safety margins in their ability to survive a high level ground motion. The ratio of spectral accelerations for two probabilities of exceedance, namely 2% and 10% in 50 years, is close to 1.5 for the WUS, whereas for the EUS this ratio is quite different, varying from 2–5. In order to maintain the same margin of safety for all regions of the U.S. the IBC-2000 code (ICC, 2000) defines a maximum considered earthquake (MCE) with a 2% probability of exceedance in 50 years and establishes a uniform factor of safety of 1.5 throughout the U.S. The ground motion at the MCE level is considered as a collapse-level strong motion. So the IBC-2000 design earthquake spectral accelerations are at two thirds of that for the MCE.

According to one of the latest versions of a new draft of the IEEE 693 document (IEEE, 2004), the level of severity for qualification testing can be calculated based on the IBC-2000 maps (ICC, 2000). For example, 0.2 sec spectral acceleration for the MCE in the CNA region can be as high as 3.0. This spectral acceleration should be divided by 2.5 to obtain the PGA for site B (so the final result is 1.2g). Since the PGA is higher than 0.5g, electrical equipment shall be tested at the high qualification level in the CNA region. The high PL spectrum does not envelop the mean of these five strong motion time histories anchored at 1.2g as shown in Figure C.2. This creates a possibility that the equipment may be undertested at the high level of qualification compared to the MCE.

The result is quite different for another fixed probability of exceedance: 10% in 50 years as adopted in the UBC-1997 (ICBO, 1997). In this case the PGA is around 0.15g for Charleston, South Carolina (Leyendecker et al., 2000) and slightly more than 0.16g for Memphis, Tennessee (Frenkel et al., 2000). The MCE PGA for Charleston and Memphis are 4.4 and 7.5 times higher, respectively, than the 10% in 50 years PGA.

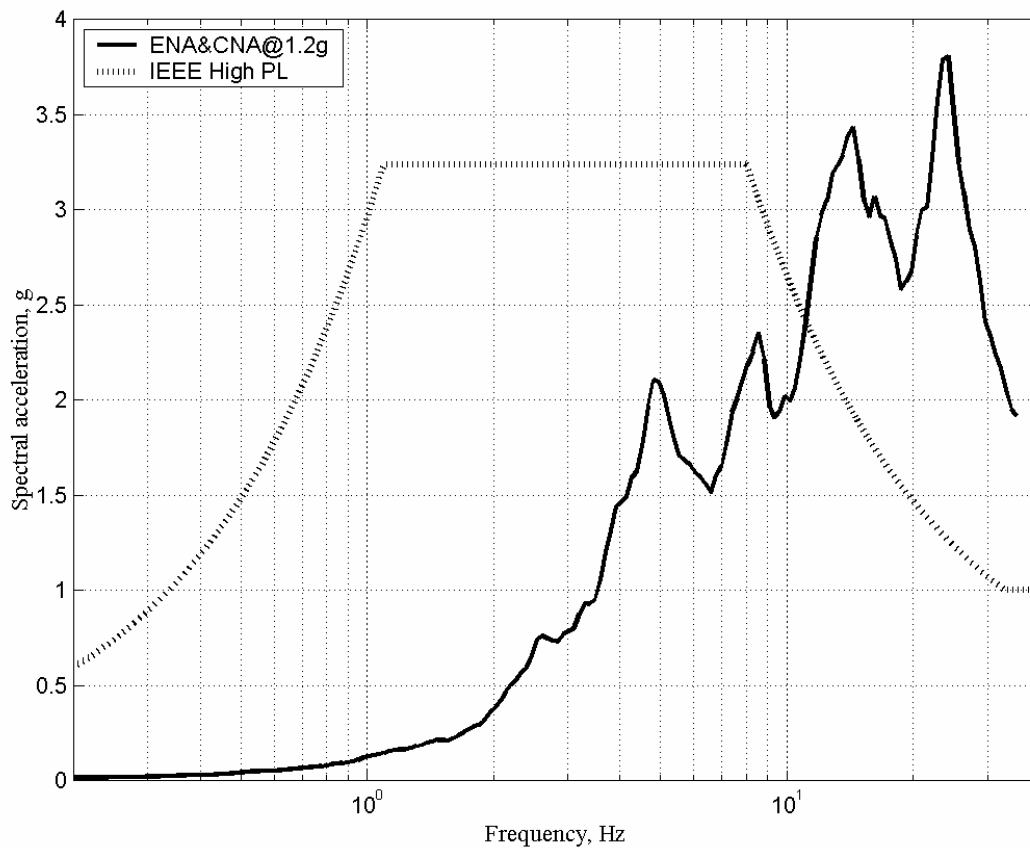


Fig. C.2 High IEEE PL spectra vs. ENA and CNA set anchored at 1.2g

C.3.2 MCE Spectra for Major Seismic Regions of U.S. Compared with IEEE Spectra

The study of the MCE spectra for all major seismic regions of the U.S. is conducted and presented in this section. As specified in the IBC-2000 code (ICC, 2000), the spectra for MCE are defined by two mapped spectral accelerations and soil conditions at the site. These spectral accelerations are as follows: (1) spectral acceleration at short periods (0.2 sec), S_s , and (2) spectral acceleration at long periods (1.0 sec), S_l . According to the current draft version of the IEEE 693 document (IEEE, 2004), the value of S_s controls the PGA of earthquakes expected to occur in the major seismic regions of the United States. The value of the PGA dictates the level of severity for qualification testing of electrical equipment.

Table C.2 shows the mapped spectral accelerations for site type B obtained from the IBC-2000 maps for the major seismic regions of the U.S. The last column presents PGA calculated in accordance with the current version of the IEEE 693 draft (IEEE 693, 2004). The spectral

acceleration at short periods produces PGA greater than 0.5g for all regions except that of the New York region; therefore the level of severity for qualification testing has to be selected as high for PGA greater than 0.5g. The PGA for the New York seismic region is greater than 0.1g but less than 0.5g; therefore the equipment shall be tested at a moderate level for installations at these sites.

Table C.2 Mapped MCE spectral accelerations and PGA for site type B (IBC-2000)

No.	Region	S_s	S_I	PGA, g	Severity Level
1	San Francisco, CA	2.18	1.59	0.87	High
2	Seattle, WA	1.50	0.50	0.60	High
3	Memphis, TN	3.00	1.00	1.20	High
4	Charleston, SC	1.66	0.47	0.66	High
5	New York, NY	0.43	0.095	0.17	Moderate

Figure C.3 shows MCE spectra for the San Francisco, Seattle, Charleston, and Memphis areas plotted against the IEEE high PL spectrum. MCE spectra for all regions except those for Memphis are enveloped by the IEEE high PL spectrum. The degree of mismatch between the IEEE spectrum and MCE spectra for Memphis region slightly varies from one soil type to another, but the major behavior remains the same: MCE spectra are shifted toward the high-frequency zone, and maximum value of the spectra is higher than that for the IEEE spectrum for all soil types except type A. The high-frequency corner of the MCE spectra plateau can be shifted as far as 15 Hz.

Figure C.4 shows MCE spectra for the New York region at various soil types as compared to the IEEE moderate PL spectrum. The IEEE spectrum envelops all MCE spectra although MCE spectra significantly shifted toward the high-frequency range. The corner frequency of MCE spectra plateau can be shifted as far as 22 Hz. The spectra acceleration at the MCE spectra plateau is significantly lower than that for the IEEE spectrum.

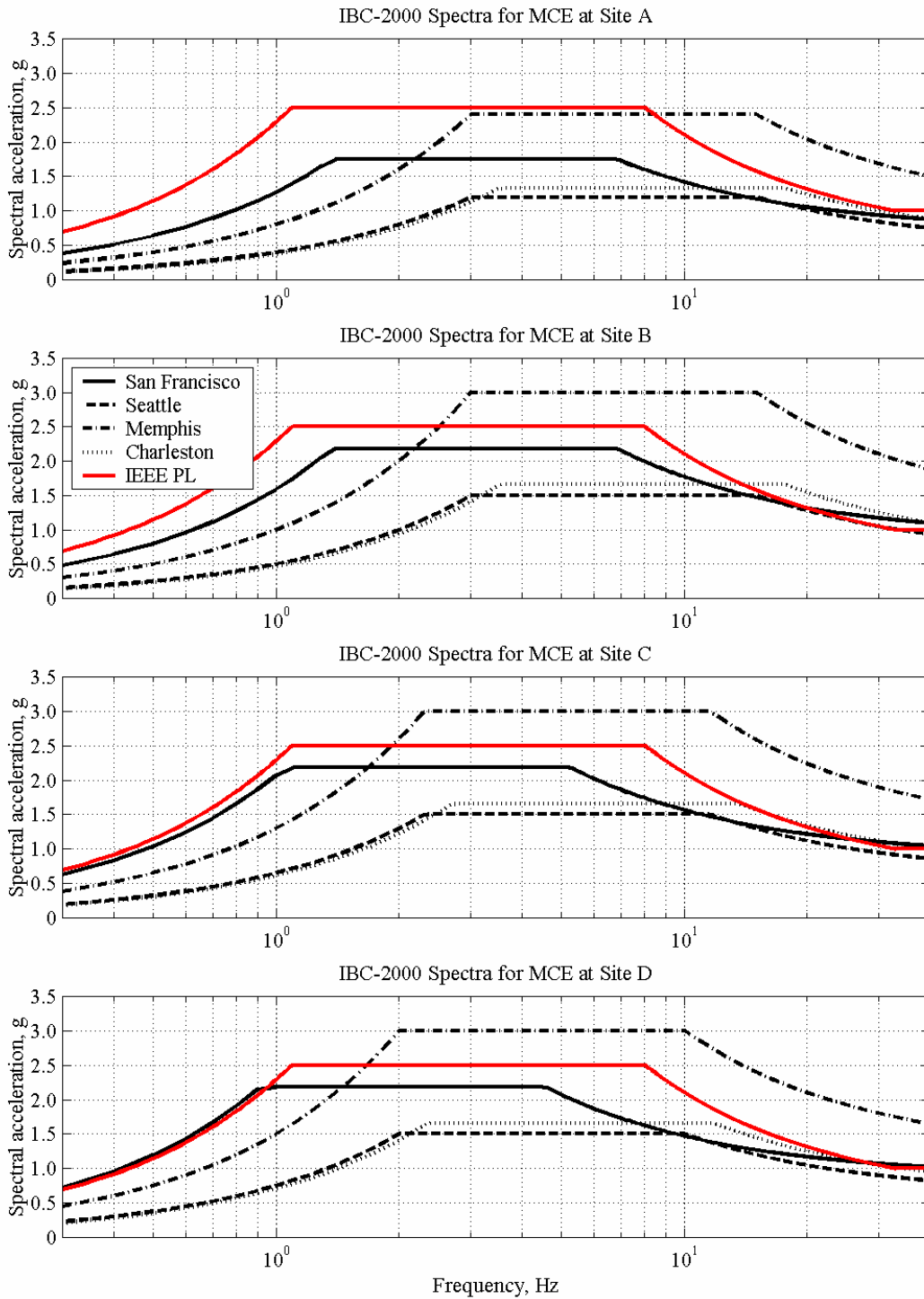


Fig. C.3 IBC-2000 response spectra for MCE at major seismic regions (New York excluded)

One possible approach for accommodating the specifics of earthquakes that occurred in the central U.S. is presented below. Since the plateau of the MCE spectra shifted toward the high-frequency range, the frequency in the IEEE RRS spectrum must also be shifted toward this range. The simplest way to achieve the shift is to multiply the frequency by some factor that should be close to 2, as can be seen from Figure C.4. In order to start the spectral plateau at 2 Hz, the proposed factor selected is 1.82:

$$f_{new} = k * f_{IEE}, (k = 1.82) \quad (4.1)$$

The spectral accelerations of IEEE RRS, S_a^{IEEE} , also have to be scaled up by a factor that is equal to the PGA calculated from the mapped spectral acceleration for site B, which is simply $S_s / 2.5$ (in our case, it is equal to $3.0/2.5=1.2$):

$$S_a = PGA * S_a^{IEEE}, (PGA = S_s / 2.5) \quad (4.2)$$

The correlation between the proposed spectrum that is scaled from the IEEE high PL spectrum and MCE spectra for the Memphis area is presented in Figure C.5 and seems to be acceptable. The CUS scaling factor for spectral accelerations would be incorporated in the IEEE RRS only if the PGA exceeds 1.0g.

The following conclusions can be drawn from the discussion in this section. The IEEE procedure of the severity level selection for qualification testing—i.e., based on the spectral accelerations of the probabilistic MCE—is appropriate for most of the seismically active regions of the U.S. except the central U.S. (CUS). The spectra for high-hazard areas of the CUS exceed the universal IEEE 693 spectrum, particularly in the high-frequency range. The higher demand on the equipment performance is consistent for all soil conditions.

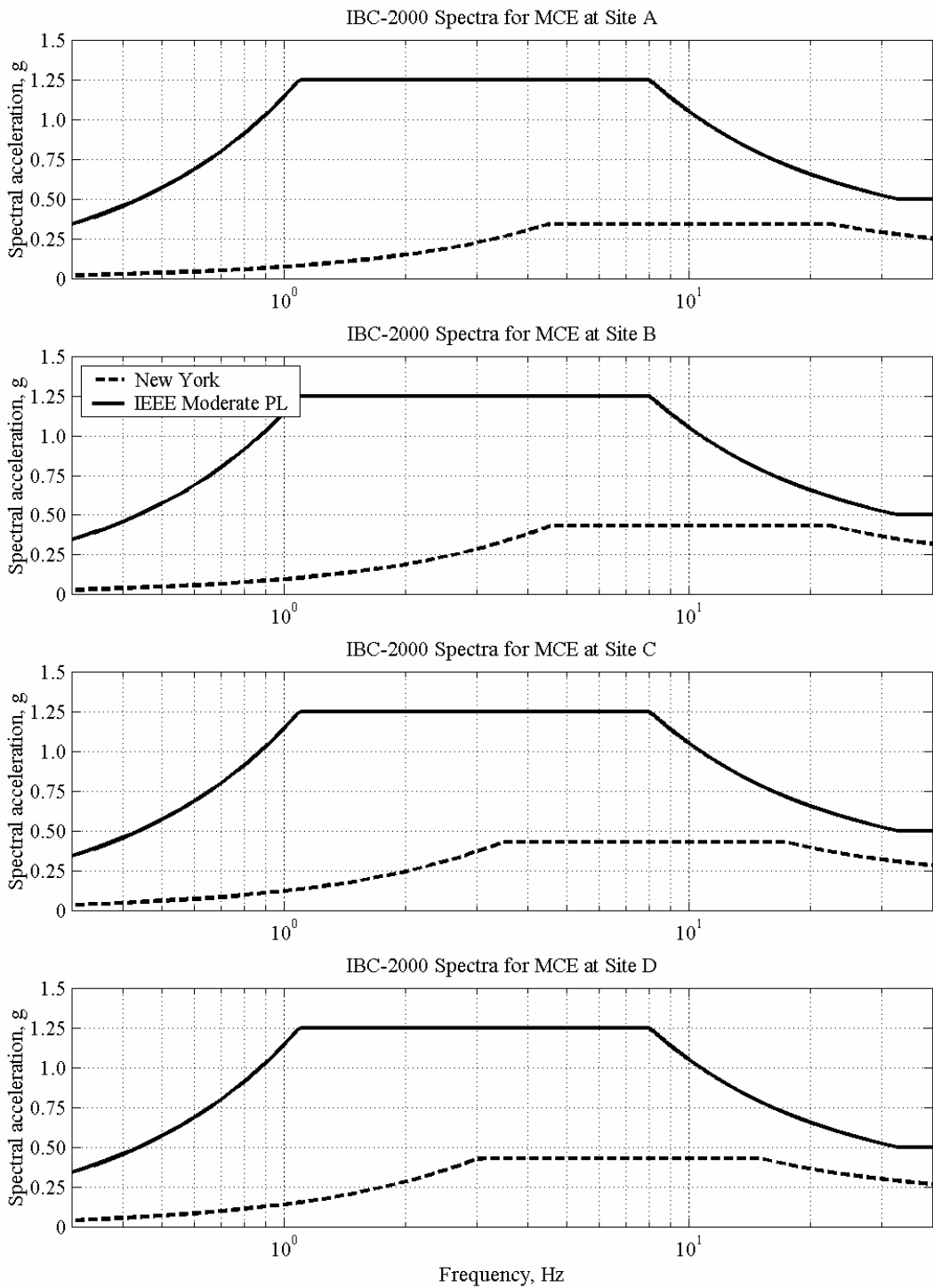


Fig. C.4 IBC-2000 response spectra for MCE at sites of New York seismic region

A suggested method for modifying the IEEE 693 spectra to provide for enveloping of CUS spectra is given below. To use more realistic PGA for the expected ground motion, the PGA should be calculated from spectral accelerations based on the deterministic MCE. If the IEEE spectra do not envelop the MCE spectra for this PGA, the IEEE required response spectra may be corrected to cover the high-frequency range. The correction may be achieved by scaling the existing IEEE RRS in order to accommodate higher spectral accelerations and a shift in the critical natural frequencies toward the high-frequency range. The scaling consists of multiplying the frequency by a factor close to 2 and the spectral accelerations by the PGA value (only for PGA greater than 1.0g for high PL) defined in g by means of the IEEE procedure for a site with soil type B.

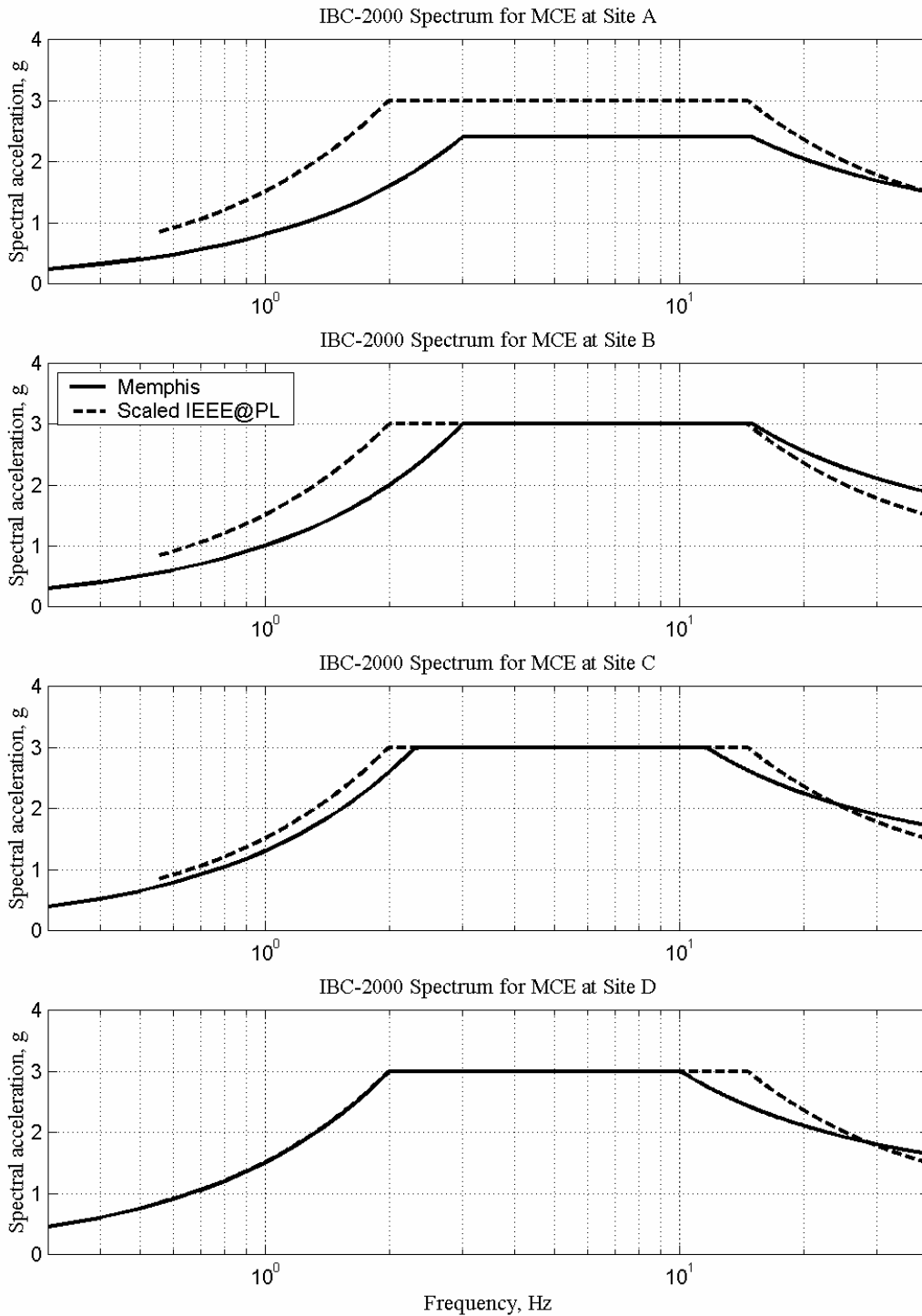


Fig. C.5 IBC-2000 response spectra for Memphis region vs. scaled IEEE spectrum

Appendix D Specification for Input Motion Used for Testing—IEEE 693 (Proposed for New IEEE 693)

The equipment and supporting structure shall be subjected to at least one time history test. The input motion time history shall satisfy the requirements given below. The recommended practice (IEEE, 1998) principally uses response spectra to establish the characteristics of the time histories used to seismically qualify substation equipment. When taken alone, it is an imprecise method of specifying excitation motions. A time history may be such that its response spectrum envelops the RRS but the energy content in certain frequency ranges will be low, so that equipment that have important natural frequencies in that range may not be adequately excited. This can be due to the design of the time history or to the interaction of the equipment and the shake table. There is a need to balance concern for adequate excitation with the desire to avoid overtesting equipment during its qualification. While imposing a power spectral density requirement on the input time history can assure an acceptable distribution of energy over the frequency range of interest, this has proved problematic in attempting to address this issue (Kennedy, 2004). If the response spectrum of a time history is reasonably smooth, a reasonable distribution of the energy in the record is also assured (Kennedy, 2004). To avoid overtesting, the TRS is permitted to dip slightly below the RRS, with appropriate limitations. All of the table motions cited below refer to accelerations or signals that will ultimately be evaluated as accelerations.

Spectral matching. The theoretical response spectrum developed for testing shall envelop the RRS according to the requirements of this section. When the high seismic level is specified, the RRS shown in Figure A.1 (IEEE, 1998) shall be used. When the moderate seismic level is specified, the RRS shown in Figure A.2 (IEEE, 1998) shall be used.

The theoretical response spectrum for testing shall be computed at 2% damping, at the resolution stated, and shall include the lower corner point frequency of the RRS (1.1 Hz), for comparison to the RRS.

Duration. The input motion shall have a duration of at least 20 sec of strong motion. Ring-down time or acceleration ramp-up time shall not be included in the 20 sec of strong motion. The duration of strong motion shall be defined as the time interval between when the plot of the time history reaches 25% of the maximum value to the time when it falls for the last time to 25% of the maximum value.

Theoretical input motion. The spectrum matching procedure shall be conducted at 1/24 octave resolution or higher, and result in a theoretical response spectrum that is within $\pm 10\%$ of the RRS at 2% damping.

Filtering limits. The theoretical input motion record used for testing may be high-pass filtered at frequencies less than or equal to 70% of the lowest frequency of the test article, but not higher than 2 Hz. The lowest frequency of the test article shall be established by test.

Filtered theoretical input motion to table. The response spectrum of the filtered table input motion shall envelop the RRS within a $-5\%/ +30\%$ tolerance band at 1/12 octave resolution or higher. A -5% deviation is allowed at a given point, provided that the spectrum of the filtered table input motion at 2 or more adjacent points meet or exceed the RRS, and not more than a total of 5 points fall below the RRS at the stated resolution. Exceedance of the $+30\%$ tolerance limit is acceptable with concurrence of the equipment manufacturer. Exceedances of the stated upper tolerance limit at frequencies above 20 Hz are generally not of interest and should be accepted unless resonant frequencies are identified in that range.

The filtered input motion to the table shall include at least 2 and a maximum of about 25 high-amplitude cycles of a single-degree-of-freedom (SDOF) oscillator response at 2% damping. A “high amplitude cycle” is a cycle defined by ASTM E1049 (ASTM, 1997; Downing, 1982) that consists of two positive or negative peaks of the same range with a peak of opposite sign between them, having an amplitude greater than or equal to 70% of the maximum response of the SDOF oscillator. SDOF oscillators in the frequency range of 0.78–11.78 Hz shall be included, and oscillator frequencies shall be selected with 1/12 octave band resolution. The minimum number of high-amplitude cycles is permitted to drop to 1 at no more than 5 frequency points in the specified frequency range. The number of high-amplitude cycles may exceed the stated maximum value with concurrence of the equipment manufacturer. Procedures for

computing the number of high-amplitude cycles are available (visit Westcoast Subcommittee's website: <http://www.westcoastsubcommittee.com/ieee693/qualified.php>).

The strong part ratio of the table input motion record shall be at least 30%. The “strong part ratio” of a given record is defined as the ratio of the time required to accumulate from 25%–75% of the total cumulative energy of the record to the time required to accumulate from 5%–95% of the total cumulative energy of the record.

Where:

$$\text{Cumulative Energy} = \int a(\tau)^2 d\tau$$

$a(\tau)$ = acceleration time history

Table output motion. The table output TRS shall envelop the RRS within a –10%/ +40% tolerance band at 1/12 octave resolution or higher. A –10% deviation is allowed at a given point, provided that the TRS at 2 or more adjacent points meet or exceed the RRS, and not more than a total of 5 points fall below the RRS at the stated resolution. Overtesting that exceeds the +40% limit is acceptable with concurrence of the equipment manufacturer. Exceedances of the stated upper tolerance limit at frequencies above 20 Hz are generally not of interest and should be accepted unless resonant frequencies are identified in that range.

PEER REPORTS

PEER reports are available from the National Information Service for Earthquake Engineering (NISEE). To order PEER reports, please contact the Pacific Earthquake Engineering Research Center, 1301 South 46th Street, Richmond, California 94804-4698. Tel.: (510) 231-9468; Fax: (510) 231-9461.

- PEER 2004/07** *Ground Motions for Earthquake Simulator Qualification of Electrical Substation Equipment.* Shakhzod M. Takhirov, Gregory L. Fenves, Eric Fujisaki, and Don Clyde. January 2005.
- PEER 2004/06** *Performance-Based Regulation and Regulatory Regimes.* Peter J. May and Chris Koski. September 2004.
- PEER 2004/05** *Performance-Based Seismic Design Concepts and Implementation: Proceedings of an International Workshop.* Peter Fajfar and Helmut Krawinkler, editors. September 2004.
- PEER 2004/03** *Evaluation and Application of Concrete Tilt-up Assessment Methodologies.* Timothy Graf and James O. Malley. October 2004.
- PEER 2004/02** *Analytical Investigations of New Methods for Reducing Residual Displacements of Reinforced Concrete Bridge Columns.* Junichi Sakai and Stephen A. Mahin. August 2004.
- PEER 2004/01** *Seismic Performance of Masonry Buildings and Design Implications.* Kerri Anne Taeko Tokoro, James C. Anderson, and Vitelmo V. Bertero. February 2004.
- PEER 2003/18** *Performance Models for Flexural Damage in Reinforced Concrete Columns.* Michael Berry and Marc Eberhard. August 2003.
- PEER 2003/17** *Predicting Earthquake Damage in Older Reinforced Concrete Beam-Column Joints.* Catherine Pagni and Laura Lowes. October 2004.
- PEER 2003/16** *Seismic Demands for Performance-Based Design of Bridges.* Kevin Mackie and Božidar Stojadinovi . August 2003.
- PEER 2003/15** *Seismic Demands for Nondeteriorating Frame Structures and Their Dependence on Ground Motions.* Ricardo Antonio Medina and Helmut Krawinkler. May 2004.
- PEER 2003/14** *Finite Element Reliability and Sensitivity Methods for Performance-Based Earthquake Engineering.* Terje Haukaas and Armen Der Kiureghian. April 2004.
- PEER 2003/13** *Effects of Connection Hysteretic Degradation on the Seismic Behavior of Steel Moment-Resisting Frames.* Janise E. Rodgers and Stephen A. Mahin. March 2004.
- PEER 2003/12** *Implementation Manual for the Seismic Protection of Laboratory Contents: Format and Case Studies.* William T. Holmes and Mary C. Comerio. October 2003.
- PEER 2003/11** *Fifth U.S.-Japan Workshop on Performance-Based Earthquake Engineering Methodology for Reinforced Concrete Building Structures.* February 2004.
- PEER 2003/10** *A Beam-Column Joint Model for Simulating the Earthquake Response of Reinforced Concrete Frames.* Laura N. Lowes, Nilanjan Mitra, and Arash Altoontash. February 2004.
- PEER 2003/09** *Sequencing Repairs after an Earthquake: An Economic Approach.* Marco Casari and Simon J. Wilkie. April 2004.
- PEER 2003/08** *A Technical Framework for Probability-Based Demand and Capacity Factor Design (DCFD) Seismic Formats.* Fatemeh Jalayer and C. Allin Cornell. November 2003.
- PEER 2003/07** *Uncertainty Specification and Propagation for Loss Estimation Using FOSM Methods.* Jack W. Baker and C. Allin Cornell. September 2003.
- PEER 2003/06** *Performance of Circular Reinforced Concrete Bridge Columns under Bidirectional Earthquake Loading.* Mahmoud M. Hachem, Stephen A. Mahin, and Jack P. Moehle. February 2003.
- PEER 2003/05** *Response Assessment for Building-Specific Loss Estimation.* Eduardo Miranda and Shahram Taghavi. September 2003.
- PEER 2003/04** *Experimental Assessment of Columns with Short Lap Splices Subjected to Cyclic Loads.* Murat Melek, John W. Wallace, and Joel Conte. April 2003.

- PEER 2003/03** *Probabilistic Response Assessment for Building-Specific Loss Estimation.* Eduardo Miranda and Hesameddin Aslani. September 2003.
- PEER 2003/02** *Software Framework for Collaborative Development of Nonlinear Dynamic Analysis Program.* Jun Peng and Kincho H. Law. September 2003.
- PEER 2003/01** *Shake Table Tests and Analytical Studies on the Gravity Load Collapse of Reinforced Concrete Frames.* Kenneth John Elwood and Jack P. Moehle. November 2003.
- PEER 2002/24** *Performance of Beam to Column Bridge Joints Subjected to a Large Velocity Pulse.* Natalie Gibson, André Filiatrault, and Scott A. Ashford. April 2002.
- PEER 2002/23** *Effects of Large Velocity Pulses on Reinforced Concrete Bridge Columns.* Greg L. Orozco and Scott A. Ashford. April 2002.
- PEER 2002/22** *Characterization of Large Velocity Pulses for Laboratory Testing.* Kenneth E. Cox and Scott A. Ashford. April 2002.
- PEER 2002/21** *Fourth U.S.-Japan Workshop on Performance-Based Earthquake Engineering Methodology for Reinforced Concrete Building Structures.* December 2002.
- PEER 2002/20** *Barriers to Adoption and Implementation of PBEE Innovations.* Peter J. May. August 2002.
- PEER 2002/19** *Economic-Engineered Integrated Models for Earthquakes: Socioeconomic Impacts.* Peter Gordon, James E. Moore II, and Harry W. Richardson. July 2002.
- PEER 2002/18** *Assessment of Reinforced Concrete Building Exterior Joints with Substandard Details.* Chris P. Pantelides, Jon Hansen, Justin Nadauld, and Lawrence D. Reaveley. May 2002.
- PEER 2002/17** *Structural Characterization and Seismic Response Analysis of a Highway Overcrossing Equipped with Elastomeric Bearings and Fluid Dampers: A Case Study.* Nicos Makris and Jian Zhang. November 2002.
- PEER 2002/16** *Estimation of Uncertainty in Geotechnical Properties for Performance-Based Earthquake Engineering.* Allen L. Jones, Steven L. Kramer, and Pedro Arduino. December 2002.
- PEER 2002/15** *Seismic Behavior of Bridge Columns Subjected to Various Loading Patterns.* Asadollah Esmaeily-Gh. and Yan Xiao. December 2002.
- PEER 2002/14** *Inelastic Seismic Response of Extended Pile Shaft Supported Bridge Structures.* T.C. Hutchinson, R.W. Boulanger, Y.H. Chai, and I.M. Idriss. December 2002.
- PEER 2002/13** *Probabilistic Models and Fragility Estimates for Bridge Components and Systems.* Paolo Gardoni, Armen Der Kiureghian, and Khalid M. Mosalam. June 2002.
- PEER 2002/12** *Effects of Fault Dip and Slip Rake on Near-Source Ground Motions: Why Chi-Chi Was a Relatively Mild M7.6 Earthquake.* Brad T. Aagaard, John F. Hall, and Thomas H. Heaton. December 2002.
- PEER 2002/11** *Analytical and Experimental Study of Fiber-Reinforced Strip Isolators.* James M. Kelly and Shakhzod M. Takhirov. September 2002.
- PEER 2002/10** *Centrifuge Modeling of Settlement and Lateral Spreading with Comparisons to Numerical Analyses.* Sivapalan Gajan and Bruce L. Kutter. January 2003.
- PEER 2002/09** *Documentation and Analysis of Field Case Histories of Seismic Compression during the 1994 Northridge, California, Earthquake.* Jonathan P. Stewart, Patrick M. Smith, Daniel H. Whang, and Jonathan D. Bray. October 2002.
- PEER 2002/08** *Component Testing, Stability Analysis and Characterization of Buckling-Restrained Unbonded BracesTM.* Cameron Black, Nicos Makris, and Ian Aiken. September 2002.
- PEER 2002/07** *Seismic Performance of Pile-Wharf Connections.* Charles W. Roeder, Robert Graff, Jennifer Soderstrom, and Jun Han Yoo. December 2001.
- PEER 2002/06** *The Use of Benefit-Cost Analysis for Evaluation of Performance-Based Earthquake Engineering Decisions.* Richard O. Zerbe and Anthony Falit-Baiamonte. September 2001.
- PEER 2002/05** *Guidelines, Specifications, and Seismic Performance Characterization of Nonstructural Building Components and Equipment.* André Filiatrault, Constantin Christopoulos, and Christopher Stearns. September 2001.

- PEER 2002/04** *Consortium of Organizations for Strong-Motion Observation Systems and the Pacific Earthquake Engineering Research Center Lifelines Program: Invited Workshop on Archiving and Web Dissemination of Geotechnical Data, 4–5 October 2001.* September 2002.
- PEER 2002/03** *Investigation of Sensitivity of Building Loss Estimates to Major Uncertain Variables for the Van Nuys Testbed.* Keith A. Porter, James L. Beck, and Rustem V. Shaikhutdinov. August 2002.
- PEER 2002/02** *The Third U.S.-Japan Workshop on Performance-Based Earthquake Engineering Methodology for Reinforced Concrete Building Structures.* July 2002.
- PEER 2002/01** *Nonstructural Loss Estimation: The UC Berkeley Case Study.* Mary C. Comerio and John C. Stallmeyer. December 2001.
- PEER 2001/16** *Statistics of SDF-System Estimate of Roof Displacement for Pushover Analysis of Buildings.* Anil K. Chopra, Rakesh K. Goel, and Chatpan Chintanapakdee. December 2001.
- PEER 2001/15** *Damage to Bridges during the 2001 Nisqually Earthquake.* R. Tyler Ranf, Marc O. Eberhard, and Michael P. Berry. November 2001.
- PEER 2001/14** *Rocking Response of Equipment Anchored to a Base Foundation.* Nicos Makris and Cameron J. Black. September 2001.
- PEER 2001/13** *Modeling Soil Liquefaction Hazards for Performance-Based Earthquake Engineering.* Steven L. Kramer and Ahmed-W. Elgamal. February 2001.
- PEER 2001/12** *Development of Geotechnical Capabilities in OpenSees.* Boris Jeremi . September 2001.
- PEER 2001/11** *Analytical and Experimental Study of Fiber-Reinforced Elastomeric Isolators.* James M. Kelly and Shakhzod M. Takhirov. September 2001.
- PEER 2001/10** *Amplification Factors for Spectral Acceleration in Active Regions.* Jonathan P. Stewart, Andrew H. Liu, Yoojoong Choi, and Mehmet B. Baturay. December 2001.
- PEER 2001/09** *Ground Motion Evaluation Procedures for Performance-Based Design.* Jonathan P. Stewart, Shyh-Jeng Chiou, Jonathan D. Bray, Robert W. Graves, Paul G. Somerville, and Norman A. Abrahamson. September 2001.
- PEER 2001/08** *Experimental and Computational Evaluation of Reinforced Concrete Bridge Beam-Column Connections for Seismic Performance.* Clay J. Naito, Jack P. Moehle, and Khalid M. Mosalam. November 2001.
- PEER 2001/07** *The Rocking Spectrum and the Shortcomings of Design Guidelines.* Nicos Makris and Dimitrios Konstantinidis. August 2001.
- PEER 2001/06** *Development of an Electrical Substation Equipment Performance Database for Evaluation of Equipment Fragilities.* Thalia Agnanos. April 1999.
- PEER 2001/05** *Stiffness Analysis of Fiber-Reinforced Elastomeric Isolators.* Hsiang-Chuan Tsai and James M. Kelly. May 2001.
- PEER 2001/04** *Organizational and Societal Considerations for Performance-Based Earthquake Engineering.* Peter J. May. April 2001.
- PEER 2001/03** *A Modal Pushover Analysis Procedure to Estimate Seismic Demands for Buildings: Theory and Preliminary Evaluation.* Anil K. Chopra and Rakesh K. Goel. January 2001.
- PEER 2001/02** *Seismic Response Analysis of Highway Overcrossings Including Soil-Structure Interaction.* Jian Zhang and Nicos Makris. March 2001.
- PEER 2001/01** *Experimental Study of Large Seismic Steel Beam-to-Column Connections.* Egor P. Popov and Shakhzod M. Takhirov. November 2000.
- PEER 2000/10** *The Second U.S.-Japan Workshop on Performance-Based Earthquake Engineering Methodology for Reinforced Concrete Building Structures.* March 2000.
- PEER 2000/09** *Structural Engineering Reconnaissance of the August 17, 1999 Earthquake: Kocaeli (Izmit), Turkey.* Halil Sezen, Kenneth J. Elwood, Andrew S. Whittaker, Khalid Mosalam, John J. Wallace, and John F. Stanton. December 2000.
- PEER 2000/08** *Behavior of Reinforced Concrete Bridge Columns Having Varying Aspect Ratios and Varying Lengths of Confinement.* Anthony J. Calderone, Dawn E. Lehman, and Jack P. Moehle. January 2001.

- PEER 2000/07** *Cover-Plate and Flange-Plate Reinforced Steel Moment-Resisting Connections.* Taejin Kim, Andrew S. Whittaker, Amir S. Gilani, Vitelmo V. Bertero, and Shakhzod M. Takhirov. September 2000.
- PEER 2000/06** *Seismic Evaluation and Analysis of 230-kV Disconnect Switches.* Amir S. J. Gilani, Andrew S. Whittaker, Gregory L. Fenves, Chun-Hao Chen, Henry Ho, and Eric Fujisaki. July 2000.
- PEER 2000/05** *Performance-Based Evaluation of Exterior Reinforced Concrete Building Joints for Seismic Excitation.* Chandra Clyde, Chris P. Pantelides, and Lawrence D. Reaveley. July 2000.
- PEER 2000/04** *An Evaluation of Seismic Energy Demand: An Attenuation Approach.* Chung-Che Chou and Chia-Ming Uang. July 1999.
- PEER 2000/03** *Framing Earthquake Retrofitting Decisions: The Case of Hillside Homes in Los Angeles.* Detlof von Winterfeldt, Nels Roselund, and Alicia Kitsuse. March 2000.
- PEER 2000/02** *U.S.-Japan Workshop on the Effects of Near-Field Earthquake Shaking.* Andrew Whittaker, ed. July 2000.
- PEER 2000/01** *Further Studies on Seismic Interaction in Interconnected Electrical Substation Equipment.* Armen Der Kiureghian, Kee-Jeung Hong, and Jerome L. Sackman. November 1999.
- PEER 1999/14** *Seismic Evaluation and Retrofit of 230-kV Porcelain Transformer Bushings.* Amir S. Gilani, Andrew S. Whittaker, Gregory L. Fenves, and Eric Fujisaki. December 1999.
- PEER 1999/13** *Building Vulnerability Studies: Modeling and Evaluation of Tilt-up and Steel Reinforced Concrete Buildings.* John W. Wallace, Jonathan P. Stewart, and Andrew S. Whittaker, editors. December 1999.
- PEER 1999/12** *Rehabilitation of Nonductile RC Frame Building Using Encasement Plates and Energy-Dissipating Devices.* Mehrdad Sasani, Vitelmo V. Bertero, James C. Anderson. December 1999.
- PEER 1999/11** *Performance Evaluation Database for Concrete Bridge Components and Systems under Simulated Seismic Loads.* Yael D. Hose and Frieder Seible. November 1999.
- PEER 1999/10** *U.S.-Japan Workshop on Performance-Based Earthquake Engineering Methodology for Reinforced Concrete Building Structures.* December 1999.
- PEER 1999/09** *Performance Improvement of Long Period Building Structures Subjected to Severe Pulse-Type Ground Motions.* James C. Anderson, Vitelmo V. Bertero, and Raul Bertero. October 1999.
- PEER 1999/08** *Envelopes for Seismic Response Vectors.* Charles Menun and Armen Der Kiureghian. July 1999.
- PEER 1999/07** *Documentation of Strengths and Weaknesses of Current Computer Analysis Methods for Seismic Performance of Reinforced Concrete Members.* William F. Cofer. November 1999.
- PEER 1999/06** *Rocking Response and Overturning of Anchored Equipment under Seismic Excitations.* Nicos Makris and Jian Zhang. November 1999.
- PEER 1999/05** *Seismic Evaluation of 550 kV Porcelain Transformer Bushings.* Amir S. Gilani, Andrew S. Whittaker, Gregory L. Fenves, and Eric Fujisaki. October 1999.
- PEER 1999/04** *Adoption and Enforcement of Earthquake Risk-Reduction Measures.* Peter J. May, Raymond J. Burby, T. Jens Feeley, and Robert Wood.
- PEER 1999/03** *Task 3 Characterization of Site Response General Site Categories.* Adrian Rodriguez-Marek, Jonathan D. Bray, and Norman Abrahamson. February 1999.
- PEER 1999/02** *Capacity-Demand-Diagram Methods for Estimating Seismic Deformation of Inelastic Structures: SDF Systems.* Anil K. Chopra and Rakesh Goel. April 1999.
- PEER 1999/01** *Interaction in Interconnected Electrical Substation Equipment Subjected to Earthquake Ground Motions.* Armen Der Kiureghian, Jerome L. Sackman, and Kee-Jeung Hong. February 1999.
- PEER 1998/08** *Behavior and Failure Analysis of a Multiple-Frame Highway Bridge in the 1994 Northridge Earthquake.* Gregory L. Fenves and Michael Ellery. December 1998.
- PEER 1998/07** *Empirical Evaluation of Inertial Soil-Structure Interaction Effects.* Jonathan P. Stewart, Raymond B. Seed, and Gregory L. Fenves. November 1998.

- PEER 1998/06** *Effect of Damping Mechanisms on the Response of Seismic Isolated Structures.* Nicos Makris and Shih-Po Chang. November 1998.
- PEER 1998/05** *Rocking Response and Overturning of Equipment under Horizontal Pulse-Type Motions.* Nicos Makris and Yiannis Roussos. October 1998.
- PEER 1998/04** *Pacific Earthquake Engineering Research Invitational Workshop Proceedings, May 14–15, 1998: Defining the Links between Planning, Policy Analysis, Economics and Earthquake Engineering.* Mary Comerio and Peter Gordon. September 1998.
- PEER 1998/03** *Repair/Upgrade Procedures for Welded Beam to Column Connections.* James C. Anderson and Xiaojing Duan. May 1998.
- PEER 1998/02** *Seismic Evaluation of 196 kV Porcelain Transformer Bushings.* Amir S. Gilani, Juan W. Chavez, Gregory L. Fennes, and Andrew S. Whittaker. May 1998.
- PEER 1998/01** *Seismic Performance of Well-Confined Concrete Bridge Columns.* Dawn E. Lehman and Jack P. Moehle. December 2000.